

***New Molecular Topologies from Main Group Elements: P/N, B/N and Al/N  
Containing Macrocycles and Pyridinophanes***

*A thesis submitted for the partial fulfilment of  
the degree of Doctor of Philosophy*

by

**Deependra Bawari**



Department of Chemical Sciences

Indian Institute of Science Education and Research (IISER) Mohali

Sector 81, Knowledge City, S. A. S. Nagar, Manauli PO, Mohali, 140306 Punjab, India.

**February 2018**



*Dedicated to my dear brother*

*late Gaurav Gahtori*



## DECLARATION

The work presented in this thesis titled “*New Molecular Topologies from Main Group Elements: P/N, B/N and Al/N Containing Macrocycles and Pyridinophanes*” has been carried out by me under the supervision of **Dr. Sanjay Singh** in the Department of Chemical Sciences, Indian Institute of Science Education and Research (IISER) Mohali, Mohali.

This work has not been submitted in part or full for a degree, diploma or a fellowship to any other university or institute.

Whenever contributions of others are involved, every effort is made to indicate this clearly with due acknowledgements of collaborative work and discussions. This thesis is a bonafide record of original work done by me and all sources listed within have been detailed in the bibliography.

**Deependra Bawari**

Date:

Place:

In my capacity as the supervisor of the candidate’s thesis work, I certify that the above statements by the candidate are true to the best of my knowledge.

**Dr. Sanjay Singh**

*Associate Professor*

*Department of Chemical Sciences*

*Indian Institute of Science Education and Research Mohali*

Date:

Place:



## *Acknowledgements*

*A blank paper becomes valuable once words inscribed on it, the same can fly in the sky once gets support from sticks and a thread. A kite can fly in the sky no longer than few minutes without the thread. All these above adjectives I have used to compare me and my supervisor therefore, foremost, from the innermost core of my heart I express my profound sense of reverence, obligations, respect and honour to Dr. Sanjay Singh, Associate Professor, Department of Chemical Sciences and Chairman of my doctoral advisory committee for his inspiration, benign cooperation, industrious guidance, impeccable supervision, timely criticism and benevolent help during the entire period of my PhD research. I would like to call it rather as a most friendly guidance which gave me so much freedom to think and learn many things independently from our friendly conversations which helped me in many ways, not only in professional front but also in personal life. I wish to express my sincere thanks to Prof. R. Kapoor, Dr. R. Vijayanand and Dr. Debashis Adhikari, Department of Chemical Sciences, members of my Advisory Committee for their valuable and sincere advice during the course of present investigation. I acknowledge special thanks to Prof. Debi Prasad Sarkar (Director IISER Mohali) and Prof. N. Sathyamurthy (former Director IISER Mohali) for providing well equipped platform with all amenities. I sincerely thank Prof. K. S. Viswanathan, former head of the department (Chemical Sciences) and Dr. S. Arulananda Babu (head of the department, Chemical Sciences) to provide all requisites in the Department. I also thank my family members, Narendra Bisht, Dr. Rajeev Kapri (physics department) and Prof. Ram S. Mohan (Chemistry department, Illinois Wesleyan University) for the moral support and the care they have shown to me.*

*I am thankful for pleasant company, friendly counselling, cooperation, practical help and patronage of my lab mates Dr. Rishu, Dr. Billa Prashanth, Dr. Kuldeep Jaiswal, Dr. Nagarjuna, Dr. Krishna Kumar Manar, Mr. Aditya Verma, Mr. G. Sai, Kumar, Mr. V. R. Sabari, Mr. Akhil Rag, Mr. Bhupendra Goswami, Mr. Sandeep Rawat, Ms. Mamta Bhandari, Mr. Sandeep Kumar Thakur, Ms. Chandrakala Negi, Mr. Manu Adhikari, Ms.*

*Tanuja Triwari, Mr. Nitish Garg, Mr. Soumydeep Chakraborty, Mr. Vishal Porwal, Mr. Rohit Kamte. I would like to thank the former and present Dean(s), IISER Mohali, for providing best research facilities and atmosphere. I am thankful to all the faculty members of IISER Mohali for their help, cooperation and encouragement at various stages.*

*I also thank all the non-teaching staff of IISER Mohali for their assistance on various occasions. I specially acknowledge Mr. Triveni Sankar and Mr. Balbir for their valuable support given to me all the time. I thank Dr. Billa Prashanth and Dr. Angshuman Roy Choudhury for their valuable suggestions in handling XRD instrument. I thank Mr. Vishal Porwal for his valuable guidance for computation. I would like to acknowledge IISER Mohali for providing the basic requirements like SCXRD Facility, NMR, HRMS, IR, and UGC, MHRD and IISER Mohali for the financial support.*

*I thank my near and dear ones whom I haven't acknowledged here for their direct or indirect help, especially the cricket team of chemistry department. This closure of acknowledgement culminates with a gesture of gratitude to my dear parents whose love and support has encouraged me to pursue this direction.*

*Deependra Bawari*

Synopsis of

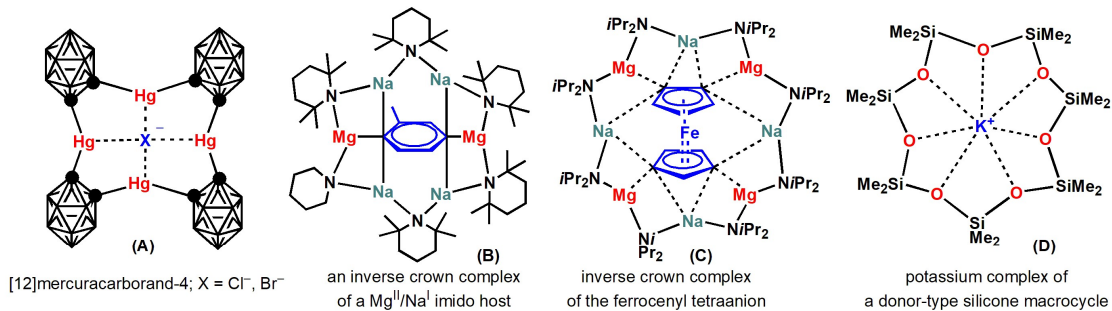
**New Molecular Topologies from Main Group Elements: P/N, B/N and Al/N  
Containing Macrocycles and Pyridinophanes**

## 1. Introduction

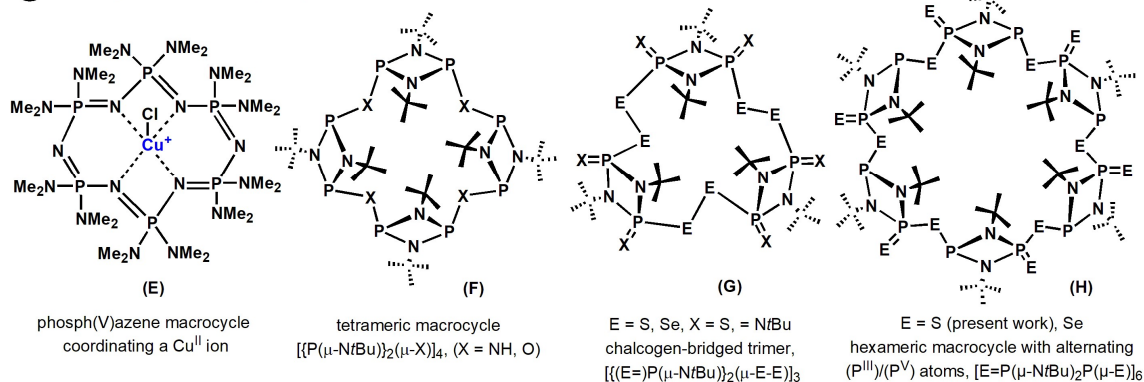
Since last few decades enormous developments in organic macrocycles domain have allowed proliferation of a variety of molecular structures. The literature pertaining to organic macrocycles encompasses a broad spectrum covering molecules such as crown ethers, cryptands, calixarenes, cyclophanes etc. The macrocyclic structure where the framework is constituted of inorganic elements has recently started to attract attention and consequently some important breakthroughs have been witnessed (see Chart). However, to match the advancements already made with the organic systems, a considerably large amount of work is needed with the inorganic macrocycles.<sup>[1]</sup> The slow progress in the area of inorganic macrocycles can be understood due to the following difficulties: (i) compared to carbon, the greater range of orbitals and hybridization states available with inorganic elements-lead to mismatch of orbital sizes and result in weaker bonds between elements from two different groups or period; (ii) variable oxidation states of inorganic elements-giving rise to formation of multiple products with different oxidation state; (iii) hydrolytic instability-hampers the separation of multiproduct; (iv) lack of a general synthetic strategy for inorganic systems compared to the organic derivatives and (v) lower thermodynamic stability and polar nature of bonds to these elements, leading to kinetically labile and/or thermodynamically less robust arrangements.<sup>[1]</sup>

Nonetheless, in spite of the challenges mentioned above, it has been possible to assemble a few robust inorganic macrocycles with stable arrangements. The Chart below shows examples of well known inorganic macrocycles. The mercuracarborands (**A**) were one of the early examples where the rigid linear geometry of  $\text{Hg}^{2+}$  atoms bridge  $\{1,2\text{-C}_2\text{B}_{10}\text{H}_{10}\}$  units into cyclic arrangements and exhibited acceptor type behaviour due to the  $\text{Hg}^{2+}$ . The inverse crowns (**B** and **C**) are good examples that show acceptor properties to a broad range of organic, inorganic and organometallic anions including highly unusual anions (2,5-C-H

**(A) Inorganic macrocycles with acceptor (A-C) and donor properties (D)**



**(B) Macrocycles based on phosphazanes**



**(C) Cyclophanes and pyridinophanes based on main group elements**

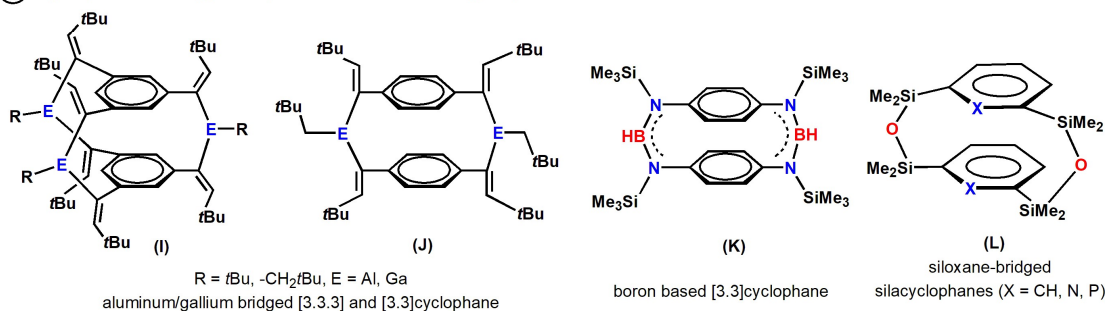


**Chart:** Some well known examples of inorganic macrocycles (**A-H**) and cyclophanes (**I-L**).

doubly deprotonated toluene **B** and tetrametallated ferrocene [(C<sub>5</sub>H<sub>3</sub>)<sub>2</sub>Fe]<sup>4+</sup> (**C**). The donor behaviour of inorganic macrocycle towards cation coordination was seen in a twelve-membered phosph(V)azane macrocycle, [(Me<sub>2</sub>N)<sub>2</sub>PN]<sub>6</sub> (**E**, captures Cu<sup>2+</sup>) followed by potassium complex of silicone analogue **D** of a crown ether. Cyclodiphosphazane, [CIP(μ-NtBu)]<sub>2</sub> and its derivatives<sup>[2]</sup> have made significant mark as a building block to assemble many inorganic macrocycles with different donor atoms (**F-H**). Chart above also shows known examples of cyclophanes (**I-K**) containing Lewis acidic atoms in the bridges.<sup>[3]</sup> The incorporation of Lewis acidic elements would allow the fine-tuning of their acceptor type

behaviour. The example of donor type of cyclophane is siloxane-bridged silacyclophanes ( $X = CH, N, P$ ) (**L**).<sup>[4]</sup> From the foregoing discussion it is understandable that the synthesis of a wide variety of building blocks based on inorganic elements and their further incorporation into macrocycles offers enormous possibility to explore this field.

## 2. Objective(s) and scope

Two main objectives of the present work are (a) Syntheses of new building blocks as derivatives of  $[CIP(\mu-NtBu)]_2$  and their further use to formulate new macrocycles; and (b) the utilization of well known dianionic amidinate fragments,  $[RN(NR')]_2^{2-}$  in the form of 'bis(trimethylsilyl)-N,N'-2,6-diaminopyridine (bap) and bis(trimethylsilyl)-N,N'-2,4-diamino-6-(R)-triazine (bat)' units to prepare the macrocyclic structures incorporating boron and aluminum. These objectives were undertaken in the sequence detailed below:

- (i) Syntheses of  $[CIP(\mu-NtBu)]_2$  derived ( $P^{III}/P^V$ ),  $[CIP(=E)(\mu-NtBu)_2PCl]$  and all ( $P^V$ ),  $[CIP(=E)(\mu-NtBu)]_2$  ( $E = S, Se, NAr$ ) building blocks.
- (ii) Wurtz type reduction of  $[CIP(=S)(\mu-NtBu)]_2$  to prepare S bridged macrocycle.
- (iii) Syntheses of boraamidinate (N–B–N) bridged macrocycles using bap and bat units.
- (iv) Syntheses of aluminum-amide (N–Al–N) bridged macrocycles using bap and bat units.

## 3. Description of the research work

### 3.1. Sequential functionalization and product isomeric distribution of cyclic- $[CIP(\mu-NtBu)]_2$

The stepwise oxidation of cyclic- $[CIP(\mu-NtBu)]_2$  framework with organic azides and chalcogens (S and Se), as monitored by in-situ  $^{31}P\{^1H\}$  NMR, revealed that conversion of the basic ( $P^{III}$ )<sub>2</sub>N<sub>2</sub> framework leads to a mixture of cis and trans isomers of ( $P^V$ )<sub>2</sub>N<sub>2</sub> via the ( $P^{III}/P^V$ )N<sub>2</sub> intermediates. Following are the examples of molecules prepared using this approach:

- (i) Diazadiphosphetidines,  $[(ArN=)ClP(\mu-NtBu)]_2$  ( $Ar = 2,6\text{-}iPr_2C_6H_3N_3$  (**1**) and  $2,4,6\text{-}Me_3C_6H_2N_3$  (**2**)).
- (ii) Monochalcogenido derivatives,  $[(Se=)ClP(\mu-NtBu)_2PCl]$  (**3**) and  $[(S=)ClP(\mu-NtBu)_2PCl]$  (**4**).
- (iii) Homo- and hetero-chalcogenido derivatives,  $[(S=)ClP(\mu-NtBu)]_2$  (**5**) and  $[(S=)ClP(\mu-NtBu)_2PCl(=Se)]$  (**6**).

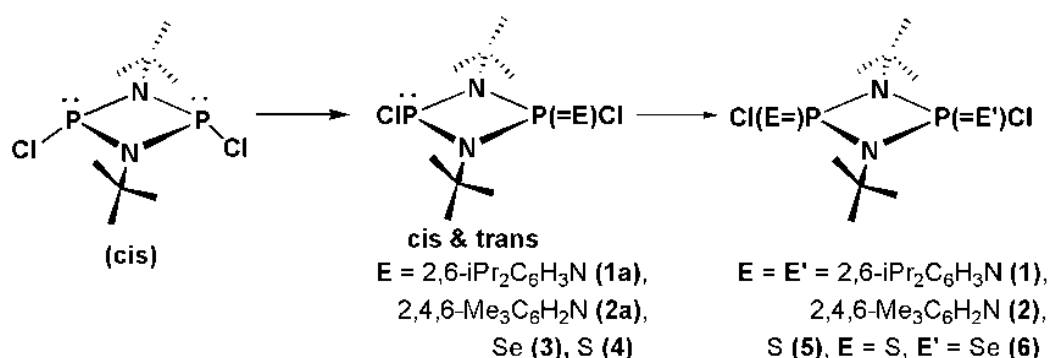


**Figure 1.** Syntheses of cyclic- $(P^V)_2N_2$  products *via* the mixed valent cyclic- $(P^{III}/P^V)N_2$  intermediates.

### 3.2. Different pathways in the Wurtz reduction of $[(S=)PCl(\mu-NtBu)]_2$ with Na

Following the syntheses of cyclic- $(P^V)_2N_2$  and the mixed valent cyclic- $(P^{III}/P^V)N_2$  compounds, we became interested to explore their utility in constructing macrocycles. Therefore, we employed reduction of cyclodiphosphazane,  $[(S=)ClP(\mu-NtBu)]_2$  (**5**) with metallic sodium that proceeds *via* two different pathways: One pathway leads to the hexameric macrocycle,  $[(\mu-S)P(\mu-NtBu)_2P(=S)]_6$  (**7**) (Figure 2) and the second yields a colourless singlet biradicaloid dianion  $trans\text{-}[S\text{-}P(Cl)(\mu-NtBu)]_2^{2-}$ . In the solid state, the later constitutes polymeric structures as three dimensional  $\{[(S\text{-})ClP(\mu-NtBu)_2PCl(S)]Na(Na \cdot 2THF)\}_n$  (**8**) and two dimensional  $\{[(S\text{-})ClP(\mu-NtBu)_2PCl(S)](Na \cdot THF)_2\}_n$  (**9**) networks. The electronic structure of the dianion core of **8** and **9** as P-centred biradicaloid was probed by computational studies on  $[S\text{-}P(Cl)(\mu-NMe)]_2^{2-}$ .

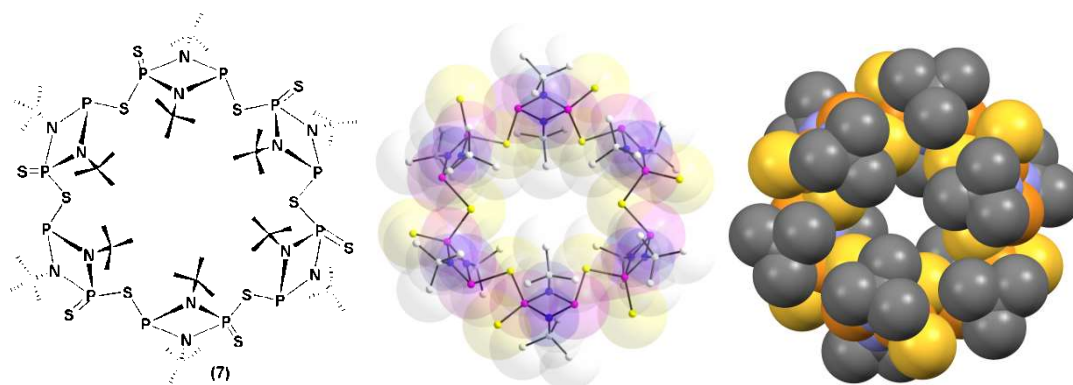


**Figure 2.** Single crystal X-ray structure of S-bridged macrocycle **7** and its space filling model.

### 3.3. Boraamidinate bridged novel [3.3](2,6)pyridinophanes and a calix like trimer

#### (i) Syntheses of boraamidinate N–B–N bridged pyridinophanes

The use of boraamidinate (N–B–N) bridges to connect the dianionic amidinate fragment, ‘bis(trimethylsilyl)-N,N’-2,6-diaminopyridine (bap) has been conceived that leads to the formation of conformationally rigid anti- and syn-pyridinophanes (**11** and **12**).

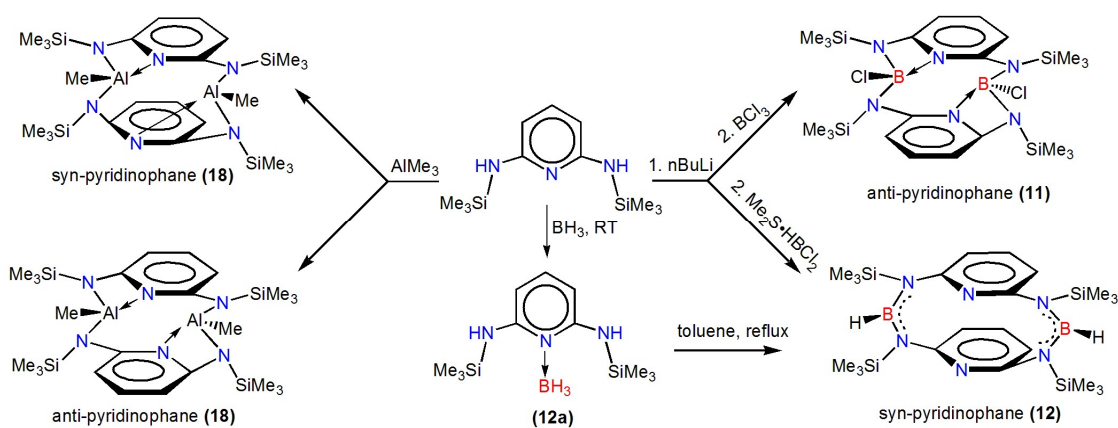


**Figure 3.** Syntheses of tetraazadibora[3.3](2,6)pyridinophanes (**11** and **12**) and the aluminum analogs (**18**).

#### (ii) Synthesis of boraamidinate N–BH<sub>2</sub>–N bridged calix like trimer and macrocycles

The unprecedented reaction of bis(trimethylsilyl)-N,N’-2,4-diamino-6-(R)-triazine (bat) with BH<sub>3</sub>·SMe<sub>2</sub> involved hydroboration of the (Me)C=N group of triazine leading to the formation of a calix like trimer (**13**).

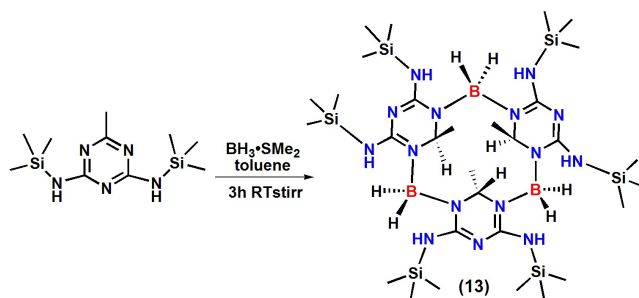


**Figure 4.** Synthesis of a calix like trimer (**13**).

### 3.4. Assembly of pyridinophanes, molecular bowls and cryptands containing aluminum

The reaction of  $\text{AlMe}_3$  and  $\text{AlH}_3$  with bis(trimethylsilyl)- $N,N'$ -2,6-diaminopyridine (bap) and bis(trimethylsilyl)- $N,N'$ -2,4-diamino-6-( $R$ )-triazine (bat) smoothly affords pyridinophanes, macrocycles and bowl shaped structures containing aluminum. The 1:1 and 1:2 reactions of bap with  $\text{AlMe}_3$  at room temperature affords methylaluminum complexes,  $[2-(\text{Me}_3\text{SiN})-6-(\text{Me}_3\text{SiNH})\text{C}_5\text{H}_3\text{N}](\text{AlMe}_2)$  (**16**) and  $[2-(\text{Me}_3\text{SiN})-6-(\text{Me}_3\text{SiNH})\text{C}_5\text{H}_3\text{N}]_2\text{AlMe}$  (**17**), respectively. Refluxing this 1:1 mixture produces a tetraazadialumino[3.3](2,6)pyridinophane,  $[2,6-(\text{Me}_3\text{SiN})_2\text{C}_5\text{H}_3\text{N}(\text{AlMe})]_2$  (**18**). Alkoxy bridged dimeric structure,  $[\{2-(\text{Me}_3\text{SiN})-6-(\text{Me}_3\text{SiNH})\text{C}_5\text{H}_3\text{N}\}_2\text{Al}(\mu\text{-OMe})]_2$  (**19**) was obtained on exposure of **17** to open atmosphere as a result of oxygen insertion in Al-Me bonds. On changing the bap and  $\text{AlMe}_3$  stoichiometry to 2:3, a bowl shaped structure,  $[2,6-(\text{Me}_3\text{SiN})_2\text{C}_5\text{H}_3\text{N}(\text{AlMe}_2)]_2[\text{AlMe}]$  (**20**) was obtained which was further reacted with the Lewis acid,  $\text{B}(\text{C}_6\text{F}_5)_3$  to generate a stable monocationic species,  $[\{2-(\text{Me}_3\text{SiN})_2-6-(\text{Me}_3\text{SiN})_2\text{C}_5\text{H}_3\text{N}\}_2(\text{AlMe}_2)(\text{AlMe})(\text{AlMe})]^\oplus[\text{MeB}(\text{C}_6\text{F}_5)_3]^\ominus$  (**21**) (Figure 5).

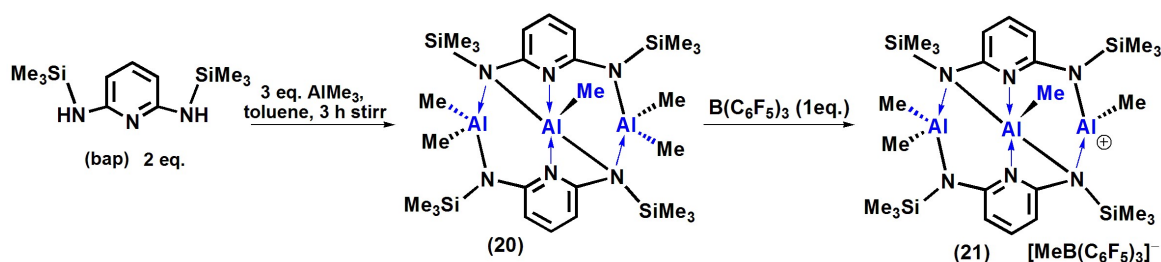


**Figure 5.** Synthesis of aluminum–amide bridged bowl type complex **20** and its monocation **21**.

Attempts to synthesize similar kind of bowl shaped structures with triazine systems resulted in dinuclear aluminum triazine complexes,  $[2,4-(\text{Me}_3\text{SiN})_2-6-(\text{R})-\text{C}_3\text{N}_3](\text{AlMe}_2)_2$  ( $\text{R} = \text{Me}$  (**22**),  $\text{NHSiMe}_3$  (**23**),  $\text{Ph}$  (**24**)). A similar 3:2 reaction of *bap* with  $\text{AlH}_3 \cdot \text{NMe}_2\text{Et}$  at room temperature afforded an aluminum based [3.3.3]cryptand,  $[2,6-(\text{Me}_3\text{SiN})_2\text{C}_5\text{H}_3\text{N}]_3\text{Al}_2$  (**25**) (Figure 6).

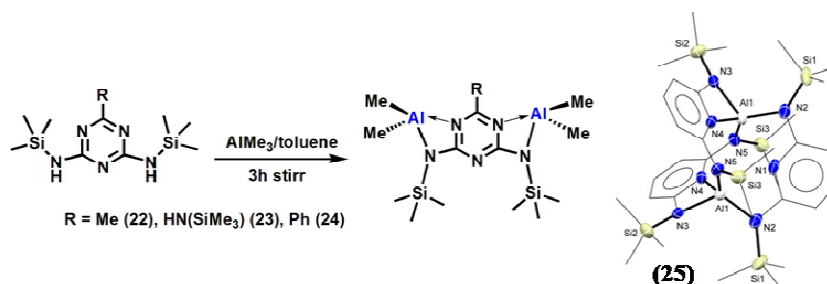


**Figure 6.** Synthesis of dinuclear aluminum triazine complexes **22-24** and [3.3.3]cryptand **25**.

#### 4. Conclusions

The synopsis presents a brief account of our efforts to develop the area of inorganic macrocycles, pyridinophanes and cryptands with a focus to use main group elements. The oxidation of  $(\text{P}^{\text{III}})_2$  centers in  $[\text{CIP}(\mu\text{-N}t\text{Bu})_2]$  to  $(\text{P}^{\text{V}})_2$  centers in  $[\text{CIP}(=\text{E})(\mu\text{-N}t\text{Bu})_2]$  ( $\text{E} = \text{S}, \text{Se}, \text{NAr}$ ) proceeds via  $(\text{P}^{\text{III}}/\text{P}^{\text{V}})$  intermediates,  $[\text{CIP}(=\text{E})(\mu\text{-N}t\text{Bu})_2\text{PCl}]$  in a stepwise manner giving *cis*- and *trans*- $[\text{CIP}(=\text{E})(\mu\text{-N}t\text{Bu})_2\text{PCl}]$  and *cis*- and *trans*- $[\text{CIP}(=\text{E})(\mu\text{-N}t\text{Bu})_2]$  compounds.

The Wurtz-type coupling on a mixture of *cis*- and *trans*- $[(\text{S}=\text{CIP}(\mu\text{-N}t\text{Bu})_2)]_2$  with sodium proceeds in two different reaction pathways, affording a sulfur-bridged hexameric macrocycle  $[(\mu\text{-S})\text{P}(\mu\text{-N}t\text{Bu})_2\text{P}(=\text{S})]_6$  as the result of *head-to-tail* cyclization. Whereas, the biradicaloid dianion  $[\text{S}-\text{P}(\text{Cl})(\mu\text{-N}t\text{Bu})_2]^{2-}$  was formed under a different pathway involving reduction of the  $\text{P}=\text{S}$  bonds to  $\text{P}-\text{S}$  bonds and forms 3D polymer,  $[\{(\text{S}-)\text{CIP}(\mu\text{-N}t\text{Bu})_2\text{PCl}(\text{S})\}\text{Na}(\text{Na} \cdot \text{THF}_2)]_n$  and 2D polymer,  $[\{(\text{S}-)\text{CIP}(\mu\text{-N}t\text{Bu})_2\text{PCl}(\text{S})\}(\text{Na} \cdot \text{THF}_2)_2]_n$  in the solid-state.

Further work on other macrocyclic topologies led to the discovery of novel conformationally rigid tetraazadibora[3.3](2,6)pyridinophanes and their aluminum analogs containing N-B-N (or N-Al-N) bridges that link substituted 2,6-diaminopyridine units. An unprecedented reaction of substituted triazine, bis(trimethylsilyl)-N,N'-2,4-diamino-6-(Me)-triazine with  $\text{BH}_3 \cdot \text{SMe}_2$  led to hydroboration and formation of a calix like structure. A bowl shaped complex based on aluminum,  $[\text{2,6-(Me}_3\text{SiN)}_2\text{C}_5\text{H}_3\text{N(AlMe}_2\text{)}]_2[\text{AlMe}]$  was formed on reaction of  $\text{AlMe}_3$  with bap. Aluminum based [3.3.3]cryptand,  $[\text{2,6-(Me}_3\text{SiN)}_2\text{C}_5\text{H}_3\text{N}]_3\text{Al}_2$  was synthesized by a 3:2 reaction of bap with  $\text{AlH}_3 \cdot \text{NMe}_2\text{Et}$ .

## 5. References

1. a) D. Bawari, B. Prashanth, S. Ravi, K. R. Shamasundar, S. Singh and D. S. Wright, *Chem. Eur. J.* **2016**, *22*, 12027–12033; b) D. Bawari, B. Prashanth, K. Jaiswal, A. R. Choudhury and S. Singh, *Eur. J. Inorg. Chem.* **2017**, 4123–4130; For reviews see: c) M. S. Balakrishna, *Dalton Trans.* **2016**, *45*, 12252–12282; d) H. Niu, A. J. Plajer, R. Garcia-Rodriguez, S. Singh and D. S. Wright, *Chem. Eur. J.* **2018**, *24*, 3073–3082.
2. a) C. G. M. Benson, V. Vasilenko, R. García-Rodríguez, A. D. Bond, S. G. Calera, L. H. Gade and D. S. Wright, *Dalton Trans.* **2015**, *44*, 14242–14247; b) H. Klare, S. Hanft, J. M. Neudörfl, N. E. Schlrer, A. Griesbeck and B. Goldfuss, *Chem.-Eur. J.* **2014**, *20*, 11847–11855; c) D. C. Haagenson, G. R. Lief, L. Stahl and R. J. Staples, *J. Organomet. Chem.* **2008**, *693*, 2748–2754.
3. a) W. Uhl, S. Haddadpour and M. Matar, *Organometallics* **2006**, *25*, 159; b) W. Uhl, M. Claesener, S. Haddadpour, B. Jasper and A. Hepp, *Dalton Trans.* **2007**, 417–423; c) W. Uhl, M. Claesener, A. Hepp, B. Jasper, A. Vinogradov, L. van Wüllen and T. K.-J. Köster, *Dalton Trans.* **2009**, 10550–10562; d) W. Uhl, A. Hepp, M. Matar and A. Vinogradov, *Eur. J. Inorg. Chem.* **2007**, 4133–4137; e) W. Uhl, F. Breher, S. Haddadpour and F. Rogel, *Organometallics* **2005**, *24*, 2210–2213; f) P. Paetzold, U. W. Osterloh and U. Englert, *Z. Anorg. Allg. Chem.* **2004**, *630*, 2569–2570.

4. K. Reuter, R. G. M. Maas, A. Reuter, F. Kilgenstein, Y. Asfaha and C. von Hänisch, *Dalton Trans.* **2017**, *46*, 4530–4541.

## Contents

	Page
<b>Chapter 1: Mechanistic Insights and Product Isomeric Distribution in the Stepwise Functionalization of Cyclic-(P<sup>(III)</sup>)<sub>2</sub>N<sub>2</sub> into Cyclic-(P<sup>(V)</sup>)<sub>2</sub>N<sub>2</sub> products</b>	1
<b>1.1 Introduction</b>	2
<b>1.2 Results and Discussion</b>	5
<b>1.3 Conclusions</b>	17
<b>1.4 Experimental Section</b>	17
1.4.1 General procedure	17
1.4.2 Starting materials	18
1.4.3 Physical measurements	18
1.4.4 Synthetic procedure	19
<b>1.5 Crystallographic Data</b>	24
<b>1.6 References</b>	24
<b>Chapter 2: Different Pathways in the Wurtz Reduction of [(S=)PCl(μ-NtBu)]<sub>2</sub> with Na</b>	28
<b>2.1 Introduction</b>	29
<b>2.2 Results and Discussion</b>	34
<b>2.3 Conclusions</b>	43
<b>2.4 Experimental Section</b>	44
2.4.1 General procedure	44
2.4.2 Starting materials	44
2.4.3 Physical measurements	44
2.4.4 Computational calculation	45
2.4.5 Synthetic procedure	45
<b>2.5 Crystallographic Data</b>	47
<b>2.6 References</b>	48

<b>Chapter 3: Boraamidinate Bridged [3.3](2,6) Pyridinophanes and a Calix Like Trimer</b>	51
<b>3.1 Introduction</b>	52
<b>3.2 Results and Discussion</b>	56
<b>3.3 Conclusions</b>	76
<b>3.4 Experimental Section</b>	77
3.4.1 General procedure	77
3.4.2 Starting materials	77
3.4.3 Physical measurements	77
3.4.4 Synthetic procedure	78
<b>3.5 Crystallographic Data</b>	83
<b>3.6 References</b>	85
<b>Chapter 4: Assembly of Pyridinophanes, Molecular bowls and Cryptands Containing Aluminum</b>	89
<b>4.1 Introduction</b>	90
<b>4.2 Results and Discussion</b>	92
<b>4.3 Conclusions</b>	108
<b>4.4 Experimental Section</b>	109
4.4.1 General procedure	109
4.4.2 Starting materials	109
4.4.3 Physical measurements	110
4.4.4 Synthetic procedure	110
<b>4.5 Crystallographic Data</b>	116
<b>4.6 References</b>	118
<b>List of Publications</b>	121

## Abbreviations

$\delta$	Chemical shift
$\tilde{\nu}$	Wave number
AP	Atmospheric solids analysis probe
Ar	Aryl
av	Average
br	Broad
bap	Bis(trimethylsilyl)-N,N'-2,6-diaminopyridine
bat	2,4-N,N'-bisilylateddiamino-6-R-triazine
BDMT	2,4-N,N'-bisilylateddiamino-6-methyl-triazine
BDPT	Bis(trimethylsilyl)-N,N'-2,4-diamino-6-Phenyl-triazine
C	Celsius
calcd.	Calculated
d	Doublet
dd	Doublet of doublet
Dipp	Diisopropylphenyl
decomp.	Decomposition
EI	Electron impact ionization
eq.	Equivalents
eV	Electron volt
g	Grams
Hz	Hertz
h	Hours
<i>i</i> Pr	<i>iso</i> -propyl
IR	Infrared
<i>J</i>	Coupling constant
K	Kelvin
L	Ligand
M	Metal
m	Multiplet
<i>m/z</i>	Mass/Charge

Mp.	Melting point
$M^+$	Molecular ion
Me	Methyl
Mes	Mesityl
min.	Minutes
MS	Mass spectrometry, mass spectra
NMR	Nuclear magnetic resonance
ppm	Parts per million
$P_2N_2$	Cyclophosphazane
Py	Pyridine
q	Quartet
R, R', R''	Organic substituents
s	Singlet
Sept	Septet
$SiMe_3$	Trimethylsilyl
t	Triplet
THF	Tetrahydrofuran
TMS	Tetramethylsilane
Tbp	Trigonal bipyramidal
TTT	tris(trimethylsilyl)-N,N',N''-2,4,6-triamino-triazine
$V$	Volume
W	Weak
Z	Number of molecules in the unit cell

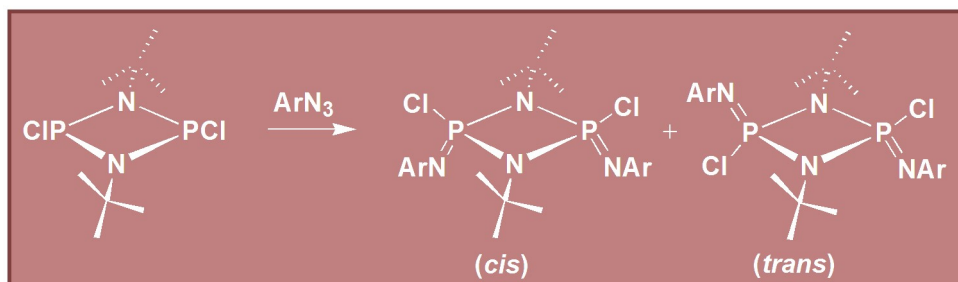




# Mechanistic Insights and Product Isomeric Distribution in the Stepwise Functionalization of Cyclic-(P<sup>III</sup>)<sub>2</sub>N<sub>2</sub> into Cyclic-(P<sup>V</sup>)<sub>2</sub>N<sub>2</sub> Products

## Chapter 1

**Abstract:** This chapter demonstrates the stepwise functionalization of the chlorophosph(III)azane, [ClP( $\mu$ -N*t*Bu)]<sub>2</sub> with organic azides and chalcogens (S and Se). The progress of these reactions were followed by in-situ <sup>31</sup>P{<sup>1</sup>H} NMR revealing that conversion of basic (P<sup>III</sup>)<sub>2</sub>N<sub>2</sub> framework leading to (P<sup>V</sup>)<sub>2</sub>N<sub>2</sub> proceed via mixed valent (P<sup>III</sup>/P<sup>V</sup>)N<sub>2</sub> intermediates. These (P<sup>III</sup>/P<sup>V</sup>)N<sub>2</sub> intermediate species provide details of the reaction pathway and distribution of cis and trans isomers of (P<sup>V</sup>)<sub>2</sub>N<sub>2</sub> products and can be isolated under controlled conditions. The work also demonstrates the expedient formation of (P<sup>V</sup>)<sub>2</sub>N<sub>2</sub> products at elevated temperature under neat condition without significantly affecting the yields and relative distribution of cis and trans isomers. All new compounds reported here are potential building blocks for the assembly of inorganic macrocycles and polymers and have been characterized thoroughly using different techniques including single crystal X-ray diffraction, multinuclear NMR, IR and high resolution mass spectrometry.



D. Bawari; B. Prashanth; K. Jaiswal; A. R. Choudhury; S. Singh

*Eur. J. Inorg. Chem.* 2017, 4123–4130.

## 1.1 Introduction

Cyclodiphosph(III)azanes,  $[XP(\mu-NR)]_2$  are saturated, four-membered rings containing alternate phosphorus(III) and nitrogen centers. Despite the fact that  $[ClP(\mu-NPh)]_2$  was the first synthesized cyclodiphosphazane in 1894 by Michaelis and Schroeter from  $PCl_3$  and aniline hydrochloride,<sup>[1]</sup> the chemistry of cyclodiphosphazanes remained unexplored for about next 100 years until the next attempts were made to synthesize few metal complexes in the 1980s. The X-ray structure of the first cyclodiphosphazane,  $[ClP(\mu-NtBu)]_2$  was determined in 1971 and reactivity, structural and spectroscopic aspects were carried out after 1990s.<sup>[1]</sup> The presence of lone pair as donor arms on phosphorus atoms allows cyclodiphosphazane,  $[XP(\mu-NtBu)]_2$  to coordinate with various metals easily while the functional group (X) attached to phosphorus atoms can react with other molecules to give nice architectural structures. Last two decades have witnessed an enormous use of phosphazanes in various areas. In this direction, Balakrishna and coworkers have effectively used the donor property of phosphorus atoms in  $[XP(\mu-NtBu)]_2$  to isolate various metal based macrocycles, homo- or heteropolynuclear complexes, and coordination polymers (Figure 1.1).<sup>[1]</sup>

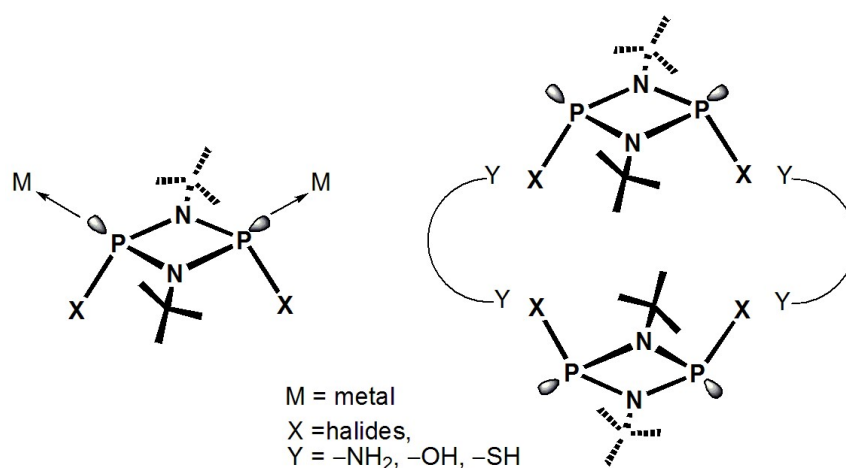


**Figure 1.1** Phosphorus lone pairs as donor arms *Vs* the reactivity of functional group on phosphorus atoms.

On the other hand Kumaraswamy and coworkers have synthesized some inorganic-organic hybrid macrocycles using  $[\text{CIP}(\mu\text{-N}t\text{Bu})]_2$  as building blocks against organic linkers. The effective use of cyclodiphosphazane units as building blocks to prepare inorganic analogues of crown ethers by Wright and coworkers has also drew the attention of scientific community. Besides the macrocyclic area, the use of cyclodiphosphazane in organic reactions by Balakrishna and Kumaraswamy and their coworkers have also created significant interest.<sup>[1]</sup>

The creative use of cyclodiphosphazane as neutral and anionic building blocks with main group or transition metal can be seen in variety of macrocycles, cages and clusters. Although, the chemistry of cyclodiphosphazane have shown continuous progress in last two decades but still it could not achieve the level what it deserves. Looking at the enormous scope that this field has to offer, in terms of new inorganic macrocycles and polymers containing  $\text{P}_2\text{N}_2$  framework, the discovery of new building blocks and a detailed understanding of their formation is therefore warranted. Our interest in this area arose to extend the less explored mixed valent,  $(\text{P}^{\text{III/V}})\text{N}_2$  and  $(\text{P}^{\text{V}})_2\text{N}_2$  building blocks of cyclodiphosphazane for the syntheses of macrocycles and polymers. The creative assembly of these building blocks have allowed the isolation of several intriguing P/N inorganic macrocycles classified as following types: (i) with all  $(\text{P}^{\text{III}})$  atoms,  $[\{\text{P}(\mu\text{-N}t\text{Bu})\}_2(\mu\text{-Y})]_4$  ( $\text{Y} = \text{NH}$  or  $\text{O}$ );<sup>[2]</sup> (ii) with alternating  $(\text{P}^{\text{III}})/(\text{P}^{\text{V}})$  atoms,  $[\text{E}=\text{P}(\mu\text{-N}t\text{Bu})_2\text{P}(\mu\text{-E})]_6$  ( $\text{E} = \text{S}, \text{Se}$ );<sup>[3]</sup> (iii) with all  $(\text{P}^{\text{V}})$  atoms,  $[(t\text{BuN}=\text{P}(\mu\text{-N}t\text{Bu})_2(\mu\text{-E}_2))]_3$  ( $\text{E} = \text{S}, \text{Se}$ )<sup>[4]</sup> and (iv) more recently the macrocycles with unique alternating  $(\text{P}^{\text{III}})_2(\text{P}^{\text{V}})_2$  backbone  $[\{(=\text{S})\text{P}(\mu\text{-N}t\text{Bu})_2\text{P}(=\text{S})\}\{\mu\text{-}(\text{S}-\text{P}(\mu\text{-N}t\text{Bu})_2\text{P}-\text{S})\}]_3$ , all  $(\text{P}^{\text{V}})$  atoms  $[(=\text{S})\text{P}(\mu\text{-N}t\text{Bu})_2\text{P}(=\text{S})(\mu\text{-S})]_6$ ,  $[\{(=\text{S})\text{P}(\mu\text{-N}t\text{Bu})\}_2(\mu\text{-Se})]_6$  and  $[\{(=\text{S})\text{P}(\mu\text{-N}t\text{Bu})\}_2(\mu\text{-Se-Se})]_3$ .<sup>[5]</sup> The metallamacrocycles and polymeric/multi-metallic assemblies involving transition metals<sup>[1c]</sup> ( $\text{Cu}, \text{Ag}, \text{Au}, \text{Rh}, \text{Ru}, \text{Ir}, \text{Pd}, \text{Pt}, \text{Zn}$ ) as well as complexes of main group elements<sup>[1g]</sup> have also been matter of interest.

Another motivation, which encouraged us to explore cyclodiphosphazanes based building blocks, is the feasibility to explore the syntheses of anionic and radicaloid species based on  $P_2N_2$  scaffolds and to explore their coordination behaviour (Figure 1.2). In this endeavour, Schulz and co-workers have used  $P_2N_2$  systems (and similar hybrid framework) to design a variety of high temperature stable radicaloid by treating chlorocyclodiphosphazanes with mild reducing agents (but containing bulky substituents) and their use in the activation of small molecules.<sup>[6]</sup> Chivers and co-workers employed dichalcogenido based ( $P^V$ ) species,  $[tBuN(H)\{(E)P(\mu-NtBu)\}]_2$  ( $E = S, Se, Te$ ) to generate double deprotonated  $P_2N_2$ -supported ambidentate dianions,  $[tBuN\{(E)P^V(\mu-NtBu)\}]_2^{2-}$  to produce “top-bottom” or “side-on” chelation resulting into spirocyclic, macrocyclic, and ladder complexes of main group elements and transition metals (Ag, Au, Hg, Rh).<sup>[7]</sup> Recently, we have reported the synthesis of a stable biradicaloid dianion,  $trans-[(S-)PCl(\mu-NtBu)]_2^{2-}$  isolated as its disodium salt (*vide infra*).<sup>[3]</sup> The aesthetic use of  $P_2N_2$  units has also been employed for many cages and clusters with main group elements.<sup>[1]</sup>

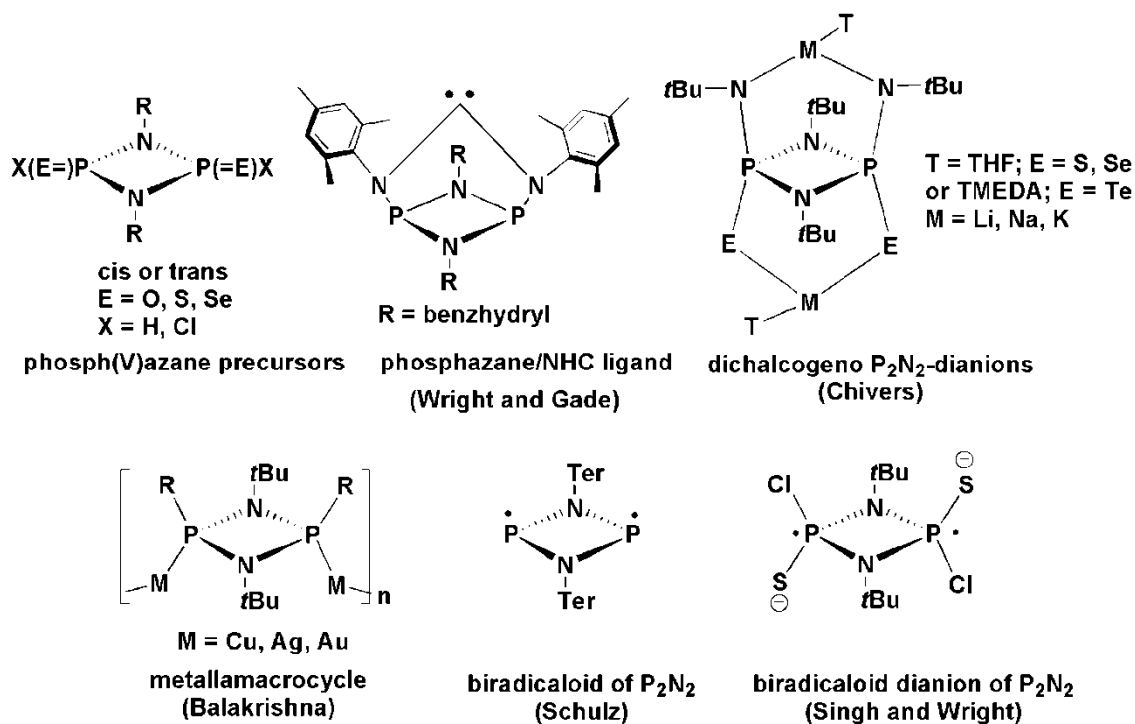


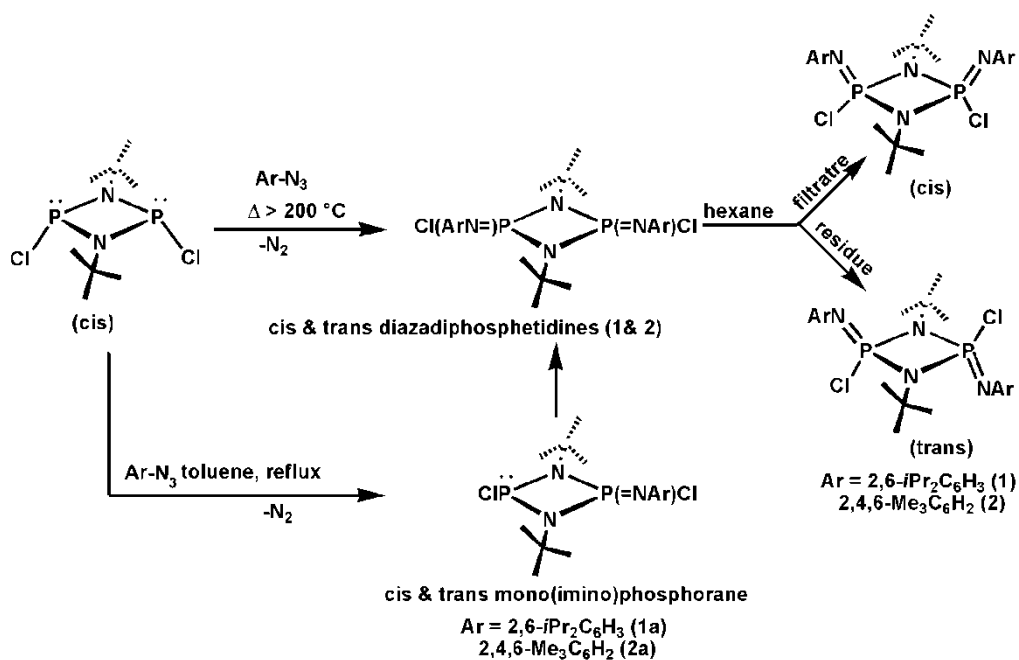
**Figure 1.2** Some interesting species based on  $P_2N_2$  unit.

The literature survey reveals the availability of a plethora of  $(P^{III})_2N_2$  and  $(P^V)_2N_2$  cyclic compounds<sup>[8]</sup> however, the systematic study on the synthesis of cyclic  $(P^{III}/P^V)_2N_2$  species has not been undertaken. The inorganic macrocycles with alternating  $(P^{III}$  and  $P^V)$  centers<sup>[3]</sup> highlight the need for such mixed valent  $(P^{III}/P^V)$  species. Herein, we have investigated some synthetic routes to prepare  $(P^V)_2N_2$  based imides and chalcogenido systems that proceed through the stable mixed valent  $(P^{III}/P^V)$  compounds.

## 1.2 Results and Discussion

**Synthesis of [(2,6-*i*Pr<sub>2</sub>C<sub>6</sub>H<sub>3</sub>N=)CIP( $\mu$ -N*t*Bu)]<sub>2</sub> (1), [(2,4,6-Me<sub>3</sub>C<sub>6</sub>H<sub>2</sub>N=)CIP( $\mu$ -N*t*Bu)]<sub>2</sub> (2), [(Se=)CIP( $\mu$ -N*t*Bu)<sub>2</sub>PCl] (3), [(S=)CIP( $\mu$ -N*t*Bu)<sub>2</sub>PCl] (4), [(S=)CIP( $\mu$ -N*t*Bu)]<sub>2</sub> (5) and [(S=)CIP( $\mu$ -N*t*Bu)(=Se)]<sub>2</sub> (6)**

It is well known from literature that sulfur and selenium can oxidize  $(P^{III})$  centres to afford  $(P^V)=E$  moieties (where E = S, Se).<sup>[8]</sup> In a similar way, easily available organic azides could also be desired oxidants and give easy access to  $(P^V)$  derivatives. Aromatic azides are interesting oxidant and oxidation of [*t*BuNHP( $\mu$ -N*t*Bu)]<sub>2</sub> with PhN<sub>3</sub> and *p*-MeC<sub>6</sub>H<sub>4</sub>N<sub>3</sub> was known.<sup>[9]</sup> However, prior to this work the only report to access diazadiphosphetidines, [(2,4,6-*t*Bu<sub>3</sub>C<sub>6</sub>H<sub>2</sub>N=)CIP( $\mu$ -NR)]<sub>2</sub> (R = *t*Bu, Et<sub>3</sub>C, 1-adamantyl) was based on the thermal decomposition of tetrazaphospholes and lacked structural characterization of the products.<sup>[10]</sup> The present work is the first report on the reactions of cis-[CIP( $\mu$ -N*t*Bu)]<sub>2</sub> with organic azides 2,6-*i*Pr<sub>2</sub>C<sub>6</sub>H<sub>3</sub>N<sub>3</sub><sup>[11a]</sup> and 2,4,6-Me<sub>3</sub>C<sub>6</sub>H<sub>2</sub>N<sub>3</sub>.<sup>[11b]</sup> The reactions were performed in the presence of a solvent (toluene) as well as under neat conditions that easily afforded [(ArN=)CIP( $\mu$ -N*t*Bu)]<sub>2</sub> derivatives **1** (Ar = 2,6-*i*Pr<sub>2</sub>C<sub>6</sub>H<sub>3</sub>) and **2** (Ar = 2,4,6-Me<sub>3</sub>C<sub>6</sub>H<sub>2</sub>) (Scheme 1.1). The in-situ <sup>31</sup>P{<sup>1</sup>H} NMR monitoring of the reaction in refluxing toluene between [CIP( $\mu$ -N*t*Bu)]<sub>2</sub> and 2,6-*i*Pr<sub>2</sub>C<sub>6</sub>H<sub>3</sub>N<sub>3</sub> attributed to the formation of a mixture of cis (−66.47 ppm) and trans



**Scheme 1.1** Syntheses of [(ArN=)CIP(μ-N*t*Bu)]<sub>2</sub> (**1**) and (**2**) via intermediates **1a** and **2a** under neat conditions and in the presence of toluene.

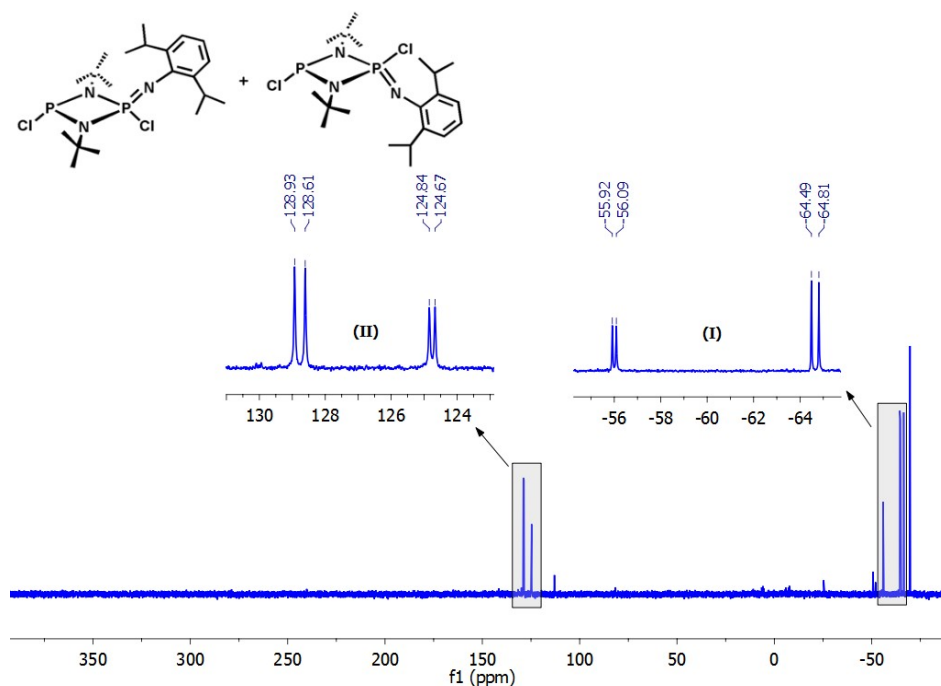


**Figure 1.3** *In-situ* <sup>31</sup>P{<sup>1</sup>H} NMR spectrum to show the formation of cis and trans [(2,6-*i*Pr<sub>2</sub>C<sub>6</sub>H<sub>3</sub>N=)CIP(μ-N*t*Bu)<sub>2</sub>PCl] (**1a**) (intermediate mono(imino)phosphorane) detected during the synthesis of [(2,6-*i*Pr<sub>2</sub>C<sub>6</sub>H<sub>3</sub>N=)CIP(μ-N*t*Bu)]<sub>2</sub> (**1**). Insets **(I)** and **(II)** show expansion for the spectral region of mono(imino)phosphorane intermediates of **1**.

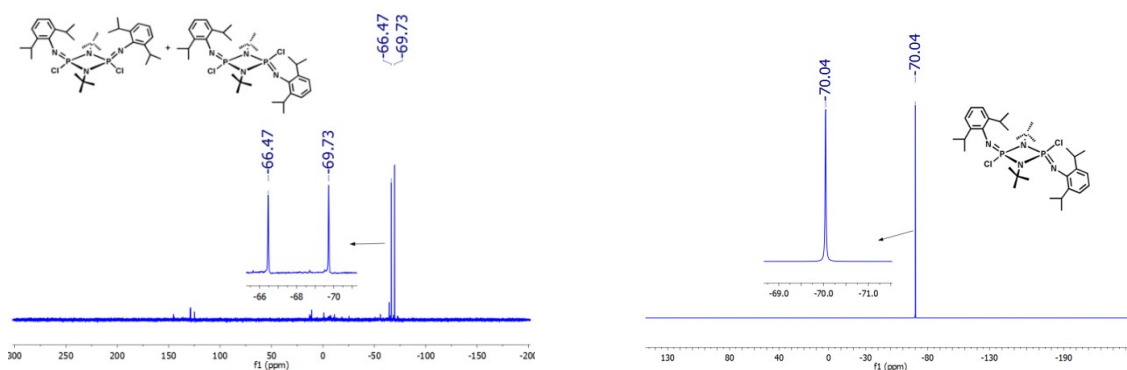


**Figure 1.4** *In-situ*  $^{31}\text{P}\{^1\text{H}\}$  NMR spectrum (left image) after completion of the reaction showing cis and trans  $[(2,6\text{-}i\text{Pr}_2\text{C}_6\text{H}_3\text{N}=\text{CIP}(\mu\text{-N}t\text{Bu}))_2]$  isomers (**1**). Inset shows expansion for the spectral region for cis and trans isomeric products of **1**.  $^{31}\text{P}\{^1\text{H}\}$  NMR spectrum (right side image) of trans  $[(2,6\text{-}i\text{Pr}_2\text{C}_6\text{H}_3\text{N}=\text{CIP}(\mu\text{-N}t\text{Bu}))_2]$  (**1**).

( $-69.73$  ppm) isomers of **1** in approximately 1:1.3 ratio. Similarly, mesityl azide gave the cis ( $-65.36$  ppm) and trans ( $-64.73$  ppm) isomers of **2** in approximately 1:2 ratio. As depicted in Scheme 1.1, the reaction progresses *via* the cis- and trans-mono(imino)phosphorane intermediates **1a** and **2a** (in approx. 1:1.5 ratio) followed by subsequent conversion of the remaining ( $\text{P}^{\text{III}}$ ) centre to ( $\text{P}^{\text{V}}$ ) producing cis, trans diazadiphosphetidine products **1** and **2** (Scheme 1.1). The presence of two sets of doublets (due to  $^2J_{\text{P-P}}$ ) in the *in-situ*  $^{31}\text{P}\{^1\text{H}\}$  NMR spectrum ( $\text{C}_6\text{D}_6$ ) confirmed the cis and trans products with ( $\text{P}^{\text{III}}/\text{P}^{\text{V}}$ ) centers. The doublets for the major isomer appeared at  $128.77$  ppm (for  $\text{P}^{\text{III}}$ ) and  $-64.65$  ppm (for  $\text{P}^{\text{V}}$ ) with  $^2J_{\text{P-P}} = 52$  Hz) and the minor isomer gave signals at  $124.75$  ppm (for  $\text{P}^{\text{III}}$ ) and  $-56.00$  ppm (for  $\text{P}^{\text{V}}$ ) with  $^2J_{\text{P-P}} = 28$  Hz as expected for **1a** leading to **1**. The HRMS spectrum of **1a** showed signal at  $m/z = 449.1670$  (calcd.  $449.1683$ ,  $[\text{M}]^+$ ). Similarly, the  $^{31}\text{P}\{^1\text{H}\}$  signals for the mono(imino)phosphorane intermediate **2a** leading to **2** were observed as two sets of doublets; for minor isomer ( $129.13$  and  $-59.18$  ppm with  $^2J_{\text{P-P}} = 50$  Hz) and for major isomer ( $125.48$  and  $-52.02$  ppm with  $^2J_{\text{P-P}} = 29$  Hz). The HRMS spectrum of **2a** showed signal at  $m/z = 407.1200$  (calcd.  $407.1214$ ,  $[\text{M}]^+$ ). Upon complete conversion

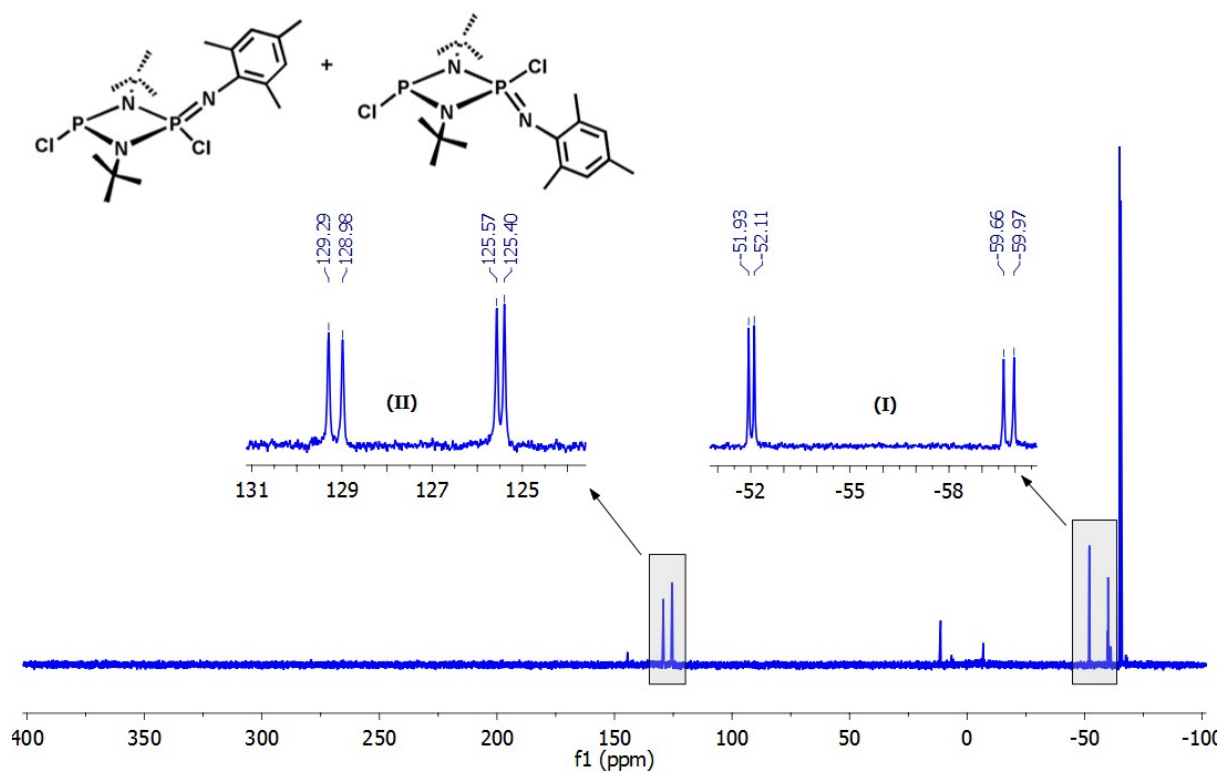


**Figure 1.5** *In-situ*  $^{31}\text{P}\{^1\text{H}\}$  NMR spectrum to show the formation of cis and trans  $[(2,4,6\text{-Me}_3\text{C}_6\text{H}_2\text{N}=\text{CIP}(\mu\text{-N}t\text{Bu})_2\text{PCl})]$  (intermediate mono(imino)phosphorane) (**2a**) detected during the synthesis of  $[(2,4,6\text{-Me}_3\text{C}_6\text{H}_2\text{N}=\text{CIP}(\mu\text{-N}t\text{Bu})_2)]_2$  (**2**). Insets (I) and (II) show expansion for the spectral region of mono(imino)phosphorane intermediates of **2**.

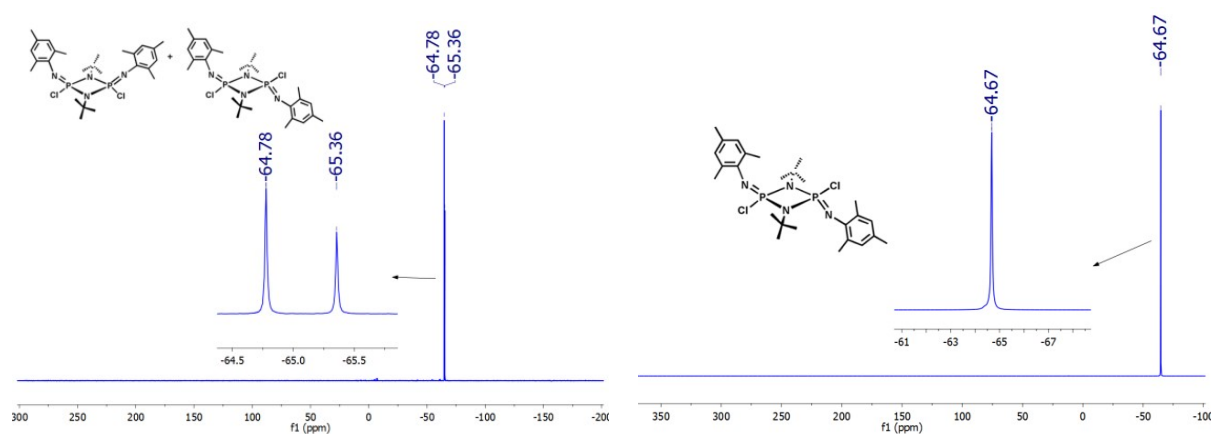


**Figure 1.6** *In-situ*  $^{31}\text{P}\{^1\text{H}\}$  NMR spectrum (left image) of cis and trans  $[(2,4,6\text{-Me}_3\text{C}_6\text{H}_2\text{N}=\text{CIP}(\mu\text{-N}t\text{Bu})_2)]_2$  isomers (**2**). Inset shows expansion for the spectral region for cis and trans isomeric products of **2**.  $^{31}\text{P}\{^1\text{H}\}$  NMR spectrum (right side image) of trans  $[(2,4,6\text{-Me}_3\text{C}_6\text{H}_2\text{N}=\text{CIP}(\mu\text{-N}t\text{Bu})_2)]_2$  (**2**).

of **1a** to **1** and **2a** to **2** their HRMS spectra gave signals at  $m/z$  624.3027 (calcd. 624.3044,  $[M]^+$ ) and  $m/z$  = 540.2028 (calcd. 540.2105,  $[M]^+$ ), respectively.

Neat reactions of  $[\text{ClP}(\mu\text{-N}t\text{Bu})_2]_2$  with 2,6-*i*Pr<sub>2</sub>C<sub>6</sub>H<sub>3</sub>N<sub>3</sub> and 2,4,6-Me<sub>3</sub>C<sub>6</sub>H<sub>2</sub>N<sub>3</sub> when performed at elevated temperature gave similar ratio (*vide supra*) of the geometric isomers of **1** and **2** (Scheme 1.1). The isomers in these mixtures could be partially separated by extracting the cis isomer (along with the traces of trans isomer and decomposed azide) with hexane whereas the residue contained the trans isomer in pure form (by  $^{31}\text{P}\{^1\text{H}\}$  NMR in CDCl<sub>3</sub>) which gave crystals of the trans-[(2,6-*i*Pr<sub>2</sub>C<sub>6</sub>H<sub>3</sub>N=)ClP(μ-N*t*Bu)]<sub>2</sub> (**1**) (−70.04 ppm) and trans-[(2,4,6-Me<sub>3</sub>C<sub>6</sub>H<sub>2</sub>N=)ClP(μ-N*t*Bu)]<sub>2</sub> (**2**) (−64.67 ppm).

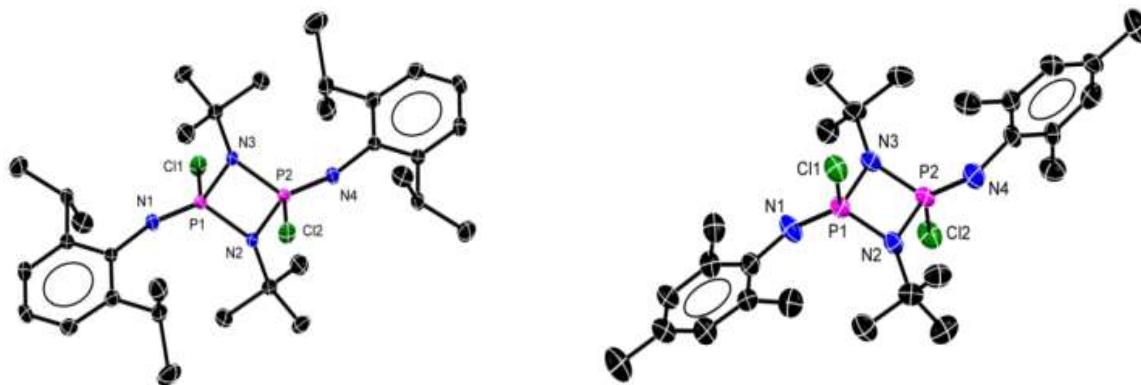
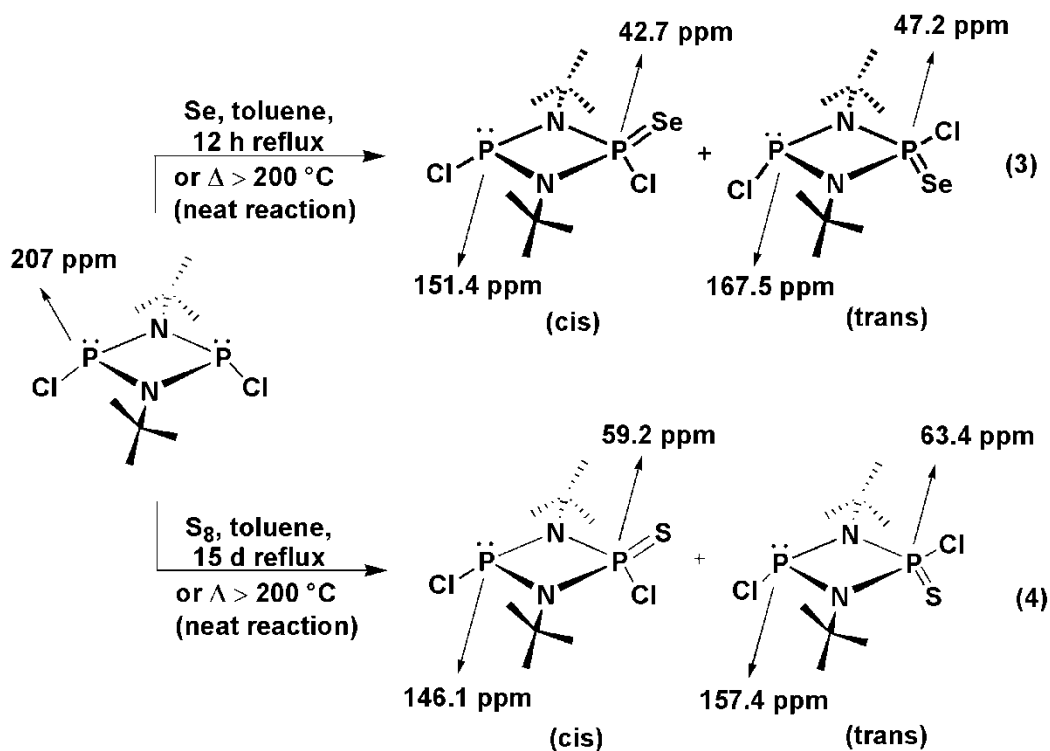


**Figure 1.7** Solid state structures of trans-[(2,6-*i*Pr<sub>2</sub>C<sub>6</sub>H<sub>3</sub>N=)ClP(μ-N*t*Bu)]<sub>2</sub> (**1**) (left) and trans-[(2,4,6-Me<sub>3</sub>C<sub>6</sub>H<sub>2</sub>N=)ClP(μ-N*t*Bu)]<sub>2</sub> (**2**) (right). All hydrogen atoms have been omitted for clarity; ellipsoids set at 50% probability. Selected bond lengths [Å] and bond angles [°] for **1**: P-Cl 2.051(9), P-N 1.678(8), P=N 1.486(4); N-P-N 84.94(4), P-N-P 95.06(3), N=P-Cl 113.13(8), N-P-Cl 124.93(2) and **2**: P-Cl 2.058(3), P-N 1.668(5), P=N 1.470(3); N-P-N 84.76(2), P-N-P 96.00(7), N=P-Cl 112.77(3), N-P-Cl 105.11(4).

As discussed above, the trans isomers of **1** and **2** can be purified by washing the impurities along with the cis isomer therefore, the crystallization of trans **1** and **2** was feasible. However, attempts to grow crystals of cis isomers of **1** and **2** remained unsuccessful. The single crystals of trans **1** and **2** were grown from toluene and crystallize in triclinic and monoclinic crystal

system with  $P\bar{1}$  and  $P2_1/c$  space group respectively (Table 1.1). The four membered phosph(V)azane rings for both the compounds (Figure 1.7) are almost planar as reported for their precursor,  $[\text{ClP}(\mu\text{-N}t\text{Bu})_2]_2$ .<sup>[13]</sup> The  $t\text{Bu}$  groups at the N atoms are staggered whereas the 2,6- $i\text{Pr}_2\text{C}_6\text{H}_3$  and 2,4,6- $\text{Me}_3\text{C}_6\text{H}_2$  substituents at the exo-cyclic N atoms are in the same plane. The angles between the mean planes  $\text{P}_2\text{N}_2\cdots 2,6\text{-}i\text{Pr}_2\text{C}_6\text{H}_3$  were found to be  $69.85^\circ$  in **1** and  $85.17^\circ$  for  $\text{P}_2\text{N}_2\cdots 2,4,6\text{-Me}_3\text{C}_6\text{H}_2$  planes in **2**.

Due to interesting applications of derivatives like  $[\text{ClP}(=\text{E})(\mu\text{-NR})_2]$  ( $\text{E} = \text{S}, \text{Se}$ )<sup>[3-5]</sup> and very limited information available on the mixed valent ( $\text{P}^{\text{III}}/\text{P}^{\text{V}}$ ) species,  $[(\text{E}=\text{O})\text{ClP}(\mu\text{-N}t\text{Bu})_2\text{PCl}]$ , oxidation of  $[\text{ClP}(\mu\text{-N}t\text{Bu})_2]$  with S and Se were performed and monitored by the in-situ  $^{31}\text{P}\{^1\text{H}\}$  NMR with the aim to see if the synthesis of monochalcogenido ( $\text{P}^{\text{III}}/\text{P}^{\text{V}}$ ) species can be controlled and are intermediate compounds towards  $[\text{ClP}(=\text{E})(\mu\text{-NR})_2]$  ( $\text{E} = \text{S}, \text{Se}$ ). It has been observed that the reaction of  $[\text{ClP}(\mu\text{-N}t\text{Bu})_2]$  with an equivalent amount of selenium in boiling toluene takes ca. 12 h to afford the monoselenide,  $[(\text{Se}=\text{O})\text{ClP}(\mu\text{-N}t\text{Bu})_2\text{PCl}]$  (**3**) whereas the same reaction with sulfur took ca. 15 days to afford monosulfide  $[(\text{S}=\text{O})\text{ClP}(\mu\text{-N}t\text{Bu})_2\text{PCl}]$  (**4**) (Scheme 1.2). The cis- and trans- $[(\text{E}=\text{O})\text{ClP}(\mu\text{-N}t\text{Bu})_2\text{PCl}]$  isomers of the ( $\text{P}^{\text{III}}/\text{P}^{\text{V}}$ ) products formed in these reactions. In the  $^{31}\text{P}\{^1\text{H}\}$  NMR spectrum, the major cis- $[(\text{Se}=\text{O})\text{ClP}(\mu\text{-N}t\text{Bu})_2\text{PCl}]$  (**3**) showed a set of two doublets containing their characteristic  $^{77}\text{Se}$  satellites and were attributed to AMX system. The doublet at 151.45 ppm corresponds to ( $\text{P}^{\text{III}}\text{-Cl}$ ) (with  $^2J_{\text{P-P}} = 15$  Hz and  $^{77}\text{Se}$  satellites from  $[(^{77}\text{Se}=\text{O})\text{ClP}(\mu\text{-N}t\text{Bu})_2\text{PCl}]$ ,  $^3J_{31\text{P-}^{77}\text{Se}} = 1350$  Hz) and another doublet at 42.77 ppm for ( $\text{P}^{\text{V}}(=\text{Se})\text{Cl}$ ) (with  $^2J_{\text{P-P}} = 15$  Hz and  $^{77}\text{Se}$  satellites from  $[(^{77}\text{Se}=\text{O})\text{ClP}(\mu\text{-N}t\text{Bu})_2\text{PCl}]$ ,  $^1J_{31\text{P-}^{77}\text{Se}} = 950$  Hz). The minor trans component showed doublets at 167.58 (for  $\text{P}^{\text{III}}\text{-Cl}$ ) and 47.20 ppm (for  $\text{P}^{\text{V}}(=\text{Se})\text{Cl}$ ) (with  $^2J_{\text{P-P}} = 36$  Hz). The  $^{77}\text{Se}$  NMR of **3** showed expected doublets for cis and trans isomers respectively, at 232.0 ( $^1J_{77\text{Se-}31\text{P}} \approx 953$  Hz) and 345.0 ppm ( $^1J_{77\text{Se-}31\text{P}} \approx 945$  Hz).



**Scheme 1.2** Syntheses of mixed valent ( $\text{P}^{\text{III}}/\text{P}^{\text{V}}$ ) monochalcogenido derivatives  $[(\text{Se}=\text{CIP}(\mu\text{-NtBu})_2\text{P}]\text{Cl}$  (**3**) and  $[(\text{S}=\text{CIP}(\mu\text{-NtBu})_2\text{P}]\text{Cl}$  (**4**), their  $^{31}\text{P}\{^1\text{H}\}$  chemical shifts are also shown.

The neat reaction for the synthesis of **3** and **4** by heating  $[\text{ClP}(\mu\text{-NtBu})_2]_2$  with elemental selenium or sulfur<sup>[8b]</sup> above  $200\text{ }^\circ\text{C}$  gave the same proportions of the cis and trans isomers as was obtained from boiling toluene (*vide supra*) (Scheme 1.2). The IR spectra of compounds **3** and **4** showed the  $\text{P}=\text{Se}$  and  $\text{P}=\text{S}$  stretch at  $557$  and  $915\text{ cm}^{-1}$ , respectively. The HRMS spectrum of **3** and **4** respectively, showed the base peak at  $m/z = 354.9549$  (calcd.  $354.9561$ ) for  $[\text{M}+\text{H}]^+$  and  $307.0132$  (calcd.  $307.0121$ ) for  $[\text{M}+\text{H}]^+$ .

The mixture of cis and trans isomers for **3** and **4** were low melting solids ( $40\text{-}44\text{ }^\circ\text{C}$ ) which when stored at room temperature gave crystals of the cis isomer suitable for X-ray diffraction (Figure 1.8) however crystals of the minor trans isomer could not be obtained even after repeated efforts. Both **3** and **4** are isostructural with same unit cell parameters and crystallized in the orthorhombic systems with *Pbca* space group (with  $Z' = 1$ ). The crystal structure of the cis isomer for **3** and **4** showed that the four membered phosphazane rings are

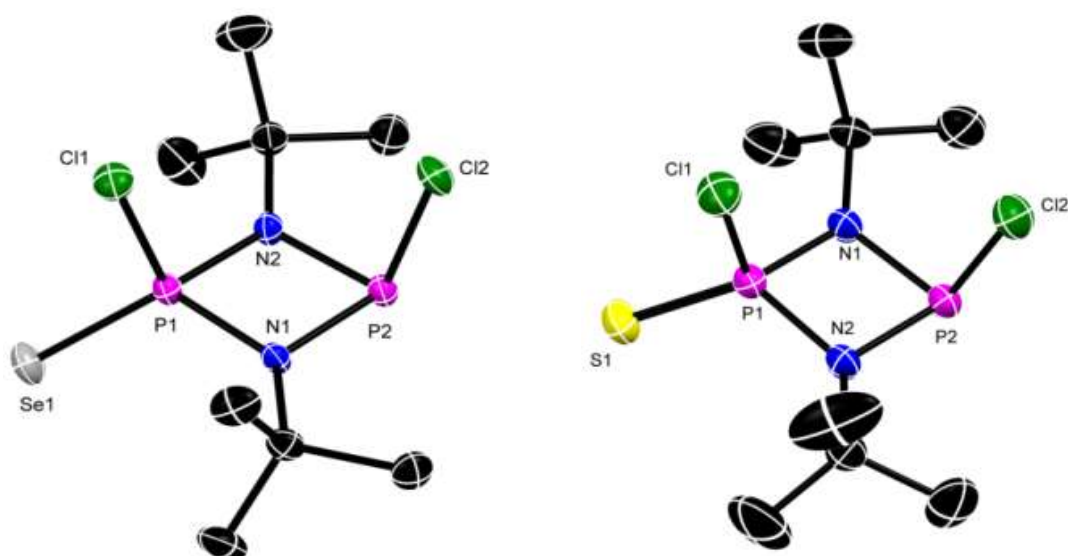


**Figure 1.8** Solid state structures of [(Se=)CIP( $\mu$ -N*t*Bu)<sub>2</sub>PCl] (**3**) (left) and [(S=)CIP( $\mu$ -N*t*Bu)<sub>2</sub>PCl] (**4**) (right). All hydrogen atoms have been omitted for clarity; ellipsoids set at 50% probability. Selected bond lengths [Å] and bond angles [°] for **3**: P(III)-Cl 2.136(3), P(V)-Cl 2.041(3), P=Se 2.057(9), P1-N1 1.671(1), P2-N2 1.711(2); P-N-P 96.73(2), N-P(III)-Cl 102.83(2), N-P(V)-Cl 107.28(2), N-P-N 84.94(4) and **4**: P(III)-Cl 2.135(2), P(V)-Cl 2.043(2), P=S 1.909(6), P1-N1 1.671(3), P2-N2 1.712(2); P-N-P 96.74(3), N-P(III)-Cl 102.90(2), N-P(V)-Cl 107.86(5), N-P-N 84.46(5).

almost planar where P<sup>III</sup>-Cl bond lengths are slightly longer (2.1395(6) Å (**3**) and 2.1352(19) Å (**4**)) than that of P<sup>V</sup>-Cl bond lengths (2.0460(6) Å (**3**) and 2.043(2) Å (**4**)). Further, the N-P<sup>III</sup>-Cl bond angles (102.89(5)° (**3**) and 102.86(12)° (**4**)) are slightly narrower than N-P<sup>V</sup>-Cl (107.27(5)° and 108.08(6)° (**3**) and 106.91(11)° and 107.84(10)° (**4**)). Compound **3** forms 2D network where two P<sub>2</sub>N<sub>2</sub> units are connected to each other due to weak *t*Bu-H $\cdots$ Se-P(V) (3.018 Å) interaction and the network grows in one direction whereas (Figure 1.9), the second direction grows due to the weak interaction *t*Bu-H $\cdots$ Cl-P(III) (2.908 Å) between two P<sub>2</sub>N<sub>2</sub> units in one direction (Figure 1.10). Unlike, **3** compound **4** shows three dimensional network formation due to the weak interaction between *t*Bu-H $\cdots$ Cl-P(III) (2.837 Å and 2.890 Å) and *t*Bu-H $\cdots$ S-P(V) (2.944 Å).

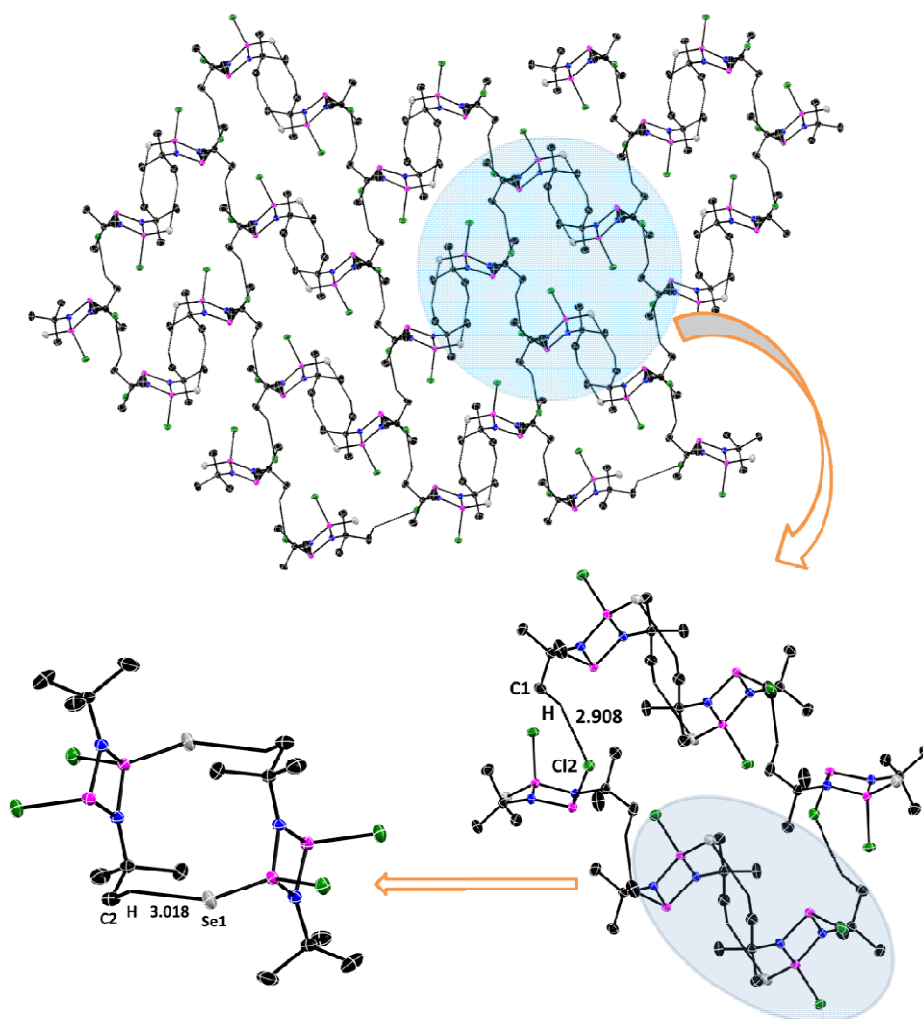


**Figure 1.9** Formation of two dimensional network due to the weak  $t\text{Bu-H}\cdots\text{Se-P(V)}$  (3.018 Å) interaction between two units of **3**.

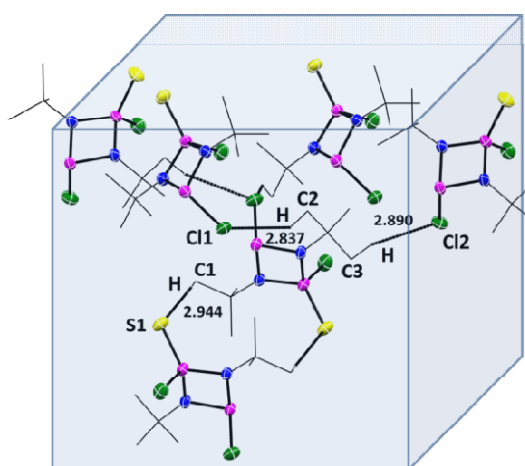
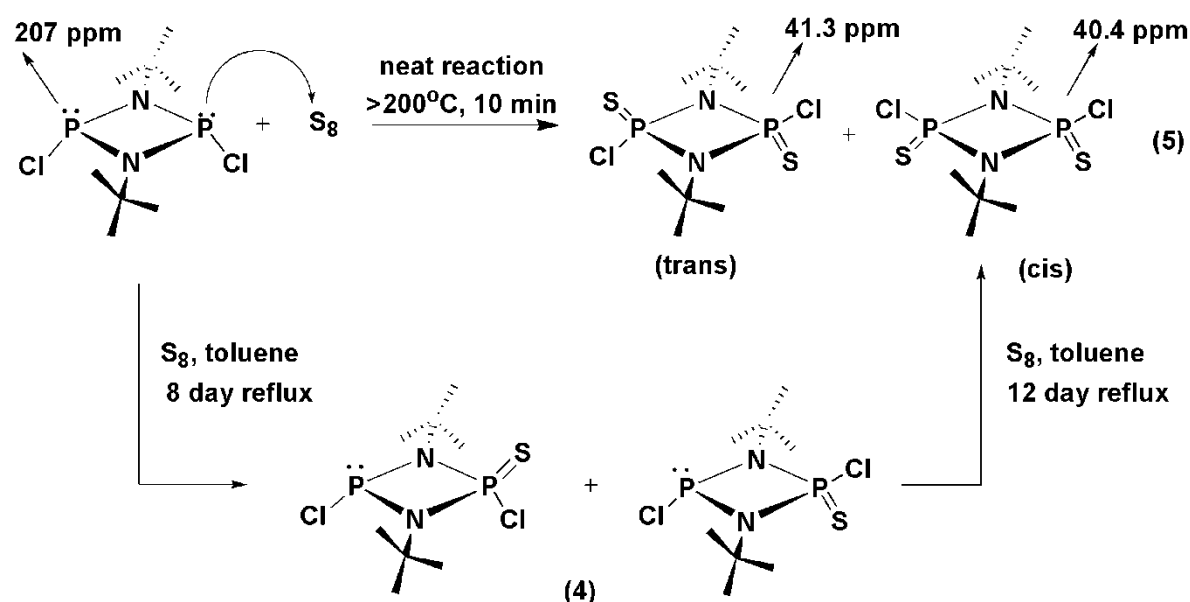


**Figure 1.10** Formation of three dimensional network due to the weak  $t\text{Bu-H}\cdots\text{Cl-P(III)}$  (2.837 Å and 2.890 Å) and  $t\text{Bu-H}\cdots\text{S-P(V)}$  (2.944 Å) interaction among different units of **3**.

It can be noted from the previous data that oxidation of both phosphorus atoms in  $[\text{ClP}(\mu\text{-NR})_2]$  with chalcogens steadily provides more proportion of cis over the trans isomer of  $[\text{ClP}(=\text{E})(\mu\text{-NR})_2]$  on going down in the group 16 (cis:trans = O,<sup>[12]</sup> Se<sup>[3b]</sup> are 0:1, 3:1, respectively). Therefore, oxidation of  $[\text{ClP}(\mu\text{-N}t\text{Bu})_2]$  with sulfur was expected to yield cis- and trans- $[(\text{S}=\text{ClP}(\mu\text{-N}t\text{Bu})_2)]$  (**5**) with a proportion of cis isomer higher than oxygen but lower than that of selenium compound. With this anticipation, a reaction of  $[\text{ClP}(\mu\text{-N}t\text{Bu})_2]$  with 2 equivalents of sulfur in boiling toluene was monitored by in-situ  $^{31}\text{P}\{^1\text{H}\}$  NMR of the reaction mixture (Scheme 1.3 and Figure 1.11).



**Scheme 1.3** Reaction pathway for the synthesis of  $(\text{P}^{\text{V}})$  disulfide derivative  $[(\text{S}=\text{ClP}(\mu\text{-N}t\text{Bu})_2)]$  (**5**).

As detailed in Scheme 1.3 and Figure 1.11, in 8 days the cis- and trans- $[(\text{S}=\text{ClP}(\mu\text{-N}t\text{Bu})_2\text{PCl})]$  (**4**) can be detected as intermediates of this reaction with the traces of disulfide  $[(\text{S}=\text{ClP}(\mu\text{-N}t\text{Bu})_2)]$  (**5**) and unreacted  $[\text{ClP}(\mu\text{-N}t\text{Bu})_2]$ . As compared to the exclusive synthesis of the monosulfide **4** (15 days reflux, Scheme 1.2), perhaps the use of more amount of sulfur here enhanced the reaction rate (8 days reflux, Scheme 1.3). Further, in about 12 days all of the  $[\text{ClP}(\mu\text{-N}t\text{Bu})_2]$  was consumed and the major amount of product constituted the cis- and trans- $[(\text{S}=\text{ClP}(\mu\text{-N}t\text{Bu})_2\text{PCl})]$  (**4**). The continued reflux for 20 days led to the

formation of cis and trans disulfide  $[(S=)ClP(\mu-NtBu)_2]$  (**5**). The signals at 40.47 and 41.32 ppm were assigned respectively to the cis and trans isomers of **5** in approximately 1.5:1 ratio. The  $^1H$  NMR spectrum of the isolated product showed a signal at 1.49 ppm for the cis isomer and the trans isomer was seen as a hump to this signal (1.48 ppm). HRMS spectrum of the product showed the base peak at  $m/z = 338.9830$  (calcd 338.9842) for  $[M+H]^+$ . A neat reaction to prepare cis- and trans- $[(S=)ClP(\mu-NtBu)_2]$  (**5**), when both the reactants were heated above 200 °C, completes in 10 minutes without significantly affecting the proportion of cis and trans products (Scheme 1.3).

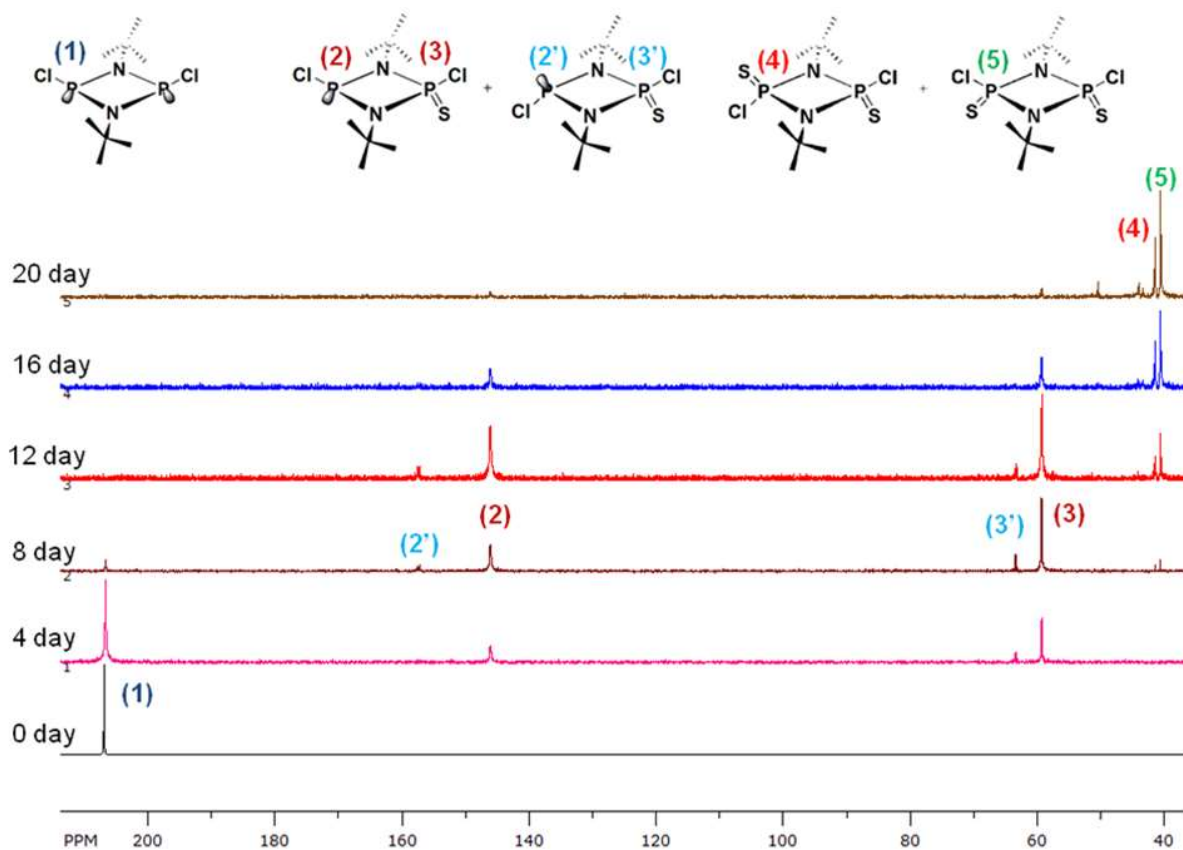
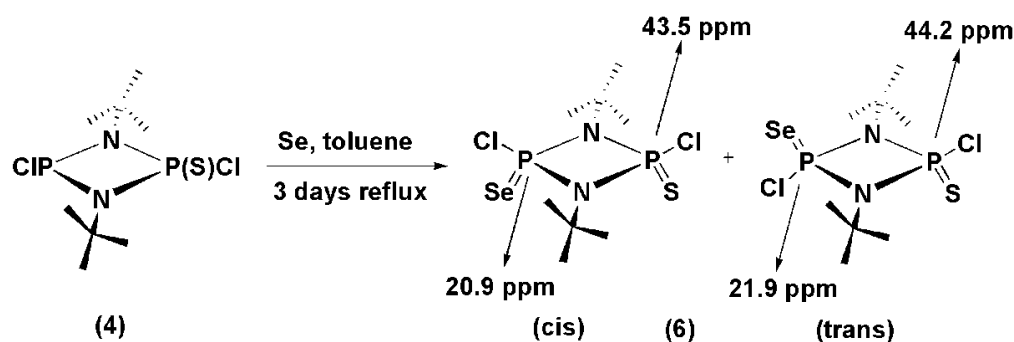


**Figure 1.11** In-situ  $^{31}P\{^1H\}$  NMR spectra (in  $C_6D_6$ ) to monitor progress of the reaction in the formation of cis- and trans- $[(S=)ClP(\mu-NtBu)_2]$  (**5**) in toluene.

Encouraged by the reactions discussed so far, we became interested to know the feasibility for the synthesis of a hetero chalcogenido compound of the type  $[(S=)ClP(\mu-NtBu)_2PCl(=Se)]$ . This could be achieved via two different routes: (i) reaction of  $[(S=)ClP(\mu-$

$NtBu)_2PCl]$  (**4**) with 1 equivalent of Se and (ii) reaction of  $[(Se=)CIP(\mu-NtBu)_2PCl]$  (**3**) with 1 equivalent of S. We attempted both the reactions under neat conditions above 200 °C that gave cis- and trans- $[(S=)CIP(\mu-NtBu)_2PCl(=Se)]$  (**6**) along with considerable scrambling of chalcogens to afford a mixture of homo-dichalcogenido  $[(E=)CIP(\mu-NtBu)_2]$  (E = Se or S). Most probably, the high reaction temperature promoted scrambling of S and Se in these cases. Therefore, reaction of  $[(S=)CIP(\mu-NtBu)_2PCl]$  (**4**) with 1 equivalent of selenium in boiling toluene was performed that took ca. 3 days to afford the mixture of cis- and trans- $[(S=)CIP(\mu-NtBu)_2PCl(=Se)]$  (**6**) in approximately 5:1 ratio (Scheme 1.4) with negligible scrambling.



**Scheme 1.4** Preparation of hetero-chalcogenido  $[(S=)CIP(\mu-NtBu)_2PCl(=Se)]$  (**6**).

The  $^{31}P\{^1H\}$  NMR spectrum of **6** can be attributed to AX spin system that showed two sets of doublets in the  $P^V$  region only, one at 44.15 and 21.93 ppm (with  $^2J_{P-P} = 11$  Hz) for the minor trans isomer and another at 43.45 and 20.85 ppm (with  $^2J_{P-P} = 6$  Hz) for the major cis isomer (together with  $^{77}Se$  satellites attributed to the  $AA'X$  isotopomer containing one  $^{77}Se$  atom ( $I = \frac{1}{2}$ , 7.6%,  $[(S=)CIP(\mu-NtBu)_2PCl(=^{77}Se)]$ ,  $^1J_{31P-77Se} = 946$  Hz). The  $^{77}Se$  NMR spectrum of **6** showed a doublet of doublet at 169.07 ppm ( $^1J_{77Se-31P} = 986$  Hz,  $^3J_{77Se-31P} = 15$  Hz) for the cis isomer similarly a doublet of doublet at 206.85 ppm ( $^1J_{77Se-31P} = 987$  Hz,  $^3J_{77Se-31P} = 18$  Hz) was observed for the trans isomer. Similarly the IR spectrum of compound **6** showed the characteristic P=S stretch at  $908\text{ cm}^{-1}$  whereas the P=Se stretch was observed at  $573\text{ cm}^{-1}$ .

The HRMS spectrum of **6** showed the base peak at  $m/z = 385.9193$  (calcd 385.9203) that was also the molecular ion signal  $[M]^+$ .

### 1.3 Conclusions

In conclusion, we have demonstrated a stepwise conversion of chlorophosph(III)azane,  $[ClP(\mu-NtBu)]_2$  into  $[ClP(=E)(\mu-NtBu)]_2$  ( $E = NAr, S, Se$ ). The in-situ  $^{31}P\{^1H\}$  NMR investigations reveal sequential conversion of the cyclic four membered  $(P^{III})_2N_2$  into mixed valent cis and trans  $(P^{III}/P^V)N_2$  derivatives,  $[ClP(=E)(\mu-NtBu)_2PCl]$  in the first step and cis and trans  $(P^V)_2N_2$  products,  $[ClP(=E)(\mu-NtBu)_2PCl]$  in the final step. These conversions can be performed using refluxing toluene or under neat conditions at elevated temperatures. These  $(P^{III}/P^V)$  and all  $(P^V)$  compounds would serve as useful precursors to synthesize new reactive species based on four-membered phosphazane systems as well as inorganic macrocycles with new connectivity.

### 1.4 Experimental Section

#### 1.4.1 General procedure

All syntheses were carried out under inert atmosphere of dry nitrogen in oven dried glassware using standard Schlenk techniques or a glove box where  $O_2$  and  $H_2O$  levels were maintained usually below 0.1 ppm. All the glassware was dried at 150 °C in an oven for at least 12 h and assembled hot and cooled *in vacuo* prior to use. Solvents were purified by MBRAUN solvent purification system MB SPS-800. THF was dried over (Na/benzophenone ketyl) and distilled under nitrogen and degassed prior to use. For NMR,  $CDCl_3$  was dried over 4 Å molecular sieves whereas  $C_6D_6$  was dried over Na.

### 1.4.2 Starting materials

All chemicals were purchased from Sigma-Aldrich and used without further purification. The molecules 2,6-*i*Pr<sub>2</sub>C<sub>6</sub>H<sub>3</sub>N<sub>3</sub>,<sup>[11a]</sup> 2,4,6-Me<sub>3</sub>C<sub>6</sub>H<sub>2</sub>N<sub>3</sub>,<sup>[11b]</sup> [CIP(μ-*Nt*Bu)]<sub>2</sub><sup>[2a]</sup> were prepared using literature procedures. Syntheses of the monosulfide [(S=)CIP(μ-*Nt*Bu)<sub>2</sub>PCl] (**4**)<sup>[8b]</sup> and the disulfide [(S=)CIP(μ-*Nt*Bu)]<sub>2</sub> (**5**)<sup>[8n]</sup> under neat conditions are reported in the literature.

### 1.4.3 Physical measurements

IR spectra of the complexes were recorded in the range 4500–400 cm<sup>-1</sup> with a Perkin–Elmer Lambda 35-spectrophotometer. The <sup>1</sup>H, <sup>13</sup>C and <sup>31</sup>P{<sup>1</sup>H} NMR spectra were recorded with a Bruker 400 MHz spectrometer with TMS and H<sub>3</sub>PO<sub>4</sub> (85%) as external reference whereas, <sup>77</sup>Se was recorded with a JEOL JNM–ECS spectrometer at operating frequencies of 76.28 MHz with Me<sub>2</sub>Se as external reference; chemical shift values are reported in ppm. High-resolution mass spectrometry was performed with a Waters SYNAPT G2–S instrument.

Single crystal X-ray diffraction data of **1**, **2** and **3** were collected using a Rigaku XtaLAB mini diffractometer equipped with Mercury375M CCD detector. The data were collected with MoK<sub>α</sub> radiation (λ = 0.71073 Å) using omega scans. During the data collection, the detector distance was 49.9 mm (constant) and the detector was placed at 2θ = 29.85° (fixed) for all the data sets. The data sets were collected Crystal Clear suite<sup>[14a]</sup> and were processed using CrysAlisPro version 1.171.39.7f.<sup>[14b]</sup> Empirical absorption correction using spherical harmonics, implemented in SCALE3 ABSPACK scaling algorithm was done using CrysAlisPro 1.171.39.7f. Single crystal X-ray diffraction data of **4** was collected on a Bruker *AXS KAPPA APEX-II* CCD diffractometer with MoK<sub>α</sub> radiation using omega scans. Unit cell determination and refinement and data collection were done using the Bruker *APPEX-II* suite,<sup>[14c]</sup> data reduction and integration were performed using SAINT v8.34A (Bruker, 2013)<sup>[14d]</sup> and absorption corrections and scaling were done using SADABS-2014/5

(Bruker,2014/5)<sup>[14e]</sup>. All the crystal structures were solved through OLEX2<sup>[14f]</sup> package using XT<sup>[14g]</sup> and the structures were refined using XL.<sup>[14g]</sup> All non-hydrogen atoms were refined anisotropically and all the H atoms were geometrically fixed and refined using the riding model. The single crystals of trans **1** and **2** were grown from toluene and crystallize in triclinic (with  $P\bar{1}$  space group and  $Z' = 0.5$ ) and monoclinic system (with  $P2_1/c$  space group and  $Z' = 0.5$ ) respectively (Table 1.1). One of the two isopropyl groups in **1** was found to be disordered while one of the *t*Bu groups in **2** was found to be disordered. These disordered atoms were refined with appropriate use of PART, EADP and EXYZ commands. The N atoms connected to the mesityl groups were also found to be disordered in **2**.

#### 1.4.4 Synthetic procedures

**Synthesis of [(2,6-*i*Pr<sub>2</sub>C<sub>6</sub>H<sub>3</sub>N=)CIP( $\mu$ -N*t*Bu)]<sub>2</sub> (**1**):** A mixture of 2,6-*i*Pr<sub>2</sub>C<sub>6</sub>H<sub>3</sub>N<sub>3</sub> (0.73 g, 3.60 mmol) and [CIP( $\mu$ -N*t*Bu)]<sub>2</sub> (0.50 g, 1.80 mmol) in a Schlenk tube was heated gradually until the mixture started to boil and turned brownish (for ca 15 min). Subsequently, a brown solid was obtained at room temperature. This brown solid was washed with hexane (7 mL) to remove impurities that also dissolved the all of the cis isomer and portion of the trans product. The white residue thus obtained was confirmed as pure trans isomer which was crystallized from toluene at -10 °C. Yield (trans isomer): 0.28 g, 24.80 %.

**Alternative synthesis of 1:** The azide 2,6-*i*Pr<sub>2</sub>C<sub>6</sub>H<sub>3</sub>N<sub>3</sub> (1.48 g, 7.30 mmol) was added at room temperature to a solution of [CIP( $\mu$ -N*t*Bu)]<sub>2</sub> (1.0 g, 3.60 mmol) in toluene (30 mL). This mixture was refluxed for 72 h and followed by removal of all volatiles under vacuum. The residue obtained was washed with hexane (10 mL) to separate impurities that also dissolved the cis isomer. The pure trans isomer was obtained as a white solid. Yield (trans isomer): 0.70 g, 31.00 %. Mp: 297-300 °C. IR ( $\tilde{\nu}$  cm<sup>-1</sup>, Nujol): 3050, 2965, 2869, 1550, 1462, 1365, 1254, 1192, 1135, 1077, 934, 908, 796, 748, 648, 558, 473. <sup>1</sup>H NMR (400 MHz, CDCl<sub>3</sub>):  $\delta$  = 7.10 (d, 4H, <sup>3</sup>J<sub>H-H</sub> = 7.6 Hz, Ar), 6.98 (t, 2H, <sup>3</sup>J<sub>H-H</sub> = 7.2 Hz, Ar), 3.54 (sept, 4H, CH(CH<sub>3</sub>)<sub>2</sub>, <sup>3</sup>J<sub>H-H</sub> =

6.8 Hz), 1.47 (s, 18H, C(CH<sub>3</sub>)<sub>3</sub>), 1.23 (d, 24H, CH(CH<sub>3</sub>)<sub>2</sub>). <sup>13</sup>C NMR (100 MHz, CDCl<sub>3</sub>): δ = 142.05, 123.05, 122.24, 57.22 (t, <sup>2</sup>J<sub>C-P</sub> = 2.0 Hz, C(CH<sub>3</sub>)<sub>3</sub>), 29.77 (t, <sup>3</sup>J<sub>C-P</sub> = 6.0 Hz, C(CH<sub>3</sub>)<sub>3</sub>), 28.79, 27.93, 23.99. <sup>31</sup>P{<sup>1</sup>H} NMR (162 MHz, CDCl<sub>3</sub>): δ = -70.04. HRMS (AP<sup>+</sup>): *m/z* calcd for C<sub>32</sub>H<sub>52</sub>Cl<sub>2</sub>N<sub>4</sub>P<sub>2</sub>: (624.3044) [M]<sup>+</sup>; found: (624.3027).

**Synthesis of [(2,4,6-Me<sub>3</sub>C<sub>6</sub>H<sub>2</sub>N=)CIP(μ-N*t*Bu)]<sub>2</sub> (**2**):** Compound **2** was synthesized in a manner similar to **1**. The quantity of reactants taken were 2,4,6-Me<sub>3</sub>C<sub>6</sub>H<sub>2</sub>N<sub>3</sub> (0.58 g, 3.60 mmol) and [CIP(μ-N*t*Bu)]<sub>2</sub> (0.50 g, 1.80 mmol). Yield (trans isomer): 0.39 g, 40.10 %.

**Alternative synthesis of 2:** The reaction for the synthesis of **2** was analogous to that of **1** performed in toluene, the amount of reactants taken were 2,4,6-Me<sub>3</sub>C<sub>6</sub>H<sub>2</sub>N<sub>3</sub> (1.20 g, 7.30 mmol) and [CIP(μ-N*t*Bu)]<sub>2</sub> (1.00 g, 3.60 mmol). This synthesis completed in 12 h. Yield (trans isomer): 1.00 g, 52.60 %. Mp: 264-266 °C. IR (ν̃ cm<sup>-1</sup>, Nujol): 2975, 2938, 2808, 1561, 1396, 1397, 1370, 1257, 1192, 1073, 929, 902, 854, 820, 728, 660, 615, 578, 543, 499, 438. <sup>1</sup>H NMR (400 MHz, CDCl<sub>3</sub>): δ = 6.86 (s, 4H, Ar), 2.35 (s, 12H, *o*-CH<sub>3</sub>), 2.25 (s, 6H, *p*-CH<sub>3</sub>), 1.50 (s, 18H, C(CH<sub>3</sub>)<sub>3</sub>) ppm. <sup>13</sup>C NMR (100 MHz, CDCl<sub>3</sub>): δ = 137.03, 131.43, 130.88, 128.59, 57.33 (C(CH<sub>3</sub>)<sub>3</sub>), 29.96 (C(CH<sub>3</sub>)<sub>3</sub>), 20.80, 20.21 ppm. <sup>31</sup>P{<sup>1</sup>H} NMR (162 MHz, CDCl<sub>3</sub>): δ = -64.67 ppm. HRMS (AP<sup>+</sup>): *m/z* calcd for C<sub>26</sub>H<sub>40</sub>Cl<sub>2</sub>N<sub>4</sub>P<sub>2</sub>: (540.2105) [M]<sup>+</sup>; found: (540.2028).

**Synthesis of [(Se=)CIP(μ-N*t*Bu)<sub>2</sub>PCI] (**3**):** A mixture of [CIP(μ-N*t*Bu)]<sub>2</sub> (5.00 g, 18.20 mmol) and selenium powder (1.44 g, 18.20 mmol) was charged in a 100 mL Schlenk tube and heated for 10 min at 200 °C to produce a transparent liquid which solidified when brought to room temperature. This low melting solid was distilled under vacuum to obtain a 4:1 mixture of cis and trans isomers of **3** which was crystallized at -10 °C to get crystals suitable for single crystal X-ray diffraction. Yield: 4.80 g, 74.30 %.

**Alternative synthesis of 3:** A mixture of [CIP( $\mu$ -NtBu)]<sub>2</sub> (15.00 g, 54.50 mmol) and selenium powder (4.31 g, 54.50 mmol) in toluene (150 mL) was refluxed for 12 h under nitrogen. The solution obtained was evaporated to dryness giving a solid which after distillation under vacuum gave a 4:1 mixture of cis and trans isomers in sufficient purity for further analysis and reactions. Yield: 14.80 g, 76.49 %. Mp: 42-45 °C. IR ( $\tilde{\nu}$  cm<sup>-1</sup>, Nujol): 2975, 2934, 2873, 1462, 1397, 1370, 1251, 1196, 1046, 926, 895, 806, 673, 557, 523 ( $\nu_{\text{P=Se}}$ ), 427. <sup>1</sup>H NMR (400 MHz, CDCl<sub>3</sub>):  $\delta$  = 1.44 (C(CH<sub>3</sub>)<sub>3</sub>) ppm. <sup>13</sup>C NMR (100 MHz, CDCl<sub>3</sub>):  $\delta$  = cis: 57.31, 30.21 (t, <sup>3</sup>J<sub>C-P</sub> = 5.9 Hz, C(CH<sub>3</sub>)<sub>3</sub>); trans:  $\delta$  = 57.25, 29.96 (t, <sup>3</sup>J<sub>C-P</sub> = 5.7 Hz, C(CH<sub>3</sub>)<sub>3</sub>) ppm. <sup>31</sup>P{<sup>1</sup>H} NMR (162 MHz, CDCl<sub>3</sub>): cis:  $\delta$  = 151.45 (d, <sup>2</sup>J<sub>31P-31P</sub> = 15 Hz, with two satellite doublets arising from [(<sup>77</sup>Se=)CIP( $\mu$ -NtBu)<sub>2</sub>PCl], <sup>1</sup>J<sub>31P-77Se</sub> = 1350 Hz), 42.77 (d, <sup>2</sup>J<sub>31P-31P</sub> = 15 Hz, with two satellite doublets arising from [(<sup>77</sup>Se=)CIP( $\mu$ -NtBu)<sub>2</sub>PCl], <sup>3</sup>J<sub>31P-77Se</sub> = 950 Hz); trans:  $\delta$  = 167.55 (d, <sup>2</sup>J<sub>31P-31P</sub> = 36 Hz), 47.20 (d, <sup>2</sup>J<sub>31P-31P</sub> = 36 Hz) ppm; <sup>77</sup>Se NMR (76.28 MHz, CDCl<sub>3</sub>):  $\delta$  = 345.93 (d, <sup>1</sup>J<sub>77Se-31P</sub> = 945 Hz; trans isomer), 232.20 (d, <sup>1</sup>J<sub>77Se-31P</sub> = 953 Hz; cis isomer) ppm. HRMS (AP<sup>+</sup>): *m/z* calcd for C<sub>8</sub>H<sub>19</sub>Cl<sub>2</sub>N<sub>2</sub>P<sub>2</sub>Se: (354.9561) [M+H]<sup>+</sup>; found: (354.9549).

**Synthesis of [(S=)CIP( $\mu$ -NtBu)<sub>2</sub>PCl] (4):** A mixture of [CIP( $\mu$ -NtBu)]<sub>2</sub> (15.00 g, 54.50 mmol) and sulfur powder (1.75 g, 54.70 mmol) in toluene (150 mL) was refluxed for 15 days under nitrogen. The solution obtained was evaporated to dryness giving a solid which after distillation under vacuum gave a 5:1 mixture of cis and trans isomers in sufficient purity for further analysis and reactions. Yield: 15.45 g, 92.30%. Mp: 40-42 °C. IR ( $\tilde{\nu}$  cm<sup>-1</sup>, Nujol): 2977, 2939, 2877, 1469, 1373, 1262, 1200, 1054, 915 ( $\nu_{\text{P=S}}$ ), 804, 746, 696, 596, 531. HRMS-AP<sup>+</sup> (*m/z*) = obs: 307.0132, cal: 307.0121 [M+H]<sup>+</sup>. The synthesis of **4** under neat conditions and its spectroscopic data are available in the literature.<sup>[8b]</sup>

**Synthesis of [(S=)CIP( $\mu$ -NtBu)]<sub>2</sub> (5):** Toluene (100 mL) was added to a mixture of [CIP( $\mu$ -NtBu)]<sub>2</sub> (2.50 g, 9.10 mmol) and sulfur (0.61 g, 19.00 mmol). This solution was refluxed

(completion of reaction was monitored by *in-situ*  $^{31}\text{P}\{^1\text{H}\}$  NMR, that takes ca. 20 days). After evaporation of all volatiles under *vacuum* a light yellow solid was obtained which on extraction with hexane afforded a mixture of *cis* and *trans* isomers (1.5:1 ratio based on  $^{31}\text{P}\{^1\text{H}\}$  NMR) in sufficient purity for further analysis and reactions. Yield: 2.56 g, 83.00 %. Mp: 102 °C. IR ( $\tilde{\nu}$   $\text{cm}^{-1}$ , Nujol): 2923, 2857, 1461, 1399, 1371, 1246, 1184, 1055, 911 ( $\nu_{\text{P}=\text{S}}$ ), 833, 782, 696, 599, 525, 474  $\text{cm}^{-1}$ .  $^1\text{H}$  NMR (400 MHz,  $\text{d}_8$ -toluene):  $\delta$  = 1.49 (t,  $^4J_{\text{H-P}} = 0.7$  Hz,  $\text{C}(\text{CH}_3)_3$ , (*cis*)), 1.48 (t,  $^4J_{\text{H-P}} = 0.7$  Hz,  $\text{C}(\text{CH}_3)_3$ , (*trans*)) ppm.  $^{13}\text{C}$  NMR (100 MHz,  $\text{d}_8$ -toluene):  $\delta$  = *trans*: 60.59 (s,  $\text{C}(\text{CH}_3)_3$ ), 29.74 (t,  $^3J_{\text{C-P}} = 5.1$  Hz,  $\text{C}(\text{CH}_3)_3$ ); *cis*: 60.39 (s,  $\text{C}(\text{CH}_3)_3$ ), 29.60 (t,  $^3J_{\text{C-P}} = 5$  Hz,  $\text{C}(\text{CH}_3)_3$ ) ppm.  $^{31}\text{P}\{^1\text{H}\}$  NMR (162 MHz,  $\text{d}_8$ -toluene):  $\delta$  = 41.32 (*trans*), 40.47 (*cis*) ppm. HRMS ( $\text{AP}^+$ ):  $m/z$  calcd for  $\text{C}_8\text{H}_{19}\text{Cl}_2\text{N}_2\text{P}_2\text{S}$ : (338.9842)  $[\text{M}+\text{H}]^+$ ; found: (338.9830).

**Alternative synthesis of 5:** A mixture of  $[\text{ClP}(\mu\text{-N}t\text{Bu})_2]$  (5.00 g, 18.20 mmol) and sulfur (1.22 g, 38.00 mmol) was heated at 200 °C in a Schlenk tube under nitrogen for 10 min. The resulting light brown compound was cooled to room temperature and subsequently extracted with hexane (60 mL) and filtered. The filtrate was evaporated to dryness to afford **5**. Yield: 4.20 g, 68.10 %. The spectroscopic data and alternative synthesis of **5** are available in the literature.<sup>[8n]</sup>

**Synthesis of  $[(\text{S}=\text{CIP}(\mu\text{-N}t\text{Bu})_2\text{PCl}(\text{=Se}))]$  (**6**):** A mixture of  $[(\text{S}=\text{CIP}(\mu\text{-N}t\text{Bu})_2]$  (**4**) (0.50 g, 1.63 mmol) and selenium powder (0.13 g, 1.63 mmol) was refluxed in 40 mL toluene for 3 days under nitrogen. The solution was evaporated to dryness followed by extraction with hexane. The hexane extract was dried under vacuum giving approximately a 5:1 mixture of *cis* and *trans* isomers. The S and Se scrambling in this method was significantly less as compared to the neat reaction at elevated temperatures, thus only traces of **5** and the diselenide congener were detected in crude product. Yield: 0.57 g, 91.00%. Mp: 99-101 °C. IR ( $\tilde{\nu}$   $\text{cm}^{-1}$ , Nujol): 2973, 2931, 2873, 1465, 1396, 1369, 1300, 1254, 1192, 1050, 908 ( $\nu_{\text{P}=\text{S}}$ ),

819, 761, 685, 634, 619, 573 ( $\nu_{\text{P=Se}}$ ).  $^1\text{H}$  NMR (400 MHz,  $\text{CDCl}_3$ ):  $\delta = 1.73$  ( $\text{C}(\text{CH}_3)_3$ ).  $^{13}\text{C}$  NMR (100 MHz,  $\text{CDCl}_3$ ):  $\delta = \text{cis: } 60.96$  (s,  $\text{C}(\text{CH}_3)_3$ ),  $30.03$  (t,  $^3J_{\text{C-P}} = 5.1$  Hz,  $\text{C}(\text{CH}_3)_3$ );  $\text{trans: } \delta = 61.28$  (s,  $\text{C}(\text{CH}_3)_3$ ),  $30.20$  (t,  $^3J_{\text{C-P}} = 4.9$  Hz,  $\text{C}(\text{CH}_3)_3$ ) ppm.  $^{31}\text{P}\{^1\text{H}\}$  NMR (162 MHz,  $\text{CDCl}_3$ ):  $\text{trans: } \delta = 44.15$  (d,  $^2J_{31\text{P-31P}} = 11$  Hz),  $21.93$  (d,  $^2J_{31\text{P-31P}} = 11$  Hz);  $\text{cis: } \delta = 43.45$  (d,  $^2J_{31\text{P-31P}} = 6.5$  Hz),  $20.85$  (d,  $^2J_{31\text{P-31P}} = 6.5$  Hz, with two satellite doublets arising from  $[(\text{S=})\text{ClP}(\mu\text{-N}t\text{Bu})_2\text{PCl}(=^{77}\text{Se})]$  at  $23.64$  and  $17.80$ ,  $^1J_{31\text{P-}^{77}\text{Se}} \approx 946$  Hz) ppm.  $^{77}\text{Se}$  NMR (76.28 MHz,  $\text{CDCl}_3$ ):  $\delta = 169.07$  (dd,  $^1J_{77\text{Se-31P}} \approx 986$  Hz,  $^3J_{77\text{Se-31P}} \approx 15$  Hz; cis isomer),  $206.85$  (dd,  $^1J_{77\text{Se-31P}} \approx 987$  Hz,  $^3J_{77\text{Se-31P}} \approx 17.5$  Hz; trans isomer) ppm. HRMS ( $\text{AP}^+$ ):  $m/z$  calcd for  $\text{C}_8\text{H}_{19}\text{Cl}_2\text{N}_2\text{P}_2\text{SeS}$ : (385.9203)  $[\text{M}]^+$ ; found: (385.9193).

## 1.5 Crystallographic Data

**Table 1.5.1** Crystallographic data for compounds 1–4.

Compound <sup>[a]</sup>	1	2	3	4
Chemical formula	C <sub>32</sub> H <sub>52</sub> Cl <sub>2</sub> N <sub>4</sub> P <sub>2</sub>	C <sub>26</sub> H <sub>40</sub> Cl <sub>2</sub> N <sub>4</sub> P <sub>2</sub>	C <sub>8</sub> H <sub>18</sub> Cl <sub>2</sub> N <sub>2</sub> P <sub>2</sub> Se	C <sub>8</sub> H <sub>18</sub> Cl <sub>2</sub> N <sub>2</sub> P <sub>2</sub> S
Molar mass	625.61	541.46	354.04	307.14
Crystal system	Triclinic	Monoclinic	Orthorhombic	Orthorhombic
Space group	<i>P</i> $\bar{1}$	<i>P</i> 2 <sub>1</sub> / <i>c</i>	<i>P</i> bca	<i>P</i> bca
<i>T</i> [K]	298.0	100.0	100.0	100.0
<i>a</i> [Å]	9.4320(10)	7.9874(8)	16.7565(8)	16.72(2)
<i>b</i> [Å]	9.6044(9)	20.747(2)	10.2266(5)	10.185(13)
<i>c</i> [Å]	11.5985(8)	8.9832(9)	17.0679(8)	17.19(2)
$\alpha$ [°]	96.978(7)	90.0	90.0	90.0
$\beta$ [°]	103.926(8)	104.710(10)	90.0	90.0
$\gamma$ [°]	114.394(10)	90.0	90.0	90.0
<i>V</i> [Å <sup>3</sup> ]	899.30(16)	1439.9(3)	2924.8(2)	2928(6)
<i>Z</i>	1	2	8	8
<i>D</i> (calcd.) [g·cm <sup>-3</sup> ]	1.155	1.249	1.608	1.394
$\mu$ (Mo- <i>K</i> $\alpha$ ) [mm <sup>-1</sup> ]	0.295	0.358	3.126	0.779
Reflections collected	12368	20540	40102	27001
Independent reflections	6136	5224	5340	4957
Data/restraints/parameters	6136/0/192	5224/0/201	5340/0/142	4957/0/142
<i>R</i> <sub>1</sub> , <i>wR</i> <sub>2</sub> [ <i>I</i> > 2 $\sigma$ ( <i>I</i> )] <sup>[a]</sup>	0.0701, 0.1991	0.0748, 0.1569	0.0338, 0.0788	0.0571, 0.1305
<i>R</i> <sub>1</sub> , <i>wR</i> <sub>2</sub> (all data) <sup>[a]</sup>	0.0860, 0.2228	0.1472, 0.1970	0.0488, 0.0856	0.1027, 0.1513
GOF	1.042	1.022	1.069	1.002

[a]  $R_1 = \frac{\sum ||F_o| - |F_c||}{\sum |F_o|}$ .  $wR_2 = \frac{[\sum w(|F_o|^2 - |F_c|^2)|^2]}{\sum w|F_o|^2}]^{1/2}$

## 1.6 References

- [1] For reviews see: a) M. S. Balakrishna, *J. Organomet. Chem.* **2010**, *695*, 925-936; b) M. S. Balakrishna, D. J. Eisler and T. Chivers, *Chem. Soc. Rev.* **2007**, *36*, 650-664; c) M. S. Balakrishna, *Dalton Trans.* **2016**, *45*, 12252-12282; d) S. G. Calera and D. S. Wright, *Dalton Trans.* **2010**, *39*, 5055-5065; e) E. L. Doyle, L. Riera and D. S. Wright, *Eur. J. Inorg. Chem.* **2003**, 3279-3289 (and references therein); f) Y. X. Shi, R. Z. Liang, K. A.

- Martin, D. G. Star, J. Díaz, X. Y. Li, R. Ganguly and F. García, *Chem. Commun.* **2015**, *51*, 16468-16471; g) L. Stahl, *Coord. Chem. Rev.* **2000**, *210*, 203-250.
- [2] a) A. Bashall, E. L. Doyle, C. Tubb, S. J. Kidd, M. McPartlin, A. D. Woods and D. S. Wright, *Chem. Commun.* **2001**, *24*, 2542-2543; b) A. Bashall, A. D. Bond, E. L. Doyle, F. García, S. Kidd, G. T. Lawson, M. C. Parry, M. McPartlin, A. D. Woods and D. S. Wright, *Chem. Eur. J.* **2002**, *8*, 3377-3385; c) S. G. Calera, D. J. Eisler, J. M. Goodman, M. McPartlin, S. Singh and D. S. Wright, *Dalton Trans.* **2009**, *8*, 1293-1296.
- [3] a) D. Bawari, B. Prashanth, S. Ravi, K. R. Shamasundar, S. Singh and D. S. Wright, *Chem. Eur. J.* **2016**, *22*, 12027-12033; b) S. G. Calera, D. J. Eisler, J. V. Morey, M. McPartlin, S. Singh and D. S. Wright, *Angew. Chem. Int. Ed.* **2008**, *47*, 1111-1114.
- [4] A. Nordheider, T. Chivers, R. Thirumoorthi, I. Vargas-Baca and J. D. Woollins, *Chem. Commun.* **2012**, *48*, 6346-6348.
- [5] A. J. Plajer, R. García-Rodríguez, C. G. M. Benson, P. D. Matthews, A. D. Bond, S. Singh, L. H. Gade and D. S. Wright, *Angew. Chem. Int. Ed.* **2017**, *56*, 9087-9090.
- [6] a) A. Hinz, A. Schulz and A. Villinger, *Angew. Chem. Int. Ed.* **2016**, *55*, 12214-12218; b) A. Hinz, A. Schulz and A. Villinger, *Chem. Eur. J.* **2014**, *20*, 3913-3916; c) A. Hinz, R. Kuzora, U. Rosenthal, A. Schulz and A. Villinger, *Chem. Eur. J.* **2014**, *20*, 14659-14673; d) A. Hinz, A. Schulz and A. Villinger, *J. Am. Chem. Soc.* **2015**, *137*, 9953-9962; e) T. Beweries, R. Kuzora, U. Rosenthal, A. Schulz and A. Villinger, *Angew. Chem. Int. Ed.* **2011**, *50*, 8974-8978.
- [7] a) T. Chivers, M. Krahn, M. Parvez and G. Schatte, *Inorg. Chem.* **2001**, *40*, 2547-2553; b) T. Chivers, M. Krahn and M. Parvez, *Chem. Commun.* **2000**, *6*, 463-464; c) A. Nordheider, T. Chivers, R. Thirumoorthi, K. S. A. Arachchige, A. M. Z. Slawin, J. D. Woollins and I. V. Baca, *Dalton Trans.* **2013**, *42*, 3291-3294; d) T. Chivers and I.

Manners, *Inorganic Rings and Polymers of the p-Block Elements: From Fundamentals to Applications*; RSC Publishing: Cambridge, U.K. **2009**; e) A. Nordheider, K. Hüll, K. S. A. Arachchige, A. M. Z. Slawin, J. D. Woollins, R. Thirumoorthi and T. Chivers, *Dalton Trans.* **2015**, *44*, 5338-5346; f) A. Nordheider, K. S. A. Arachchige, A. M. Z. Slawin, J. D. Woollins and T. Chivers, *Dalton Trans.* **2015**, *44*, 8781-8783; g) A. Nordheider, K. Hüll, J. K. D. Prentis, K. S. A. Arachchige, A. M. Z. Slawin, J. D. Woollins and T. Chivers, *Inorg. Chem.* **2015**, *54*, 3043-3054.

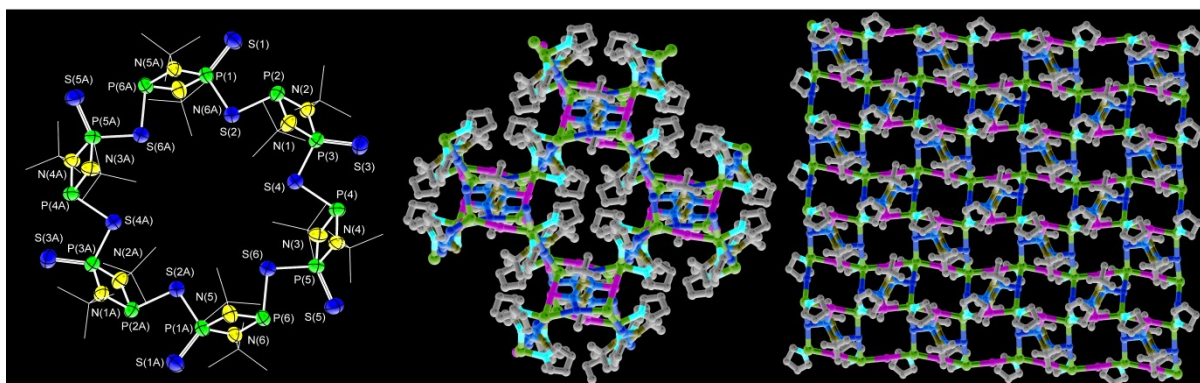
- [8] a) C. G. M. Benson, V. Vasilenko, R. García-Rodríguez, A. D. Bond, S. G. Calera, L. H. Gade and D. S. Wright, *Dalton Trans.* **2015**, *44*, 14242-14247; b) R. Jefferson, J. F. Nixon, T. M. Painter, R. Keat and L. Stobbs, *J. Chem. Soc., Dalton Trans.* **1973**, *13*, 1414-1419; c) G. Bulloch, R. Keat, D. S. Rycroft and D. G. Thompson, *Organic Magnetic Resonance*, **1979**, *12*, 708-712; d) T. G. Hill, R. C. Haltiwanger, M. L. Thompson, S. A. Katz and A. D. Norman, *Inorg. Chem.* **1994**, *33*, 1770-1777; e) T. Chivers, M. Krahn and M. Parvez, *Chem. Commun.* **2000**, 463-464; f) G. Bulloch and R. Keat, *J. Chem. Soc., Dalton Trans.* **1974**, *18*, 2010-2014; g) R. Keat and D. G. Thompson, *J. Chem. Soc., Dalton Trans.* **1980**, *6*, 928-936; h) C. D. Flint, R. A. Shaw, E. H. M. Ibrahim, B. C. Smith and C. P. Thakur, *J. Chem. Soc. (A)*, **1971**, 3513-3516; i) R. A. Shaw and D. A. Watkins, *J. Chem. Soc., Dalton Trans.* **1988**, *10*, 2591-2596; j) R. Keat, D. S. Rycroft and D. G. Thompson, *J. Chem. Soc., Dalton Trans.* **1979**, *7*, 1224-1230; k) C. D. Flint, E. H. M. Ibrahim, R. A. Shaw, B. C. Smith and C. P. Thakur, *Tetrahedron Lett.* **1969**, *36*, 3061-3062; l) H. Klare, S. Hanft, J. M. Neudörfl, N. E. Schlrer, A. Griesbeck and B. Goldfuss, *Chem. Eur. J.* **2014**, *20*, 11847-11855; m) D. C. Haagensohn, G. R. Lief, L. Stahl and R. J. Staples, *J. Organomet. Chem.* **2008**, *693*, 2748-2754; n) Y. X. Shi, R. Z. Liang, K. A. Martin, N. Weston, S. G. Calera, R. Ganguly, Y.

- Li, Y. Lu, A. J. M. Ribeiro, M. J. Ramos, P. A. Fernandes and F. García, *Inorg. Chem.* **2015**, *54*, 6423-6432.
- [9] a) G. R. Lief, C. J. Carrow and L. Stahl, *Organometallics* **2001**, *20*, 1629-1635; b) D. F. Moser, C. J. Carrow, L. Stahl and R. J. Staples, *J. Chem. Soc., Dalton Trans.* **2001**, 1246-1252.
- [10] E. Niecke, V. von der Gönna and M. Nieger, *Chem. Ber.* **1990**, *123*, 2329-2333.
- [11] a) L. P. Spencer, R. Altwer, D. Wei, L. Gelmini, J. Gauld and D. W. Stephan, *Organometallics* **2003**, *22*, 3841-3854; b) S. Murata, S. Abe and H. Tomioka, *J. Org. Chem.* **1997**, *62*, 3055-3061.
- [12] a) R. Keat, L. Manojlović-Muir and K. W. Muir, *Angew Chem. Int. Ed.* **1973**, *4*, 311-312; b) (j) L. M. Muir and K. W. Muir, *J. Chem. Soc. Dalton Trans.* **1974**, *22*, 2395-2398.
- [13] a) K. W. Muir and J. F. Nixo, *Chem. Commun.* **1971**, 1405-1406; b) K. W. Muir, *J. Chem. Soc., Dalton Trans.* **1975**, *3*, 259-62.
- [14] a) *CrystalClear 2.0*; Rigaku Corporation: Tokyo, Japan, 2013; b) CrysAlisPro, v1.171.39.7f Rigaku-Oxford Diffraction Oxfordshire, England, 2016; c) Bruker (2012). *Apex-III*. Bruker AXS Inc., Madison, Wisconsin, USA; d) Bruker (2013). *SAINT v8.34A*. Bruker AXS Inc., Madison, Wisconsin, USA; e) Bruker (2014/5). *Sadabs, 2014/5*. Bruker AXS Inc., Madison, Wisconsin, USA; f) O. V. Dolomanov, L. J. Bourhis, R. J. Gildea, J. A. K. Howard, H. Puschmann, *J. Appl. Crystallogr.* **2009**, *42*, 339-341; g) G. M. Sheldrick, *Acta Cryst. A* **2015**, *71*, 3-8.

## Different Pathways in the Wurtz Reduction of $[(S=)PCl(\mu-NtBu)]_2$ with Na

## Chapter 2

**Abstract:** Reduction of a mixture of isomeric cyclodiphosphazane, *cis*- and *trans*- $[(S=)CIP(\mu-NtBu)]_2$  (**5**) with metallic sodium, under reflux in toluene, proceeds *via* two different pathways. One Wurtz-type pathway involves the elimination of NaCl from **5** followed by *head-to-tail* cyclization of the intermediate anion to give the hexameric macrocycle,  $[(\mu-S)P(\mu-NtBu)_2P(=S)]_6$  (**7**). The other pathway involves reduction of the P=S bonds of *trans*- $[(S=)CIP(\mu-NtBu)]_2$  (**5**) to generate a colourless singlet biradicaloid dianion *trans*- $[S-P(Cl)(\mu-NtBu)]_2^{2-}$ , that is seen in the polymeric structures of three dimensional  $[\{(S-)CIP(\mu-NtBu)_2PCl(S)\}Na(Na \cdot THF_2)]_n$  (**8**) and two dimensional  $[\{(S-)CIP(\mu-NtBu)_2PCl(S)\}(Na \cdot THF_2)]_n$  (**9**). The electronic structure of the dianion core of **8** and **9** as P-centred biradicaloid was supported by computational studies on  $[S-P(Cl)(\mu-NMe)]_2^{2-}$ .



D. Bawari; B. Prashanth; S. Ravi; K. R. Shamasundar; S. Singh; D. S. Wright

*Chem. Eur. J.* 2016, 22, 12027–12033.

## 2.1 Introduction

The expansion of diverse families of organic macrocycles has far reaching impacts on vast area of molecular and supramolecular chemistry, extended across the fields of material and coordination chemistry, and the biological area. Since last few decades, significant developments in organic macrocycles domain have allowed proliferation of a variety of molecular structures. Simple examples of organic macrocycles which have been extensively investigated in numerous studies encompass a broad spectrum, such as: (a) crown ethers, (b) porphyrins, (c) cryptands, (d) cyclophanes, (e) calixarenes, and (f) cavitands (Figure 2.1).<sup>[1]</sup>

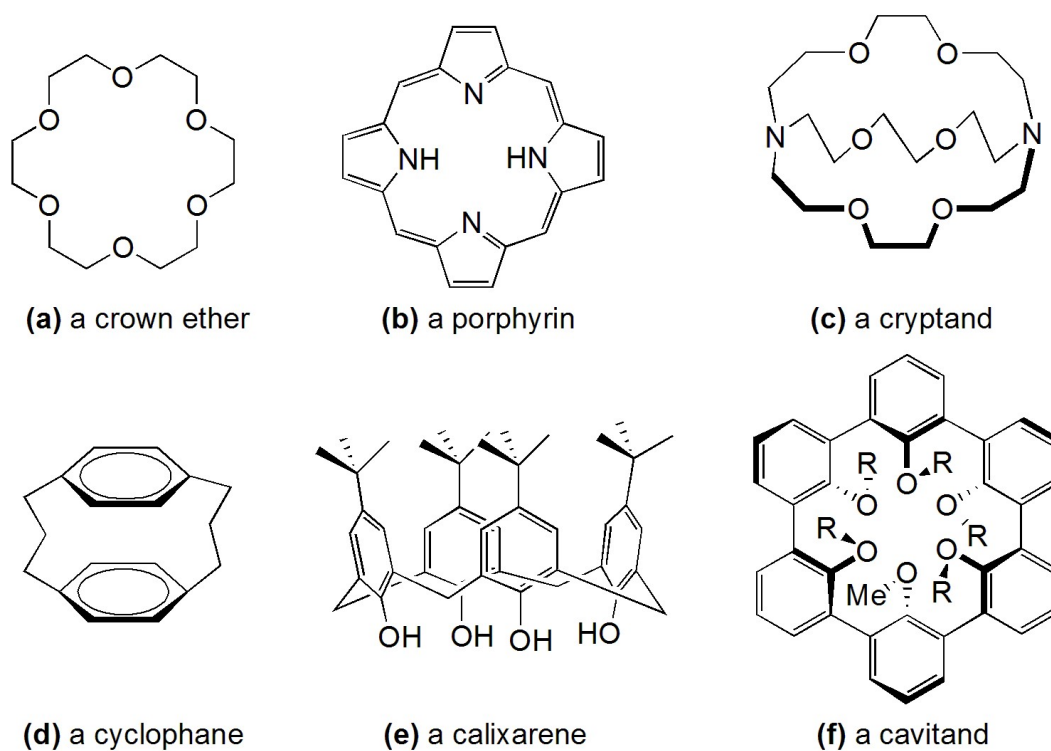


**Figure 2.1** Some common organic macrocycles.

While organic macrocycles based on carbon frameworks have been a central theme of modern chemistry, the functional inorganic macrocycles where the framework is constituted solely from inorganic elements are rare. There is therefore a lot more work required to match the well developed field of organic macromolecular chemistry.<sup>[1]</sup> The slow progress in the

area of inorganic macrocycles can be understood due to the following difficulties: (i) compared to carbon, the greater range of orbitals and hybridization states available with inorganic elements-lead to mismatch of orbital sizes and result in weaker bonds between elements from two different groups or period; (ii) variable oxidation states of inorganic elements-giving rise to the formation of multiple products with different oxidation state; (iii) hydrolytic instability-hampers the separation of multiproduct; (iv) lack of a general synthetic strategy for inorganic systems compared to the organic derivatives and (v) lower thermodynamic stability and polar nature of bonds to these elements, leading to kinetically labile and/or thermodynamically less robust arrangements.<sup>[1]</sup> Figure 2.2 shows some recent examples in the field of inorganic macrocycles which function as acceptors or as donors to a broad range of organic, inorganic and organometallic anions. Of the few inorganic macrocycles investigated so far, in limited cases where the host-guest chemistry has been

(A) Inorganic macrocycles with acceptor properties (A-E) and donor properties (F-H)

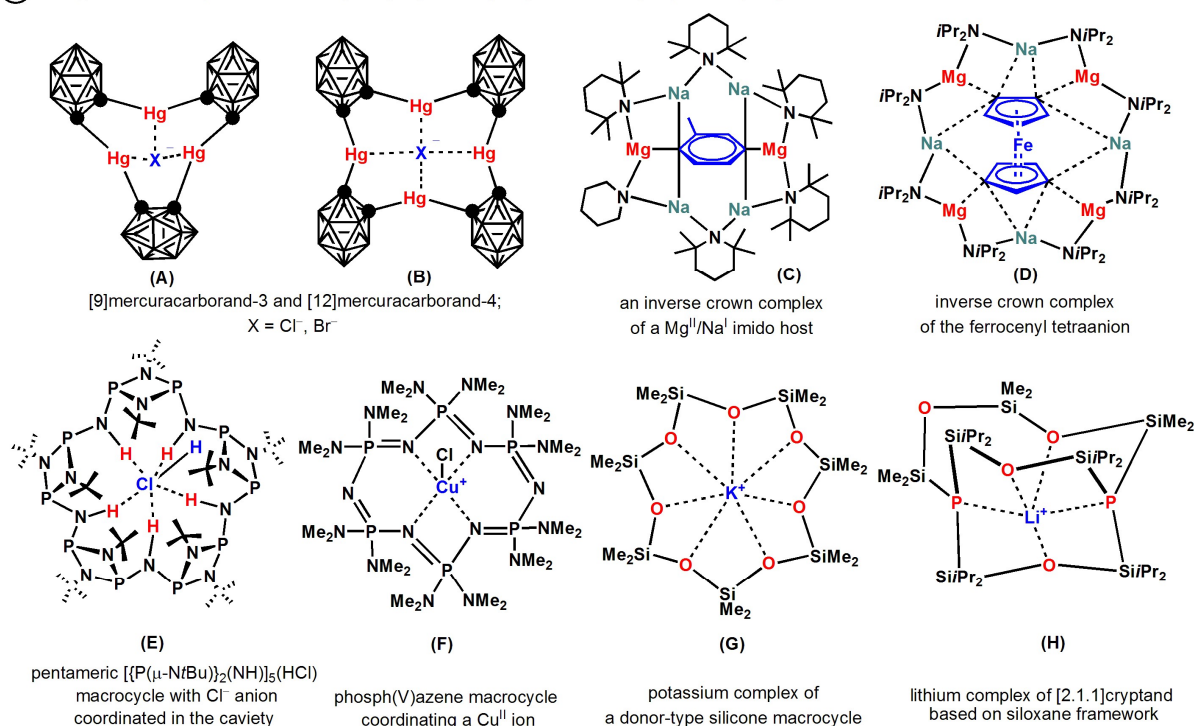


**Figure 2.2** Some well known examples of inorganic macrocycles (A-E: acceptor type, F-H: donor type).

explored, shows the acceptor type behaviour, particularly those based on electropositive metals.<sup>[1]</sup> Hawthorne's mercuracarborands such as [9]mercuracarborand-3 (**A**) and [12]mercuracarborand-4 (**B**) (X = Cl<sup>-</sup>, Br<sup>-</sup>) were the early examples of inorganic macrocycles exhibiting acceptor type behaviour. These species take advantage of the rigid linear geometry of Hg<sup>2+</sup> atoms, that bridge {1,2-C<sub>2</sub>B<sub>10</sub>H<sub>10</sub>} units into cyclic arrangements and exhibited acceptor type behaviour due to the electropositive character of Hg<sup>2+</sup>.<sup>[1h]</sup> The ionically-bonded, metallacyclic "inverse crowns" (**C** and **D**) introduced by Mulvey are good examples exhibiting acceptor properties to a broad range of organic, inorganic and organometallic anions including highly unusual anions (2,5-C-H doubly deprotonated toluene **C** and tetrametallated ferrocene [(C<sub>5</sub>H<sub>3</sub>)<sub>2</sub>Fe]<sup>4-</sup> (**D**)).<sup>[1i-j]</sup> Wright and coworkers have shown a nice example of host-guest complex, [P(μ-N*t*Bu)]<sub>2</sub>(NH)<sub>5</sub>(HCl) (**E**), composed of a pentameric, [P(μ-N*t*Bu)]<sub>2</sub>(NH)<sub>5</sub> macrocycle which coordinates to a Cl<sup>-</sup> anion using the five NH groups of the macrocyclic framework.<sup>[1k]</sup> From the foregoing discussion it can be understood that in contrast to organic macrocycle (generally donor type), inorganic macrocyclic area is dominated by examples exhibiting acceptor type behaviour and very few donor type inorganic macrocycles have been reported. An early example of donor type inorganic macrocycles was seen in a twelve-membered phosph(V)azane macrocycle, [(Me<sub>2</sub>N)<sub>2</sub>PN]<sub>6</sub> (**F**) that was found to coordinate Cu<sup>2+</sup> within its cavity.<sup>[1l-m]</sup> Other recent examples of cation coordination were seen in the case of cyclic silicones (**G** and **H**) (analogous to crown ether and cryptands) which show their coordinating behaviour towards alkali metals.<sup>[1n-p]</sup>

Cyclodiphosph(III)azanes, [XP(μ-N*t*Bu)]<sub>2</sub> are well known precursors for many inorganic and organic systems including P-N based macrocycles, metal complexation,<sup>[1]</sup> dichalcogen based systems. In the past decade or so, the [CIP(μ-N*t*Bu)]<sub>2</sub> units of cyclic phosph(III)azanes have proved to be robust building blocks for the assembly of hybrid-type inorganic-organic macrocycles [P(μ-NR)]<sub>2</sub>(μ-LL')<sub>n</sub> (where LL' is an organic linker).<sup>[1,2,3a]</sup>

Similarly, inorganic-type macrocycles with N-bridges  $[\{P(\mu\text{-NR})\}_2(\mu\text{-NR})]_n$  ( $n = 4$  (**I**), and 5) were obtained by the condensation reactions of  $[\text{CIP}(\mu\text{-NR})]_2$  with  $[\text{NH}_2\text{P}(\mu\text{-NR})]_2$  in the presence of a Brønsted base.<sup>[1k,3b]</sup> The significant use of  $[\text{CIP}(\mu\text{-NR})]_2$  as a building block to assemble intriguing macrocycles with different donor atoms have been shown in Figure 2.3 (**I-VI**).

Attempts have been made to mimic organic macrocycles using  $[\text{CIP}(\mu\text{-N}t\text{Bu})]_2$  as potential building blocks with bridging elements (Se, O) other than N-bridged species. In this series the O-bridged tetramer,  $[\{P(\mu\text{-N}t\text{Bu})\}_2(\mu\text{-O})]_4$  (**II**) was the first example of such a crown-type macrocycle.<sup>[3c]</sup> However, the syntheses of this type of macrocycle are fought with

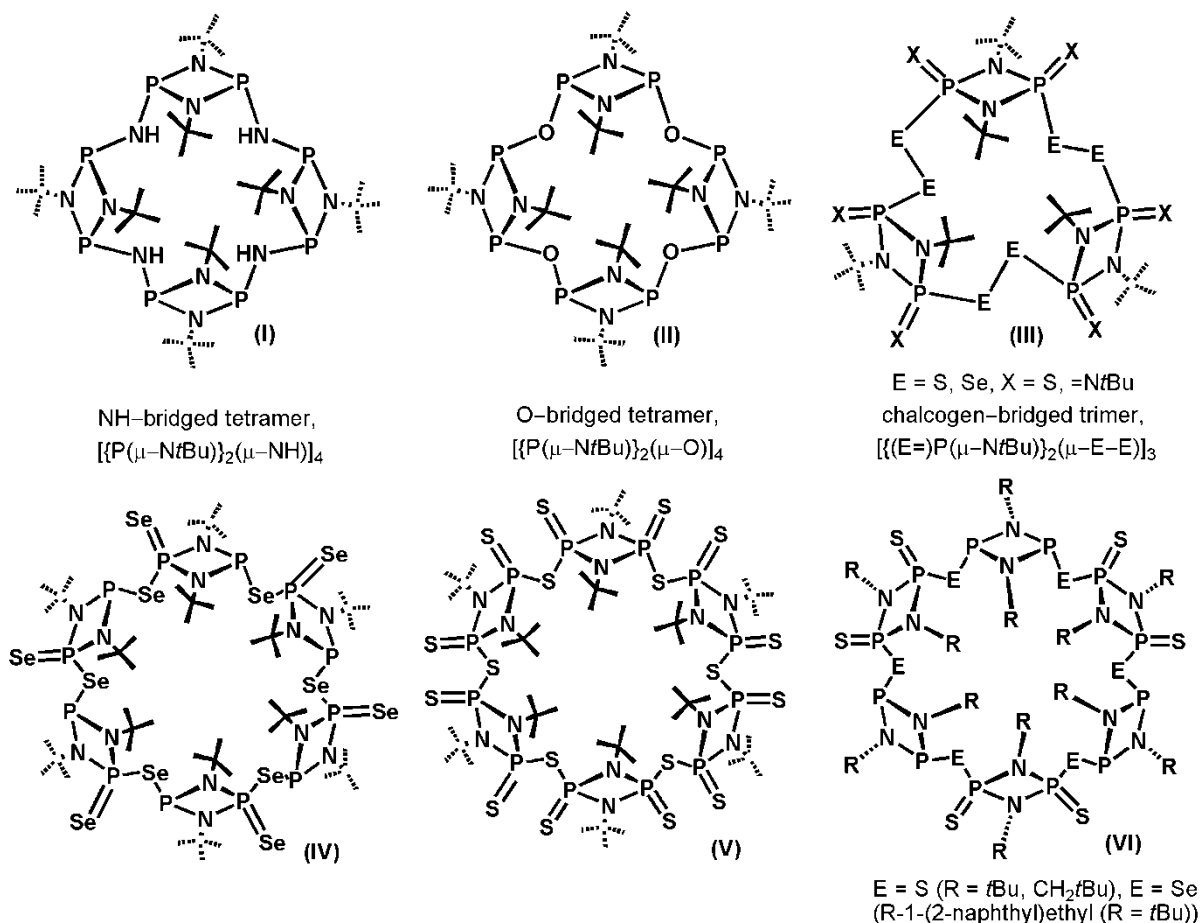


**Figure 2.3** Examples of NH- and chalcogen bridged macrocycles based on  $[\text{CIP}(\mu\text{-NR})]_2$  unit and its derivatives.

synthetic challenges and the approach used for N-bridged macrocycles (**I**) could not be applied in this case. Therefore, the lack of a general approach led the necessity to investigate other pathways to obtain crown-like phosphazane macrocycles of this class, with the ultimate aim of developing a new area of host-guest chemistry. Switching from O- to S- or Se-bridged inorganic macrocycles should have two important effects (i) expansion of the size of the macrocyclic cavity and (ii) producing softer hosts for the coordination of a range of metal ions.

The extension of O-bridged systems to Se-macrocycles was achieved using Wurtz-type reaction to afford a hexameric macrocycle, [(Se=)P( $\mu$ -N*t*Bu)<sub>2</sub>P( $\mu$ -Se)]<sub>6</sub> (**IV**) by reaction of Na metal with a cis and trans mixture of [(Se=)ClP( $\mu$ -N*t*Bu)]<sub>2</sub>.<sup>[3d]</sup> However, pre-organization has been an important factor to construct the above mentioned macrocycles (**I** and **II**), but the rational synthetic routes have not been much explored to segregate the polymeric or undesirable aggregation formed during the course of macrocyclic syntheses. The example of segregation can be seen apparently in the synthesis of selenium-bridged hexamer, [( $\mu$ -Se)P( $\mu$ -N*t*Bu)<sub>2</sub>P(=Se)]<sub>6</sub> (**IV**) from its cis isomer on reducing the isomeric mixture of cis and trans-[(Se=)ClP( $\mu$ -N*t*Bu)]<sub>2</sub> where the fate of trans isomer could not be determined and can be considered to produce the polymeric product rather than macrocycle due to lack of pre-organization.

More recently, a new high-yielding modular approach has also been developed to synthesize a variety of chalcogenide (S- and Se-) bridged trimeric (**III**) and hexameric (**V-VI**) inorganic macrocycles based on cyclophosphazane frameworks.<sup>[3e]</sup> This approach involves the reaction of in-situ generated dianionic intermediate [E(S)P-( $\mu$ -NR)]<sub>2</sub><sup>2-</sup> (E=S or Se) with electrophilic [ClP( $\mu$ -NR)]<sub>2</sub> to give hexameric macrocycles with unique alternating (P<sup>III</sup>)<sub>2</sub>(P<sup>V</sup>)<sub>2</sub> backbone [ {(S=)P( $\mu$ -N*t*Bu)<sub>2</sub>P(=S)} { $\mu$ -(S-P( $\mu$ -N*t*Bu)<sub>2</sub>P-S)} ]<sub>3</sub> (E = S (R = *t*Bu, CH<sub>2</sub>*t*Bu), E = Se (R-1-(2-naphthyl)ethyl (R = *t*Bu)).<sup>[3f]</sup> The reaction of this dianionic units with I<sub>2</sub> give

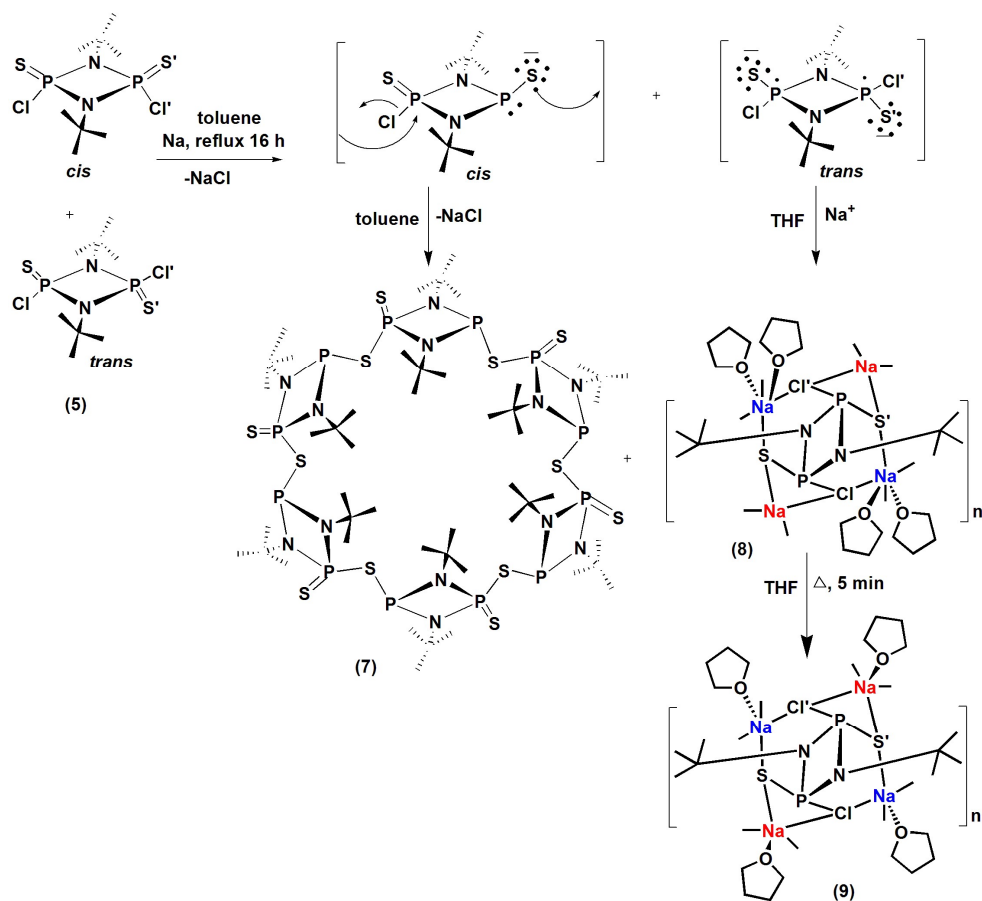
mixed S, Se-chalcogenide trimeric macrocycles with P<sup>V</sup> variants of the type, [ $\{(S=)P(\mu\text{-}NtBu)\}_2(\mu\text{-}Se\text{-}Se)\}_3$ . Moreover, a hexameric macrocycle with all P<sup>V</sup> variants of the type,  $[(S=)P(\mu\text{-}NtBu)_2P(=S)(\mu\text{-}S)]_6$  has also been reported by the oxidation of S-bridged macrocycle  $[(\mu\text{-}S)P(\mu\text{-}NtBu)_2P(=S)]_6$  (**7**).<sup>[3e]</sup>

In the present work, we have explored the analogous reaction of Na metal with cis- and trans- $[(S=)PCl(\mu\text{-}NtBu)]_2$  (**5**).<sup>[1f]</sup> We show that unlike the related Se-system, two reaction pathways occur in this case, (i) Wurtz-type coupling to give the S-bridged macrocycle  $[(\mu\text{-}S)P(\mu\text{-}NtBu)_2P(=S)]_6$  (**7**) and (ii) the unexpected reduction of the P=S bonds of **5** to give the trans biradicaloid dianion  $[S\text{-}P(Cl)(\mu\text{-}NtBu)]_2^{2-}$ . Our results suggest that the reaction pathway is influenced by which isomer of the precursor **5** (cis or trans) is involved, with **7** potentially arising from the cis- or trans-isomers and the  $[S\text{-}P(Cl)(\mu\text{-}NtBu)]_2^{2-}$  resulting from reduction of the trans-isomer alone.

## 2.2 Results and Discussion

### Synthesis of $[(\mu\text{-}S)P(\mu\text{-}NtBu)_2P(=S)]_6$ (**7**), $\{[(S\text{-})CIP(\mu\text{-}NtBu)_2PCl(S)]Na(Na\cdot THF_2)\}_n$ (**8**) and $\{[(S\text{-})CIP(\mu\text{-}NtBu)_2PCl(S)](Na\cdot THF_2)\}_n$ (**9**)

Reaction of a mixture of cis- and trans- $[(S=)CIP(\mu\text{-}NtBu)]_2$  (**5**) (discussed in Chapter 1) with excess sodium metal in toluene at reflux gave a mixture of products along with a brown slurry (Scheme 2.1). The brown slurry was separated by filtration and storage of the filtrate at room temperature for 3 days gave colorless crystals of  $[(\mu\text{-}S)P(\mu\text{-}NtBu)_2P(=S)]_6$  (**7**) in 13.6% yield (with respect to **5** supplied). The presence of P<sup>(III)</sup> and P<sup>(V)</sup> centers in **7** was evident from the room-temperature  $^{31}P\{^1H\}$  NMR spectrum in *d*<sub>8</sub>-toluene that showed two apparent doublet of doublets (P<sup>(III)</sup> 159.9, and P<sup>(V)</sup> 81.2 ppm), resulting from P<sup>(III)</sup>- $(\mu\text{-}N)$ -P<sup>(V)</sup> ( $^2J_{31P-31P} = 35.4$  Hz) and P<sup>(III)</sup>- $(\mu\text{-}S)$ -P<sup>(V)</sup> ( $^2J_{31P-31P} = 12.5$  Hz) coupling within the P<sub>2</sub>N<sub>2</sub> ring units and



**Scheme 2.1** Synthesis of the S-bridged macrocycle **7** and the  $[\text{S-P(Cl)}(\mu\text{-N}t\text{Bu})_2]_2^{2-}$  dianion complexes **8** and **9**.

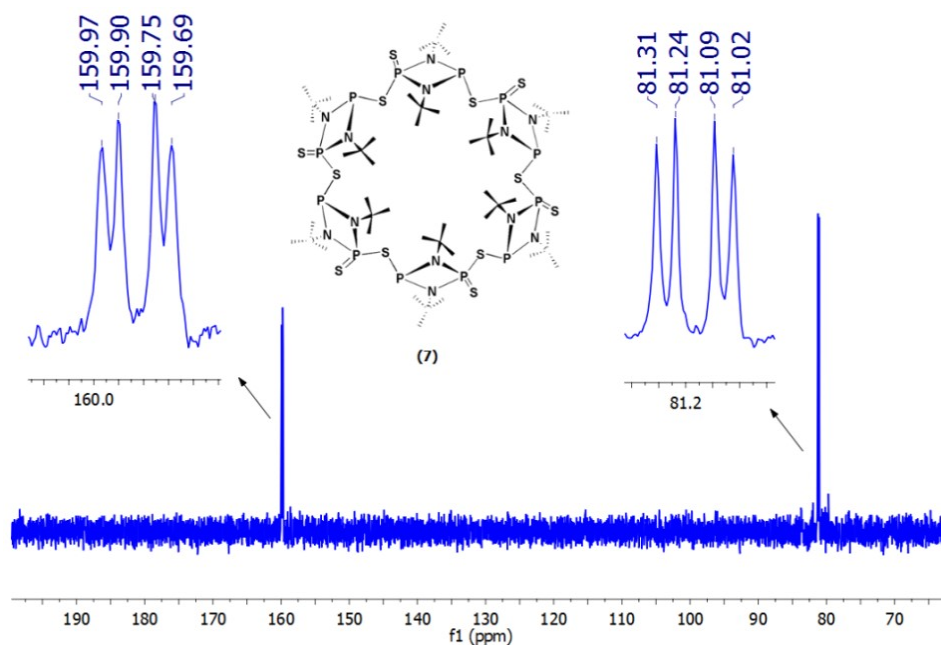


**Figure 2.4**  $^{31}\text{P}\{^1\text{H}\}$  NMR spectrum of S-bridged hexameric macrocycle,  $[(\mu\text{-S})\text{P}(\mu\text{-N}t\text{Bu})_2\text{P}(=\text{S})]_6$  (**7**).

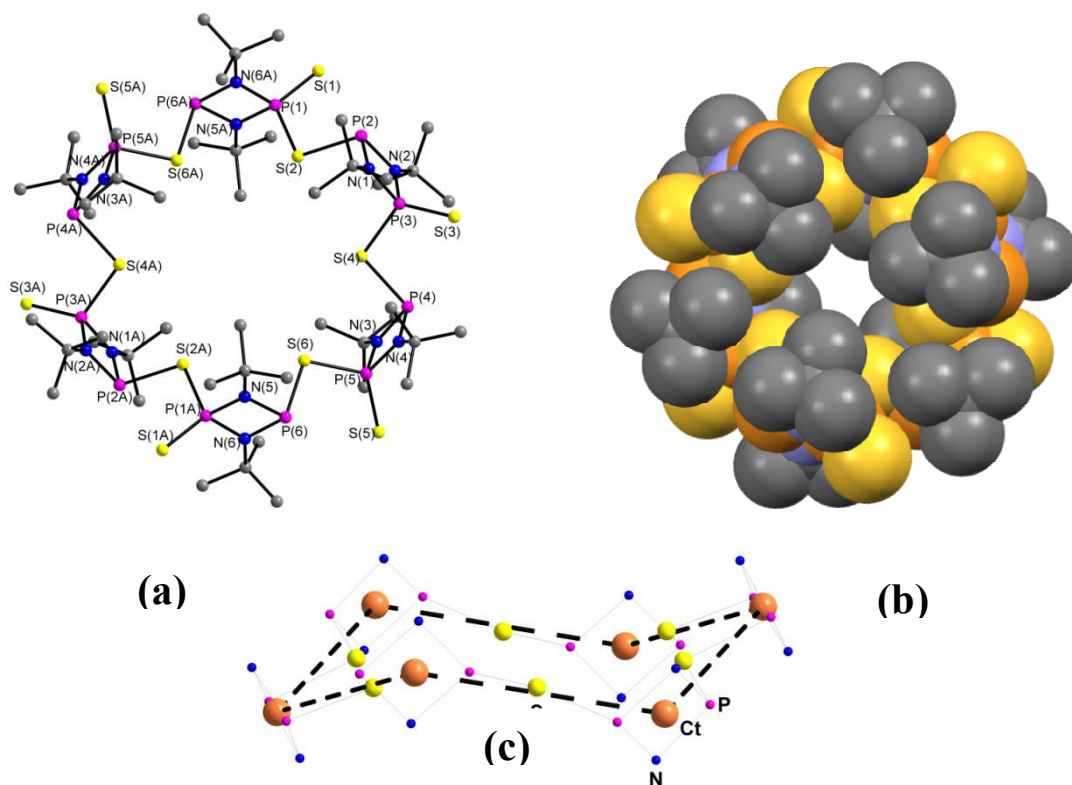


**Figure 2.5** Single crystal X-ray structure **(a)** and space-filling diagram **(b)** of the hexameric macrocycle  $[(\mu\text{-S})\text{P}(\mu\text{-N}t\text{Bu})_2\text{P}(=\text{S})]_6$  (**7**). As shown in **(c)** the centroids (**Ct**) of the six  $\text{P}_2\text{N}_2$  rings constitute a chair conformation. All hydrogen atoms and toluene molecule have been omitted for clarity. Selected bond lengths [Å] and bond angles [°]: P=S 1.915(4), P(V)-S 2.092(4), P(III)-S 2.198(3), P(III)-N 1.715(1), P(V)-N 1.675(1); P-S-P 102.80(2), S-P(V)-N 105.44(2) 109.63(2), S-P(III)-N 105.87(8) 98.77(3).

across the S-bridges of the macrocyclic arrangement (Figure 2.4). While the room-temperature  $^1\text{H}$  and  $^{13}\text{C}$  NMR spectra indicate the presence of only one *t*Bu-environment. These spectroscopic features are consistent with the subsequent single-crystal structure of **7**. In addition, high-resolution MS spectrum showed the presence of a prominent ion at  $m/z = 805.1230$  (calcd. 805.1238) which we attribute to the dication of **7**,  $[\text{M}+2\text{H}]^{2+}$ .

The single crystal X-ray structure of **7** confirms the formulation of this product as the hexameric macrocycle,  $[(\mu\text{-S})\text{P}(\mu\text{-N}t\text{Bu})_2\text{P}(=\text{S})]_6$  (Figure 2.5a). Eighteen atoms of the macrocyclic framework of **7**,  $[(\text{P}\cdots\text{P})(\mu\text{-S})]_6$  are non-planar in such a manner that the

centroids of six P<sub>2</sub>N<sub>2</sub> rings form a chair conformation (Figure 2.5c). This cavity is slightly smaller than that reported for isostructural Se-based hexameric macrocycle (8.2 Å).<sup>[3e]</sup> The *exo*-P=S bonds [1.915(4) Å] are as expected significantly shorter than the P-S single bonds within the core of **7** [2.092(4)-2.198(3) Å]. Sulfur-containing macrocycles are interesting owing to the unusual redox properties of S and the ability to stabilize low-oxidation-state metals.<sup>[7-9]</sup> Cooper and co-workers have reported on sulfur analogues of crown ethers,<sup>[7]</sup> hexathio-18-crown-6, (18S6) and hexathio-24-crown-6 (24S6), and their transition metal [Cu(II),<sup>[7c]</sup> Cu(I),<sup>[7c]</sup> Ni(II),<sup>[7d,e,f]</sup> Co(II)<sup>[7g]</sup>] complexes. Prior to this work, phosphazane-based macrocycles comprising of heavier group 16 element bridges were limited only to [(Se=)P( $\mu$ -N*t*Bu)<sub>2</sub>P( $\mu$ -Se)]<sub>6</sub> (**IV**) and the di-chalcogenide (-E-E-) bridged trimers [(*t*BuN=)P( $\mu$ -N*t*Bu)<sub>2</sub>( $\mu$ -E<sub>2</sub>)]<sub>3</sub> (E = S, Se) (**III**).<sup>[8]</sup> Compound **7** represents a completely new type of S-based macrocyclic arrangement, unique in possessing a large cavity size and a rigid, crown-like arrangement even in the absence of a metal. Presence of  $\mu$ -S bridging atoms in **7** and *cisoid* geometry with respect to the P<sub>2</sub>N<sub>2</sub> rings makes it an ideal donor for metal coordination.

Extraction of the brown residue with THF at room temperature followed by concentration of the solvent and storage for 2 days at room temperature gave colorless crystals of [ {(S-)ClP( $\mu$ -N*t*Bu)<sub>2</sub>PCl(S)}Na(Na·THF<sub>2</sub>) ]<sub>n</sub> (**8**) in 19.4% yield (with respect to **5** supplied). If the brown residue is extracted with hot THF, colorless crystals of [ {(S-)ClP( $\mu$ -N*t*Bu)<sub>2</sub>PCl(S)}(Na·THF)<sub>2</sub> ]<sub>n</sub> (**9**) were obtained at room temperature in 15.8% yield (with respect to **5** supplied). Both **8** and **9** were shown later by single-crystal X-ray analysis to be closely related, differing only in the extent of THF solvation of Na<sup>+</sup>. They contain the singlet biradicaloid dianion<sup>[5]</sup> [S-P(Cl)( $\mu$ -N*t*Bu)]<sub>2</sub><sup>2-</sup> also supported by computational studies (Figure 2.6 and 2.10). This is colourless and gives sharp NMR signals (<sup>1</sup>H, <sup>31</sup>P and <sup>13</sup>C) at room temperature. This diamagnetism is similar to that seen recently by Schulz for a similar biradicaloid [P( $\mu$ -N*Ter*)]<sub>2</sub> (Ter = 2,6-Mes<sub>2</sub>-C<sub>6</sub>H<sub>3</sub>, Mes = 2,4,6-Me<sub>3</sub>C<sub>6</sub>H<sub>2</sub>).<sup>[6]</sup> However, the

biradicaloid dianion of **8** and **9** does not require steric protection using bulky substituents at the N atoms. The stability of the dianion is probably due to the dual effects of P<sup>(V)</sup> and the electronegativity of the S and Cl atoms attached to phosphorus.

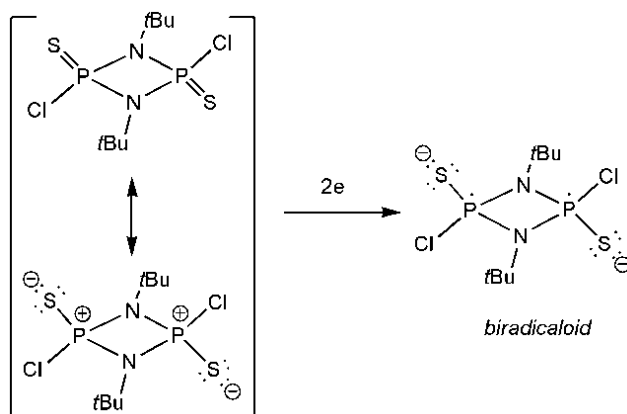


**Figure 2.6** Biradicaloid dianion  $[S-P(Cl)(\mu-NtBu)]_2^{2-}$  generated from  $trans-[(S=)ClP(\mu-NtBu)]_2$ .

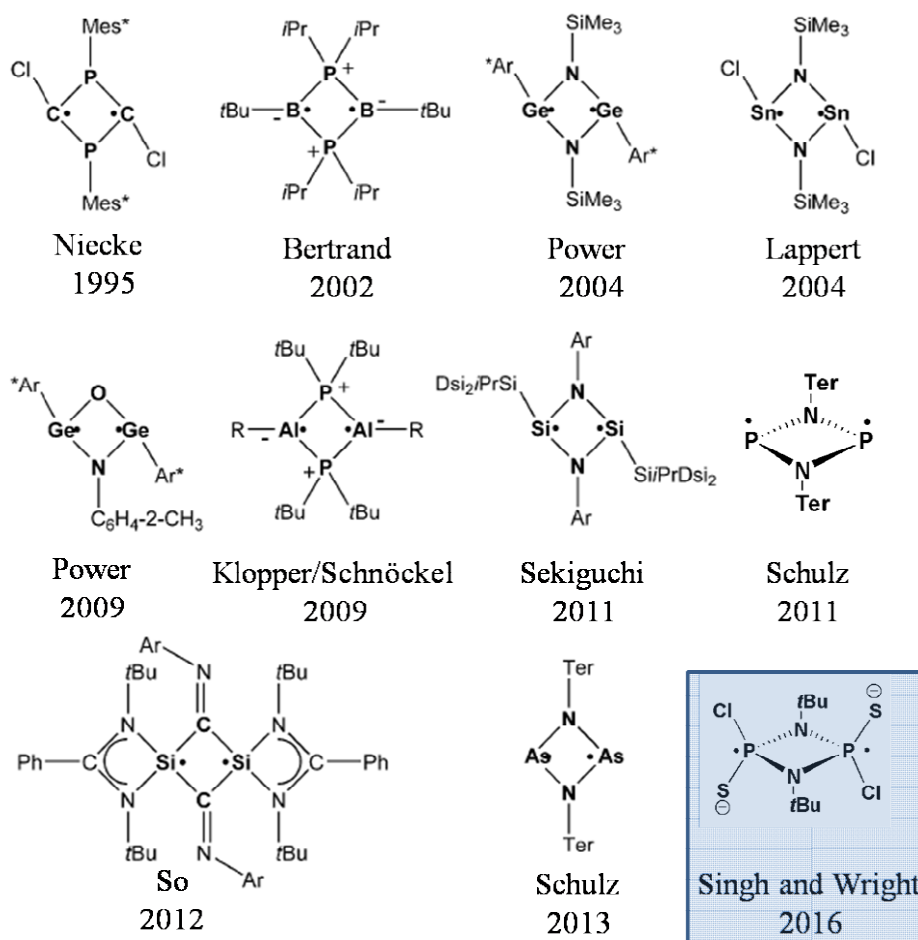


**Figure 2.7** Experimentally known, cyclo-butanediyl based four membered heterocyclic biradicaloids.

To the best of our knowledge  $[\text{S-P}(\text{Cl})(\mu\text{-N}t\text{Bu})]_2^{2-}$  is the first example of a  $\text{P}_2\text{N}_2$ -based biradicaloid dianion. Figure 2.7 shows various examples of experimentally known, four membered heterocyclic biradicaloids of main group elements derived from cyclobutanediyl.<sup>[6]</sup> Scheme 2.1 shows the mechanisms by which the macrocycle **7** and the singlet biradicaloid  $[\text{S-P}(\text{Cl})(\mu\text{-N}t\text{Bu})]_2^{2-}$  dianion of **8** and **9** are generated. Like the previously reported Se-analogue, the likely mechanism by which **7** is produced involves a reaction sequence in which the first step is reduction of a P-Cl bond of the precursor **5**. Although it is tempting to suggest that **7** can only be generated from the cis-isomer of **5**, there is an obvious potential for P-lone pair inversion of the intermediate anion generated by the reduction of a P-Cl bond of the trans-isomer. However, it is clear that the trans-geometry of the  $[\text{S-P}(\text{Cl})(\mu\text{-N}t\text{Bu})]_2^{2-}$  dianions found in the solid-state structures of **8** and **9** must result from reduction of the P=S bonds of the trans isomer of the precursor **5**.

Once isolated and dried under vacuum the spectroscopic and spectrometric data for **8** and **9** were found to be identical. Both compounds show a single resonance in their room-temperature  $^{31}\text{P}\{^1\text{H}\}$  NMR spectra in  $d_8$ -THF ( $\delta$  82.0 ppm), while their high-resolution MS both show peak at  $m/z$  503.0020 (**8**), 503.0000 (**9**) (calcd 503.0008) which we assign to  $[\text{M}+\text{H}]^+$  for the  $\text{C}_8\text{H}_{18}\text{P}_2\text{N}_2\text{S}_2\text{Cl}_2\text{Na}_4\cdot\text{THF}$  fragment. Furthermore, vacuum-dried crystals of **8** and **9** exhibit the same melting behavior (decomposing at *ca.* 320 °C). All of these features strongly suggest the loss of most of the THF from both complexes, producing unsolvated  $\{\text{Na}_2[\text{S-P}(\text{Cl})(\mu\text{-N}t\text{Bu})]_2\}_n$  after drying under vacuum. The absence of coordinated THF in both is confirmed by the  $^1\text{H}$  NMR spectrum which shows little or no THF remains. Further support for the lability of the coordinated THF molecules comes from the fact that complex **9** can be crystallized from a solution of an isolated sample of **8** dissolved in hot THF.

The single-crystal X-ray structures of the 3D- and 2D-polymers  $[\{(\text{S-})\text{ClP}(\mu\text{-N}t\text{Bu})_2\text{PCl}(\text{S})\}\text{Na}(\text{Na}\cdot\text{THF}_2)]_n$  (**8**) and  $[\{(\text{S-})\text{ClP}(\mu\text{-N}t\text{Bu})_2\text{PCl}(\text{S})\}(\text{Na}\cdot\text{THF})_2]_n$  (**9**) both show

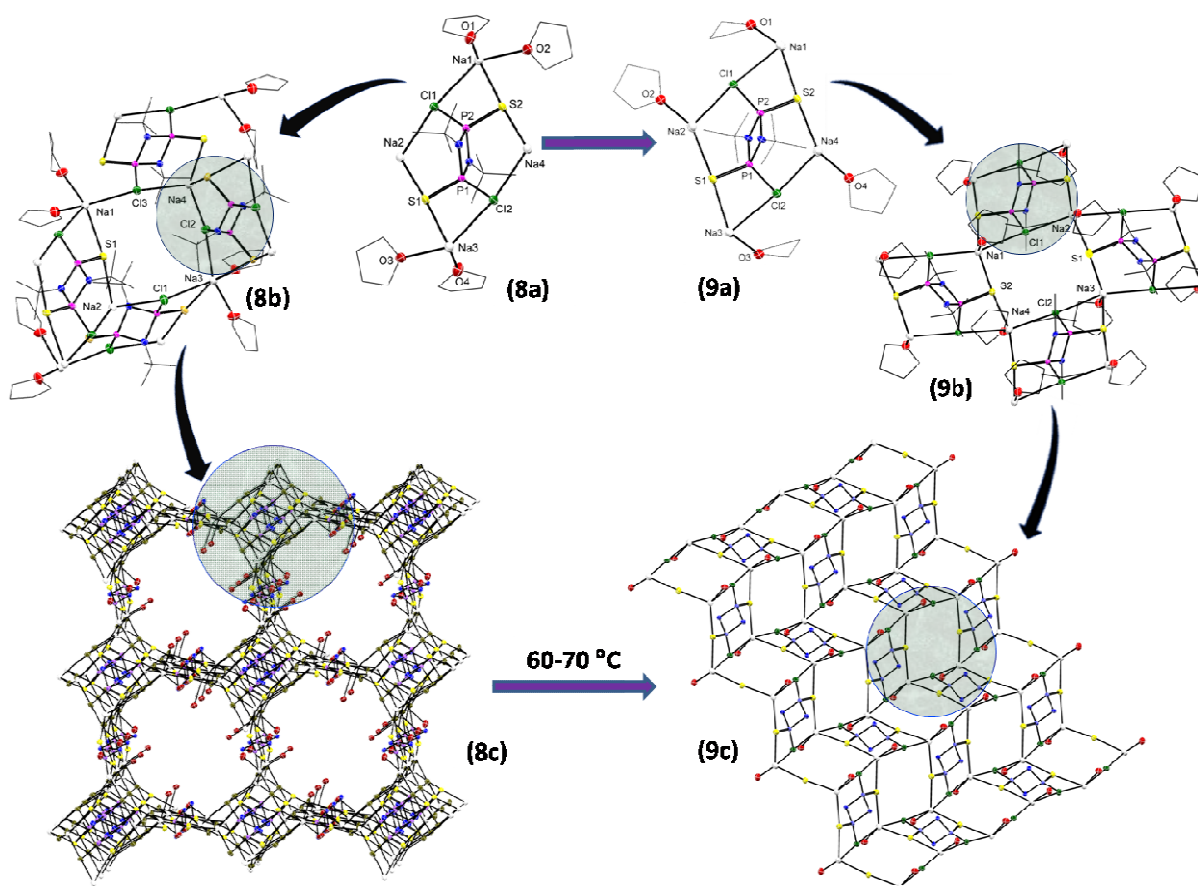


**Figure 2.8** Perspective view of sections of the 3D polymer **8** and 2D polymer **9**: Structures **8a** and **9a** show top-bottom and side-on chelation of  $\text{Na}^+$  with the dianion  $[\text{S-P}(\text{Cl})(\mu\text{-N}t\text{Bu})]_2^{2-}$ . Structures **8b** and **9b** show the formation of 8-membered  $[\text{Na}_4\text{Cl}_3\text{S}]$  and  $[\text{Na}_4\text{S}_2\text{Cl}_2]$  rings, respectively. Structures **8c** and **9c** show sections of the infinite extended molecular structure of the 3D polymer **8** and 2D polymer **9**, respectively, *t*Bu and THF carbon atoms have been omitted for clarity in structures **8c** and **9c**.

the presence of the novel  $[(\text{S-})\text{CIP}(\mu\text{-N}t\text{Bu})]_2^{2-}$  dianion. The P-Cl bond lengths in the dianions of **8** and **9** (1.984(4) and 1.975(1) Å, respectively) are similar to those found in the precursor  $[(\text{S=})\text{CIP}(\mu\text{-N}t\text{Bu})]_2$  (**5**)<sup>[4]</sup> [1.996(3) Å]. However, as expected there is a significant elongation of the P-S bonds by 0.07-0.08 Å in the dianion  $[\text{S-P}(\text{Cl})(\mu\text{-N}t\text{Bu})]_2^{2-}$  in **8** and **9** [1.987(6) Å and 1.989(3) Å, respectively] compared to the P=S bond length in **5** [1.911(2) Å], consistent with the reduction of the double bond to a single bond (P=S to P-S). The essential difference between the two arrangements of **8** and **9** stems from the presence of unsolvated and *bis*-THF

Na<sup>+</sup> cations in **8** and exclusively *mono*-solvated Na<sup>+</sup> cations in **9**. As noted previously, **8** is converted into **9** after heating in THF solution. The structural relationship between the polymeric arrangements of both compounds is shown schematically in Figure 2.8. Figure 2.9

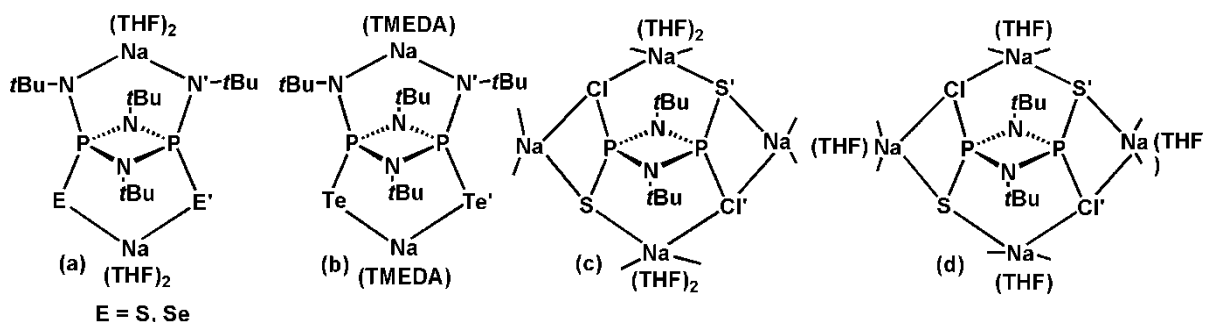


**Figure 2.9** Sodium salts of (a) sulfur-, selenium-based and (b) tellurium-based phosphazane dianions  $[(E=)(tBuN)P(\mu-NtBu)]_2^{2-}$ , (c) and (d) *top-bottom* (Cl, S' and S, Cl') and *side-on* (S, Cl and S', Cl') chelation of the  $[S-P(Cl)(\mu-NtBu)]_2^{2-}$  dianion in the current work.

shows the building units of **8** and **9** and their relationship to previously reported molecular Na-complexes of  $[(E=)(tBuN)P(\mu-NtBu)]_2^{2-}$  (E = S, Se, Te) anions that bind only in a *top-bottom* mode.<sup>[10,11]</sup> The aggregation of **8** into a 3D polymer can be seen to result from two cation coordination modes, (i) *top-bottom* (Cl, S' and S, Cl') chelation of the  $Na(THF)_2$  cations leads to 6-membered  $[NaS(P\cdots P)NCl]$  ring units within the polymer in which these cations have six-coordinate geometries (see Scheme 2.1 and structure **8a**, Figure 2.8), and (ii) *side-on* (S, Cl and S', Cl') chelation of the unsolvated Na<sup>+</sup> cations produces 4-membered  $[SPClNa]$  ring units in which the Na<sup>+</sup> cations are 4-coordinate (see Scheme 2.1 and structure **8a**, Figure 2.8). The resulting units are further connected to each other by *top-bottom* chelation of one unit with another to produce larger 8-membered  $[Na_4Cl_3S]$  rings (**8b**, Figure 2.8). These 8 membered rings associate to produce channels in the structure *via*  $[S-Na-Cl]$  bridges. The arrangement in complex **9** is closely related (see structures **9a** and **9b**, Figure 2.8), only the absence of un-(THF)-solvated Na<sup>+</sup> cation means that the assembly cannot build

into a 3D structure. Instead, a step-like 2D polymer (built up from  $[\text{Na}_4\text{S}_2\text{Cl}_2]$  8-membered rings) is formed (**9c**, Figure 2.8).

To clarify the electronic nature of novel  $\text{P}_2\text{N}_2$ -based biradicaloid dianion shown in Figure 2.6, we have carried out *ab initio* calculations on a simpler model compound in which the *t*Bu groups have been replaced by methyl groups. The optimized geometry of the neutral species was found to have  $C_i$  symmetry and we have maintained this symmetry for the dianion calculations. To describe the biradicaloid nature correctly, multi-reference CASSCF and MRCI methods were used with aug-cc-pVDZ basis sets. A two-orbital active space CAS(2,2) with  $A_g$  and  $A_u$  symmetry orbitals was found to describe the biradicaloid singlet state adequately. After geometry optimization of the biradicaloid state at the CAS(2,2) level, a single-point state-averaged CASSCF(2,2) calculation including three singlet and one triplet states was carried out. This was followed by MRCI calculations on the lowest singlet and triplet states for each symmetry. The results of these calculations along with other details can be found in the supplementary information.

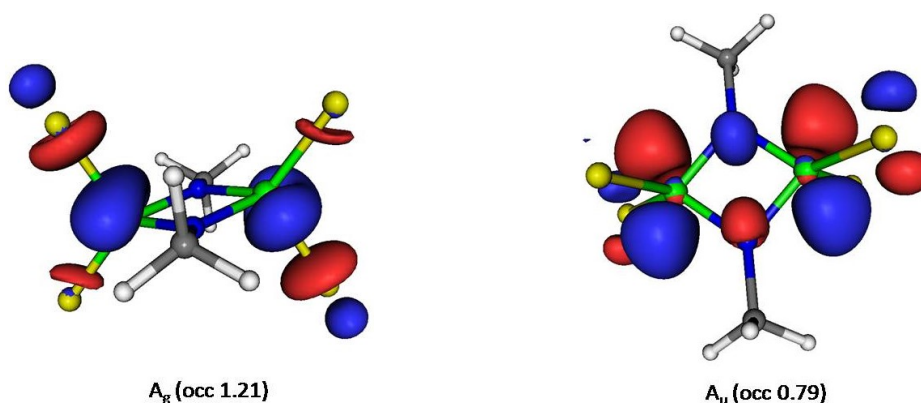


**Figure 2.10** Active orbitals of the model compound (with their symmetry and natural occupancies) supporting the biradicaloid nature of the  $[\text{S-P}(\text{Cl})(\mu\text{-NMe})_2]^{2-}$  dianion.

As can be seen in Figure 2.10, the active orbitals, of the model compound, are predominantly P-centered with small contributions from neighbouring S atom. Their natural occupation numbers (1.21 for the  $A_g$  and 0.79 for the  $A_u$  orbital) are perfectly consistent with

the biradicaloid nature of the dianion. The Mulliken population analysis showing a negative charge of 0.75e on the S and a positive charge of 0.76e on the P atoms (as compared to -0.48e on S and +1.57e on P for the neutral model compound) indicates that the additional electrons have gone on to the P atoms. The Na cations found in **8** and **9** help to further stabilize the resulting biradicaloid further through ionic interactions. The MRCI calculations show that the  $A_g$  symmetry biradicaloid state is separated by 0.5 kcal/mol from the lower-lying  $A_u$  symmetry open-shell triplet state. This is in agreement with the IUPAC definition of biradicaloids.

### 2.3 Conclusions

In conclusion, on attempting a Wurtz-type coupling reaction using cis- and trans-[(S=)ClP( $\mu$ -N*t*Bu)]<sub>2</sub> (**5**) with sodium two different reaction pathways are found. The sulfur-bridged hexameric macrocycle [( $\mu$ -S)P( $\mu$ -N*t*Bu)<sub>2</sub>P(=S)]<sub>6</sub> (**7**) is the result of *head-to-tail* cyclization. Whereas, the biradicaloid dianion [S-P(Cl)( $\mu$ -N*t*Bu)]<sub>2</sub><sup>2-</sup> as its disodium salt formed from a different pathway involving reduction of the P=S bonds of **5** to P-S bonds. In the solid state this biradicaloid dianion assembles as a 3D polymer, [{(S-)ClP( $\mu$ -N*t*Bu)<sub>2</sub>PCl(S)}Na(Na·THF<sub>2</sub>)]<sub>n</sub> (**8**) at room temperature and that converts into a 2D polymer, [{(S-)ClP( $\mu$ -N*t*Bu)<sub>2</sub>PCl(S)}(Na·THF)<sub>2</sub>]<sub>n</sub> (**9**) after heating for a few minutes in THF. The electronic structure of the dianion core of **8** and **9** as P-centered biradicaloid was supported by computational studies on the model dianion [S-P(Cl)( $\mu$ -NMe)]<sub>2</sub><sup>2-</sup>. Future studies will explore the host-guest behaviour of macrocycle **8** and explore the bonding and coordination behaviour of the dianion [S-P(Cl)( $\mu$ -N*t*Bu)]<sub>2</sub><sup>2-</sup>.

## 2.4 Experimental Section

### 2.4.1 General procedure

All syntheses were carried out under an inert atmosphere of dinitrogen in oven dried glassware using standard Schlenk techniques or a glove box where O<sub>2</sub> and H<sub>2</sub>O levels were maintained usually below 0.1 ppm. Solvents were purified by MBRAUN solvent purification system MB SPS-800. THF was dried over (Na/benzophenone ketyl) and distilled under nitrogen and degassed prior to use.

### 2.4.2 Starting materials

All chemicals used in this work were purchased from commercial sources and were used without further purification. [ClP( $\mu$ -N*t*Bu)]<sub>2</sub> was prepared as per the reported procedure.<sup>[3b]</sup>

### 2.4.3 Physical measurements

The <sup>1</sup>H, <sup>13</sup>C and <sup>31</sup>P{<sup>1</sup>H} spectra were recorded with a Bruker 400 MHz spectrometer with TMS and H<sub>3</sub>PO<sub>4</sub> (85 %) respectively, as external references and chemical shifts were reported in ppm. Downfield shifts relative to the reference were quoted positive while the upfield shifts were assigned negative values. High resolution mass spectra were recorded on a Waters SYNAPT G2-S instrument. IR spectra of the complexes were recorded in the range 4000–400 cm<sup>-1</sup> using a Perkin Elmer Lambda 35-spectrophotometer over KBr plates. The absorptions of the characteristic functional groups were only assigned and other absorptions (moderate to very strong) were only listed. Melting points were obtained in sealed capillaries on a Büchi B-540 melting point instrument.

Single-crystal X-ray diffraction data were collected with a Bruker AXS KAPPA APEX-II CCD diffractometer (monochromatic MoK $\alpha$  radiation) equipped with Oxford Cryosystem 700 Plus at 100 K. Data collection and unit-cell refinement of the data sets were

done with the Bruker APPEX-II suite, data reduction and integration were performed with SAINT V7.685A (Bruker AXS, 2009), and absorption corrections and scaling were done with SADABS V2008/1 (Bruker AXS, 2009). The structures were solved by direct methods and refined by full-matrix least-squares procedures by using the SHELXL-97 software package in the Olex2 suite. All non-hydrogen atoms were refined anisotropically.

#### **2.4.4 Details of computational calculation of the model compound $[\text{S-P}(\text{Cl})(\mu\text{-NMe})_2]^{2-}$**

Ab initio calculations were carried out using MOLPRO package<sup>[13]</sup> at CASSCF and MRCI levels with aug-cc-pVDZ basis sets. The  $C_i$  symmetry was imposed in all calculations. The active space employed was the two-orbital-two-electron active space CAS(2,2) including one-orbital of Ag and Au symmetries. Geometry optimization of the biradical singlet state was carried out using this active space. At the optimized geometry, single-point calculations were carried out at CASSCF and MRCI levels of theory. The state-averaged calculations used all the three resulting singlet states (2 Ag states and 1 Au symmetry open-shell singlet) and one Au symmetry triplet state. The MRCI calculations were performed using internally contracted MRCI wave function, (in literature many variants of MRCI wave functions are available), method used in this work was developed by Werner and co-workers. The new internally contraction scheme would enable the highly correlated electronic structure calculations to the large molecules and molecules containing heavy atoms.<sup>[14]</sup> The active orbitals at CAS(2,2)/cc-pVDZ level have been visualized with MOLEKEL package.<sup>[15]</sup>

#### **2.4.5 Synthetic procedure**

**Synthesis of  $[(\mu\text{-S})\text{P}(\mu\text{-N}t\text{Bu})_2\text{P}(=\text{S})]_6$  (7), 3D polymer (8) and 2D polymer (9):** A mixture of **5** (1.02 g, 3.0 mmol) and sodium (0.33 g, 14.3 mmol) in toluene (60 mL) was refluxed for 16 h. The resulting brown slurry was filtered off and the filtrate was concentrated till some solid just started to appear. At this point the evaporation was stopped and the solid was

dissolved by gentle heating. This solution gave crystals of  $[(\mu\text{-S})\text{P}(\mu\text{-N}t\text{Bu})_2\text{P}(=\text{S})]_6$  (**7**) at room temperature in three days. Yield: 0.11 g, 13.6% (with respect to **5** supplied), Mp: 175 °C. The original brown residue was extracted with THF (40 mL) and filtered, on concentration of this solution colourless crystals of the 3D polymer (**8**) were obtained at room temperature in 2 days Yield: 0.22 g, 19.4% (with respect to **5** supplied), Mp: 320 °C (decomp). Using the correct stoichiometric ratio of Na metal relative to **5** resulted in a slightly reduced yield of **7**.

In repetitions of this reaction, extraction of the brown residue with hot THF gave crystals of 2D polymer **9** only. Yield: 0.180 g, 15.8% (with respect to **5** supplied), Mp 320 °C (decomp). Subsequently, it was also confirmed that the room temperature THF extract of **8** when heated (or dried crystals of **8** when dissolved in THF with heating), led to irreversible conversion of **8** to **9**. Spectroscopic data for **8** and **9** were identical. Once extracted from their mother liquor compounds **7-9** showed very limited solubility in wide range of solvents.

**Spectroscopic data for  $[(\mu\text{-S})\text{P}(\mu\text{-N}t\text{Bu})_2\text{P}(=\text{S})]_6$  (**7**):** IR (KBr): 2971, 1625, 1460, 1397, 1368, 1259, 1197, 1081, 1026, 899, 807, 715, 669, 616, 581, 535  $\text{cm}^{-1}$ .  $^1\text{H}$  NMR (400 MHz,  $d_8$ -toluene):  $\delta = 1.60$  (s,  $\text{C}(\text{CH}_3)_3$ ).  $^{31}\text{P}\{^1\text{H}\}$  NMR (162 MHz,  $d_8$ -toluene):  $\delta = 159.9$  (dd,  $J_{\text{P(III)}-\mu\text{N-P(V)}} = 35.4$  Hz,  $J_{\text{P(III)}-\mu\text{S-P(V)}} = 12.5$  Hz), 81.2 (dd  $J_{\text{P(V)}-\mu\text{N-P(III)}} = 35.4$  Hz,  $J_{\text{P(V)}-\mu\text{S-P(III)}} = 12.5$  Hz). HRMS ( $\text{AP}^+$ ):  $m/z$  calcd for  $\text{C}_{24}\text{H}_{55}\text{P}_6\text{N}_6\text{S}_6$ : (805.1238)  $[\text{M}+2\text{H}]^{2+}$ ; found: (805.1230).

**Spectroscopic data for 3D polymer (**8**) and 2D polymer (**9**):** IR (KBr): 2958, 1634, 1386, 1362, 1250, 1201, 1047, 928, 883, 809, 653, 527  $\text{cm}^{-1}$ .  $^1\text{H}$  NMR: (400 MHz,  $d_8$ -THF):  $\delta = 1.77$  (s,  $\text{C}(\text{CH}_3)_3$ ).  $^{13}\text{C}$  NMR (100 MHz,  $d_8$ -THF):  $\delta = 56.3$  (s,  $\text{C}(\text{CH}_3)_3$ ), 30.0 (t,  $J_{\text{P-C}} = 4.7$  Hz,  $\text{C}(\text{CH}_3)_3$ ).  $^{31}\text{P}\{^1\text{H}\}$  NMR (162 MHz,  $d_8$ -THF):  $\delta = 82.0$  ppm.  $^1\text{H}$  NMR (400 MHz,  $\text{D}_2\text{O}$ ):  $\delta = 1.67$  (s,  $\text{C}(\text{CH}_3)_3$ ).  $^{13}\text{C}$  NMR (100 MHz,  $\text{D}_2\text{O}$ ):  $\delta = 58.1$  (s,  $\text{C}(\text{CH}_3)_3$ ), 30.8 (t,  $J_{\text{P-C}} = 4.5$  Hz,  $\text{C}(\text{CH}_3)_3$ ).  $^{31}\text{P}\{^1\text{H}\}$  NMR (162 MHz,  $\text{D}_2\text{O}$ ):  $\delta = 82.5$

ppm. HRMS (AP<sup>+</sup>): *m/z* calcd for C<sub>8</sub>H<sub>18</sub>P<sub>2</sub>N<sub>2</sub>S<sub>2</sub>Cl<sub>2</sub>Na<sub>4</sub>·THF: (503.0008) [M+H]<sup>+</sup>; found: (503.0020) (for **8**), (503.0000) (for **9**).

## 2.5 Crystallography Data

**Table 2.1.** Crystallographic data for compounds **7-9**.

Compound <sup>[a]</sup>	<b>7</b>	<b>8</b>	<b>9</b>
Chemical formula	C <sub>9</sub> H <sub>19</sub> N <sub>2</sub> P <sub>2</sub> S <sub>2</sub>	C <sub>32</sub> H <sub>66</sub> Cl <sub>4</sub> N <sub>4</sub> Na <sub>4</sub> O <sub>4</sub> P <sub>4</sub> S <sub>4</sub>	C <sub>8</sub> H <sub>17</sub> ClNaOPS
Molar mass	281.32	1056.76	264.69
Crystal system	Cubic	Triclinic	Monoclinic
Space group	<i>Pa</i> -3	<i>P</i> $\bar{1}$	<i>P2</i> <sub>1</sub> / <i>c</i>
<i>T</i> [K]	100(2)	100(2)	100(2)
<i>a</i> [Å]	20.663(2)	12.721(5)	12.047(2)
<i>b</i> [Å]	20.663(2)	12.855(5)	9.135(2)
<i>c</i> [Å]	20.663(2)	17.454(6)	11.822(2)
$\alpha$ [°]	90	106.43(4)	90
$\beta$ [°]	90	102.73(6)	100.16(3)
$\gamma$ [°]	90	99.86(3)	90
<i>V</i> [Å <sup>3</sup> ]	8823(2)	2585.9(3)	1280.8(3)
<i>Z</i>	24	2	4
<i>D</i> (calcd.) [g·cm <sup>-3</sup> ]	1.271	1.357	1.373
$\mu$ (Mo- <i>K</i> $\alpha$ ) [mm <sup>-1</sup> ]	0.555	0.585	0.590
Reflections collected	89716	39413	17332
Independent reflections	2695	9441	2332
Data/restraints/parameters	2695/0/142	9441/0/499	2332/0/130
<i>R</i> <sub>1</sub> , <i>wR</i> <sub>2</sub> [ <i>I</i> >2 $\sigma$ ( <i>I</i> )] <sup>[a]</sup>	0.0588, 0.1625	0.0634, 0.636	0.0301, 0.0886
<i>R</i> <sub>1</sub> , <i>wR</i> <sub>2</sub> (all data)[a]	0.0902, 0.1856	0.0821, 0.1729	0.0332, 0.0922
GOF	1.067	1.096	1.099

[a]  $R_1 = \sum ||F_o| - |F_c|| / \sum |F_o|$ ,  $wR_2 = [\sum w(|F_o|^2 - |F_c|^2)^2 / \sum w|F_o|^2]^{1/2}$

## 2.6 References

- [1] For reviews, see a) M. S. Balakrishna, *Dalton Trans.* **2016**, *45*, 12252–12282; b) H. Niu, A. J. Plajer, R. García-Rodríguez, S. Singh and D. S. Wright, *Chem. Eur. J.* **2018**, *24*, 3073-3082; c) S. G. Calera and D. S. Wright, *Dalton Trans.* **2010**, *39*, 5055-5065; d) M. S. Balakrishna, D. J. Eisler and T. Chivers, *Chem. Soc. Rev.* **2007**, *36*, 650-664; e) E. L. Doyle, L. Riera and D. S. Wright, *Eur. J. Inorg. Chem.* **2003**, 3279-3289 (and references cited therein); f) D. Bawari, B. Prashanth, S. Ravi, K. R. Shamasundar, S. Singh and D. S. Wright, *Chem. Eur. J.* **2016**, *22*, 12027–12033; g) D. Bawari, B. Prashanth, K. Jaiswal, A. R. Choudhury and S. Singh, *Eur. J. Inorg. Chem.* **2017**, 4123-4130; h) M. F. Hawthorne and Z. Zheng, *Acc. Chem. Res.* **1997**, 276-276; i) D. R. Armstrong, A. R. Kennedy, R. E. Mulvey and R. B. Rowlings, *Angew. Chem. Int. Ed.* **1999**, *38*, 131-133; j) W. Clegg, K. W. Henderson, A. R. Kennedy, R. E. Mulvey, C. T. OHara, R. B. Rowlings, and D. M. Tooke, *Angew. Chem. Int. Ed.* **2001**, *40*, 3902-3905; k) A. Bashall, A. D. Bond, E. L. Doyle, F. García, S. Kidd, G. T. Lawson, M. C. Parry, M. McPartlin, A. D. Woods and D. S. Wright, *Chem. Eur. J.* **2002**, *8*, 3377-3385; l) W. C. Marsh, N. L. Paddock, J. Stewart, J. Trotter, *Chem. Commun.* **1970**, 1190-1991; m) W. C. Marsh and J. Trotter, *J. Chem. Soc.* **1971**, 1482-1486; n) M. R. Churchill, C. H. Lake, Sun-Hua L. Chao and O. T. Beachley, *J. Chem. Soc. Chem. Commun.* **1993**, 1577-1578; o) J. S. Ritch and T. Chivers, *Angew. Chem. Int. Ed.* **2007**, *46*, 4610–4613; p) C. von Hänisch, O. Hampe, F. Wigend, S. Stahl, *Angew. Chem. Int. Ed.* **2007**, *46*, 4775.
- [2] a) P. Kommana, K. V. P. Pavan Kumar and K. C. Kumara Swamy, *Indian J. Chem.* **2003**, *42A*, 2371-2375; b) P. Kommana and K. C. Kumara Swamy, *Inorg. Chem.* **2000**, *39*, 4384-4385.
- [3] a) G. S. Ananthnag, S. Kuntavalli, J. T. Mague and M. S. Balakrishna, *Inorg. Chem.* **2012**, *51*, 5919-5930; b) A. Bashall, E. L. Doyle, C. Tubb, S. J. Kidd, M. McPartlin, A.

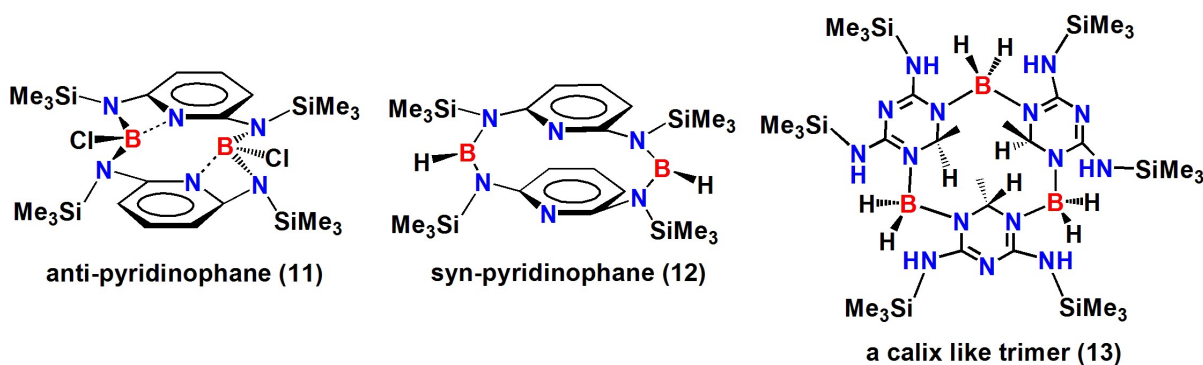
- D. Woods and D. S. Wright, *Chem. Commun.* **2001**, 24, 2542-2543; c) S. G. Calera, D. J. Eisler, J. M. Goodman, M. McPartlin, S. Singh and D. S. Wright, *Dalton Trans.* **2009**, 8, 1293-1296; d) S. G. Calera, D. J. Eisler, J. V. Morey, M. McPartlin, S. Singh and D. S. Wright, *Angew. Chem. Int. Ed.* **2008**, 47, 1111-1114; e) A. J. Plajer, R. R. García-Rodríguez, C. G. M. Benson, P. D. Matthews, A. D. Bond, S. Singh, L. H. Gade, and D. S. Wright, *Angew. Chem. Int. Ed.* **2017**, 56, 9087-9090.
- [4] Y. X. Shi, R. Z. Liang, K. A. Martin, N. Weston, S. G. Calera, R. Ganguly, Y. Li, Y. Lu, A. J. M. Ribeiro, M. J. Ramos, P. A. Fernandes and F. García, *Inorg. Chem.* **2015**, 54, 6423-6432.
- [5] Singlet biradicaloids are characterized by a small energy gap between their lowest energy singlet and triplet states, see F. Breher, *Coord. Chem. Rev.* **2007**, 251, 1007–1043.
- [6] a) T. Beweries, R. Kuzora, U. Rosenthal, A. Schulz and A. Villinger, *Angew. Chem. Int. Ed.* **2011**, 50, 8974-8978; b) A. Hinz, R. Kuzora, U. Rosenthal, A. Schulz and A. Villinger, *Chem. Eur. J.* **2014**, 20, 14659-14673.
- [7] a) J. R. Hartman, R. E. Wolf, B. M. Foxman and S. R. Cooper, *J. Am. Chem. Soc.* **1983**, 105, 131-132; b) R. E. Wolf, J. R. Hartman, J. M. E. Storey, B. M. Foxman and S. R. Cooper, *J. Am. Chem. Soc.* **1987**, 109, 4328-4335; c) J. R. Hartman and S. R. Cooper, *J. Am. Chem. Soc.* **1986**, 108, 1202-1208; d) E. J. Hints, J. R. Hartman and S. R. Cooper, *J. Am. Chem. Soc.* **1983**, 105, 3738-3739; e) S. R. Cooper, S. C. Rawle, J. R. Hartman, E. J. Hints and G. A. Admans, *Inorg. Chem.* **1988**, 27, 1209-1214; f) S. C. Rawle, J. R. Hartman, D. J. Watkin and S. R. Cooper, *J. Chem. Soc., Chem. Commun.* **1986**, 1083-1084; g) J. R. Hartman, E. J. Hints and S. R. Cooper *J. Chem. Soc., Chem. Commun.* **1984**, 386-387.
- [8] A. Nordheider, T. Chivers, R. Thirumoorthi, I. V. Baca and J. D. Woollins, *Chem. Commun.* **2012**, 48, 6346-6348.

- [9] a) A neutral ( $\mu$ -S) bridged planar boron disulfide  $B_8S_{16}$  saturated macrocycle composed of four five-membered  $B_2S_3$  rings is known: W. Siebert, in *The Chemistry of Inorganic Homo- and Heterocycles*, ed. I. Haiduc and D. B. Sowerby, Academic Press, London, **1987**, pp. 143; b) Octahedral Ru(II) and Os(II) complexes of the dianionic 14-membered  $[Et_4As_6S_{10}]^{2-}$  and 16-membered  $[Et_6As_8S_{10}]^{2-}$  sulfur-arsenic rings are also known: T. Hausler, W. S. Sheldrick, *Chem. Ber.* **1996**, *129*, 131-136.
- [10] a) T. Chivers, M. Krahn, M. Parvez and G. Schatte, *Inorg. Chem.* **2001**, *40*, 2547-2553; b) T. Chivers, M. Krahn and M. Parvez, *Chem. Commun.* **2000**, *6*, 463-464; c) A. Nordheider, T. Chivers, R. Thirumoorthi, K. S. A. Arachchige, A. M. Z. Slawin, J. D. Woollins and I. V. Baca, *Dalton Trans.* **2013**, *42*, 3291-3294.
- [11] a) T. Chivers, I. Manners, *Inorganic Rings and Polymers of the p-Block Elements: From Fundamentals to Applications*; RSC Publishing: Cambridge, U.K. **2009**; b) A. Nordheider, K. Hüll, K. S. A. Arachchige, A. M. Z. Slawin, J. D. Woollins, R. Thirumoorthi and T. Chivers, *Dalton Trans.* **2015**, *44*, 5338-5346; c) A. Nordheider, K. S. A. Arachchige, A. M. Z. Slawin, J. D. Woollins and T. Chivers, *Dalton Trans.* **2015**, *44*, 8781-8783; d) A. Nordheider, K. Hüll, J. K. D. Prentis, K. S. A. Arachchige, A. M. Z. Slawin, J. D. Woollins and T. Chivers, *Inorg. Chem.* **2015**, *54*, 3043-3054.
- [12] G. M. Sheldrick, *Acta Crystallogr. Sect. A* **2008**, *64*, 112-122.
- [13] (a). H.-J. Werner, P. J. Knowles, G. Knizia, F. R. Manby and M. Schutz, *WIREs Comput Mol Sci* **2012**, *2*, 242–253; b) MOLPRO, version 2012.1, a package of ab initio programs; (b) H.-J. Werner, P. J. Knowles, G. Knizia, F. R. Manby and M. Schutz, and others, see <http://www.molpro.net>.
- [14] K. R. Shamasundar, G. Knizia and H.-J. Werner, *J. Chem. Phys.* **2011**, *135*, 054101.
- [15] Ugo Varetto, Molekel 5.4., Swiss national supercomputing centre, Lugano, (Switzerland).

## Boraamidinate Bridged [3.3](2,6) Pyridinophanes and a Calix Like Trimer

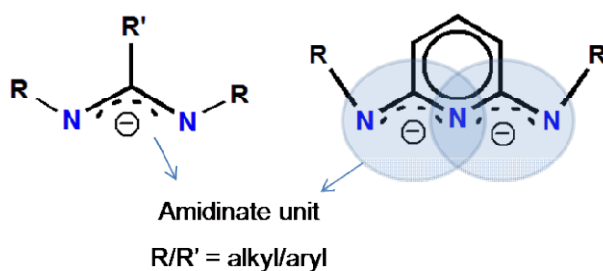
### Chapter 3

**Abstract:** This chapter presents the syntheses and characterization of boron containing tetraazadibora[3.3](2,6)pyridinophanes (**11** and **12**), a calix like trimer (**13**) and macrocycles (**14** and **15**) assembled using the boraamidinate N-B-N bridges. The presence of B as acceptor atoms in the bridges and their coordination with pyridine nitrogen has very strong influence on the conformational rigidity of the pyridinophanes **11** and **12**. The calix like trimer **13** was obtained by the reaction of bis(trimethylsilyl)-N,N'-2,4-diamino-6-(Me)-triazine (BDMT) with  $\text{BH}_3 \cdot \text{SMe}_2$  at room temperature as a result of Markovnikov hydroboration of a  $\text{Me-C=N}$  bond of the triazine ring. Reaction of tris(trimethylsilyl)-N,N',N''-2,4,6-triamino-triazine (TTT) and bis(trimethylsilyl)-N,N'-2,4-diamino-6-(Phenyl)-triazine (BDPT) derivatives of triazine with  $\text{BH}_3 \cdot \text{SMe}_2$  afforded their corresponding adducts **14** and **15** at room temperature. The adducts **14** and **15** were highly stable and did not convert into macrocyclic compounds.



### 3.1 Introduction

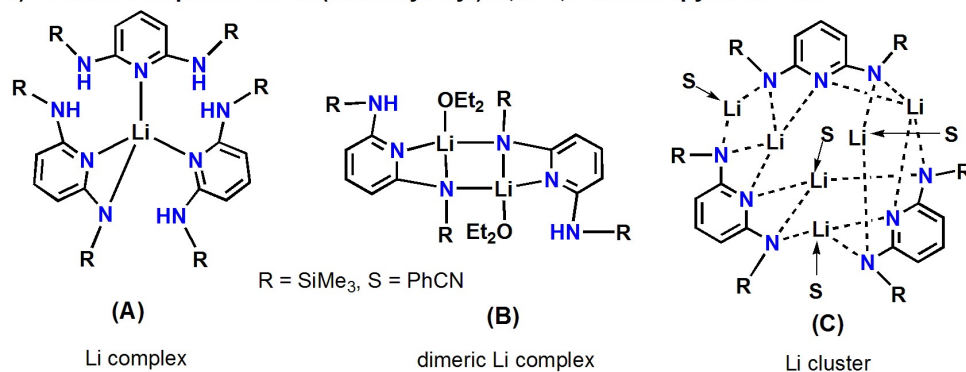
The bonding characteristics of a ligand play a very important role to control the stability, chemical properties and subsequent applications of a coordination compound. Therefore, designing and/or selection of a suitable ligand is a crucial step to modulate coordination abilities (denticity) along with its electronic and steric features.<sup>[1]</sup> In this context, the use of pyridine ring in dianionic chelating amidinate fragment  $[R'N(NR)_2]_2^{2-}$  ( $R'N$  = pyridine,  $R$  = alkyl/aryl) provides combination of various coordination modes and flexibility whereas, the fine tuning of substituents on nitrogen and carbon atoms allows the modifications in steric as well as electronic properties, leading to enormous structural diversity and therefore modified property in inorganic chemistry.



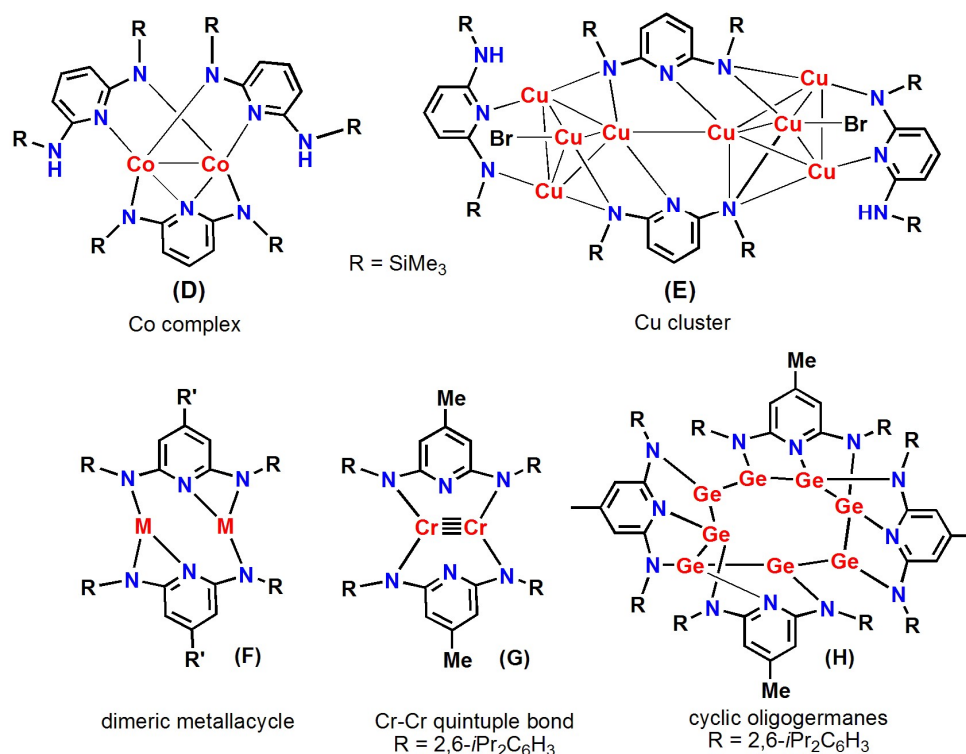
Typical amidinates (left) and 2,6-diaminopyridine system (right) showing amidinate units

2,6-disubstituted pyridine based systems have been important precursors to stabilize multiply bonded systems<sup>[2]</sup> as well as complexes of some transition<sup>[3]</sup> and lanthanide and actinide elements<sup>[4]</sup> where the substituents on their appended nitrogen atoms were altered to modify the ligand characteristics. The work groups of Kempe, Guillet and Trifonov have used N,N'-bis-(trimethylsilyl)-pyridine-2,6-diamine unit to synthesize several metal complexes of lithium, copper and cobalt (**A-E**) (Figure 3.1).<sup>[5]</sup> Tsai and coworkers have used dilithiated 2,6-diamidopyridine units to assemble metallacycles based on chromium (**F**) which are very useful precursor to generate quintuple metal-metal bonds (**G**).<sup>[6]</sup> The same group has also used dilithiated 2,6-diamidopyridine to prepare acyclic and cyclic oligogermanes (**H**).<sup>[7]</sup>

a) Lithium complexes of bis(trimethylsilyl)-N,N'-2,6-diaminopyridine unit



b) Metallacycle and multiple bonds



M = Cr(THF), R = 2,6-*i*Pr<sub>2</sub>C<sub>6</sub>H<sub>3</sub>, R' = Me  
 or R = Si-*i*Pr<sub>3</sub>, R' = H  
 when M = Sn, Ge, R = Si-*i*Pr<sub>3</sub>, R' = H

c) Alkylttrium/lutetium complexes of amidine-amidopyridinate ligands

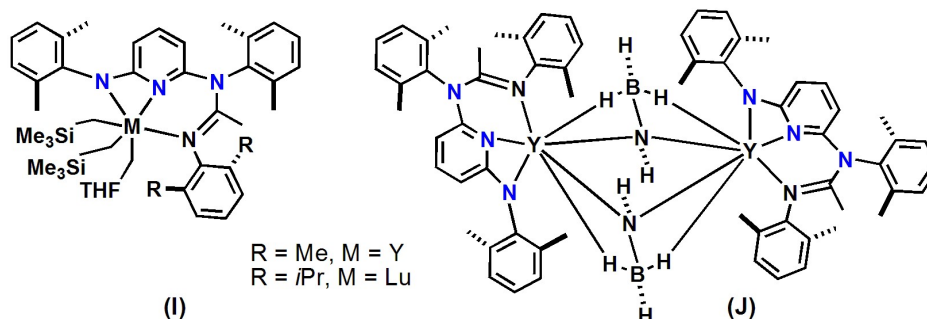
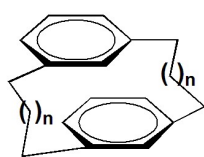


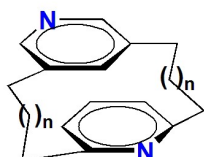
**Figure 3.1** Examples of known molecular assemblies based on 2,6-substituted diaminopyridine unit emphasizing on their diverse application as building blocks.

I Conventional cyclophanes and pyridinophanes ( $n = 1, 2, 3, \dots$ )



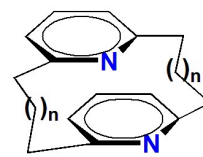
(A)

cyclophane



(B)

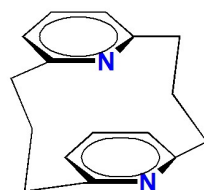
anti-(3,5)pyridinophane



(C)

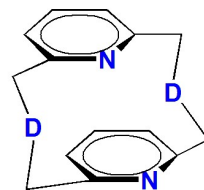
syn-(2,6)pyridinophane

II [3.3](2,6)pyridinophanes with different atoms in bridges



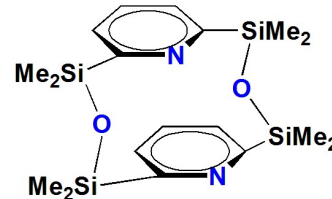
(D)

$-(\text{CH}_2)_3$ -bridge



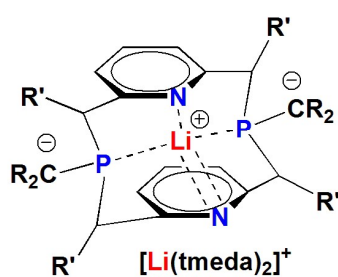
(E)  $D = \text{NH}, \text{O}, \text{S}, \text{Se}$

$-\text{CH}_2\text{-D-CH}_2$ -bridge



(F)

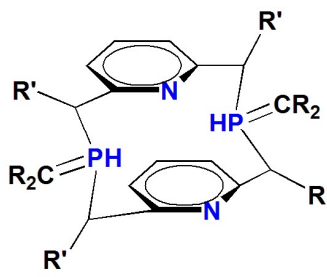
$-\text{SiMe}_2\text{-O-SiMe}_2$ -bridge



(G)

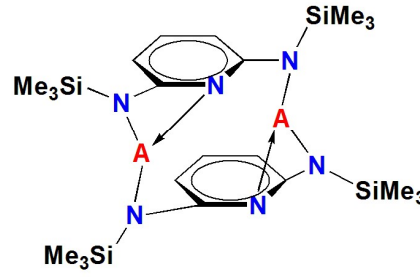
$R = R' = \text{SiMe}_3$

$-\text{CR}'\text{-P}(\text{CR}_2)\text{-CR}'$ - bridge



(H)

$-\text{CR}'\text{-PH}(\text{=CR}_2)\text{-CR}'$ - bridge



(I)

$A = \text{B}, \text{Al}$

$-\text{N-A-N-}$  bridge (present work)  
A = acceptor elements

**Figure 3.2:** Examples of: I) cyclophanes (A) and syn/anti pyridinophanes (B-C); II) [3.3](2,6)pyridinophanes with bridge containing trimethylene unit (D) and different donor atoms (E-H); present work (A = acceptor atom (B, Al)).

Trifonov and coworkers have reported multidentate chelating ligand system by combining amidopyridinate and amidine fragments to synthesize organolanthanides (alkylttrium and lutetium bisalkyl) complexes of amidine–amidopyridinate ligands and their intramolecular  $\text{C}(\text{sp}^3)\text{-H}$  activation and reactivity studies (I-J).<sup>[8]</sup> Many other classical examples include designing of organic donor type molecules/hosts such as, crown ethers,<sup>[9]</sup> azacalixpyridine,<sup>[10]</sup> macrocycles and cryptands,<sup>[11]</sup> with 2,6-disubstituted pyridine units. In particular, such systems have been used as hosts for

transition and lanthanide ions, which possess valuable luminescence properties, as well as of being great importance in inorganic synthesis as catalysts.<sup>[4]</sup> The literature survey shows a huge work particularly on 2,6-disubstituted pyridine based motifs to design the organic pyridinophanes, and their derivatives which show significant applications as pyridoxal models and for metal complexation.<sup>[12,13]</sup> In comparison to conventional cyclophanes (**A**), the introduction of pyridine rings between the bridging units in pyridinophanes results in tunable conformations and additional donor sites. Two types of [3.3]pyridinophanes based on the substitution pattern/position of the pyridine ring, are well known, the first type contains the 3,5-disubstituted pyridine units and provide the building blocks for [3.3](3,5)pyridinophanes (**B**), the second type consists of 2,6-disubstituted pyridine units to assemble [3.3](2,6)pyridinophanes (**C**) (Figure 3.2).<sup>[14]</sup> The [3.3]-bridges that connect the 2,6-disubstituted pyridine rings in pyridinophanes have either been trimethylene  $-(\text{CH}_2)_3-$  (**D**), or heteroatom bridges that contain donor atoms such as  $-\text{CH}_2-\text{D}-\text{CH}_2-$  ( $\text{D} = \text{NH}, \text{O}, \text{S}, \text{Se}$ ) (**E**),  $-\text{SiMe}_2-\text{O}-\text{SiMe}_2-$  (**F**) and  $-\text{CR}'-\text{P}(\text{CR}_2)-\text{CR}'-$  (**G**) or  $-\text{CR}'-\text{PH}(\text{=CR}_2)-\text{CR}'-$  (**H**) ( $\text{R} = \text{R}' = \text{SiMe}_3$ ).<sup>[15]</sup>

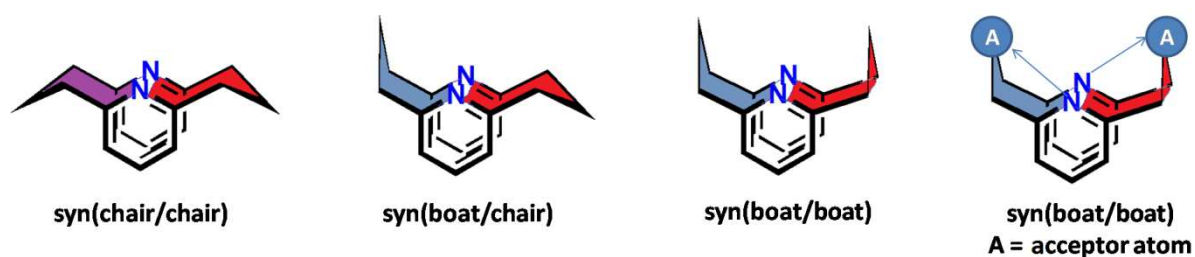


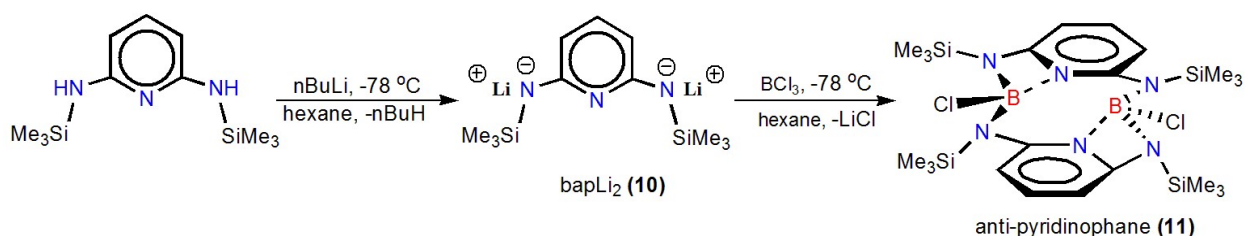
**Figure 3.3** syn-[3.3](2,6)pyridinophanes with different conformations.

Here it is noteworthy to mention that [3.3] pyridinophanes are expected to have two possible isomers i.e, syn and anti, due to the different orientation of pyridine rings across the [3.3] bridges. Out of these two isomers the syn isomer in solution is dynamic in nature and expected to have three stable conformers due to the flipping of bridge between chair and boat

form in solution. The dynamic nature of these conformeric structures such as chair/chair(CC) (similar to cyclooctane ring), chair/boat(CB) and boat/boat(BB) can be elucidated by the variable temperature NMR spectroscopy and computational study (Figure 3.3). It is clear from the examples mentioned above on [3.3](2,6)-pyridinophanes that their [3.3]-bridges have been based on either completely carbon or along with donor heteroatoms whereas, the pyridinophanes containing acceptor atoms in the [3.3]-bridges have not been explored (**I**).<sup>[16]</sup> Herein, we have analyzed the concept that whether the presence of a suitably placed acceptor atom in the bridge would be crucial in bringing conformational rigidity by engaging the pyridine N to interact with itself. As a consequence of successful application of this concept we have assembled conformationally rigid novel tetraazadibora[3.3](2,6)pyridinophanes (**11** and **12**) and their aluminum analogue (Chapter 4, compound **18**) involving donor-acceptor interactions between pyridine nitrogen with group 13 acceptors in the bridges.

### 3.2 Results and Discussion

Colorless crystals of lithium bis(trimethylsilyl)-N,N'-2,6-diamidopyridine (bapLi<sub>2</sub>) (**10**)<sup>5a</sup> as a hexanuclear lithium amido cluster was obtained at -4 °C using reported method by the reaction of bis(trimethylsilyl)-N,N'-2,6-diaminopyridine<sup>[17]</sup> with 2 equivalents of *n*BuLi in hexane (Scheme 3.1). The molecular structure of **10** is depicted in Figure 3.4, which consists of three dianionic diamido ligands coordinated to six Li atoms, where two lithium ions are



**Scheme 3.1** synthesis of anti tetraazadibora[3.3](2,6)pyridinophane (**11**) via bapLi<sub>2</sub> (**10**).

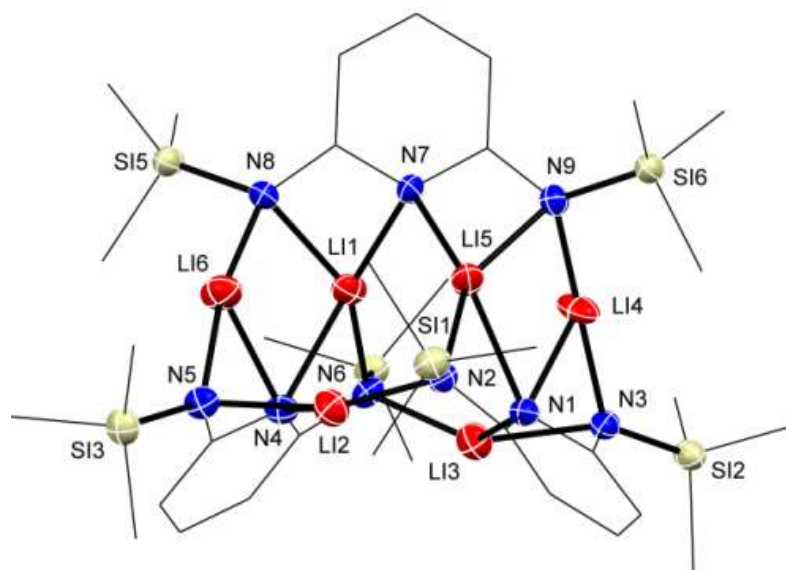


**Figure 3.4** Solid state structure of  $\text{bapLi}_2$  (**10**) with thermal ellipsoids at the 50% probability level.

Selected bond distances [Å] and angles [°]: N(1)–Li(3) 2.192(13), N(1)–Li(4) 2.184(13), N(1)–Li(5) 2.324(13), N(2)–Li(2) 1.966(13), N(2)–Li(5) 1.977(12), N(3)–Li(3) 2.050(13), N(3)–Li(4) 1.975(12), N(7)–Li(1) 2.068(12), N(7)–Li(5) 2.098(12), N(8)–Li(1) 2.048(13), N(8)–Li(6) 1.959(13), N(9)–Li(4) 1.967(12), N(9)–Li(5) 2.032(12), Li(1)⋯Li(2) 3.277(16), Li(1)⋯Li(3) 3.079(17), Li(1)⋯Li(5) 2.920(16), Li(1)⋯Li(6) 2.568(17), Li(2)⋯Li(5) 2.937(16), Li(2)⋯Li(6) 2.694(18), Li(3)⋯Li(4) 2.731(16), Li(4)⋯Li(5) 2.565(17); N(1)–Li(5)–N(2) 64.49(4), N(1)–Li(3)–N(3) 65.34(2), N(1)–Li(4)–N(3) 66.72(4), Li(3)–N(1)–Li(4) 77.23(5), Li(3)–N(1)–Li(5) 106.6(5), Li(4)–N(1)–Li(5) 69.28(4), Li(2)–N(2)–Li(5) 95.7(5), N(2)–Li(2)–N(5) 151.6(7), N(2)–Li(5)–N(7) 143.8(6), N(2)–Li(5)–N(9) 149.2(7), Li(1)–N(7)–Li(5) 88.99(5), Li(1)–N(8)–Li(6) 79.7(5), N(7)–Li(1)–N(8) 68.7(4).

four coordinated and other four are three coordinated. The structure also shows the coordination of one of the pyridine nitrogen to two lithium ions whereas the nitrogen atoms of two other pyridine rings are coordinated to three lithium ions. The stoichiometric reaction of  $\text{bapLi}_2$  (**10**) with  $\text{BCl}_3$  in hexane (Scheme 3.1) afforded a brown solid which on crystallization from hexane at 4 °C in a few days gave colorless crystals of the tetraazadibora[3.3](2,6) pyridinophane (**11**) (yield 37.4 %). The single resonance at 8.11 ppm

in the  $^{11}\text{B}$  NMR spectrum of this product indicated the presence of tetra-coordinated boron. Two signals for the  $\text{SiMe}_3$  groups in the  $^1\text{H}$  NMR (0.33 and 0.08 ppm),  $^{13}\text{C}$  NMR (1.96 and 0.16 ppm) and  $^{29}\text{Si}$  NMR (6.29 and 4.18 ppm) spectra indicated two magnetically different  $\text{SiMe}_3$  groups on each pyridine ring. Additionally, five signals in the  $^{13}\text{C}$  NMR spectra also support the asymmetric environment around each pyridine ring. Based on the HRMS spectrum, the composition of this compound was expected as dimer of two *bap* units bridged by two B-Cl units due to the peak at  $m/z$  595.2179 (cal. 595.2201) for  $[\text{M}+\text{H}]^+$ , and was later confirmed by the single crystal X-ray diffraction analysis (see below).

The solid state structure of pyridinophane **11** was determined using single crystal X-ray diffraction. Compound **11** crystallized in the triclinic system with  $P\bar{1}$  space group. The pyridinophane **11** adopts an anti conformation in the solid state with chair-chair form of the central eight membered  $[\text{N}_4\text{B}_2\text{C}_2]$  ring (Figure 3.5c) similar to that observed in cyclooctane chair-chair conformation. The coordination of pyridine N to the B atom ( $\text{Npy}\cdots\text{B}$ ) plays a crucial role in making this pyridinophane conformationally rigid and results in two planar four membered  $[\text{N}_2\text{BC}]$  chelate that are fused to two diagonally opposite edges (B-N) of the central eight membered  $[\text{N}_4\text{B}_2\text{C}_2]$  ring. Thus the presence of tetra-coordinated boron and the mutual trans orientation of the chlorides are the key factors to provide conformational rigidity to the molecule. The  $\text{SiMe}_3$  groups on the N-B-N bridges adopt gauche conformation to reduce the steric congestion around the central  $[\text{N}_4\text{B}_2\text{C}_2]$  ring. Overall, both pyridine rings in the pyridinophane **11** are bridged by two boraamidinate  $[\text{N-B-N}]$  bridges, the covalent B-N bonds in 4-membered  $[\text{N}_2\text{BC}]$  rings as expected are shorter than the coordinate B-N bonds. The  $\text{N}\cdots\text{N}$  separation between two pyridine rings in **11** is 3.185 Å (Figure 3.5) and their centroids are 5.505 Å apart. The central  $[\text{N}_4\text{B}_2\text{C}_2]$  ring shows a short  $\text{B}\cdots\text{B}$  separation (3.618 Å) much closer as compared to remotely related [4.4]paracyclophane (8.26 Å).<sup>[18]</sup> The structure of **11** showed the weak  $\text{C-H}\cdots\text{Cl}$  interaction (2.939 Å) between one of the hydrogen

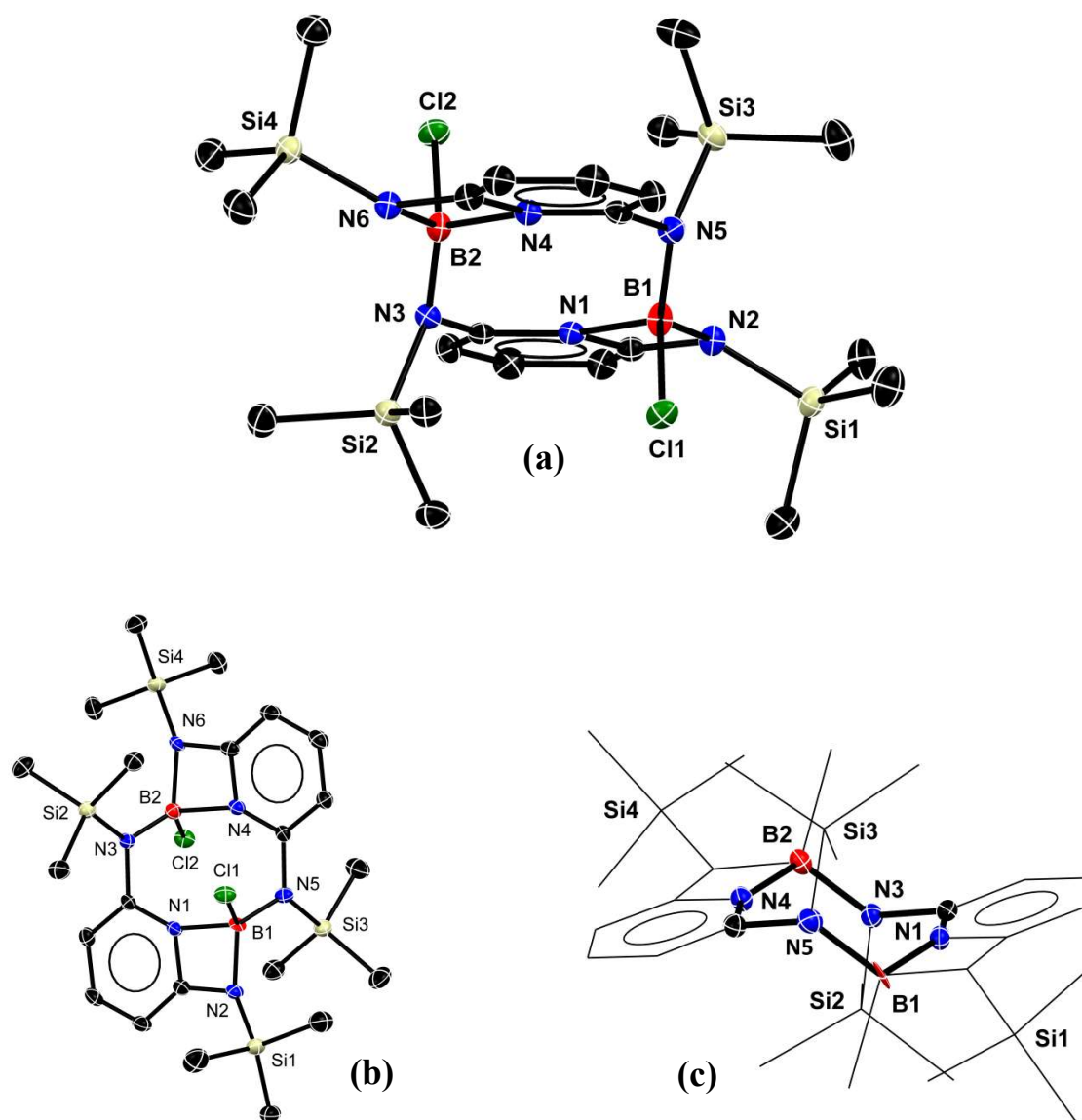


**Figure 3.5** Solid state structure of tetraazadibora[3.3](2,6)pyridinophane **11**; **(a)** with parallel py rings and trans chlorides and showing  $N_{py} \cdots B$  interaction; **(b)** showing central 8 membered  $[N_4B_2C_2]$  ring; and **(c)** the chair-chair conformation of the central  $[N_4B_2C_2]$  ring and anti arrangement of py rings. Thermal ellipsoids are shown at 50% probability level. Selected bond distances [ $\text{\AA}$ ] and angles [ $^\circ$ ]: B1-C11 1.8726(16), B2-Cl2 1.8566(16), B1-N1 1.6465(19), B1-N2 1.5546(19), B2-N3 1.4831(19), B2-N4 1.6554(19), B1-N5 1.4743(19); N2-B1-N1 82.85(9), N5-B1-N1 116.28(12), N5-B1-N2 117.54(12), N6-B2-N3 118.30(12), N4-B2-N3 115.98(11), N6-B2-N4 82.29(9), N1-B1-C11 108.63(9), N2-B1-C11 114.29(10), N5-B1-C11 113.51(10), N4-B2-Cl2 109.14(9), N3-B2-Cl2 113.54(10), N3-B2-Cl2 113.54(10), B1-N2-Si1 132.35(9), B1-N5-Si3 122.79(10), B2-N3-Si2 124.15(10), B2-N6-Si4 135.70(10).

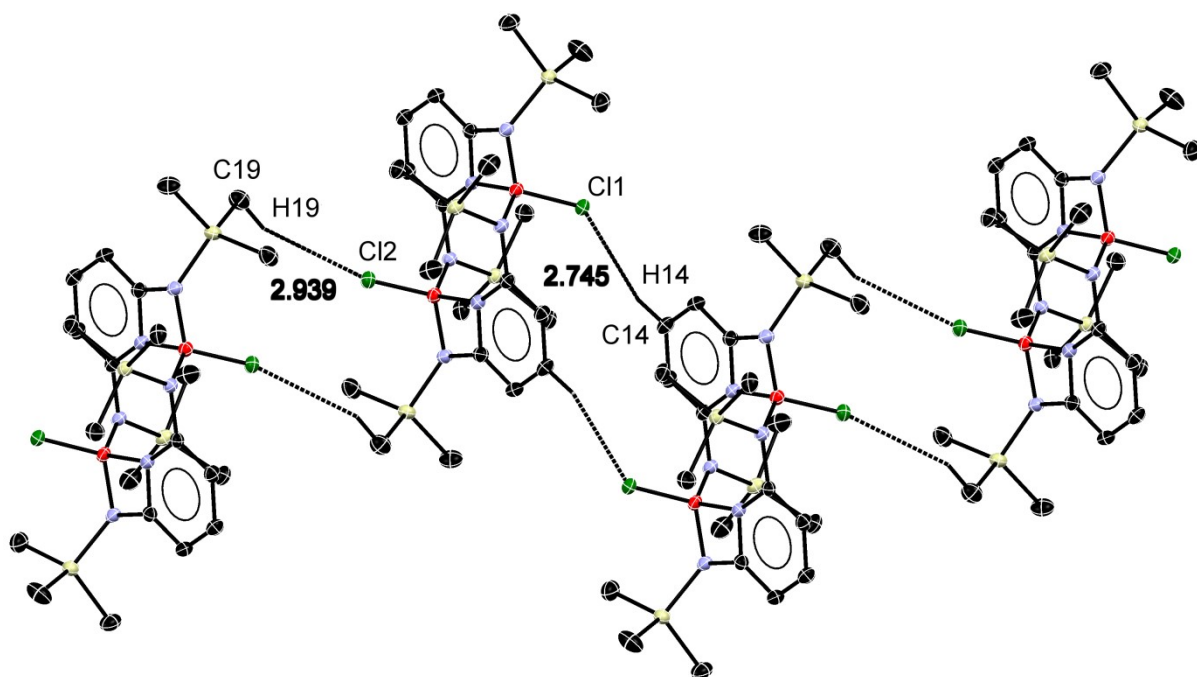
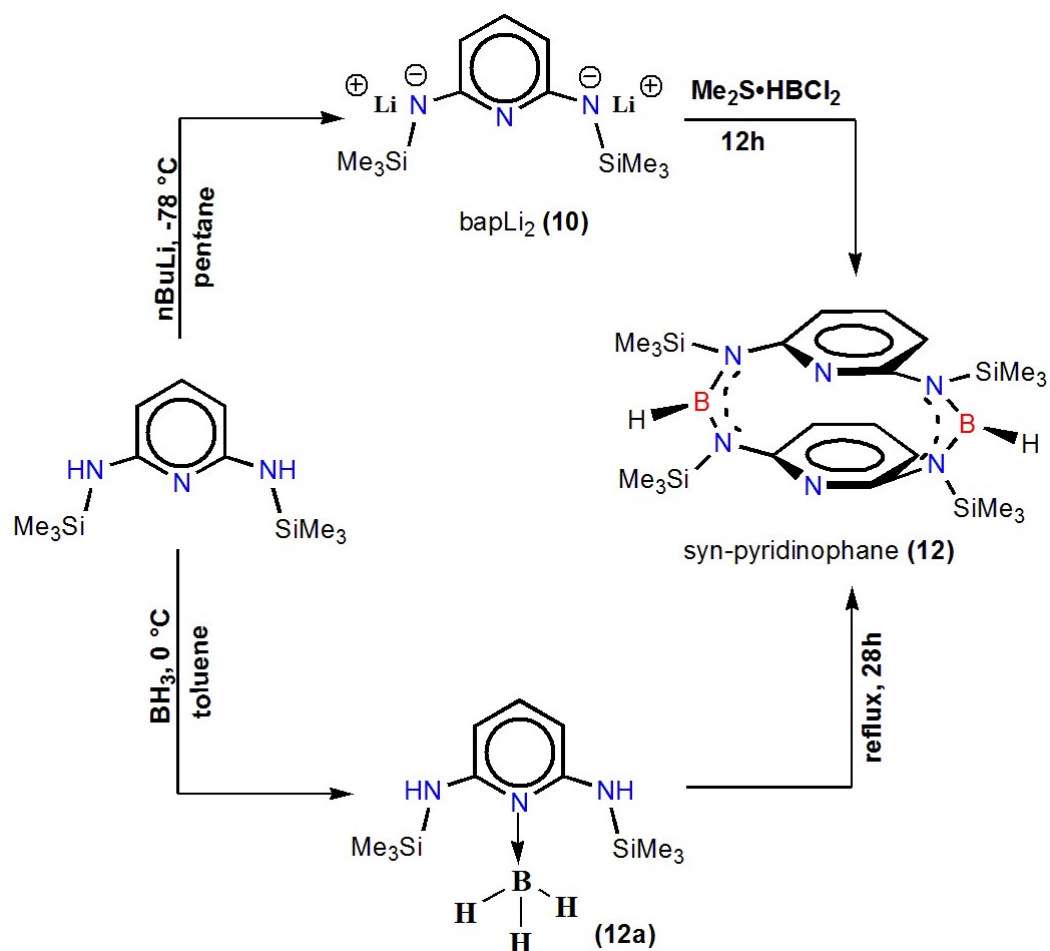


**Figure 3.6** Formation of one dimensional network due to the weak C–H···Cl interaction (2.939 Å and 2.745 Å) between units of tetraazadibora[3.3](2,6)pyridinophane (**11**).

on SiMe<sub>3</sub> group with the chloride atoms of another unit and the another weak interaction (2.745 Å) between the hydrogen of pyridine ring of one unit with the chloride atoms of another unit (Figure 3.6).

Similar reaction of  $\text{bapLi}_2$  (**10**) with  $\text{HBCl}_2 \cdot \text{SMe}_2$  in pentane for 12 h afforded an orange coloured sticky material which on crystallization from pentane at  $-20$  °C produced orange crystals of the tetraazadibora[3.3](2,6)pyridinophane (**12**) (21 % yield) (Scheme 3.2). The IR spectrum of **12** showed a band at  $2450 \text{ cm}^{-1}$  attributed as the B–H stretch.<sup>[19]</sup> A single resonance at 27 ppm in the  $^{11}\text{B}$  NMR spectrum of **12** was assigned to three-coordinated boron centre (unlike the  $^{11}\text{B}$  NMR signal for tetra-coordinated boron in **11** (8.11 ppm)). Contrary to the pyridinophane **11**, the single peak for SiMe<sub>3</sub> groups in the  $^1\text{H}$  NMR (0.05 ppm),  $^{13}\text{C}$  NMR (1.2 ppm) and  $^{29}\text{Si}$  NMR (11 ppm) spectra attributed to a symmetrical structure of **12**. The HRMS pattern at  $m/z$  527.2979 (cal. 527.2992  $[\text{M}+\text{H}]^+$ ) suggested that **12** also exists as dimer of two *bap* units bridged by two B–H groups.



**Scheme 3.2** Synthesis of syn tetraazadibora[3.3](2,6)pyridinophane (**12**)

High sensitivity of  $\text{bapLi}_2$  (**10**) towards adventitious moisture and an extra step involved in the synthesis of **12** prompted us to discover alternate, convenient and high yielding synthesis by reacting equimolar amounts of bis(trimethylsilyl)-N,N'-2,6-diaminopyridine with  $\text{BH}_3\cdot\text{SMe}_2$  in toluene at  $0\text{ }^\circ\text{C}$  (for 3 h) followed by reflux for 28 h. Based on the in-situ NMR investigations, this reaction first leads to the formation of the adduct [bis(trimethylsilyl)-N,N'-2,6-diaminopyridine] $\cdot\text{BH}_3$  (**12a**) (Scheme 3.2). This adduct formation was identified by a broad quartet at  $-23.43$  to  $-25.67$  ppm in  $^{11}\text{B}$  NMR and the presence of a broad B–H signal in both IR ( $2324\text{ cm}^{-1}$ ) and  $^1\text{H}$  NMR (2.11–1.79 ppm) spectra. The N–H peak for adduct **12a** was observed as downfield shifted at 6.38 ppm in  $^1\text{H}$  NMR spectrum (*c.f.* 4.46 ppm for starting material) also a

red shift in the IR frequency for the N-H stretch at  $3302\text{ cm}^{-1}$  ( $3394\text{ cm}^{-1}$ , compared to starting material). Refluxing the adduct **12a** in toluene for 28 h produced exclusively compound **12** in more than 88 % yield. The formation of this product could be easily followed due to the disappearance of N-H signal (present in starting material) in IR as well as in  $^1\text{H}$  NMR spectra. Moreover, the appearance of a new signal at  $2450\text{ cm}^{-1}$  in IR spectrum and the presence of a peak at 28 ppm in  $^{11}\text{B}$  NMR spectrum articulate that the N-H protons have been displaced by the boron atoms.

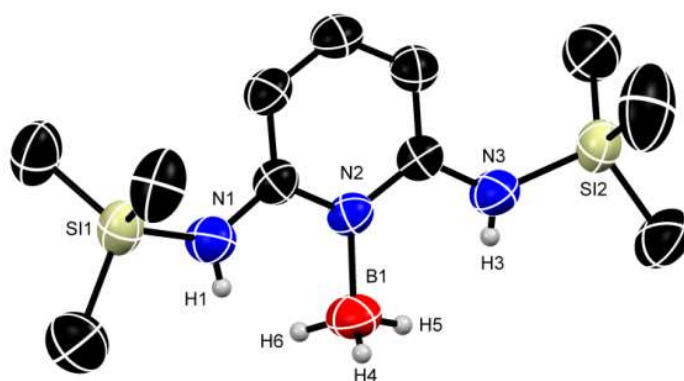


**Figure 3.7** Solid state structure of trihydridoborane adduct with bis(trimethylsilyl)-N,N'-2,6-diaminopyridine (**12a**). All hydrogens except that on boron and nitrogen have been omitted for clarity. Thermal ellipsoids are drawn at 50% probability. Selected bond lengths [ $\text{\AA}$ ] and angles [ $^\circ$ ]: B1-H1 0.960(4), B1-H2 0.960(4), B1-H3 0.960(4), N1-H1 0.769(3), N3-H3 0.684(2), B1-N2 1.601(3); N2-B1-H4 109.47(2), N2-B1-H5 109.47(2), N2-B1-H6 109.47(2), H4-B1-H5 109.47(3), H5-B1-H6 109.47(3), H4-B1-H6 109.47(3).

The solid state structure of adduct **12a** and pyridinophane **12** were determined using single crystal X-ray diffraction. Adduct **12a** crystallized in the monoclinic system with  $P2_1/c$  space group whereas, pyridinophane **12** crystallized in the triclinic system with  $P\bar{1}$  space group. Single crystal X-ray structure of **12a** showed the formation of borane-pyridine adduct with a B-N distance of  $1.601(3)\text{ \AA}$ . Other features of **12a** were consistent with the spectroscopic data.

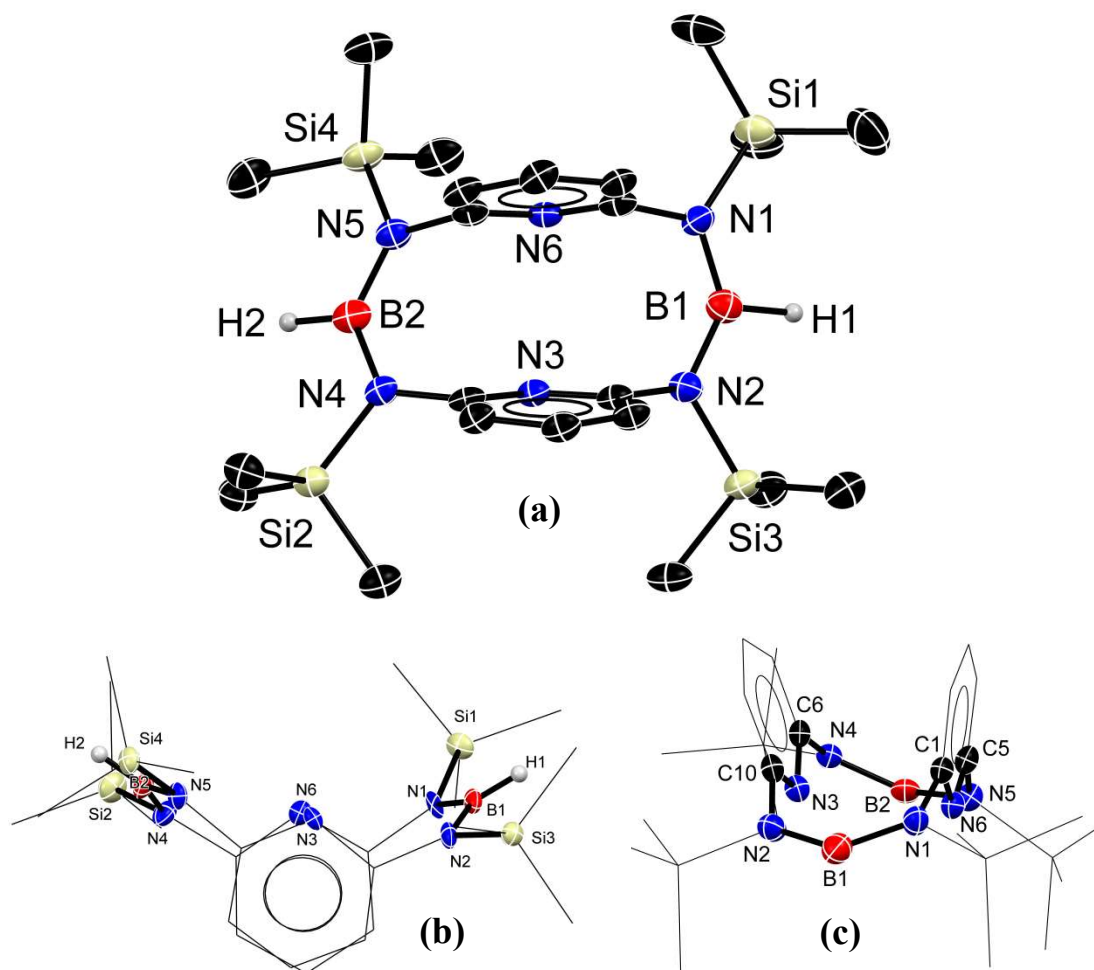


**Figure 3.8** Solid state structure of tetraazadibora[3.3](2,6)pyridinophane **12**; **(a)** depicting the pyridinophane form of **12** with syn orientation of py rings and mutual cis orientation of hydrides and absence of  $N_{py} \cdots B$  interaction; **(b)** Syn (boat, boat) conformation of **12**, and **(c)** the boat conformation of the central  $C_2N_4B_2$  ring. Thermal ellipsoids are shown at the 50% probability level; selected bond distances [Å] and angles [°]: B1-H1 1.27(3), B2-H2 1.14(3), B1-N1 1.417(5), B1-N2 1.437(5), B2-N4 1.447(5), B2-N5 1.423(5), N1-Si1 1.764(3), N2-Si3 1.770(3), N4-Si2 1.773(3), N5-Si4 1.767(3); N1-B1-N2 129.3(4), N4-B2-N5 128.4(4), N1-B1-H1 115.3(14), N2-B1-H1 115.3(14), N4-B2-H2 118.2(15), N5-B2-H2 113.3(15) Si1-N1-B1 120.1(3), Si3-N2-B1 117.6(3), Si2-N4-B2 119.6(3), Si4-N5-B2 124.1(3).

Unlike **11**, the pyridine rings in **12** occupy syn conformation possibly due to absence of the coordination of pyridine nitrogen with the boron (Figure 3.8). The similar B-N bond lengths and three-coordinated planar arrangement around boron atoms in the N-B-N bridges

(sum of bond angles  $359.93^\circ$ ) are suggestive of considerable electronic delocalization leading to partial double bond character and rigidity in these bridges. The structure of **12** showed the pyridinophane structure comprised of the central twelve membered  $[N_3BC_2]_2$  ring. The B $\cdots$ B separation between transannular B atoms in **12** is 5.736 Å in contrast to **11** (which showed close B $\cdots$ B separation 3.618 Å) causing the centroids of the pyridine rings to move closer in **12** (3.282 Å) as compared to **11** (5.506 Å). The N-B-N and N-B-H bond angles in **12** respectively, lie in the range ( $128.41$ – $129.37^\circ$ ) and ( $113.32$ – $118.26^\circ$ ). The hydrides on B atoms have mutual cis orientation. The structure of **12** showed the weak C–H $\cdots$ N interaction (2.518 Å) between the para hydrogen on pyridine ring and the nitrogen atom on pyridine ring of another molecule hence forms one dimensional network (Figure 3.9).

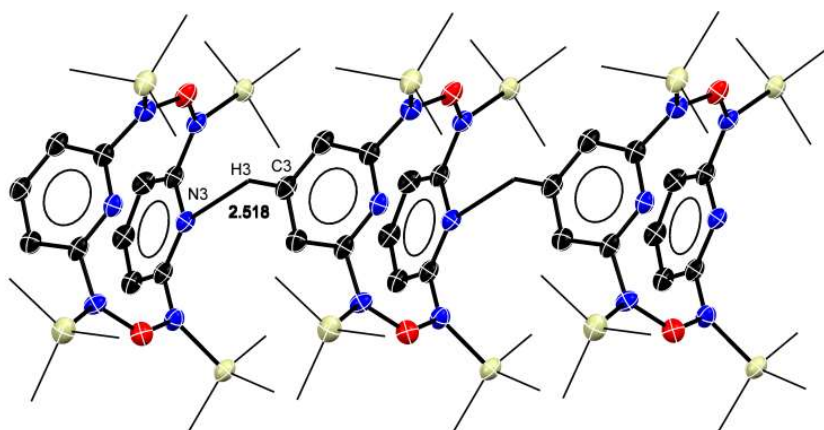


**Figure 3.9** Formation of one dimensional network due to the weak C–H $\cdots$ N interaction (2.518 Å) between adjacent units of tetraazadibora[3.3](2,6)pyridinophane (**12**) in the solid state.

The  $^1\text{H}$  NMR spectra of the pyridinophane **11** at various temperatures are shown in Figure 3.10. At 15 °C, two broad, partially coalesced lines (6.05 and 5.82 ppm) are seen for the pyridine H at 3- and 5-positions; complete coalescence occurs on raising the temperature to 30 °C and the single broad peak starts to broaden as the temperature is raised further to 45 °C. At 60 °C a clear broad doublet was observed (5.97 ppm,  $J = 8$  Hz) due to fast exchange/switching of B between the two N,N' donor pairs of a bap unit and the result is the

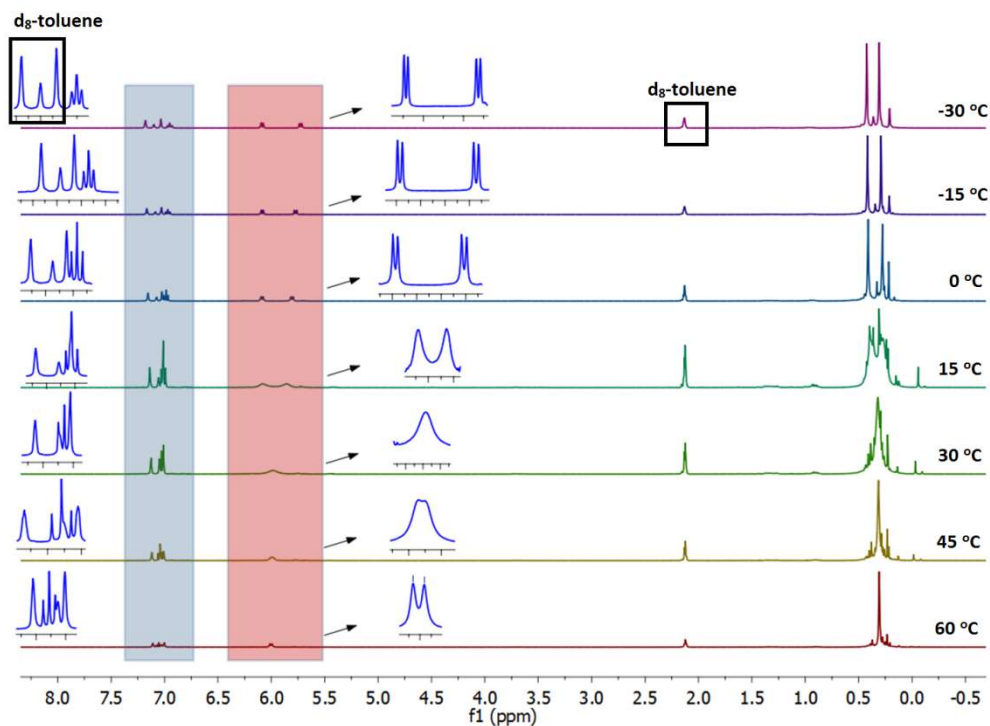


**Figure 3.10** Variable temperature  $^1\text{H}$  NMR spectra (in  $\text{d}_8$ -toluene) of pyridinophane **11** to show its conformational rigidity.

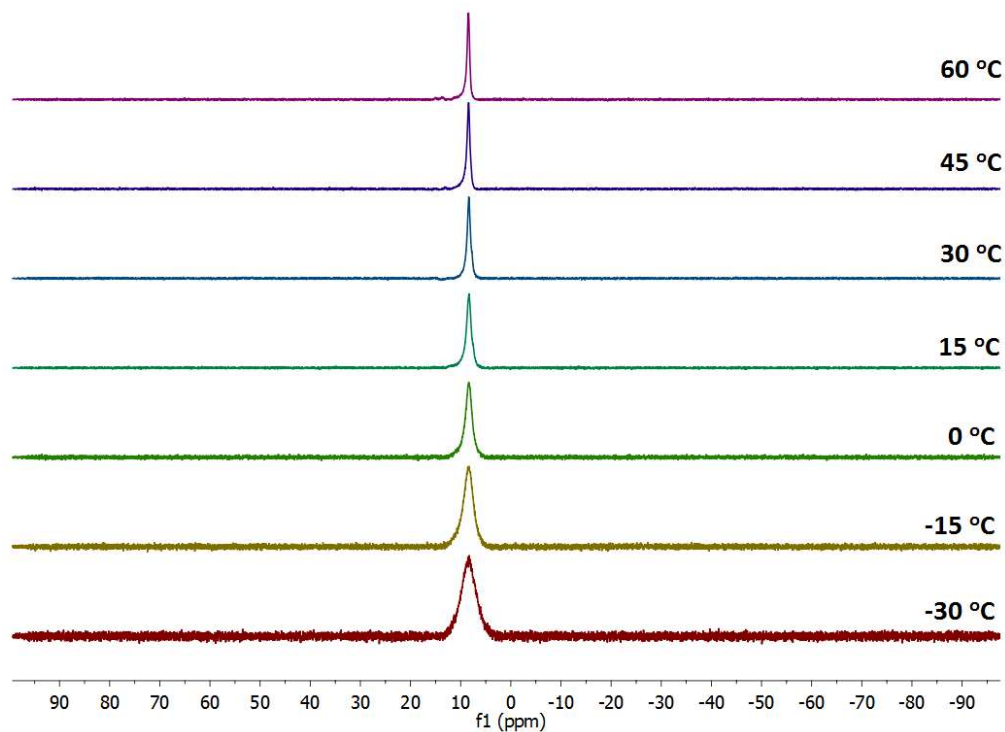


**Figure 3.11** Variable temperature  $^{11}\text{B}$  NMR spectra (in  $\text{d}_8$ -toluene) of pyridinophane **11** to show its conformational rigidity.

AX<sub>2</sub> pattern for pyridyl hydrogens. Below 0 °C, the static spectrum with clear coupling constants ( $J = 8$  Hz) was observed demonstrating that in cold solutions (below 0 °C) **11** is static with respect to any exchange processes. Below 0 °C, two sets of doublets for hydrogens at 3- and 5-position of pyridyl were observed as they become chemically and magnetically different and the three H of a pyridyl unit form AMX spin system. The H at 4-position of the pyridyl shows two overlapped doublets which coincidentally appear as a triplet below 0 °C. <sup>11</sup>B NMR spectra of **11** at various temperatures showed a single resonance at 8.4 ppm (Figure 3.11) indicating that boron centres remained in the same coordination static state as far as the <sup>11</sup>B NMR time scale is concerned, except slight variation in the peak width due to the change in temperature. The <sup>1</sup>H NMR spectra of the pyridinophane **12** in the temperature range +50 to –60 °C are shown in Figure 3.12. The spectra show that the NMR spectral feature (a doublet (6.07 ppm,  $J = 8$  Hz) and a triplet (6.72 ppm,  $J = 8$  Hz) due to pyridiyl hydrogens and a singlet due to SiMe<sub>3</sub> group (0.19 ppm)) of **12** remains unchanged at elevated as well as lower temperatures indicating its conformational rigidity in solution.

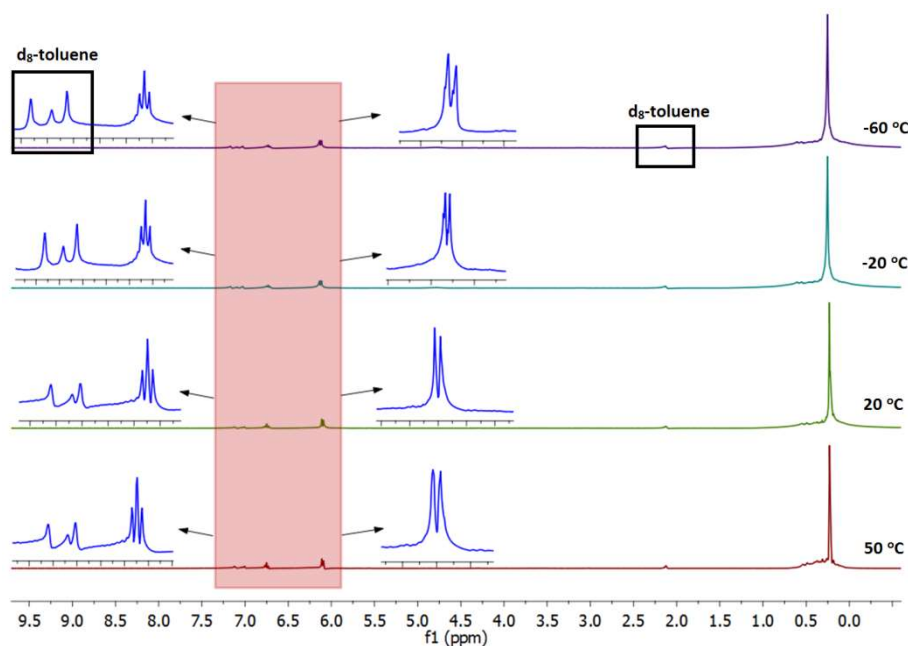
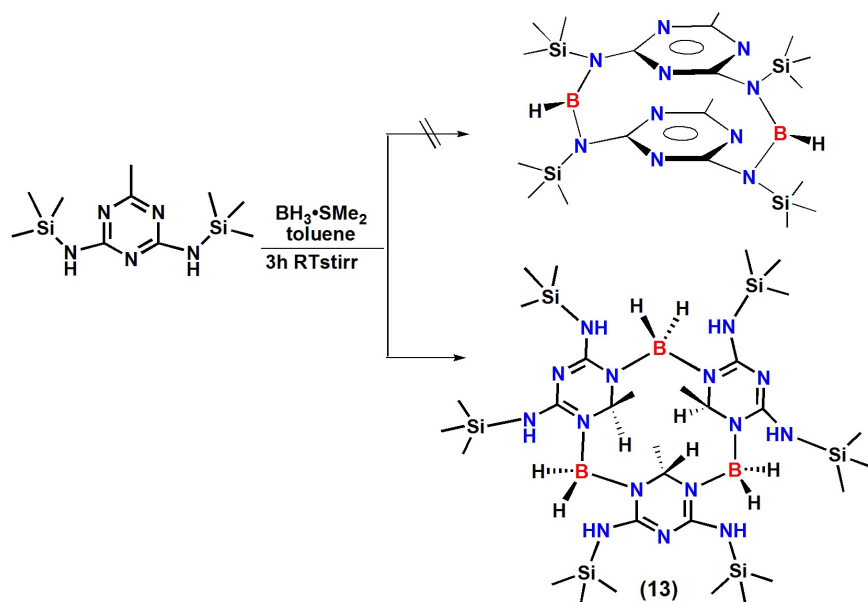


**Figure 3.12** Variable temperature <sup>1</sup>H NMR spectra (in d<sub>8</sub>-toluene) of pyridinophane **12** to show its conformational rigidity.

Similar to the formation of **12**, the reaction of  $\text{BH}_3 \cdot \text{SMe}_2$  with bis(trimethylsilyl)-*N,N'*-2,4-diamino-6-(Me)-triazine (BDMT) was also expected to produce a cyclic structure with evolution of  $\text{H}_2$  gas however, in this case an unexpected product was obtained due to the Markovnikov hydroboration (addition of B–H bond) of one of the Me–C=N bond of triazine ring (Scheme 3.3). The reaction did not show any visible evolution of  $\text{H}_2$  gas however, after few minutes the solution turned from slight turbid to clear transparent. The HRMS spectrum of the isolated product showed the presence of a signal at 849.5459 (calcd. 849.5459 for  $[\text{M}^+]$ ) indicating the formation of a cyclic trimer.



**Scheme 3.3** Synthesis of an unprecedented boraamidinate bridged calix like trimer (**13**).

The initial spectroscopic investigation of this trimer showed the presence of unreacted N–H bonds ( $3355 \text{ cm}^{-1}$ ) with a newly emerged B–H signals ( $2331 \text{ cm}^{-1}$ ) in the IR spectrum. The  $^1\text{H}$  NMR spectrum also showed N–H signals at three different positions (5.59, 5.06 and 4.89 ppm) with each corresponding to two NH protons (Figure 3.13). A broad signal at 2.64 ppm (B–H) for 6 hydrogens in  $^1\text{H}$  NMR spectrum in addition to a broad signal at  $-13.13$  ppm in  $^{11}\text{B}$  NMR spectrum attributed to the tetracoordinated boron centre. On looking carefully, the  $^1\text{H}$  NMR spectrum showed a drastic shift (2.20 ppm for BDMT) for the methyl groups

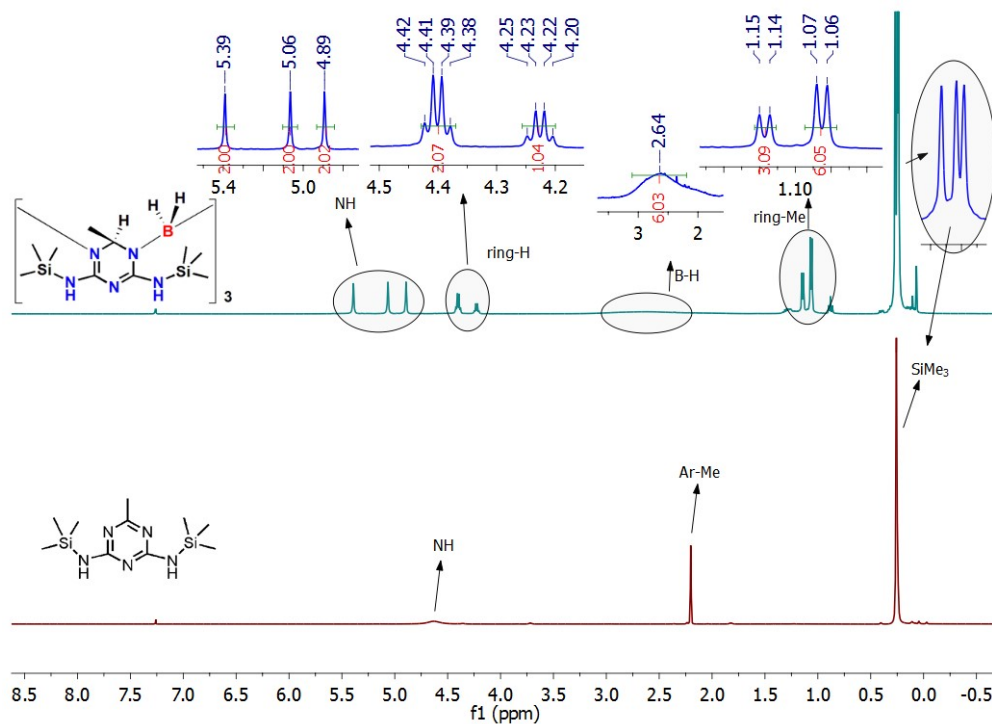


**Figure 3.13** Comparative  $^1\text{H}$  NMR spectra of BDMT (bottom) in reaction with  $\text{BH}_3\cdot\text{SMe}_2$  yielding a calix like trimer (**13**) (top).

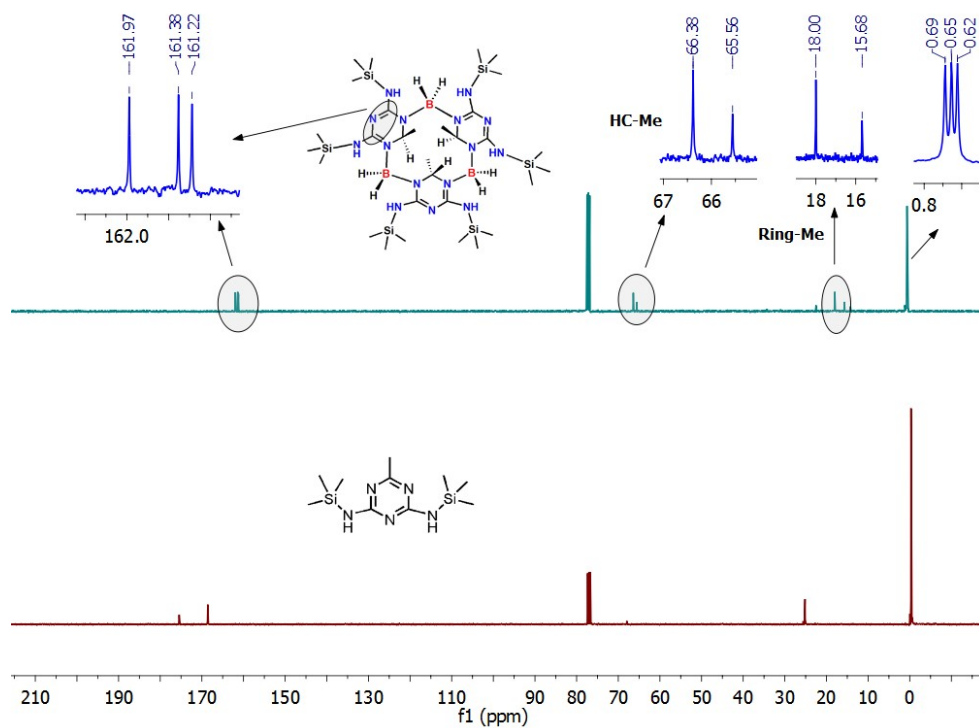


**Figure 3.14** Comparative  $^{13}\text{C}$  NMR spectra of BDMT (bottom) in reaction with  $\text{BH}_3\cdot\text{SMe}_2$  yielding a calix like trimer (**13**) (top).

(Ar–Me) of triazine rings, observed as two separate sets of doublets (1.13 and 1.07 ppm) in 3:6 ratio with a coupling of 4 Hz (Figure 3.13). In addition to these two doublets a set of two newly emerged quartets (4.40 and 4.22 ppm) was also observed (Ar–H) showing a 1:2 ratio with a coupling of 4 Hz. The ratio (1:2) and coupling constant (4 Hz) of both these doublets and quartets features indicated that the aromaticity of triazine ring has been diminished by the addition of B–H bonds across the Me–C=N bond of triazine ring.  $^1\text{H}$  NMR (0.27, 0.25 and 0.24 ppm),  $^{13}\text{C}$  NMR (0.69, 0.65 and 0.62 ppm) and  $^{29}\text{Si}$  NMR (5.07, 4.90 and 4.63 ppm) spectra showed three different signals for  $\text{SiMe}_3$  groups (Figure 3.14). Overall these observations indicate the presence of two types of triazine rings in 1:2 ratios which was later

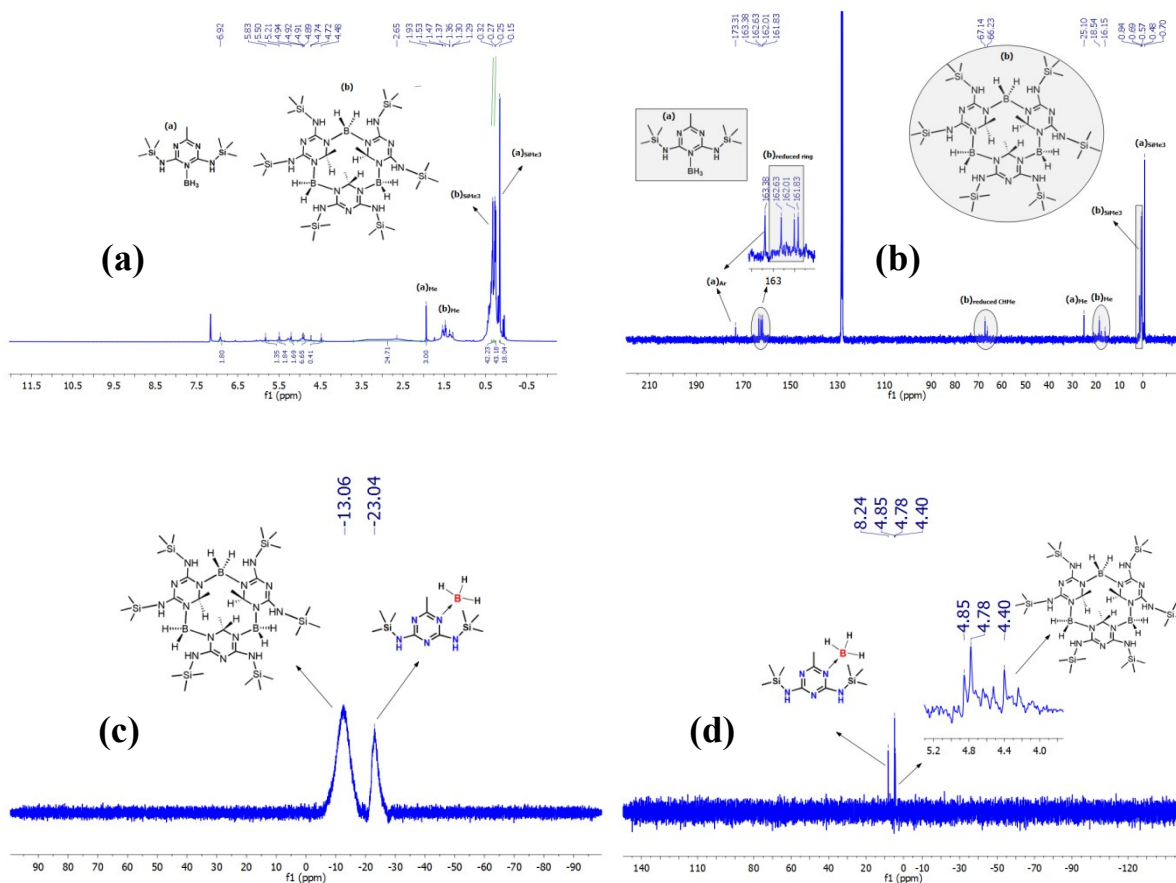


**Figure 3.15** Heteronuclear NMR spectra ( $\text{CDCl}_3$ ) to show the formation of  $\text{BDMT}\cdot\text{BH}_3$  adduct and subsequent formation of the trimer (**13**) in the reaction mixture after 5 min: (a)  $^1\text{H}$  NMR spectrum; (b)  $^{13}\text{C}$  NMR spectrum; (c)  $^{11}\text{B}$  NMR spectrum and (d)  $^{29}\text{Si}$  NMR spectrum.

confirmed by the single crystal structure of **13**. This trimeric macrocycle was stable against air and moisture for weeks without decomposition, also it is highly hydrophobic and showed no decomposition in  $\text{CDCl}_3\text{-D}_2\text{O}$  mixture as analyzed by NMR even after 2 days. The careful investigation of trimeric product attributed its very fast formation (in 15 minute only) therefore attempt to isolate the intermediate triazine-borane adduct (**13c**) during the course of the reaction in pure form was not possible. However, a mixture of trimeric macrocycle was obtained along with the expected intermediate triazine-borane adduct on acquiring the NMR data at very less time (5 min reaction).  $^1\text{H}$  and  $^{13}\text{C}$  NMR spectra of adduct **13c** were consistent with its expected values along with the signals at -23.04 and 8.24 ppm respectively, in  $^{11}\text{B}$  and  $^{29}\text{Si}$  NMR spectra which confirmed its formation (Figure 3.15).

The single crystal X-ray structure of trimeric macrocycle **13** showed its two isomorphous structures, one in orthorhombic and the other in monoclinic system with  $P222$  and  $P2_1/c$  space group, respectively (Figure 3.16). Both of these isomorphous structures are almost mirror image to each other and consist of a 12 member macrocycle that is comprised of a trimeric unit connected through three boraamidinate (N-B-N) units where each boron centre is connected to two hydride groups. The structure corroborates the formulation of a trimeric macrocycle by the hydroboration of triazine ring instead of reacting to the terminal N-H groups. The reduction of triazine rings in both isomorphs could be seen by the tetrahedral geometry around the carbons after hydroboration. The average bond lengths of reduced C-N bond in triazine rings are 1.458 Å (N1-C1, N2-C1 in **13**) and 1.487 Å (N1-C1, N3-C1 in **13'**) showing single bond character whereas, the rest of backbone still contain the double bond character 1.33–1.34 Å for all C=N (Figure 3.13). As observed in  $^{11}\text{B}$  NMR (-13.13 ppm) the tetrahedral geometry around boron centres was also supported by the X-ray structure attributing their connection to two reduced triazine units and two hydride atoms.

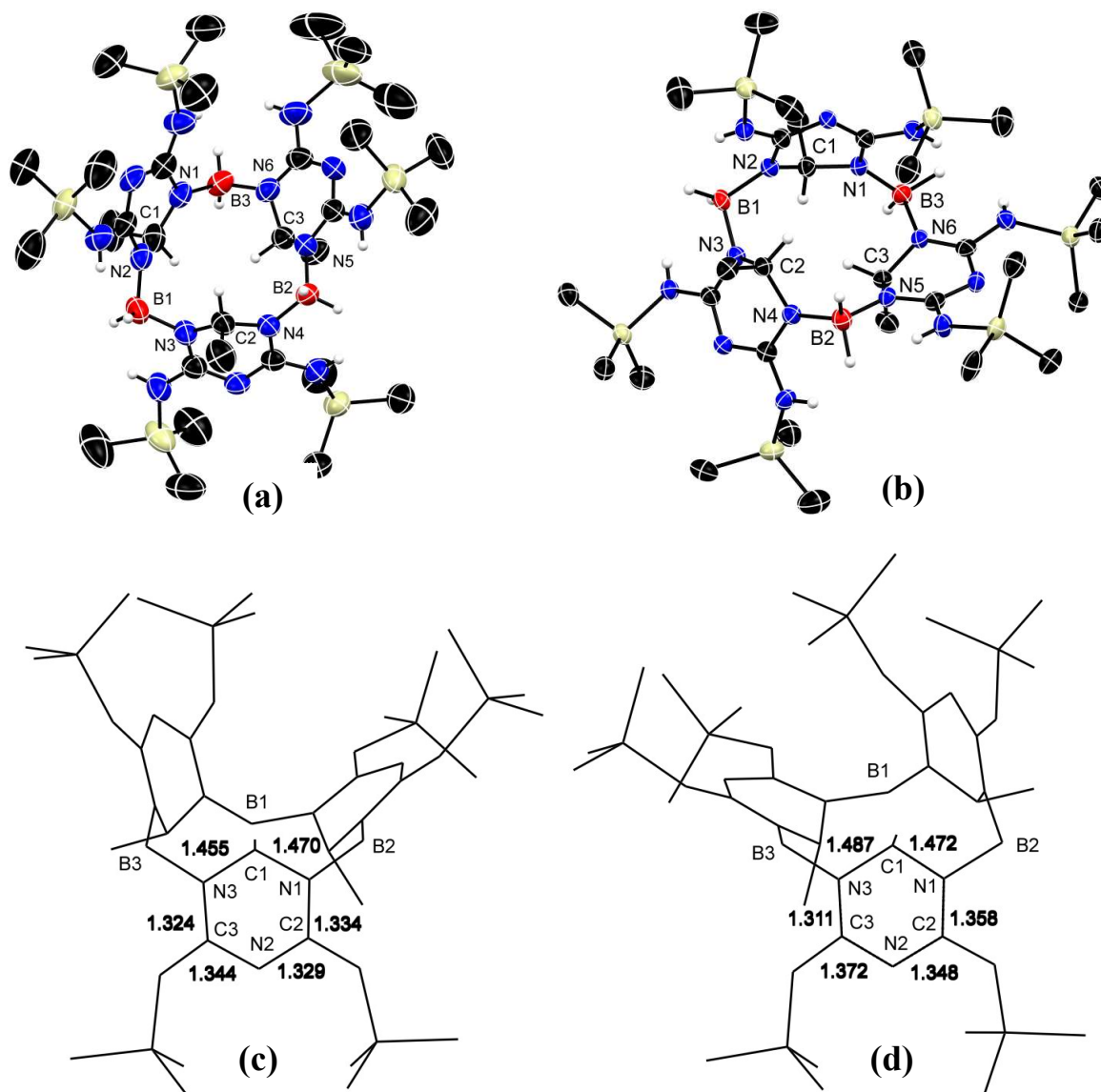


**Figure 3.16** Solid state structures of the calix like trimer (**13**) with thermal ellipsoids at the 50% probability level; (a) and (b) show single crystal X-ray structure for **13** and its isomeric structure **13'** respectively along with their calixarene view as (c) and (d). Selected bond distances [ $\text{\AA}$ ] and angles [ $^\circ$ ]: for **13**: B-H 0.970(11), B1-N2 1.546(9), B1-N3 1.552(7), B2-N4 1.533(7), B2-N5 1.568(11), B3-N1 1.562(9), B3-N6 1.551(9), C1-N1 1.470(7), C1-N2 1.455(7); N2-B1-N3 109.06(3), N4-B2-N5 110.37(11), N1-B3-N6 108.74(6), H-B1-H 108.29(6), N1-C1-N2 110.59(9), N3-C2-N4 111.32(6); for **13'**: B-H 1.163(4), B1-N2 1.548(11), B1-N3 1.584(11), B2-N4 1.552(3), B2-N5 1.573(5), B3-N1 1.556(3), B3-N6 1.564(11), C1-N1 1.472(6), C1-N2 1.468(7); N2-B1-N3 107.05(5), N4-B2-N5 110.04(3), N1-B3-N6 107.25(2), H-B1-H 111.19(7), N1-C1-N2 110.40(5), N3-C2-N4 109.32(4).

The formation of the trimeric macrocycle can be seen as linkage of three reduced triazine units by intermolecular coordinate N→B bonds that keep them intact even in solution which can be seen by the presence of two types of signals (2:1) in heteronuclear NMR spectra and consistent with the X-ray structure where one of the ring is oriented opposite to other two comprising a calix type of structure.

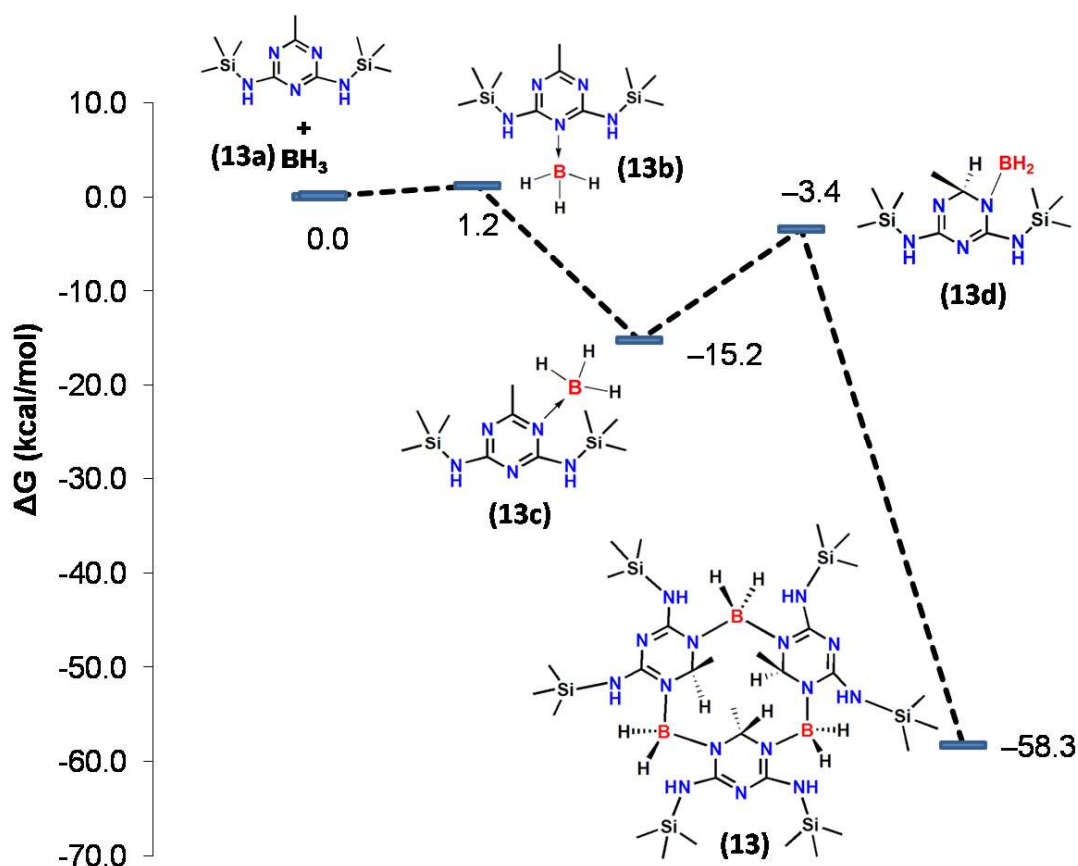


**Figure 3.17** Energy profile diagram: for schematically depicted plausible mechanism for the complexes (13a-13d and 13) involved in dearomative hydroboration of BDMT.

Attempts to hydroborate all C=N bonds of triazine ring using either excess of  $\text{BH}_3 \cdot \text{SMe}_2$  or with Lewis acid,  $\text{B}(\text{C}_6\text{F}_5)_3$  as catalyst were unsuccessful.<sup>[21]</sup> To clarify the nature of transformation involved during the dearomative hydroboration the geometries of different structures of BDMT and borane (13a-d and 13) have been optimized using density functional theory (DFT/B3LYP) in their ground states. The geometry optimization and frequency calculations of all these structures have been

carried out at B3LYP/6-311++G(d,p) level. The results of these calculations were in good agreement with the experimental observations and show the formation of trimer through a series of transformations between borane and BDMT.

Figure 3.17 depicts the energy profile diagram for the intermediate species involved during the dearomative hydroboration. The energy profile suggested that out of two possible adducts (**13b** and **13c**) of BDMT·BH<sub>3</sub> the reaction proceeds through the formation of more stable adduct **13c** ( $\Delta G = -15.2$  kcal/mol) (more stable than **13b** ( $\Delta G = 1.2$  kcal/mole)). The adduct **13c** undergoes dearomatization of the triazine rings via hydroboration and forms, **13d** ( $\Delta G = -3.4$  kcal/mol) as the dearomatized product. The self sorting of three molecules of **13d** affords a highly stable macrocycle as a trimer **13** ( $\Delta G = -58.3$  kcal/mol).

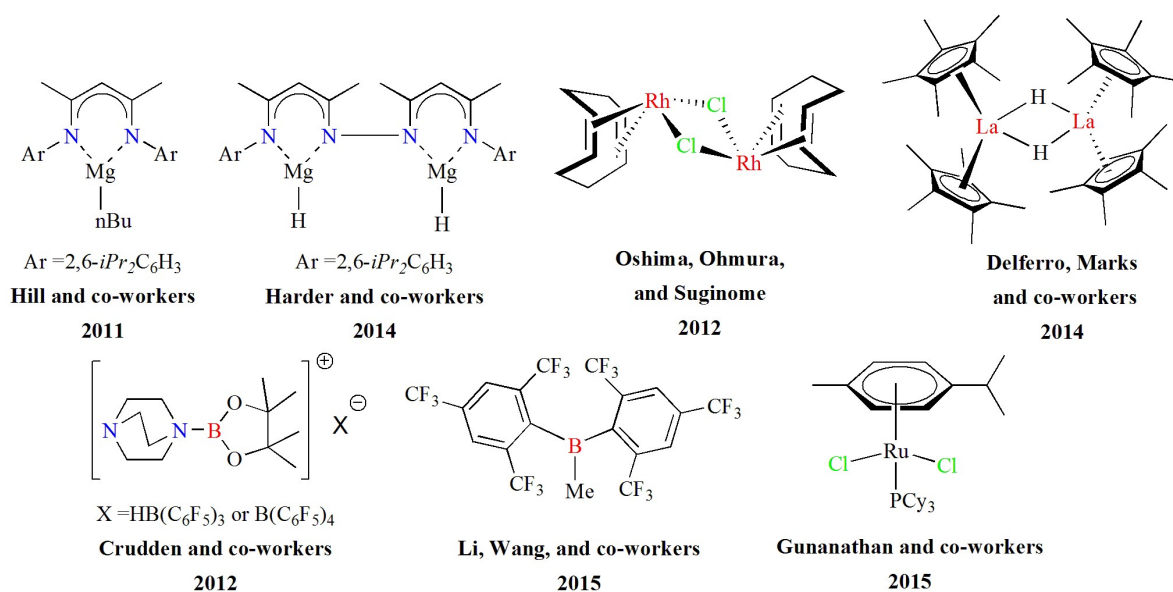
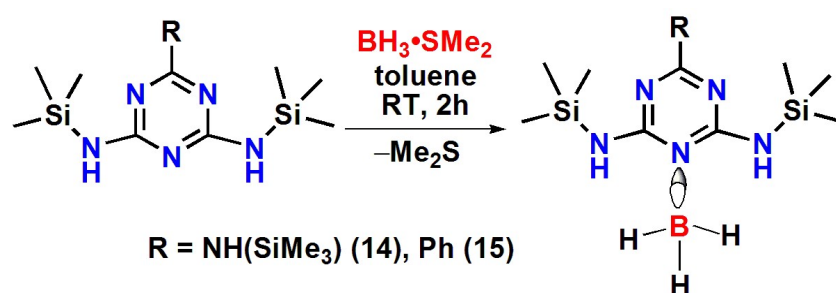


**Figure 3.18** Some known examples of complexes for the catalytic reduction of pyridine based systems.

Catalytic reduction of heteroaromatic rings is one of the important process and the reduced products obtained such as piperidines and partially reduced azacyclic compounds, serve as important building blocks for the syntheses of many bioactive alkaloids and commercial drugs. The first approach on catalytic hydroboration by Hill and coworkers was reported in

2011 to afford dearomatized derivatives of pyridines,<sup>[20]</sup> this approach has drawn enormous interest but still there are only few catalysts known (Figure 3.18) and have been dominated by metals. However in 2012, Crudden and co-workers used borenium salt for the hydroboration of acridine but the first example of metal-free approach was reported by Li, Wang and co-workers in 2015.<sup>[21]</sup> Figure 3.18 shows examples of catalysts known so far for hydroboration of pyridines whereas, the hydroboration of triazine systems is still unknown.<sup>[22]</sup>



**Scheme 3.4** synthesis of triazine-borane adducts; TTT·BH<sub>3</sub> (**14**) and BDPT·BH<sub>3</sub> (**15**).

To see the feasibility of extension of this strategy, we employed two more substrate, namely tris(trimethylsilyl)-N,N',N''-2,4,6-triamino-triazine (TTT) and bis(trimethylsilyl)-N,N'-2,4-diamino-6-(Phenyl)-triazine (BDPT) and their reaction with BH<sub>3</sub>·SMe<sub>2</sub> at 0 °C in equimolar ratio. The products obtained in these reactions were confirmed as the simple adducts TTT·BH<sub>3</sub> (**14**) and BDPT·BH<sub>3</sub> (**15**). The formation of these adducts were identified by a broad quartet at -24.55 (**14**) and -24.07 ppm (**15**) in their <sup>11</sup>B NMR spectrum and the presence of a broad B–H signal in both IR (2324 cm<sup>-1</sup> (**14**) and 2340 cm<sup>-1</sup> (**15**)) as well as in <sup>1</sup>H NMR spectrum (1.95 (**14**) and 1.92 ppm (**15**)). For adduct **14** the N–H peak was observed as downfield shifted at 6.34 ppm in <sup>1</sup>H NMR (4.49 ppm for starting material) also with a lower shift of N-H stretching frequency (3394 cm<sup>-1</sup> (starting material) to 3302 cm<sup>-1</sup>) in its IR spectrum. The similar downfield shift (6.63 ppm) was observed for the N–H signal of adduct **15** (4.84 ppm in starting material). The solid state structures of **14** and **15** corroborate the formulation of TTT·BH<sub>3</sub> (**14**) and BDPT·BH<sub>3</sub> (**15**) adducts (Figure 3.19).

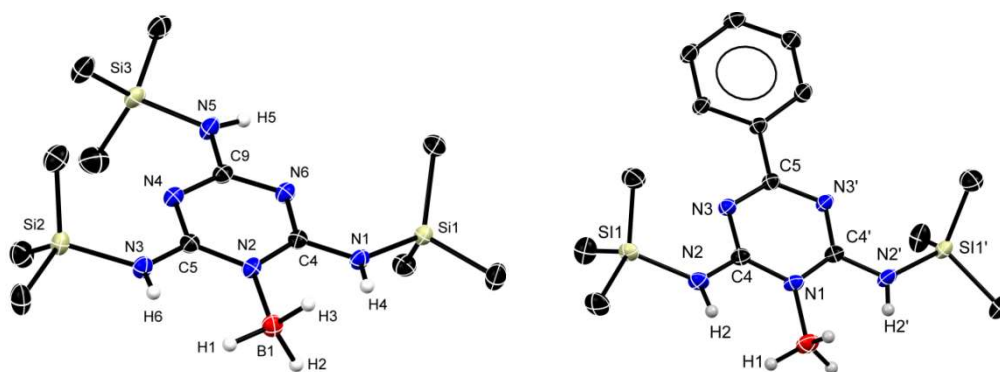


**Figure 3.19** Single crystal X-ray structure of TTT·BH<sub>3</sub> (**14**) (left) and BDPT·BH<sub>3</sub> (**15**) (right). All hydrogen atoms have been omitted for clarity. Selected bond lengths [Å] and angles [°]: for **14**: B1–H1 1.10(3), B1–N2 1.598(3), N2–C5 1.375(3), N2–C4 1.367(3), N4–C9 1.349(3), N6–C9 1.348(3); N4–C5–N2 123.69(19), N6–C4–N2 124.03(19), N6–C9–N4 125.3(2); **15**: N1–B1 1.598(3), B1–H1 0.9800, C5–N3 1.3374(14), N1–C4 1.3705(16); C4–N3 C5 115.89(12), N3–C4–N1 123.91(12).

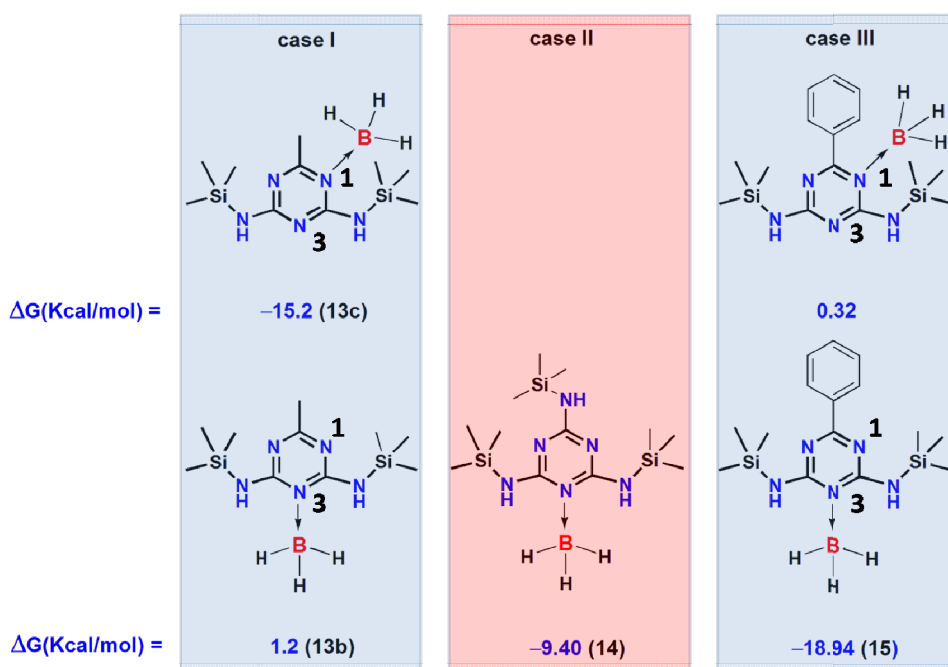


**Figure 3.20** Free energy values of triazine adducts: BDMT·BH<sub>3</sub> (**13a** and **13c**), TTT·BH<sub>3</sub> (**14**) and BDPT·BH<sub>3</sub> (**15**).

Figure 3.20 shows the comparison of calculated free energy values for different adduct structures which are possible to form between the borane and triazine systems,

bis(trimethylsilyl)-N,N'-2,4-diamino-6-(R)-triazine (bat) (R = Me, NH(SiMe<sub>3</sub>), Ph) (used in this work). The results of these calculations show that in case I (R = Me) borane forms a stable adduct **13c** at position 1 (nitrogen) ( $\Delta G = -15.2$  kcal/mol) of triazine ring whereas, the borane adduct **13b** at position 3 of triazine ring is less stable ( $\Delta G = 1.2$  kcal/mol). In case II, (R = NH(SiMe<sub>3</sub>)) the triazine ring can form only one adduct **14**, ( $\Delta G = -9.40$  kcal/mol) which is than case the adduct **13b**. Case III shows that in comparison to position 1 ( $\Delta G = 0.32$  kcal/mol) of triazine ring the adduct (**15**) formation is more feasible at position 3 ( $\Delta G = -18.89$  kcal/mol). The conclusion from these calculations matched well with the experimental observations.

### 3.3 Conclusions

In summary, the synthesis of boron containing conformationally rigid “N-B-N” heteroatomic bridged [3.3](2,6)pyridinophanes have been demonstrated for the first time. The crucial factor to incorporate conformational rigidity in these pyridinophanes is the presence of Npy...B donor-acceptor interactions with the py ring present in the proximity. These macrocyclic structures are a step closer towards the highly unexplored pyridinophanes assembled using inorganic linkers.

We have shown two different pathways for reactivity of borane with bap and BDMT: (i) evolution of H<sub>2</sub> gas due to basic nature of hydride (B-H) resulting in the formation of tetraazadibora[3.3](2,6)pyridinophane (**12**), (ii) another pathway involves reducing nature of hydride (B-H) result in formation of an unexpected boraamidinate bridged calix like trimer (**13**).

The work presents first dearomative hydroboration of triazine system under ambient catalyst free condition. The pathway involve in this transformation has been supported by the DFT calculations on different species between BDMT and borane.

The similar attempt with TTT and BDPT systems could not undergo hydroboration and gave their corresponding adducts **14** and **15** at room temperature. The stability of adducts **14** and **15** were also in accordance with the outcomes from DFT calculation.

## 3.4 Experimental Section

### 3.4.1 General procedure

All the syntheses were carried out under an inert atmosphere of dinitrogen in oven dried glassware using standard Schlenk techniques or a glovebox where O<sub>2</sub> and H<sub>2</sub>O levels were maintained usually below 0.1 ppm. All the glassware were dried at 150 °C in an oven for at least 12 h and assembled hot and cooled *in vacuo* prior to use. Solvents were purified by MBRAUN solvent purification system MB SPS-800. THF was dried over (Na/benzophenone ketyl) and distilled under nitrogen and degassed prior to use. CDCl<sub>3</sub> for NMR was dried over 4 Å molecular sieves.

### 3.4.2 Starting materials

All manipulations were performed under nitrogen/argon atmosphere using Schlenk line or glove box techniques. All chemicals were purchased from Sigma-Aldrich and used without further purification. The starting materials bis(trimethylsilyl)-N,N'-2,6-diaminopyridine,<sup>[17]</sup> lithium bis(trimethylsilyl)-N,N'-2,6-diamidopyridine<sup>[5a]</sup> and bis(trimethylsilyl)-N,N'-2,4-diamino-6-(R)-triazine (bat) (R = Me, NH(SiMe<sub>3</sub>), Ph)<sup>[23]</sup> were prepared by following the reported procedures.

### 3.4.3 Physical measurements

The <sup>1</sup>H, <sup>13</sup>C, and <sup>11</sup>B NMR spectra were recorded with a Bruker 400 MHz spectrometer with TMS and BF<sub>3</sub>·OEt<sub>2</sub> respectively, as external references and chemical shifts were reported in

ppm. Downfield shifts relative to the reference were quoted positive while the upfield shifts were assigned negative values. High resolution mass spectra were recorded on a Waters SYNAPT G2-S instrument. IR spectra of the complexes were recorded in the range 4000–400  $\text{cm}^{-1}$  using a Perkin Elmer Lambda 35-spectrophotometer. The absorptions of the characteristic functional groups were only assigned and other absorptions (moderate to very strong) were only listed. Melting points were obtained in sealed capillaries on a Büchi B-540 melting point instrument.

Single crystal X-ray diffraction data of **11** was collected on a Bruker *AXS KAPPA APEX-II* CCD diffractometer with  $\text{MoK}\alpha$  radiation using omega scans. Unit cell determination and refinement and data collection were done using the Bruker APPEX-II suite, data reduction and integration were performed using SAINT v8.34A (Bruker, 2013) and absorption corrections and scaling were done using SADABS-2014/5 (Bruker, 2014/5). Single crystal X-ray diffraction data of **12a**, **12** and **13** were collected using a Rigaku XtaLAB mini diffractometer equipped with Mercury375M CCD detector. The data were collected with  $\text{MoK}\alpha$  radiation ( $\lambda = 0.71073 \text{ \AA}$ ) using omega scans. During the data collection, the detector distance was 49.9 mm (constant) and the detector was placed at  $2\theta = 29.85^\circ$  (fixed) for all the data sets. The data collection and data reduction were done using Crystal Clear suite.<sup>[24]</sup> and all the crystal structures were solved through OLEX2 package<sup>[25]</sup> using XT and the structures were refined using XL.<sup>[26]</sup> All non hydrogen atoms were refined anisotropically. All the figures were generated using Mercury 3.2. The geometric data reported here are taken from the CIF.

#### 3.4.4 Synthetic procedure

**Synthesis of tetraazadibora[3.3](2,6)pyridinophane (11):** A solution of  $\text{LLi}_2$  (**10**) (19.76 mmol, 5.24 g) in hexane (150 mL) was added slowly to a solution of  $\text{BCl}_3$  (19.8 mL, 19.76 mmol, 1 M in toluene) in hexane (150 mL) at  $-78^\circ\text{C}$ . The reaction mixture allowed to warm

to room temperature and stirred for further 12 hours. The mixture was then filtered to remove LiCl and the volume of the filtrate was reduced to (250 mL) and stored at 4 °C to afford transparent crystals of **11**. Yield: 2.2 g (37.42 %). Mp: 247–251 °C. IR (Nujol)  $\nu$ : 3085, 2923, 2852, 1601, 1456), 1401, 1342, 1287, 1250, 1096, 1029, 956, 912, 846, 794, 728, 682, 599, 510, 420  $\text{cm}^{-1}$ .  $^1\text{H}$  NMR (400 MHz,  $\text{CDCl}_3$ ):  $\delta$  = 7.55 (t, 2H, *p*-ArH,  $^3J_{\text{H-H}}$  = 8 Hz), 6.21 (broad, 4H, *m*-ArH), 0.33 (s, 18H, SiMe<sub>3</sub>), 0.08 (s, 18H, SiMe<sub>3</sub>) ppm.  $^{13}\text{C}$  NMR (100 MHz,  $\text{CDCl}_3$ ):  $\delta$  = 164.0, 155.9, 143.9, 112.5, 101.8, 1.9 (SiMe<sub>3</sub>), 0.2 (SiMe<sub>3</sub>) ppm.  $^{11}\text{B}$  NMR (128 MHz,  $\text{CDCl}_3$ ):  $\delta$  = 8.1 ppm.  $^{29}\text{Si}$  NMR (79.5 MHz,  $\text{CDCl}_3$ ):  $\delta$  = 6.29, 4.18 ppm. HRMS ( $\text{AP}^+$ ):  $m/z$  calcd for  $\text{C}_{22}\text{H}_{43}\text{B}_2\text{Cl}_2\text{N}_6\text{Si}_4$ : (595.2201)  $[\text{M}+\text{H}]^+$ ; found: (595.2179).

**Synthesis of tetraazadibora[3.3](2,6)pyridinophane (12):** A solution of  $\text{LLi}_2$  (**10**) (19.76 mmol, 5.24 g) in hexane (70 mL) was added slowly to a solution of  $\text{BHCl}_2\cdot\text{SMe}_2$  (2.3 mL, 19.76 mmol, 8.7 M in  $\text{SMe}_2$ ) in hexane (100 mL) at  $-78$  °C. The reaction mixture allowed to come at room temperature and stirred for further 12 hours. The mixture was then filtered to remove LiCl and the volume of the filtrate was reduced to (10 mL) and stored at  $-20$  °C to afford transparent crystals of **12**. Yield: 1.1 g (21.0 %). Mp: 116–120 °C. IR (in Nujol)  $\nu$ : 3051, 2955, 2855, 2444, 1938, 1581, 1453, 1355, 1258, 1017, 842  $\text{cm}^{-1}$ .  $^1\text{H}$  NMR (400 MHz,  $\text{CDCl}_3$ ):  $\delta$  = 7.02 (t, 2H, *p*-ArH,  $^3J_{\text{H-H}}$  = 7.6 Hz), 6.17 (d, 4H, *m*-ArH,  $^3J_{\text{H-H}}$  = 7.6 Hz), 0.05 (s, 36H, SiMe<sub>3</sub>) ppm.  $^{13}\text{C}$  NMR (100 MHz,  $\text{CDCl}_3$ ):  $\delta$  = 157.5, 137.7, 119.4, 1.2 (SiMe<sub>3</sub>) ppm.  $^{11}\text{B}$  NMR (128 MHz,  $\text{CDCl}_3$ ):  $\delta$  = 27.0 ppm.  $^{29}\text{Si}$  NMR (79.5 MHz,  $\text{CDCl}_3$ ):  $\delta$  = 11 ppm. HRMS ( $\text{AP}^+$ ):  $m/z$  calcd for  $\text{C}_{22}\text{H}_{45}\text{B}_2\text{N}_6\text{Si}_4$ : (527.2979)  $[\text{M}+\text{H}]^+$ ; found: (527.2992).

**Synthesis of trihydridoborane adduct with bis(trimethylsilyl)-N,N'-2,6-diaminopyridine (12a):** A solution of  $\text{BH}_3\cdot\text{SMe}_2$  (0.4 mL, 3.9 mmol, 10 M in  $\text{SMe}_2$ ) was added slowly to a stirred solution of bis(trimethylsilyl)-N,N'-2,6-diaminopyridine (1.0 g, 3.9 mmol) in pentane (30 mL) at 0 °C. The reaction mixture was allowed to come to room temperature and stirred for 12 hours. This was followed by removal of all volatiles under vacuum to afford a white

solid (99.0 % conversion). This solid was crystallized by hexane solution at 4 °C. Yield: 0.88 g (84.4 %). Mp: 97-100 °C. IR (Nujol)  $\nu$ : 3302 (N–H), 2958, 2924, 2856, 2324 (B–H), 1623, 1582, 1466, 1381, 1313, 1255, 1221, 1176, 1108, 1057, 935, 846, 778, 730, 699, 625, 567, 455  $\text{cm}^{-1}$ .  $^1\text{H}$  NMR (400 MHz,  $\text{CDCl}_3$ ):  $\delta$  = 7.25 (t, 1H, *p*-ArH, Ar,  $^3J_{\text{H-H}}$  = 8.0 Hz), 6.38 (s, 2H, *m*-ArH, NH), 5.96 (d, 2H, Ar,  $^3J_{\text{H-H}}$  = 8 Hz), 0.32 (s, 18H, SiMe<sub>3</sub>) ppm.  $^{13}\text{C}$  NMR (100 MHz,  $\text{CDCl}_3$ ):  $\delta$  = 156.2, 138.2, 98.4, 0.3 SiMe<sub>3</sub> ppm.  $^{29}\text{Si}$  NMR (79.5 MHz,  $\text{CDCl}_3$ ):  $\delta$  = 5.5 ppm.  $^{11}\text{B}$  NMR (128 MHz,  $\text{CDCl}_3$ ):  $\delta$  = -24.5 (broad) ppm. HRMS (AP<sup>+</sup>): *m/z* calcd for C<sub>11</sub>H<sub>25</sub>BN<sub>3</sub>Si<sub>2</sub>: (266.1683) [M–H]<sup>+</sup>; found: (266.1671).

**Alternative synthesis of tetraazadibora[3.3](2,6)pyridinophane (12):** The freshly made adduct **12a** (using the above method) (5.3 g, 19.76 mmol) was dissolved in toluene (70 mL) and refluxed for 28 hours. Alternatively, BH<sub>3</sub>·SMe<sub>2</sub> (2 mL, 19.76 mmol, 10 M in SMe<sub>2</sub>) was added slowly to a stirred solution of bis(trimethylsilyl)-N,N'-2,6-diaminopyridine (5.0 g, 19.76 mmol) in toluene (80 mL) at 0 °C. The reaction mixture was allowed to come to room temperature and stirred for 2 hours at room temperature, followed by reflux for next 28 hours. In both the approaches, on reflux after half an hour there was a change in color of the reaction mixture from transparent to orange colour. After 28 hours, all the volatiles were removed under vacuum to afford an orange solid. Yield: 4.2 g (88 %). The spectroscopic characterization of this product was identical to that mentioned above.

**Synthesis of calix like trimer (13):** BH<sub>3</sub>·SMe<sub>2</sub> (3.72 mmol) was added slowly to a stirred solution of BDMT (1.0 g, 3.72 mmol) in toluene (30 mL) at 0 °C. The reaction mixture was allowed to come to room temperature and stirred for 24 h. All the volatiles were removed under vacuum to give white solid. This solid was crystallized at -10 °C in pentane. Yield: 0.91 g (86.3 %). Mp: 86-90 °C. IR (Nujol)  $\nu$ : 3355 (N–H), 2957, 2925, 2859, 2331 (B–H), 1639, 1582, 1457, 1371, 1333, 1252, 1202, 1110, 1016, 887, 845, 785, 736, 700, 620  $\text{cm}^{-1}$ .  $^1\text{H}$  NMR (400 MHz,  $\text{CDCl}_3$ ):  $\delta$  = 5.39 (s, 2H, NH), 5.06 (s, 2H, NH), 4.89 (s, 2H, NH), 4.40

(q, 2H, CH,  $^3J_{\text{H-H}} = 4$  Hz), 4.22 (q, 1H, CH,  $^3J_{\text{H-H}} = 4$  Hz), 2.64 (broad singlet, 6H, BH), 1.13 (d, 3H, CH<sub>3</sub>,  $^3J_{\text{H-H}} = 4$  Hz), 1.07 (d, 6H, CH<sub>3</sub>,  $^3J_{\text{H-H}} = 4$  Hz), 0.27 (s, 18H, SiMe<sub>3</sub>), 0.24 (d, 36H, SiMe<sub>3</sub>). <sup>13</sup>C NMR (100 MHz, CDCl<sub>3</sub>):  $\delta = 161.97, 161.38, 161.22, 66.38, 65.56, 18.00, 15.68, 0.69$  SiMe<sub>3</sub>,  $0.65$  SiMe<sub>3</sub>,  $0.62$  SiMe<sub>3</sub>. <sup>29</sup>Si NMR (79.5 MHz, CDCl<sub>3</sub>):  $\delta = 5.07, 4.90, 4.63$ . <sup>11</sup>B NMR (128 MHz, CDCl<sub>3</sub>):  $\delta = -13.13$ . HRMS (AP<sup>+</sup>):  $m/z$  calcd for C<sub>30</sub>H<sub>78</sub>B<sub>3</sub>N<sub>15</sub>Si<sub>6</sub>: (849.5459), [M<sup>+</sup>]; found: 849.5459.

**Synthesis of TTT·BH<sub>3</sub> (14):** BH<sub>3</sub>·SMe<sub>2</sub> (2.9 mmol) was added slowly to a stirred solution of TTT (1.0 g, 2.9 mmol) in hexane (10 mL) at 0 °C. The reaction mixture was allowed to come to room temperature and stirred for 12 h. All the volatiles were removed under vacuum to give tinted solid. This solid gave colorless crystals on crystallizing from pentane at -30 °C. Yield: 0.87 g (84.4 %). Mp. 122-124 °C. IR (Nujol)  $\nu$ : 3357 (N–H), 3312 (N–H), 2954, 2927, 2858, 2335 (B–H), 1602, 1547, 1465, 1248, 1131, 1104, 935, 842, 759, 732, 701, 632 cm<sup>-1</sup>. <sup>1</sup>H NMR (400 MHz, CDCl<sub>3</sub>):  $\delta = 6.51, 6.34$  (br, 2H, NH), 4.49 (s, 1H, NH), 1.96-1.69 (br, 3H, BH), 0.30 (s, 27H, SiMe<sub>3</sub>). <sup>13</sup>C NMR (100 MHz, CDCl<sub>3</sub>):  $\delta = 165.1, 162.9, 0.15$  SiMe<sub>3</sub>,  $-0.14$  SiMe<sub>3</sub>. <sup>29</sup>Si NMR (79.5 MHz, CDCl<sub>3</sub>):  $\delta = 7.31$  (SiMe<sub>3</sub>),  $6.24$  (SiMe<sub>3</sub>). <sup>11</sup>B NMR (128 MHz, CDCl<sub>3</sub>):  $\delta = -24.32$  (broad). HRMS (AP<sup>+</sup>):  $m/z$  calcd for C<sub>12</sub>H<sub>33</sub>BN<sub>6</sub>Si<sub>3</sub>: (355.2093) [M–H]<sup>+</sup>; found: (355.2077).

**Synthesis of BDPT·BH<sub>3</sub> (15):** BH<sub>3</sub>·SMe<sub>2</sub> (3.0 mmol) was added slowly to a stirred solution of BDPT (1.0 g, 3.0 mmol) in hexane (20 mL) at 0 °C. The reaction mixture was allowed to come to room temperature and stirred for 12 h. All the volatiles were removed under vacuum to give white crystalline solid. This solid gave colorless crystals on crystallizing with toluene at 4 °C. Yield: 0.83 g (80.1 %). Mp: 153–155 °C. IR (Nujol)  $\nu$ : 3344 (N–H), 2925, 2857, 2340 (B–H), 1585, 1536, 1469, 1419, 1378, 1246, 1144, 936, 846, 774, 732, 702, 654, 623, 578 cm<sup>-1</sup>. <sup>1</sup>H NMR (400 MHz, CDCl<sub>3</sub>):  $\delta = 8.34$  (d, 2H,  $^3J_{\text{H-H}} = 8$  Hz, Ar), 7.50 (m, 3H, Ar), 6.63 (s, 2H, NH), 1.92 (br, 3H, BH), 0.42 (s, 18H, SiMe<sub>3</sub>). <sup>13</sup>C NMR (100 MHz, CDCl<sub>3</sub>):  $\delta =$

167.4, 163.4, 135.6, 135.5, 128.8, 128.6, -0.24 SiMe<sub>3</sub>. <sup>29</sup>Si NMR (79.5 MHz, CDCl<sub>3</sub>):  $\delta$  = 8.78 (SiMe<sub>3</sub>). <sup>11</sup>B NMR (128 MHz, CDCl<sub>3</sub>):  $\delta$  = -24.07 (broad). HRMS (AP<sup>+</sup>):  $m/z$  calcd for C<sub>15</sub>H<sub>28</sub>BN<sub>5</sub>Si<sub>2</sub>: (345.1976) [M]<sup>+</sup>; obs: (345.1976).

### 3.5 Crystallographic Data

**Table 3.1** Crystallographic data for compounds **10-12**.

Compound <sup>[a]</sup>	10	11	12a	12
Chemical formula	C <sub>33</sub> H <sub>59</sub> Li <sub>6</sub> N <sub>9</sub> Si <sub>6</sub>	C <sub>22</sub> H <sub>42</sub> B <sub>2</sub> Cl <sub>2</sub> N <sub>6</sub> Si <sub>4</sub>	C <sub>11</sub> H <sub>26</sub> BN <sub>3</sub> Si <sub>2</sub>	C <sub>22</sub> H <sub>44</sub> B <sub>2</sub> N <sub>6</sub> Si <sub>4</sub>
Molar mass	183.15	595.50	267.34	526.61
Crystal system	orthorhombic	triclinic	monoclinic	triclinic
Space group	<i>Pca</i> 2 <sub>1</sub>	<i>P</i> $\bar{1}$	<i>P</i> 2 <sub>1</sub> / <i>c</i>	<i>P</i> $\bar{1}$
<i>T</i> [K]	100(2)	100(2)	280(2)	100(2)
<i>a</i> [Å]	20.4630(15)	11.3419(4)	7.1703(17)	6.5190(18)
<i>b</i> [Å]	19.7303(15)	14.9551(5)	18.860(4)	14.118(3)
<i>c</i> [Å]	24.1098(19)	16.2731(5)	12.843(3)	17.136(6)
$\alpha$ [°]	90	98.8330(10)	90	84.72(4)
$\beta$ [°]	90	110.2060(10)	98.818(12)	89.46(6)
$\gamma$ [°]	90	102.878(2)	90	84.14(3)
<i>V</i> [Å <sup>3</sup> ]	9734.1(13)	2443.71(14)	1716.2(6)	1562.3(8)
<i>Z</i>	8	2	4	2
<i>D</i> (calcd.) [g·cm <sup>-3</sup> ]	1.081	1.214	1.035	1.120
$\mu$ (Mo- <i>K</i> $\alpha$ ) [mm <sup>-1</sup> ]	0.203	0.369	0.193	0.211
Reflections collected	22256	18442	12182	12117
Independent reflections	15925	8893	3885	5321
Data/restraints/parameters	15925/0/1005	8893/0/505	3885/0/172	5321/0/327
<i>R</i> <sub>1</sub> , <i>wR</i> <sub>2</sub> [ <i>I</i> >2 $\sigma$ ( <i>I</i> )] <sup>[a]</sup>	0.0714, 0.1603	0.0269, 0.0707	0.0516, 0.1407	0.0699, 0.1600
<i>R</i> <sub>1</sub> , <i>wR</i> <sub>2</sub> (all data) <sup>[a]</sup>	0.1004, 0.1860	0.0310, 0.0737	0.0623, 0.1542	0.1093, 0.2064
GOF	1.054	1.046	1.060	1.010

[a]  $R_1 = \sum ||F_o| - |F_c|| / \sum |F_o|$ ,  $wR_2 = [\sum w(|F_o|^2 - |F_c|^2)^2 / \sum w|F_o|^2]^{1/2}$

**Table 3.2** Crystallographic data for compounds **13-15**.

<b>Compound</b> <sup>[a]</sup>	<b>13</b>	<b>13'</b>	<b>14</b>	<b>15</b>
Chemical formula	C <sub>30</sub> H <sub>78</sub> B <sub>3</sub> N <sub>15</sub> Si <sub>6</sub>	C <sub>32.5</sub> H <sub>84</sub> B <sub>3</sub> N <sub>15</sub> Si <sub>6</sub>	C <sub>12</sub> H <sub>33</sub> BN <sub>6</sub> Si <sub>3</sub>	C <sub>7.5</sub> H <sub>14</sub> B <sub>0.5</sub> N <sub>2.5</sub> Si
Molar mass	850.04	886.11	356.52	172.71
Crystal system	orthorhombic	monoclinic	orthorhombic	monoclinic
Space group	<i>P</i> 2 <sub>1</sub> 2 <sub>1</sub> 2 <sub>1</sub>	<i>P</i> 2 <sub>1</sub> / <i>c</i>	<i>P</i> 2 <sub>1</sub> 2 <sub>1</sub> 2 <sub>1</sub>	<i>P</i> 2 <sub>1</sub> / <i>c</i>
<i>T</i> [K]	100(2)	280(2)	100(2)	100(2)
<i>a</i> [Å]	14.0559(16)	14.207(2)	11.3362(15)	15.467(5)
<i>b</i> [Å]	15.932(2)	13.3504(19)	12.4711(17)	20.387(6)
<i>c</i> [Å]	23.274(3)	29.239(4)	15.373(2)	7.1648(17)
$\alpha$ [°]	90	90	90	90
$\beta$ [°]	90	99.330(7)	90	92.726(10)
$\gamma$ [°]	90	90	90	90
<i>V</i> [Å <sup>3</sup> ]	5212.0(11)	5472.5(14)	2173.4(5)	2256.7(11)
<i>Z</i>	4	4	4	8
<i>D</i> (calcd.) [g·cm <sup>-3</sup> ]	1.083	1.076	1.090	1.017
$\mu$ (Mo- <i>K</i> $\alpha$ ) [mm <sup>-1</sup> ]	0.197	0.190	0.223	0.162
Reflections collected	55613	47216	23428	11798
Independent reflections	11894	12440	4964	2575
Data/restraints/parameters	11894/0/564	12440/0/588	4964/0/232	2575/0/115
<i>R</i> 1, <i>wR</i> <sub>2</sub> [ <i>I</i> >2 $\sigma$ ( <i>I</i> )] <sup>[a]</sup>	0.0463, 0.1127	0.0904, 0.2357	0.0337, 0.0836	0.0499, 0.1402
<i>R</i> 1, <i>wR</i> <sub>2</sub> (all data) <sup>[a]</sup>	0.0512, 0.1183	0.1252, 0.2833	0.0350, 0.0850	0.0539, 0.1441
GOF	1.047	1.028	1.063	1.091

[a]  $R1 = \Sigma||Fo| - |Fc||/\Sigma|Fo|$ ,  $wR2 = [\Sigma w(|Fo|^2 - |Fc|^2)^2/\Sigma w|Fo|^2]^{1/2}$

### 3.6 References

- [1] P. Kumar and R. Gupta, *Dalton Trans.* **2016**, *45*, 18769-18783.
- [2] a) N. V. S. Harisomayajula, A. K. Nair and Y. C. Tsai, *Chem. Commun.* **2014**, *50*, 3391–3412 (and references cited therein); b) A. Noor, E. S. Tamne, B. Oelkers, T. Bauer, S. Demeshko, F. Meyer, F. W. Heinemann and R. Kempe, *Inorg. Chem.* **2014**, *53*, 12283–12288; c) A. Falceto, K. H. Theopold and S. Alvarez, *Inorg. Chem.* **2015**, *54*, 10966–10977; d) N. Curado, M. Carrasco, E. Álvarez, C. Maya, R. Peloso, A. Rodríguez, J. L. Serrano and E. Carmona, *J. Am. Chem. Soc.* **2015**, *137*, 12378–12387; e) A. Noor, S. Schwarz and R. Kempe, *Organometallics* **2015**, *34*, 2122–2125.
- [3] a) Y. Fedorova, O. Fedorova, A. Peregudov, S. Kalmykov, B. Egorova, D. Arkhipov, A. Zubenko and M. Oshchepkov, *J. Phys. Org. Chem.* **2016**, *29*, 244-150; b) K. M. Lincoln, M. E. Offutt, T. D. Hayden, R. E. Saunders and K. N. Green, *Inorg. Chem.* **2014**, *53*, 1406–1416; c) J. Casabb, L. Escriche, S. Alegret, C. Jaime, C. PCrez-JimCnez, L. Mestres, J. Rius, E. Molins, C. Miravittles and F. Teixidor, *Inorg. Chem.* **1991**, *30*, 1893–1898; d) Subhi A. Al-Jibori, Shihab A.O. Ahmed, C. Wagner, H. Schmidt and G. Hogarth, *Inorg. Chim. Acta* **2014**, *410*, 118–121; e) T. Sciarone, J. Hoogboom, P. P. J. Schlebos, P. H. M. Budzelaar, Rene' de Gelder, J. M. M. Smits, and A. Ga, *Eur. J. Inorg. Chem.* **2002**, 457–464; f) F. Tang, F. Qu, J. R. Khusnutdinova, N. P. Rath and L. M. Mirica, *Dalton Trans.* **2012**, *41*, 14046–14050; g) J. R. Khusnutdinova, J. Luo, N. P. Rath and L. M. Mirica, *Inorg. Chem.* **2013**, *52*, 3920–3932; h) H. Kelm and H. J. KrÜger, *Inorg. Chem.* **1996**, *35*, 3533-3540; i) S. P. Meneghetti, P. J. Lutz and J. Kress, *Organometallics* **2001**, *20*, 5050–5055; j) S. P. Meneghetti, P. J. Lutz, J. Fischer and J. Kress, *Polyhedron* **2001**, *20*, 2705–2710; k) Y. Meng, Y. R. Gui, P. C. Wu, N. N. Li and M. Zhou, *Russian J. Coord. Chem.* **2011**, *37*, 294–301.

- [4] a) A. Gerus, K. Ślepokura and J. Lisowski, *Inorg. Chem.* **2013**, *52*, 12450–12460; b) V. Alexander, *Chem. Rev.* **1995**, *95*, 273–342; c) C. Galaup, J. M. Couchet, C. Picard and P. Tisne`s, *Tetrahedron Lett.* **2001**, *42*, 6275–6278; d) C. Galaup, M. C. Carrie, J. Az~ma and C. Picard, *Tetrahedron Lett.* **1998**, *39*, 1573–1576; e) A. de Bettencourt-Dias, P. S. Barber and S. Viswanathan, *Coord. Chem. Rev.* **2014**, 273–274; f) A. Roca-Sabio, C. S. Bonnet, M. M. Iglesias, D. E. Gómez, É. Tóth, A. de Blas, T. R. Blas and C. P. Iglesias, *Inorg. Chem.* **2012**, *51*, 10893–10903; g) W. P. To, T. W. S. Chow, C. W. Tse, X. Guan, J. S. Huanga and C. M. Che, *Chem. Sci.* **2015**, *6*, 5891.
- [5] a) G. G. Skvortsov, G. K. Fukin, S. Y. Ketkov, A. V. Cherkasov, K. A. Lyssenko and A. A. Trifonov, *Eur. J. Inorg. Chem.* **2013**, 4173–4183; b) G. Glatz and R. Kempe, *Z. Kristallogr. NCS*, **2008**, *223*, 307–308; c) G. Glatz and R. Kempe, *Z. Kristallogr. NCS*, **2008**, *223*, 309–310; d) G. Glatz and R. Kempe, *Z. Kristallogr. NCS*, **2008**, *223*, 313–315.
- [6] Y. L. Huang, D. Y. Lu, H. C. Yu, J. S. K. Yu, C. W. Hsu, T. S. Kuo, G. H. Lee, Y. Wang and Y. C. Tsai, *Angew. Chem. Int. Ed.* **2012**, *51*, 7781–7785.
- [7] Y. T. Wey, F. S. Yang, H. C. Yu, T. S. Kuo and Y. C. Tsai, *Angew. Chem. Int. Ed.* **2017**, *56*, 15108–15112.
- [8] V. Rad'kov, V. Dorcet, J. F. Carpentier, A. Trifonov and E. Kirillov, *Organometallics*, **2013**, *32*, 1517–1527.
- [9] A. T. Le, A. T. Soldatenkov, *Chem. Heterocycl. Compd.* **2016**, *52*, 152–154.
- [10] M. X. Wang, *Acc. Chem. Res.* **2012**, *45*, 182–195.
- [11] a) S. O. Kang, J. M. Llinares, V. W. Dayc and K. B. James, *Chem. Soc. Rev.* **2010**, *39*, 3980–4003; b) S. O. Kang, V. W. Day and K. B. James, *Inorg. Chem.* **2010**, *49*, 8629–8636; c) B. A. Moyer, R. Custelcean, B. P. Hay, J. L. Sessler, K. B. James, V. W. Day and S. O. Kang, *Inorg. Chem.* **2013**, *52*, 3473–3490.

- [12] a) G. Castro, R. Bastida, A. Macías, P. P. Lourido, C. P. Iglesias and L. Valencia, *Inorg. Chem.* **2015**, *54*, 1671–1683; b) G. Castro, R. Bastida, A. Macías, P. P. Lourido, C. P. Iglesias and L. Valencia, *Inorg. Chem.* **2013**, *52*, 6062–6072.
- [13] a) M. R. Wasielewski, U. H. Smith, B. T. cope and J. J. Katz, *J. Am. Chem. Soc.* **1977**, *99*, 4173; b) H. Kuzuhara, N. Watanabe and M. Ando, *J. Chem. Soc., Chem. Commun.* **1987**, 95–96; c) K. Fuchigami, N. P. Rath and L. M. Mirica, *Inorg. Chem.* **2017**, *56*, 9404–9408; d) F. Tang, N. P. Rath and L. M. Mirica, *Chem. Commun.* **2015**, *51*, 3113–3116.
- [14] a) M. Shibahara, M. Watanabe, M. Suenaga, K. Ideta, T. Matsumoto, T. Shinmyozu, *Tetrahedron Lett.* **2009**, *50*, 1340–1344; b) T. Satou and T. Shinmyozu, *J. Chem. Soc., Perkin Trans.* **2002**, *2*, 393–397.
- [15] a) K. Reuter, R. G. M. Maas, A. Reuter, F. Kilgenstein, Y. Asfaha and C. von Hänisch, *Dalton Trans.* **2017**, *46*, 4530–4541; b) M. Newcomb, J. M. Timko, D. M. Walba and D. J. Cram, *J. Am. Chem. Soc.* **1977**, 6392–6398; c) G. R. Newkome, S. Pappalardo and F. R. Fronczek, *J. Am. Chem. Soc.* **1983**, *105*, 5152–5153; d) H. Higuchi and S. Misumi, *Tetrahedron Lett.* **1982**, *23*, 5571; e) S. Muralidharan, M. Hojjatie, M. Firestone and H. Freiser, *J. Org. Chem.* **1989**, *54*, 393–399; f) S. Ekici, D. Gudat, M. Nieger, L. Nyulaszi and E. Niecke, *Angew. Chem., Int. Ed.* **2002**, *41*, 3367–3371.
- [16] For examples of cyclophanes containing group 13 elements see: a) W. Uhl, S. Haddadpour and M. Matar, *Organometallics* **2006**, *25*, 159; b) W. Uhl, M. Claesener, S. Haddadpour, B. Jasper and A. Hepp, *Dalton Trans.* **2007**, 417–423; c) W. Uhl, M. Claesener, A. Hepp, B. Jasper, A. Vinogradov, L. van Wüllen and T. K.-J. Köster, *Dalton Trans.* **2009**, 10550–10562; d) F. P. Gabbaï, *Angew. Chem., Int. Ed.*, **2012**, *51*, 6316–6318.

- [17] L. Beer, J. F. Britten, J. L. Brusso, A. W. Cordes, R. C. Haddon, M. E. Itkis, D. S. MacGregor, R. T. Oakley, R. W. Reed and C. M. Robertson *J. Am. Chem. Soc.* **2003**, *125*, 14394–14403.
- [18] M. Sánchez, H. Höpfl, M. Ochoa, N. Farfán, R. Santillan and S. Rojas-Lima, *Chem. Eur. J.* **2002**, *8*, 612–621.
- [19] P. Paetzold, U. W. Osterloh and U. Englert, *Z. Anorg. Allg. Chem.* **2004**, *630*, 2569–2570.
- [20] M. Arrowsmith, M. S. Hill, T. Hadlington, G. Kociok-Köhn and C. Weetman, *Organometallics* **2011**, *30*, 5556–5559.
- [21] a) P. Eisenberger, A. M. Bailey and C. M. Crudden, *J. Am. Chem. Soc.* **2012**, *134*, 17384–17387; b) X. Fan, J. Zheng, Z. H. Li and H. Wang, *J. Am. Chem. Soc.* **2015**, *137*, 4916–4919.
- [22] a) K. Oshima, T. Ohmura and M. Suginome, *J. Am. Chem. Soc.* **2012**, *134*, 3699–3702; b) A. Kaithal, B. Chatterjee and C. Gunanathan, *Org. Lett.* **2016**, *18*, 3402–3405; c) J. Intemann, M. Lutz and S. Harder, *Organometallics* **2014**, *33*, 5722–5729.
- [23] B. Parker and D. Y. Son, *Inorg. Chem. Commun.* **2002**, *5*, 516–518.
- [24] CrystalClear 2.0; Rigaku Corporation: Tokyo, Japan, **2013**.
- [25] O. V. Dolomanov, L. J. Bourhis, R. J. Gildea, J. A. K. Howard and H. Puschmann, *J. Appl. Crystallogr.* **2009**, *42*, 339–341.
- [26] G. M. Sheldrick, *Acta Cryst. A* **2015**, *71*, 3–8.

**Abstract:** This chapter presents the versatility of bis(trimethylsilyl)-N,N'-2,6-diaminopyridine (bap) and substituted triazine modules to construct aluminum containing molecular bowls and cryptands. The control over the reaction, by varying the reagents stoichiometry and temperature, has been successfully applied. Thus, 1:1 and 1:2 reactions of bap with AlMe<sub>3</sub> at room temperature afforded mononuclear aluminum-methyl complex, [2-(Me<sub>3</sub>SiN)-6-(Me<sub>3</sub>SiNH)C<sub>5</sub>H<sub>3</sub>N](AlMe<sub>2</sub>) **(16)** and [2-(Me<sub>3</sub>SiN)-6-(Me<sub>3</sub>SiNH)C<sub>5</sub>H<sub>3</sub>N]<sub>2</sub>AlMe **(17)**, respectively. Refluxing the 1:1 mixture of bap and AlMe<sub>3</sub> completes the cyclization to afford a tetraazadialumino[3.3](2,6)pyridinophane, [2,6-(Me<sub>3</sub>SiN)<sub>2</sub>C<sub>5</sub>H<sub>3</sub>NAlMe]<sub>2</sub> with two structures **18-syn** and **18-anti** in the solid state. Complex **17** was found to be sensitive to oxygen and produced methoxy bridged dimer, [{2-(Me<sub>3</sub>SiN)-6-(Me<sub>3</sub>SiNH)C<sub>5</sub>H<sub>3</sub>N}<sub>2</sub>Al(μ-OMe)]<sub>2</sub> **(19)** due to the oxygen insertion in aluminum-methyl bonds. On changing the bap and AlMe<sub>3</sub> stoichiometry to 2:3, a bowl shaped structure, [2,6-(Me<sub>3</sub>SiN)<sub>2</sub>C<sub>5</sub>H<sub>3</sub>N(AlMe<sub>2</sub>)]<sub>2</sub>[AlMe] **(20)** was obtained which was further reacted to the Lewis acid, B(C<sub>6</sub>F<sub>5</sub>)<sub>3</sub> to generate a stable monocationic species, [2-(Me<sub>3</sub>SiN)<sub>2</sub>-6-(Me<sub>3</sub>SiN)<sub>2</sub>C<sub>5</sub>H<sub>3</sub>N]<sub>2</sub>(AlMe<sub>2</sub>)(AlMe)<sup>+</sup>[AlMe][MeB(C<sub>6</sub>F<sub>5</sub>)<sub>3</sub>]<sup>-</sup> **(21)**. Attempts to synthesize similar bowl shaped structures of aluminum with triazine systems resulted in their dinuclear complexes, [2,4-(Me<sub>3</sub>SiN)<sub>2</sub>-6-(R)-C<sub>3</sub>N<sub>3</sub>](AlMe<sub>2</sub>)<sub>2</sub> (R = Me **(22)**, NHSiMe<sub>3</sub> **(23)**, Ph **(24)**). A similar 3:2 reaction of bap with AlH<sub>3</sub>·NMe<sub>2</sub>Et at room temperature afforded an aluminum based [3.3.3]cryptand, [2,6-(Me<sub>3</sub>SiN)<sub>2</sub>C<sub>5</sub>H<sub>3</sub>N]<sub>3</sub>Al<sub>2</sub> **(25)**.

## 4.1 Introduction

There has been significant interest in the chemistry of group 13 compounds and particularly aluminum has featured prominently in this area as an important metal to which most of the ligands readily coordinate. Past five decades have been witnessed the discovery of a variety of reagents and reactions involving organoaluminum compounds. In context of coordination chemistry, aluminum complexes exhibit wide structural diversity with various bonding features and structures, in addition to their utilities in preparative chemistry.<sup>[1]</sup> The use of various aluminum complexes is known to show a range of applications, such as ion-exchange materials, catalysts, catalyst supports, flame retardants, molecular sieves and sensors.<sup>[2]</sup>

Among various ligand systems, amidinate units have attracted a considerable amount of attention as versatile precursors to stabilize various complexes of aluminum due to their robustness, ease of synthesis and modification by changing substituents. There has been a plethora of amidinate units based on N,N'-disubstituted frameworks.<sup>[3]</sup> In the past, numerous research groups have worked on a variety of complexes based on aluminum that mostly includes their mononuclear complexes.<sup>[3]</sup> However, the use of aluminum to assemble its macrocyclic systems is less known and largely depends on the selection of basic unit and the designing of reaction pathway. In this context, 2,6-N,N'-disubstituted pyridine units of the type,  $[\text{RN}(\text{NR}')_2]_2^{2-}$  (RN = pyridine) are important units due to the desired orientation of –NR' group in their dianionic chelating amidinate fragment which makes them ideal for forming cyclic assemblies with suitable acceptors and provides a combination of various coordination modes. In addition to this a variety of, substituents that can be installed on nitrogen allows the modifications in steric as well as the fine tuning of electronic properties, leading enormous diversity in inorganic chemistry.<sup>[4]</sup>

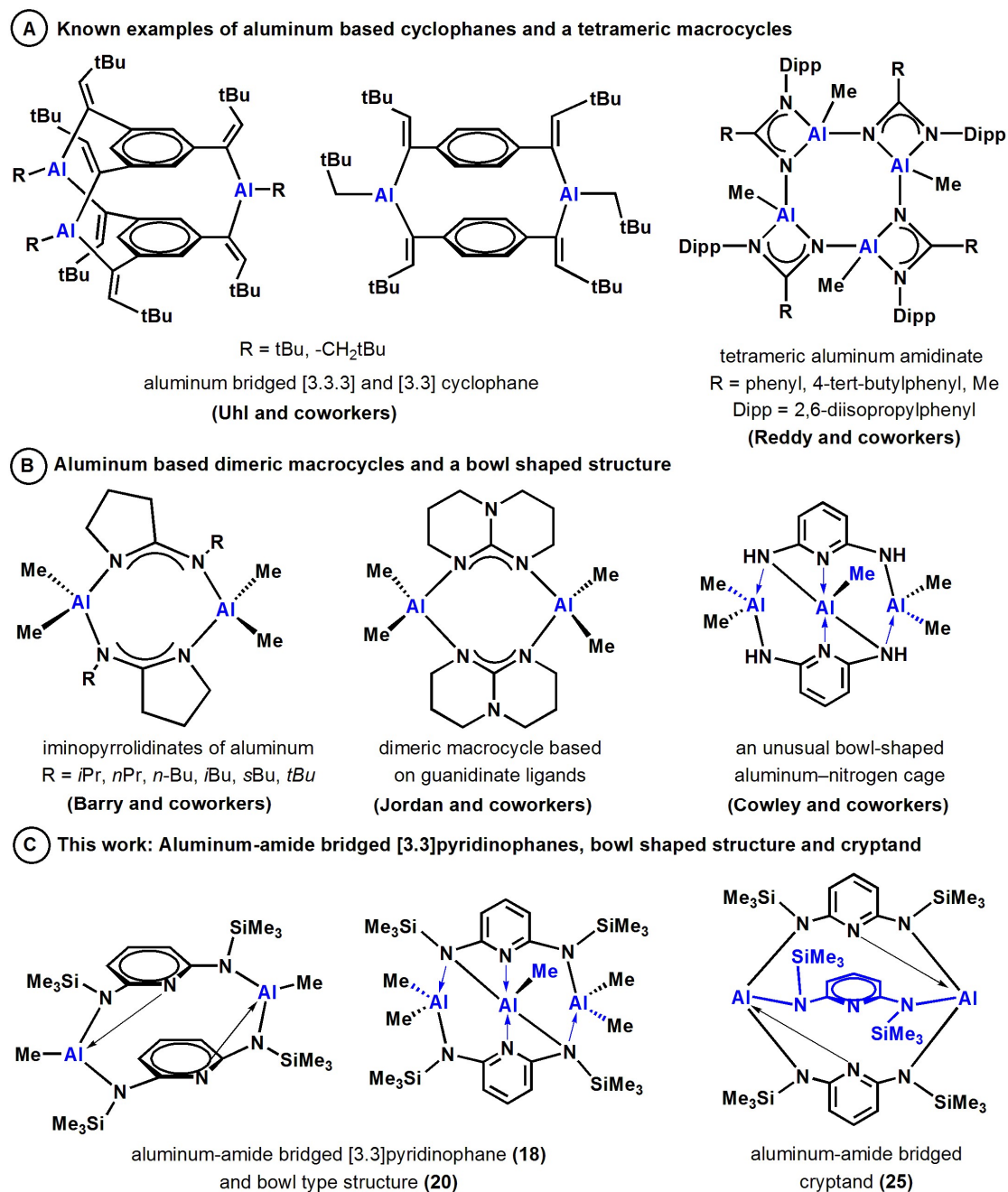


**Figure 4.1** known examples of aluminum based: A) cyclophanes and tetrameric macrocycles; B) dimeric macrocycles and a bowl shaped structure and C) present work: aluminum-amide bridged, [3.3](2,6)pyridinophane (**18**), bowl shaped structure (**20**) and cryptand (**25**).

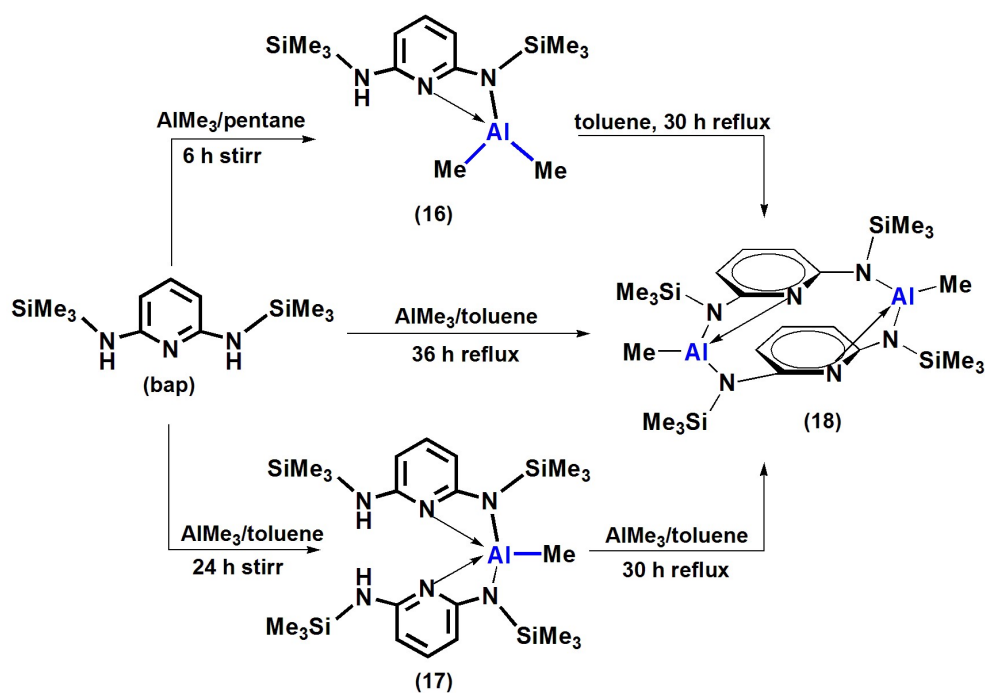
In attempts to assemble macrocycles based on aluminum, Uhl and coworkers have used hydroalumination approach to prepare a few aluminum bridged [3.3] and [3.3.3]cyclophanes, which involve the addition of Al–H bond to C≡C triple bond in the alkyl group connected with the phenyl rings (Figure 4.1).<sup>[5]</sup> Reddy and coworkers have assembled tetrameric

macrocycles based on aluminum amidine units.<sup>[6]</sup> Barry and coworkers have used various ligands to synthesize the dimethyl aluminum iminopyrrolidinate by reaction with AlMe<sub>3</sub> at room temperature.<sup>[7]</sup> Jordan and coworkers have synthesized dimeric aluminum alkyl complexes,  $\{(\mu\text{-hpp})\text{-AlMe}_2\}_2$  supported by guanidinate ligands by the reaction of 1,3,4,6,7,8-hexahydro-2H-pyrimido[1,2-a]pyrimidine (hppH) with AlMe<sub>3</sub>.<sup>[8]</sup> Cowley and coworkers have synthesized an unusual cage-type compound, AlMe[Al-Me<sub>2</sub>{N(H),N(H)-C<sub>5</sub>H<sub>3</sub>N}]<sub>2</sub> by 3:2 mole ratio reaction of AlMe<sub>3</sub> and 2,6-diaminopyridine.<sup>[9]</sup>

Continuing in this area, we felt that silylamide ligands based on aminopyridines/triazines would be of particular interest due to their readily and inexpensive accessibility. This work involves the use of two building blocks, bis(trimethylsilyl)-N,N'-2,6-diaminopyridine (bap) and bis(trimethylsilyl)-N,N'-2,4-diamino-6-(R)-triazine (bat) to assemble aluminum-amide bridged macrocyclic systems including tetraazadialumino[3.3](2,6)pyridinophane (**18**), a bowl shaped structure (**20**) and [3.3.3]cryptand (**25**).

## 4.2 Results and Discussion

The equimolar (1:1) reaction between bis(trimethylsilyl)-N,N'-2,6-diaminopyridine (bap) and AlMe<sub>3</sub> in pentane at 0 °C over 6 h afforded a mononuclear dimethyl-aluminum complex,  $[2\text{-(Me}_3\text{SiN)-6-(Me}_3\text{SiNH)C}_5\text{H}_3\text{N}]\text{(AlMe}_2\text{)}$  (**16**) (Scheme 4.1). The HRMS spectrum of **16** showed a signal at  $m/z$  310.1702 (calcd. 310.1715 [M+H]<sup>+</sup>) as the mononuclear complex (also supported by single crystal X-ray structure). The occurrence of a signal at 3392 cm<sup>-1</sup> in IR spectrum of **16** showed the presence of N-H signal. Two singlets in the <sup>1</sup>H NMR (0.11 and -0.97 ppm) as well as in the <sup>13</sup>C NMR (1.47 and 0.41 ppm) spectra of **16** attributed to the presence of an AlMe<sub>2</sub> moiety. The SiMe<sub>3</sub> groups on bap skeleton in **16** appeared to be identical in solution at room temperature and showed a single resonance in the <sup>1</sup>H (0.30 ppm),



**Scheme 4.1** Synthesis of methyl-aluminum complexes,  $[2-(\text{Me}_3\text{SiN})-6-(\text{Me}_3\text{SiNH})\text{C}_5\text{H}_3\text{N}](\text{AlMe}_2)$  (**16**),  $[2-(\text{Me}_3\text{SiN})-6-(\text{Me}_3\text{SiNH})\text{C}_5\text{H}_3\text{N}]_2\text{AlMe}$  (**17**) and tetraazadi-alumino[3.3](2,6)pyridinophane,  $[2,6-(\text{Me}_3\text{SiN})_2\text{C}_5\text{H}_3\text{NAlMe}]_2$  (**18-syn and 18-anti**).

$^{13}\text{C}$  (2.64 ppm) and  $^{29}\text{Si}$  (8.58 ppm) NMR spectra. On changing the stoichiometry of bap and  $\text{AlMe}_3$  to 2:1, the reaction at room temperature afforded a mononuclear complex,  $[2-(\text{Me}_3\text{SiN})-6-(\text{Me}_3\text{SiNH})\text{C}_5\text{H}_3\text{N}]_2\text{AlMe}$  (**17**) (Scheme 4.1). The formulation of **17** was confirmed by the  $^1\text{H}$  and  $^{13}\text{C}$  NMR spectra that clearly showed 2 equivalents of bap reacted with 1 equivalent of  $\text{AlMe}_3$ . Unlike **16**, the structure of **17** in the solution appeared to be more rigid and showed different signals for a pair of  $\text{SiMe}_3$  groups. Two equal intensity signals for four  $\text{SiMe}_3$  groups in the  $^1\text{H}$  NMR spectrum (0.27 and  $-0.07$  ppm) were consistent with the observation of two signals in the  $^{13}\text{C}$  (1.21 and  $-0.10$  ppm) and  $^{29}\text{Si}$  (4.70 and  $-1.45$  ppm) NMR spectra. All these features indicated towards chemically non-equivalent environment around the pyridine ring. The HRMS spectrum of complex **17** showed a peak at  $m/z = 531.2501$  (calcd. 531.2520) corresponding to  $[\text{M}-\text{Me}+\text{H}]^+$ .

The solid state structures of compounds **16** and **17** were confirmed by X-ray diffraction analyses, and are illustrated in Figure 4.2. Details of the crystallographic analyses for all these compounds are provided in Table 4.1. Compounds **16** and **17** crystallize in monoclinic system with space group of  $P2_1/c$ . The metric parameters within the ligand framework in both of these compounds were very similar. The solid state structure of [2-(Me<sub>3</sub>SiN)-6-(Me<sub>3</sub>SiNH)C<sub>5</sub>H<sub>3</sub>N](AlMe<sub>2</sub>), (**16**) confirmed its earlier formulation as mononuclear bidentate pyridinato complex containing tetracoordinated aluminum that adopts distorted tetrahedral geometry with two nitrogen atoms and two methyl groups attached to it.

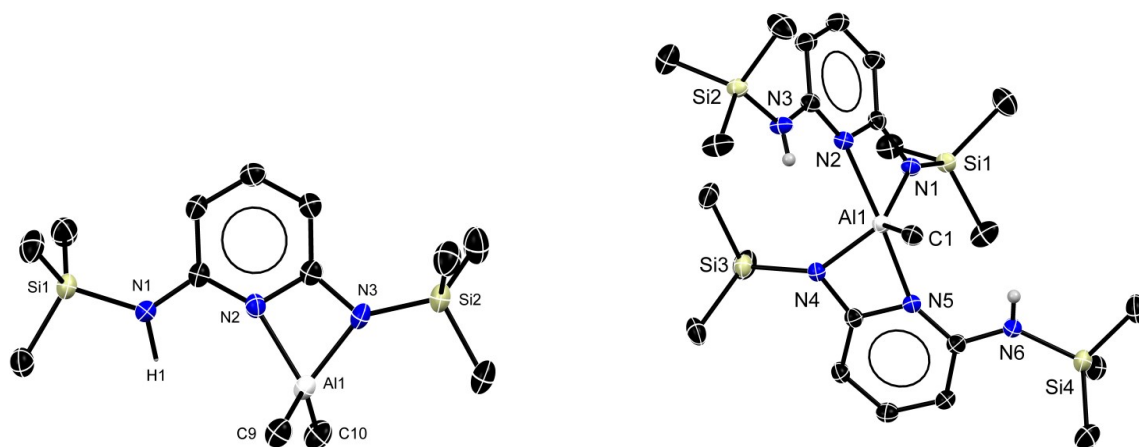


**Figure 4.2** Single crystal X-ray structure of [2-(Me<sub>3</sub>SiN)-6-(Me<sub>3</sub>SiNH)C<sub>5</sub>H<sub>3</sub>N](AlMe<sub>2</sub>) (**16**) and [2-(Me<sub>3</sub>SiN)-6-(Me<sub>3</sub>SiNH)C<sub>5</sub>H<sub>3</sub>N]<sub>2</sub>AlMe (**17**). All hydrogen atoms have been omitted for clarity. Selected bond lengths [Å] and bond angles [°]: for (**16**): Al1–N2 1.984(3), Al1–N3 1.903(3), Al1–C9 1.954(3), Al1–C10 1.960(3), N1–Si1 1.747(3), N3–Si2 1.724(3); N2–Al1–N3 70.07(10), C9–Al1–C10 120.78(15), C9–Al1–N2 110.31(13), C10–Al1–N2 114.62(13), C9–Al1–N3 114.83(13), C10–Al1–N3 115.43(14); for (**17**): Al1–N1 1.9238(17), Al1–N2 2.0551(18), Al1–C1 1.975(2), N1–Si1 1.7357(18), N3–Si2 1.7534(19); N1–Al1–N2 68.15(7), N1–Al1–N5 102.42(7), N1–Al1–C1 125.88(8), N2–Al1–N4 104.05(7).

This structure consists of a four membered [N<sub>2</sub>CAI] ring where, the pyridyl and amino sites of bap bind to aluminum centre. The molecular structure of [2-(Me<sub>3</sub>SiN)-6-(Me<sub>3</sub>SiNH)C<sub>5</sub>H<sub>3</sub>N]<sub>2</sub>AlMe (**17**) is comprised of a nice noncoplanar structure around the

pentacoordinated aluminum centre where two of the bap units are oriented opposite to each other constituting the uncyclized structure. The structure also forms N,N' chelates where, both the pyridiyl and amino sites of bap bind to aluminum centre to form  $[N_2CAI]$  four membered chelate while another amino site does not coordinate to aluminum.

The occurrence of N-H stretch in IR spectrum for **16** showed that it could not cyclize at room temperature and it was further supported by its single crystal X-ray structure. Therefore, to obtain the cyclic product the stoichiometric amount (1:1) of bap and  $AlMe_3$  were refluxed for 36 h which afforded an oily product that converted to a solid on drying for a long time. This solid was further crystallized by dry pentane at  $-30\text{ }^\circ\text{C}$  to produce colorless crystals of tetraazadialumino[3.3](2,6)pyridinophane,  $[2,6-(Me_3SiN)_2C_5H_3NAlMe]_2$  (**18**) in 65.5% yield (Scheme 4.1). The absence of N-H signal (present in starting material (bap)) in IR and  $^1H$  NMR spectra of **18** corroborates complete deprotonation of both  $-NHSiMe_3$  units of bap and a possible cyclization due to the liberation of methane gas. In addition, the resonance at 0.49 ppm in  $^1H$  and 10.50 ppm in  $^{13}C$  NMR spectra indicated the presence of methyl group on aluminum. The  $^1H$  NMR spectrum of **18** also showed a single peak (at 0.13 ppm) for the  $SiMe_3$  groups whereas two signals were observed in the  $^{29}Si$  (3.76 and  $-2.38$  ppm) and  $^{13}C$  NMR spectra (2.23 and 0.45 ppm) for the  $SiMe_3$  groups indicating different orientation of  $SiMe_3$  groups. The presence of a triplet at 7.18 ppm and a broad singlet at 5.80 ppm could not clarify the different chemical environment for protons of pyridine ring however the  $^{13}C$  NMR attributes different peaks for all five carbons in pyridine ring. The presence of these five signals for the pyridine ring is indicative of the coordination of pyridine nitrogen to the Al ( $Npy \cdots Al$ ) (similar to pyridinophane **11**, Chapter 3) (supported by the X-ray structure later). The formation of pyridinophane **18** as the N-Al(Me)-N bridged dimer was also indicated in the HRMS measurements that showed a signal at  $m/z$  587.2708 (calcd. 587.2726 for  $[M+H]^+$ ).

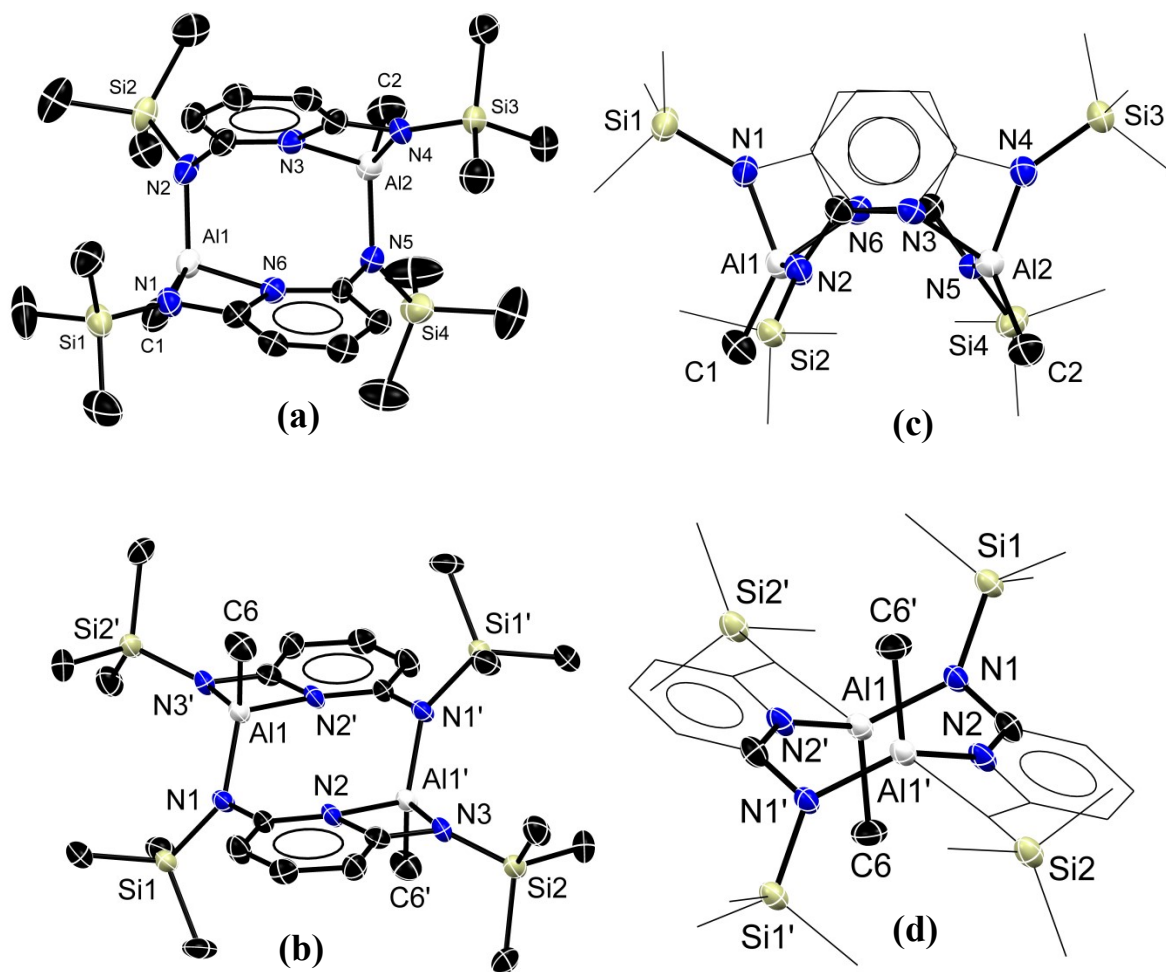
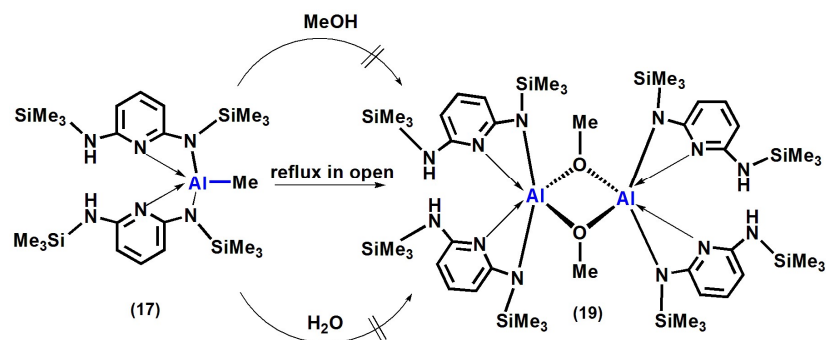


**Figure 4.3** Single crystal X-ray structure of tetraazadialumino[3.3](2,6)pyridinophane; **(a)** syn(boat,boat) conformation (**18-syn**) and **(b)** the anti conformation (**18-anti**), **(c)** and **(d)** show another view of **18-syn** and **18-anti**, respectively. All hydrogen atoms have been omitted for clarity. Selected bond lengths [Å] and bond angles [°]: for **18-syn**: Al1–N1 1.914(2), Al1–N2 1.838(2), Al1–N6 1.941(2), Al1–C1 1.939(3), N1–Si1 1.735(2), N2–Si2 1.742(2); N1–Al1–N2 113.81(10), N2–Al1–N6 107.90(9), N1–Al1–N6 70.30(9), N1–Al1–C1 117.96(12), N2–Al1–C1 119.33(12), N6–Al1–C1 117.45(12), for **18-anti**: Al1–N1 1.851(2) Al1–N2 1.951(2), Al1–N3 1.900(2), Al1–C6 1.944(3), N1–Si1 1.752(2), N3–Si2 1.730(2); N1–Al1–C6 114.25(11) N1–Al1–N3 117.99(10).

Attempts to synthesize **18** via refluxing **16** or the reaction of **17** with 1 eq. of AlMe<sub>3</sub> gave the expected dimeric macrocycle, [2,6–(Me<sub>3</sub>SiN)<sub>2</sub>C<sub>5</sub>H<sub>3</sub>NAlMe]<sub>2</sub> (**18**) along with a little amount of [2,6–(Me<sub>3</sub>SiN)<sub>2</sub>C<sub>5</sub>H<sub>3</sub>N(AlMe<sub>2</sub>)<sub>2</sub>]<sub>2</sub>[AlMe] (**20**) (Scheme 4.1 and 4.3).

Although the heteronuclear NMR for **18** showed its formation as the only product and it was seen as the dimeric structure,  $[2,6-(\text{Me}_3\text{SiN})_2\text{C}_5\text{H}_3\text{NAlMe}]_2$  by HRMS. The structural elucidation of tetraazadialumino[3.3](2,6)pyridinophane (**18**) by single crystal X-ray diffraction authenticated its structure as syn(boat,boat) (**18-syn**) and anti (**18-anti**) conformers. Both conformers of **18** have identical solution behaviour (NMR data at room temperature) and both of them crystallized in the monoclinic system (space group  $P2_1/c$ ). Both conformers of **18** are composed of eight membered  $[\text{N}_4\text{Al}_2\text{C}_2]$  central ring providing the basic framework of a [3.3](2,6)pyridinophane. The pyridine N within this framework coordinate to Al centers ( $\text{Npy}\cdots\text{Al}$ ) and are responsible for the overall conformational rigidity and the formation of two planar four member  $[\text{N}_2\text{AlC}]$  chelates that are fused to two diagonally opposite edges (Al-N) of the central eight membered  $[\text{N}_4\text{Al}_2\text{C}_2]$  ring. This coordination also explains the slight distortion in **18-syn** conformer from a regular syn(boat,boat) structure. The methyl groups on the N-Al(Me)-N bridges are mutually cis in **18-syn** and trans in **18-anti** (Figure 4.3). The separation between transannular Al atoms (4.037 Å for **18-syn** and 3.732 Å for **18-anti**) compare well with the structurally related tetraazadibora[3.3](2,6)pyridinophane **11** ( $\text{B}\cdots\text{B}$  separation of 3.618 Å, Chapter 3). The distance between the centroids of the pyridine rings in **18-syn** and **18-anti** are 3.979 Å and 6.060 Å, respectively.

Surprisingly one reaction, among the repeated attempts for the reaction **17** under reflux, afforded a product,  $[\{2-(\text{Me}_3\text{SiN})-6-(\text{Me}_3\text{SiNH})\text{C}_5\text{H}_3\text{N}\}_2\text{Al}(\mu\text{-OMe})]_2$  (**19**) that contained methoxide bridges between two Al centres (Scheme 4.2). This product is the consequence of insertion of oxygen between a pair of Al-Me bonds and has been isolated as a light brown powder, which could be easily purified by washing with a small amount of cold pentane.<sup>[10]</sup> The formation of **19** was also seen, by exposing **17** to oxygen, whereas controlled



**Scheme 4.2** Synthesis of rhombus core complex,  $[\{2-(\text{Me}_3\text{SiN})-6-(\text{Me}_3\text{SiNH})\text{C}_5\text{H}_3\text{N}\}_2\text{Al}(\mu\text{-OMe})_2]$  (19).

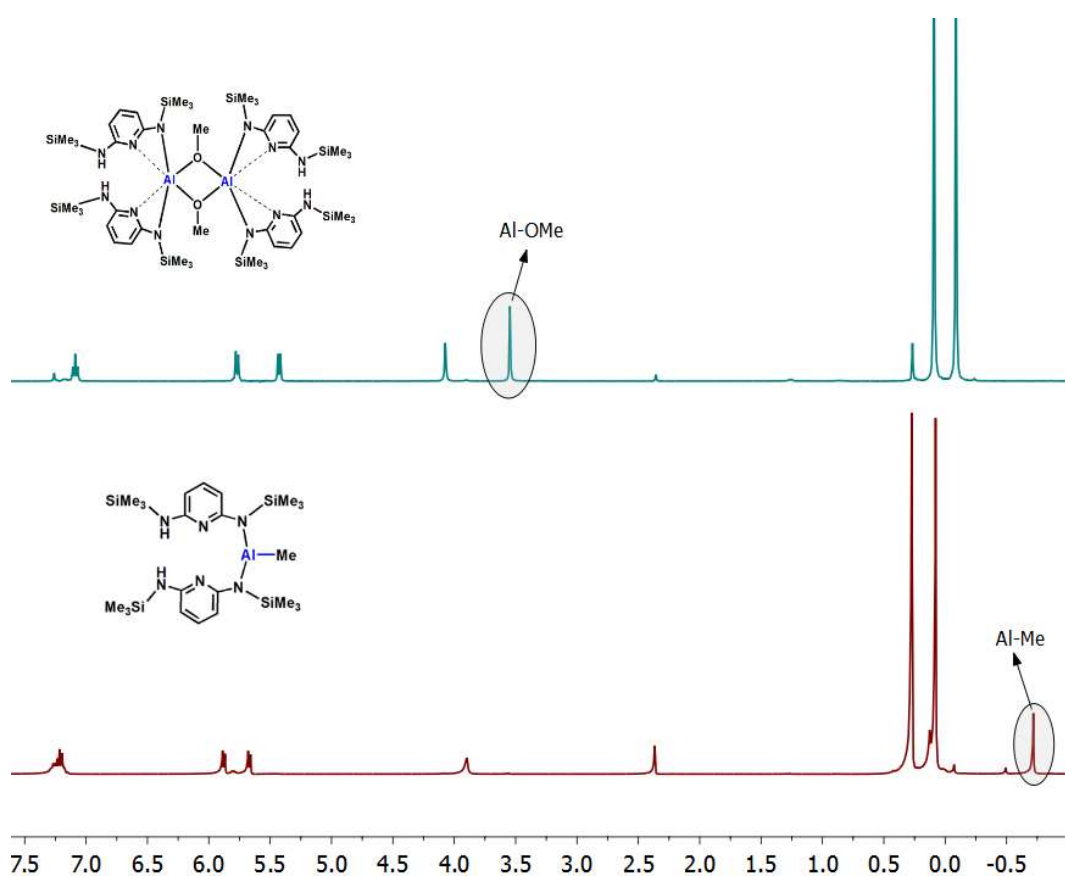


**Figure 4.4.** Comparison of  $^1\text{H}$  NMR spectra of bap with that of **19** to show the oxygen insertion in Al-Me bonds in  $[2-(\text{Me}_3\text{SiN})-6-(\text{Me}_3\text{SiNH})\text{C}_5\text{H}_3\text{N}]_2\text{AlMe}$  (**17**) to form  $[\{2-(\text{Me}_3\text{SiN})-6-(\text{Me}_3\text{SiNH})\text{C}_5\text{H}_3\text{N}\}_2\text{Al}(\mu\text{-OMe})_2]$  (**19**).

Reaction of **17** with MeOH and H<sub>2</sub>O showed its decomposition. Similar to complex **17**, the  $^1\text{H}$  (0.09 and -0.09 ppm) and  $^{29}\text{Si}$  NMR (2.77 and -4.08 ppm) spectra for complex **19** also showed the presence of two different types of SiMe<sub>3</sub> groups. Also, the presence of a

triplet (7.09 ppm) and two doublets (5.77 and 5.43 ppm) in the aromatic region supported different environment for protons of pyridine rings. Complex **19** showed a singlet at 3.55 ppm (Figure 4.4) in its  $^1\text{H}$  NMR spectrum for the  $-\text{OCH}_3$  and its corresponding signal in  $^{13}\text{C}$  NMR spectrum appeared at 51.32 ppm. The HRMS data showed an isotope distribution pattern at  $m/z$  1125.5431 (calc. 1125.5486 for  $[\text{M}^+]$ ) which can be assigned as methoxide bridged dinuclear complex **19**.

The solid state structure of compound  $[\{2-(\text{Me}_3\text{SiN})-6-(\text{Me}_3\text{SiNH})\text{C}_5\text{H}_3\text{N}\}_2\text{Al}(\mu\text{-OMe})_2]$  (**19**) confirmed its formulation as the dimeric species where each hexacoordinated aluminum centre is coordinated to nitrogen of two pyridine rings of different bap ligands in axial position with the Al–N distance of 2.025–2.043 Å. The equatorial positions of aluminum are occupied with two bridging oxygen atoms and two amino sites of different bap

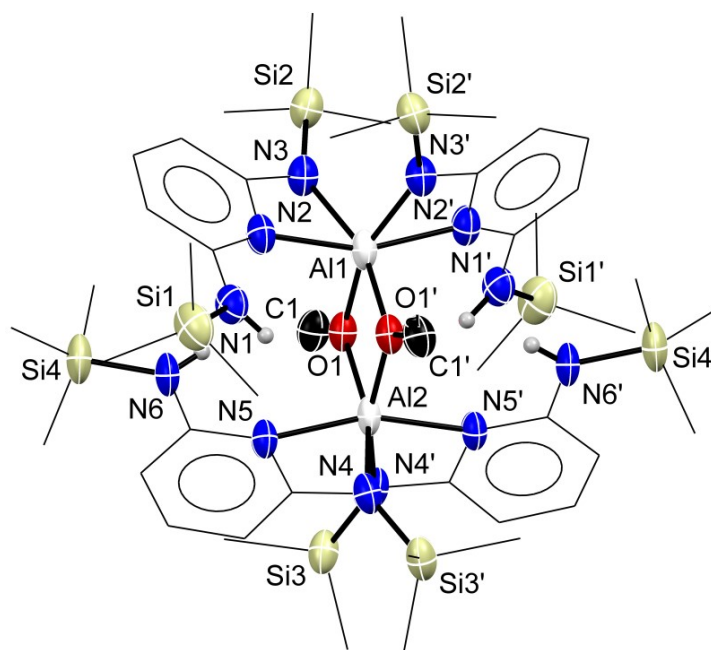
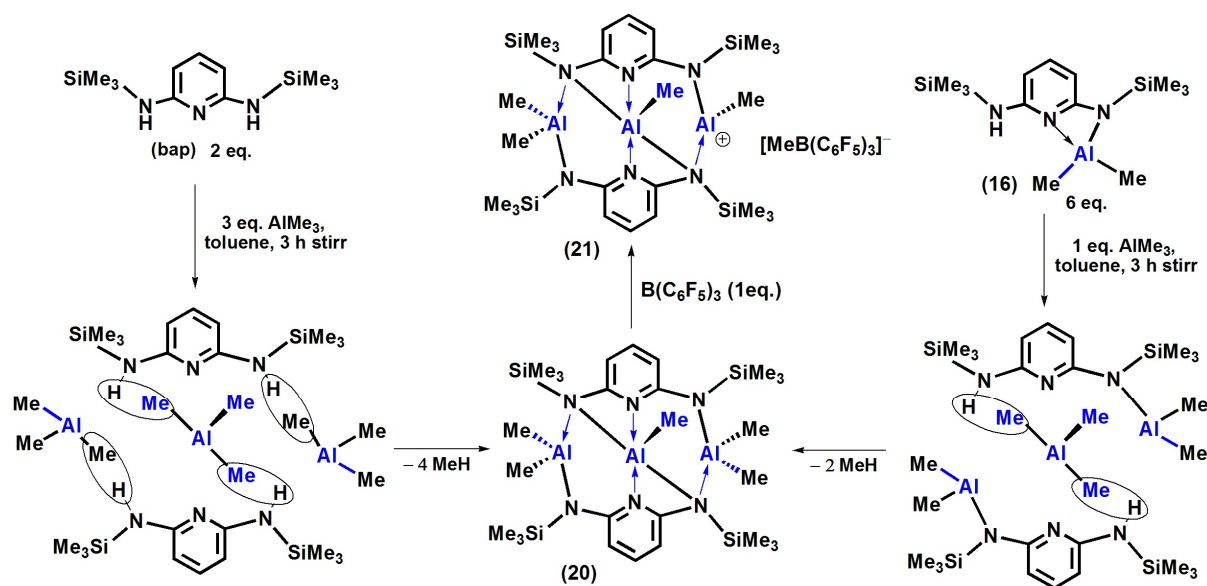


**Figure 4.5** Single crystal X-ray structure of  $[\{2-(\text{Me}_3\text{SiN})-6-(\text{Me}_3\text{SiNH})\text{C}_5\text{H}_3\text{N}\}_2\text{Al}(\mu\text{-OMe})_2]$  (**19**). All hydrogen atoms have been omitted for clarity. Selected bond lengths [Å] and bond angles [°]: Al1–N2 2.040(3), Al1–N3 1.986(4), Al1–C1 1.954(3), Al1–O1 1.887(4), Al2–O1 1.889(3), N1–Si1 1.746(4), N3–Si2 1.741(4), Al1–Al2 2.997(3), O1–C1 1.438(5); O1–Al1–O1' 75.0(2), O1–Al1–N2 99.14(15), C1–O1–Al1 128.0(3).

ligands with the lengths of Al–O 1.888–1.898 Å and Al–N 1.994–2.007 Å.<sup>[11]</sup> This dimeric structure consists of a four member rhombus [AlO]<sub>2</sub> ring where, the four units of bap binds to two aluminum centres through pyridiyl and one of the amido sites while the other as amino site doesn't coordinate to aluminum. Both the aluminum centres are -OMe bridged consisting slightly distorted octahedral geometry with a distance of 3.004 Å (Al···Al) and 2.298 Å (O···O).

Although, an unusual bowl-shaped aluminum-nitrogen cage compound was synthesized by Cowley and coworkers in 2005 by the reaction of trialkyls with bifunctional primary amines (Figure 4.1).<sup>[9]</sup> No significant attention however, has been paid thereafter to perform such reactions with this kind of systems. Our further investigation on the reaction between bap and AlMe<sub>3</sub> in 2:3 stoichiometry at room temperature for 2 h resulted in the formation of a bowl shaped cage, [2,6-(Me<sub>3</sub>SiN)<sub>2</sub>C<sub>5</sub>H<sub>3</sub>N(AlMe<sub>2</sub>)<sub>2</sub>]<sub>2</sub>[AlMe] (**20**). Initial characterization of this product showed the disappearance of N–H signals in IR as well as in <sup>1</sup>H NMR spectra that were similar to complex **18**. However, the <sup>1</sup>H NMR spectrum also showed the presence of three Al–Me signals in 1:2:2 proportion (for 3H:6H:6H) ratios at –0.23, –0.55 and –1.50 ppm which can be attributed to the formation of a dimeric structure of **16** with an additional diagonal (N–Al–N) bridge between two bap moieties via the elimination of methane gas (Scheme 4.3). The values for these three Al–Me signals were also consistent in <sup>13</sup>C NMR spectrum at –0.06, –2.01, –8.22 ppm. The presence of a single peak for SiMe<sub>3</sub> group in <sup>1</sup>H, <sup>13</sup>C and <sup>29</sup>Si NMR spectra for **20** indicates the symmetrical nature of this molecule. Further the signal at *m/z* 659.3218 (calcd. 659.3246) in HRMS corroborated the formation of **20** as a diagonally aluminum bridged species. The formation of **20** can be compared with the formation of bowl shaped structure by Jones and coworkers.<sup>[9]</sup> Scheme 4.3 shows the formation of **20** through the dimerization of two [2-(Me<sub>3</sub>SiN)–6-(Me<sub>3</sub>SiNH)C<sub>5</sub>H<sub>3</sub>N](AlMe<sub>2</sub>) (**16**) molecules followed by the reaction with one extra equivalent of AlMe<sub>3</sub>.



**Scheme 4.3.** Synthesis of aluminum-amide bridged bowl shaped complex, [2,6-(Me<sub>3</sub>SiN)<sub>2</sub>C<sub>5</sub>H<sub>3</sub>N(AlMe<sub>2</sub>)<sub>2</sub>][AlMe] (**20**) and its monocationic macrocycle, [2-(Me<sub>3</sub>SiN)<sub>2</sub>-6-(Me<sub>3</sub>SiN)<sub>2</sub>C<sub>5</sub>H<sub>3</sub>N]<sub>2</sub>(AlMe<sub>2</sub>)(AlMe)<sup>+</sup>[AlMe][MeB(C<sub>6</sub>F<sub>5</sub>)<sub>3</sub>]<sup>-</sup> (**21**).

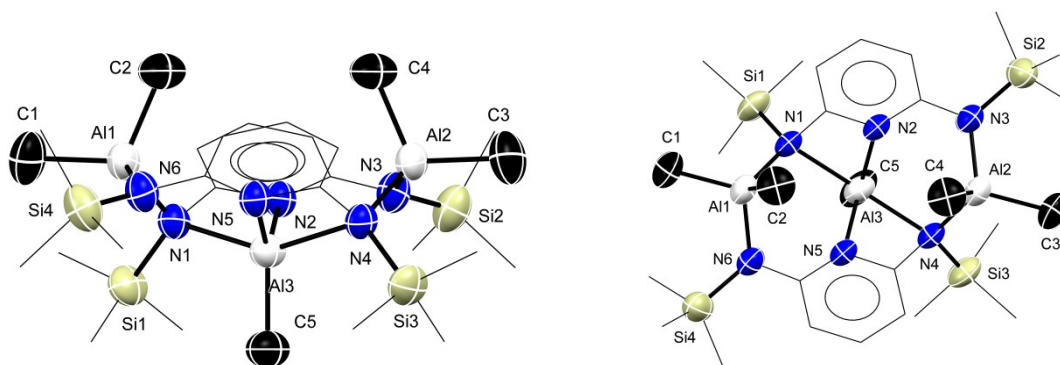


**Figure 4.6** Single crystal X-ray structure of [2,6-(Me<sub>3</sub>SiN)<sub>2</sub>C<sub>5</sub>H<sub>3</sub>N(AlMe<sub>2</sub>)<sub>2</sub>][AlMe] (**20**) (left image – side view, right image – top view). All hydrogen atoms have been omitted for clarity. Selected bond lengths [Å] and bond angles [°]: Al1–N1 1.997(3), Al1–N6 1.901(7), Al1–C1 1.952(13), Al1–C2 1.976(5), Al3–C5 1.968(11); N1–Al1–N6 105.93(10), N2–Al3–N5 114.17(6), C1–Al1–C2 109.77(11).

The X-ray structural analysis of [2,6-(Me<sub>3</sub>SiN)<sub>2</sub>C<sub>5</sub>H<sub>3</sub>N(AlMe<sub>2</sub>)<sub>2</sub>][AlMe] (**20**) showed its bicyclic nature where two bapAlMe<sub>2</sub> units are connected to each other via a diagonal bridge (N–Al–N) (Figure 4.6). This structure can be considered as the

dimeric form of **16** connected via an aluminum bridge. The structure showed that both of the pyridine rings are almost perpendicular to each other constituting bowl shaped symmetry. The cyclic structure consists of three aluminum centres, out of them two terminal aluminum centres are tetracoordinated having tetrahedral geometry whereas the third one is pentacoordinated having square pyramidal geometry. Both the tetracoordinated terminal aluminum centres have two methyl groups where one of the methyl groups orient towards inside and the other one orients away from the macrocyclic cavity hence, both of these methyl groups are chemically non-equivalent as seen in the  $^1\text{H}$  NMR spectrum.

The facile synthesis, structural rigidity and presence of several reactive methyl groups on **20** encouraged us to see its reaction chemistry with Lewis acid,  $\text{B}(\text{C}_6\text{F}_5)_3$ . Indeed it was found to be very interesting candidate to generate cationic species. On performing its NMR tube reaction with a Lewis acid,  $\text{B}(\text{C}_6\text{F}_5)_3$  in  $\text{CDCl}_3$  a stable monocationic species,  $[\text{2}-(\text{Me}_3\text{SiN})_2-6-(\text{Me}_3\text{SiN})_2\text{C}_5\text{H}_3\text{N}]_2(\text{AlMe}_2)(\text{AlMe})^+[\text{AlMe}][\text{MeB}(\text{C}_6\text{F}_5)_3]^-$  (**21**) was obtained. This cationic species was stable at room temperature for several weeks and does not show the possible  $\text{CH}_3$  and  $\text{C}_6\text{F}_5$  exchange between the cationic and anionic part. Compound **21** settled as clathrate oil from solvents like benzene and toluene whereas it dissolved freely in polar solvents like chloroform and THF. Several attempts to crystallize the cationic species were unsuccessful. The initial evidence towards the cation formation was seen by a change in  $^1\text{H}$  NMR spectrum in the signal intensity for terminal  $\text{Al}-\text{Me}$  of **20** in few minutes. The presence of four signals for a total of twelve methyl protons with a ratio of 1:1:1:1 (for 3H:3H:3H:3H) at 0.15, 0.20, 0.24 and  $-1.24$  ppm for  $\text{Al}-\text{Me}$  show that one of the terminal methyl groups ( $\text{Al}-\text{Me}$ ) had been abstracted by  $\text{B}(\text{C}_6\text{F}_5)_3$  to form a new  $\text{B}-\text{Me}$  bond (at 0.52 ppm) as the counter anion  $[\text{MeB}(\text{C}_6\text{F}_5)_3]^-$  (Figure 4.6).

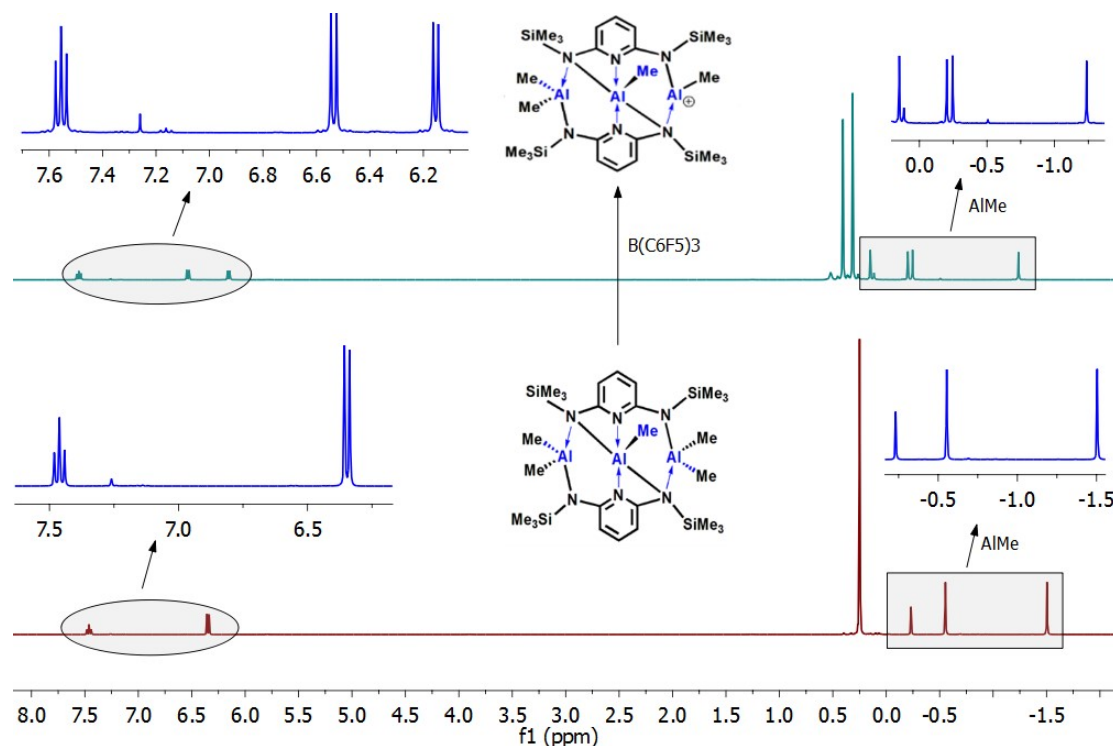
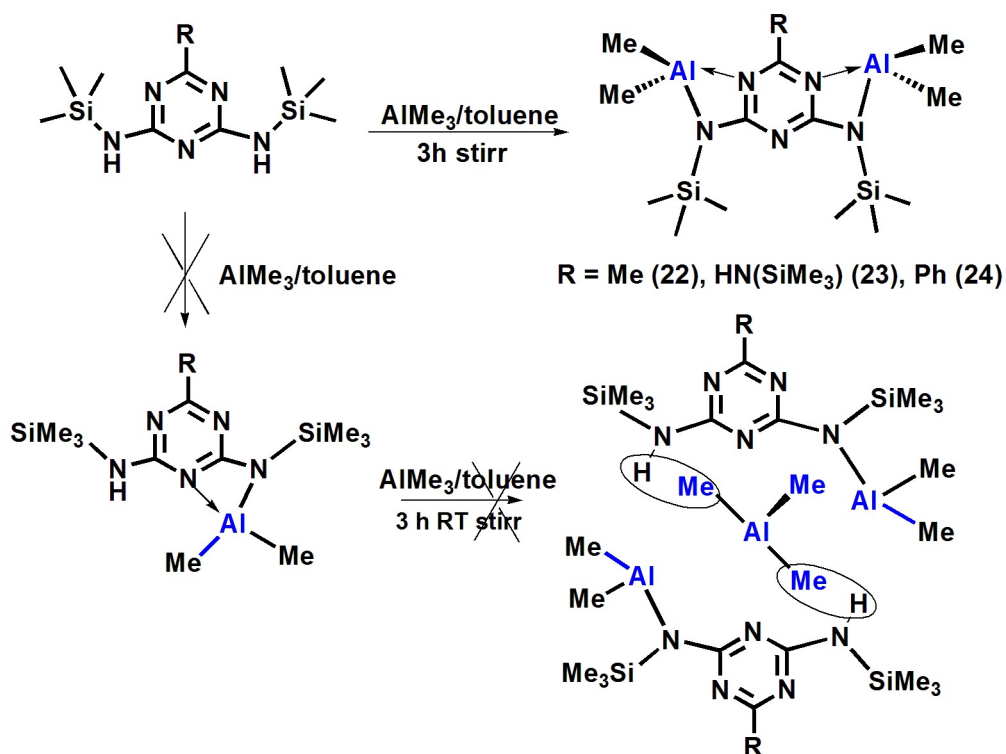


**Figure 4.6.** Comparison of  $^1\text{H}$  NMR (400 MHz,  $\text{CDCl}_3$ ) spectra to show the formation of monocationic macrocycle,  $[2-(\text{Me}_3\text{SiN})_2-6-(\text{Me}_3\text{SiN})_2\text{C}_5\text{H}_3\text{N}]_2(\text{AlMe}_2)(\text{AlMe})^+[\text{AlMe}][\text{MeB}(\text{C}_6\text{F}_5)_3]^-$  (**21**) from  $[2,6-(\text{Me}_3\text{SiN})_2\text{C}_5\text{H}_3\text{N}(\text{AlMe}_2)]_2[\text{AlMe}]$  (**20**) and its in-situ reaction with  $\text{B}(\text{C}_6\text{F}_5)_3$ .

Another indication for the monocation formation was seen by the presence of two different equal intensity signals for  $\text{SiMe}_3$  groups in  $^1\text{H}$  (0.41 and 0.31 ppm),  $^{13}\text{C}$  (1.66 and 1.30 ppm) and  $^{29}\text{Si}$  NMR (20.33 and 5.88 ppm) spectra in addition to two doublets (6.53 and 6.15 ppm) and a triplet (7.56 ppm) in aromatic region which indicated the nonequivalent chemical environment around the aluminum centres of **21** in comparison to its precursor, **20** (Figure 4.6). The chemical nonequivalency of carbon atoms around the pyridine ring could also be seen by the presence of five carbon signals in  $^{13}\text{C}$  NMR spectrum.  $^{11}\text{B}$  NMR spectrum of **21** showed the tetracoordinated anionic borane due to a sharp signal at  $-14.92$  ppm. An attempt to generate the cation on other aluminum centres resulted in several indistinguishable products. Attempt to synthesize



**Scheme 4.4.** Synthesis of aluminum-amide complexes,  $[2,4-(\text{Me}_3\text{SiN})_2-6-(\text{R})-\text{C}_3\text{N}_3](\text{AlMe}_2)_2$  ( $\text{R} = \text{Me}$  (**22**),  $\text{NHSiMe}_3$  (**23**),  $\text{Ph}$  (**24**)).

similar bowl shaped structures by reacting 1 eq. of bis(trimethylsilyl)-N,N'-2,4-diamino-6-(R)-triazine (bat) systems ( $\text{R} = \text{Me}$ ,  $\text{NH}(\text{SiMe}_3)$ ,  $\text{Ph}$ ) with 1.5 eq.  $\text{AlMe}_3$  couldn't afford the expected product however, on optimising the reaction of 1 eq. bat at room temperature in toluene with 2 eq. of  $\text{AlMe}_3$  gave a dinuclear aluminum complex with  $\text{AlMe}_2$  groups  $[2,4-(\text{Me}_3\text{SiN})_2-6-(\text{R})-\text{C}_3\text{N}_3](\text{AlMe}_2)_2$  ( $\text{R} = \text{Me}$  (**22**),  $\text{NHSiMe}_3$  (**23**),  $\text{Ph}$  (**24**)) (Scheme 4.4). Initial investigation of all these reactions (**22–24**) showed vigorous evolution of methane gas leading to a slight turbid to transparent solutions. The disappearance of N–H signals in IR spectrum as well as in  $^1\text{H}$  NMR spectrum confirmed the deprotonation of both amino protons however, the presence of Al–Me signals for **22** as a single peak (12H) at  $-0.69$  ppm, two singlets (with 6H each) at  $-0.63$ ,  $-0.68$  ppm for **23** and a single resonance (12H) at  $-0.61$  ppm for **24** with respect to other signals attributed formation of dinuclear

dimethylaluminium complex. The chemical shift values in  $^{13}\text{C}$  NMR spectrum for complexes **22** ( $-10.73$  ppm), **23** ( $-9.01$  ppm) and **24** ( $-0.07$  ppm) were consistent with the observations in  $^1\text{H}$  NMR spectrum of the corresponding molecules.  $^{29}\text{Si}$  NMR spectra showed signal at  $3.13$  (**22**),  $8.56$ ,  $1.32$ ,  $0.57$  (**23**) and  $3.18$  (**24**) ppm. Moreover, the signal at  $m/z = 382.1971$  (calcd.  $382.1984$ ),  $453.2155$  (calcd.  $453.2175$ ) and  $444.2126$  (calcd.  $444.2140$ ,  $[\text{M}+\text{H}]^+$ ) in HRMS confirmed the formation of **22-24** as dinuclear dimethylaluminum complexes.

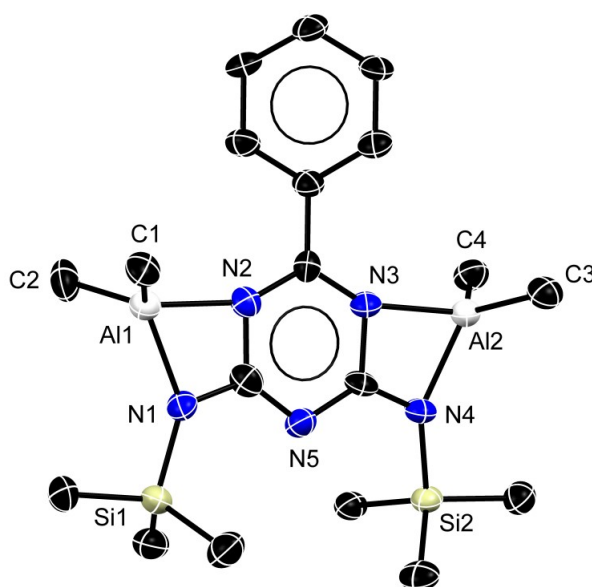
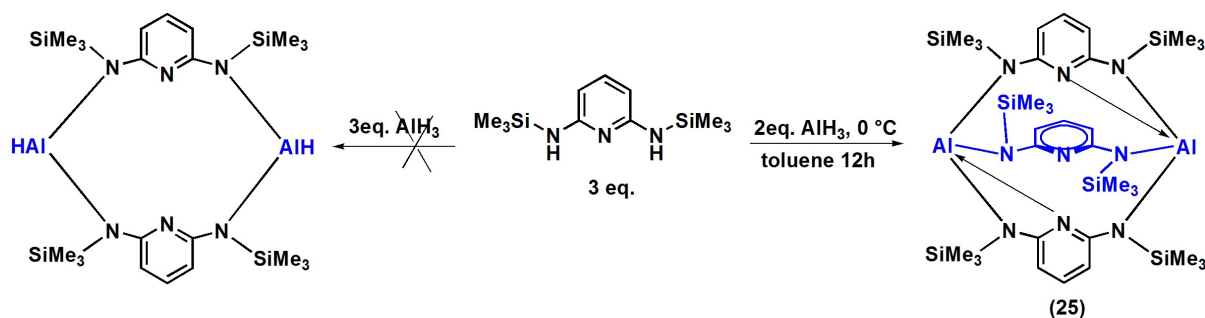


**Figure 4.7** Single crystal X-ray structure of  $[2,4-(\text{Me}_3\text{SiN})_2-6-(\text{Ph})-\text{C}_3\text{N}_3](\text{AlMe}_2)_2$  (**24**). All hydrogen atoms have been omitted for clarity. Selected bond lengths [ $\text{\AA}$ ] and bond angles [ $^\circ$ ]: Al1–N2 1.940(3), Al1–N2 1.984(3), Al1–C1 1.949(3), Al1–C2 1.950(3), Al2–C3 1.963(3), Al2–C4 1.963(3), N1–Si1 1.748(3), N4–Si2 1.754(3); N1–Al1–N2 69.29(10), N3–Al2–N4 70.10(10), C1–Al1–C2 121.15(15), C3–Al2–C4 121.82(15), C1–Al1–N1 118.00(13), C2–Al1–N1 110.42(13), C1–Al1–N2 114.29(13), C2–Al1–N2 112.60(13), C3–Al2–N3 119.25(13), C4–Al2–N3 115.23(13), C3–Al2–N3 115.23(13), C4–Al2–N4 113.68(14).

Repeated efforts to crystallize compounds **22** and **23** were unsuccessful due to gel formation on storing these complexes for several days however, complex **24** could be crystallized and its single crystal X-ray structure analysis revealed that it crystallized in

triclinic system with  $P\bar{1}$  space group. The solid state structure of complex **24** showed that both the aluminum centres are tetracoordinated and adopt distorted tetrahedral geometry with two nitrogen atoms and two methyl atoms forming a four membered  $[N_2CAI]$  ring (Figure 4.7). This structure consists of two four member  $[AlCN_2]$  chelate ring where both the triazine and amido sites of bat bind to centre in comparison to dialkyl complex **16** (pyridiyl nitrogen is bonded to Al and one of the amino site is not interacting with Al). The guanidinate bite angles (N-Al-N) in **24** are acute  $69.02^\circ$ - $69.77^\circ$  and are comparable to the amidinate bite angles in  $[2-(Me_3SiN)-6-(Me_3SiNH)C_5H_3N](AlMe_2)$  (**16**) range. In complex **24** the observed Al-C bond lengths are almost identical (1.950(4) and 1.963(4) Å).



**Scheme 4.5.** Synthesis of aluminum based cryptand,  $[2,6-(Me_3SiN)_2C_5H_3N]_3Al_2$  (**25**)

Attempts to obtain the structure similar to **12** (Chapter 3) and **18** using equimolar amount of  $AlH_3 \cdot NMe_2Et$  and bat were unsuccessful however, a 3:2 ratio reaction between bat with  $AlH_3 \cdot NMe_2Et$  in toluene proceeded over 12 h to afford a sticky product which on crystallization at  $-20^\circ C$  produced colorless crystals of a [3.3]cryptand,  $[2,6-(Me_3SiN)_2C_5H_3N]_3Al_2$  (**25**) in 56.2% yield (Scheme 4.5). The absence of N-H signal (present in the starting material (bat)) in IR and  $^1H$  NMR spectra of **25** showed that both N-H protons have been abstracted. The presence of only one signal for  $SiMe_3$  groups in  $^1H$  (0.11 ppm),  $^{13}C$  (1.68 ppm) and  $^{29}Si$  (0.02 ppm) NMR spectra attributed the symmetric nature of the product. The HRMS data showed a  $m/z$  pattern at 807.3423  $[M^+]$ , (calcd. 807.3453), which can be assigned to bicyclic molecule, where three bat units are connected by two Al centres.

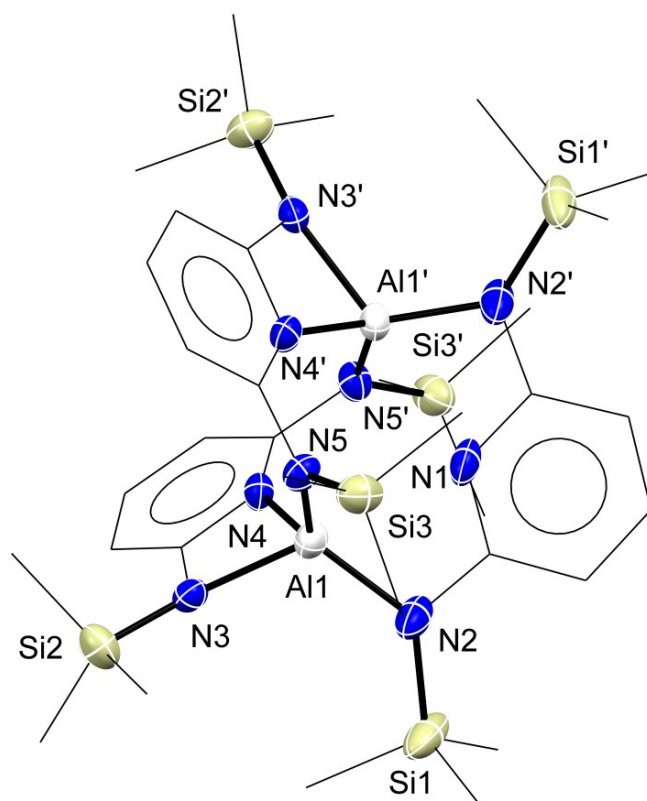


**Figure 4.8** Single crystal X-ray structure of aluminum based cryptand, [2,6-(Me<sub>3</sub>SiN)<sub>2</sub>C<sub>3</sub>H<sub>3</sub>N]<sub>3</sub>Al<sub>2</sub> (**25**). All hydrogen atoms have been omitted for clarity. Selected bond lengths [Å] and bond angles [°]: Al1–N2 1.844(5), Al1–N4 1.941(5), Al1–N5 1.848(5), N2–Si1 1.732(5), N3–Si2 1.723(5), N5–Si3 1.749(4), Al1···Al1 3.425(4), N1···N4 3.209(5), N4···N4' 3.004(7); N2–Al1–N3 116.20(4), N2–Al1–N5 118.95(2), N3–Al1–N4 70.24(4), N3–Al1–N5 106.80(2), N2–Al1–N4 113.11(2).

Single crystal X-ray structural analysis of **25** showed that it crystallized in orthorhombic system with  $C222_1$  space group. The cryptand **25** comprised of two tetracoordinated aluminum atoms adopting distorted tetrahedral geometry flanked with three units of bap ligand (Figure 4.8). The coordination results in the formation of two central rings (i) two ten membered, [N<sub>5</sub>Al<sub>2</sub>C<sub>3</sub>] rings flanked with four -SiMe<sub>3</sub>, where two pyridine rings are connected by N-Al-N arms, and (ii) a eight membered, [N<sub>4</sub>Al<sub>2</sub>C<sub>2</sub>] rings flanked with four -SiMe<sub>3</sub>, where two pyridine rings are connected by N-Al-N arms. The crystal structure of compound **25**

showed the Al $\cdots$ Al distance of 3.425(4) Å, however the N $\cdots$ N distance between nitrogen atoms of two pyridine rings are 3.209(5) Å (N<sub>1</sub> $\cdots$ N<sub>4</sub>) and 3.004(4) Å (N<sub>4</sub> $\cdots$ N<sub>4</sub>').

It is noteworthy, that in the case of the BH<sub>3</sub>·SMe<sub>2</sub> reaction with *bap*, a dimeric structure was obtained as tetraazadibora[3.3](2,6)pyridinophane (**12**) (Chapter 3) whereas, the reaction of AlH<sub>3</sub>·NEtMe<sub>2</sub> could not afford the analogous structure. Figure 4.9 depicts a comparison between the boron (85 pm) and aluminum (143) atomic radii. Perhaps, in the case of tetraazadibora[3.3](2,6)pyridinophane (**12**) the third unit of *bap* could not be accommodated between the boron atoms due to their small atomic radii. Whereas, the bigger atom aluminum allowed the third *bap* unit to form third bridge to a macrocyclic precursor under evolution of H<sub>2</sub>. The overall result is the formation of a cryptand like structure.

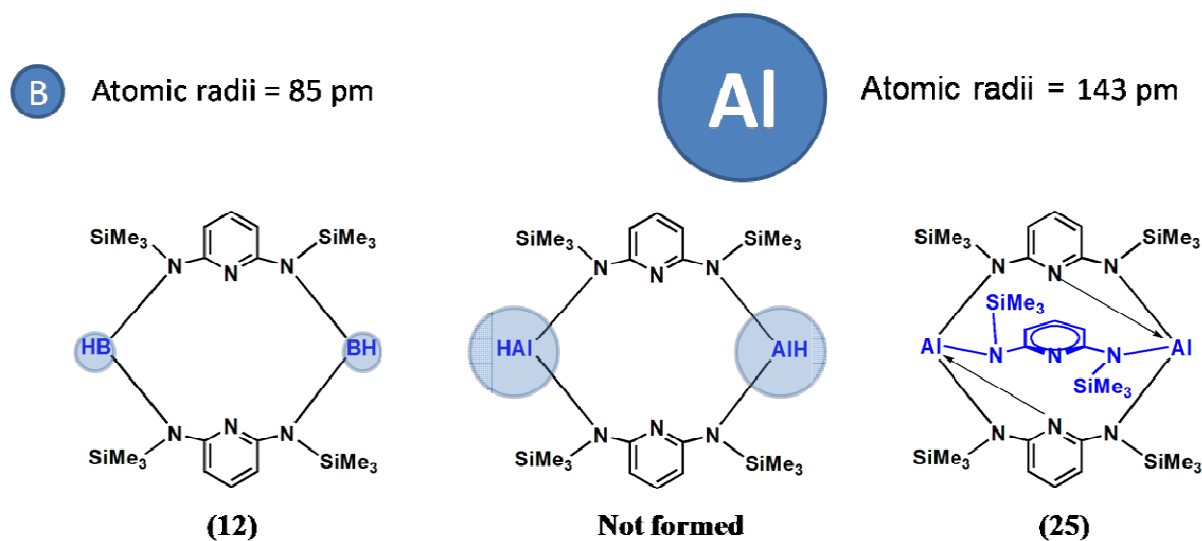


**Figure 4.9.** Structural comparison of tetraazadibora[3.3](2,6)pyridinophane (**12**) and the aluminum based cryptand, [2,6-(Me<sub>3</sub>SiN)<sub>2</sub>C<sub>5</sub>H<sub>3</sub>N]<sub>3</sub>Al<sub>2</sub> (**25**).

### 4.3 Conclusions

In summary, a variety of organoaluminum species are synthesized by changing the stoichiometry of *bap* and AlMe<sub>3</sub>. These complexes include aluminum-methyl complexes, [2-(Me<sub>3</sub>SiN)-6-(Me<sub>3</sub>SiNH)C<sub>5</sub>H<sub>3</sub>N](AlMe<sub>2</sub>) (**16**), [2-(Me<sub>3</sub>SiN)-6-(Me<sub>3</sub>Si

NH)C<sub>5</sub>H<sub>3</sub>N]<sub>2</sub>AlMe (**17**), tetraazadialumino[3.3](2,6)pyridinophane, [2,6-(Me<sub>3</sub>SiN)<sub>2</sub>C<sub>5</sub>H<sub>3</sub>NAI Me]<sub>2</sub> (**18-syn and 18-anti**). The sensitivity of complex **17** towards oxygen was used to afford methoxy bridged dimeric structure, [{2-(Me<sub>3</sub>SiN)-6-(Me<sub>3</sub>SiNH)C<sub>5</sub>H<sub>3</sub>N}<sub>2</sub>Al(μ-OMe)]<sub>2</sub> (**19**). On changing the bap and AlMe<sub>3</sub> (2:3) stoichiometry a bowl type structure, [2,6-(Me<sub>3</sub>SiN)<sub>2</sub>C<sub>5</sub>H<sub>3</sub>N(AlMe<sub>2</sub>)]<sub>2</sub>[AlMe] (**20**) was obtained which was further reacted with Lewis acid, B(C<sub>6</sub>F<sub>5</sub>)<sub>3</sub> to generate its monocationic species, [2-(Me<sub>3</sub>SiN)<sub>2</sub>-6-(Me<sub>3</sub>SiN)<sub>2</sub>C<sub>5</sub>H<sub>3</sub>N]<sub>2</sub>(AlMe<sub>2</sub>)(AlMe)<sup>+</sup>[AlMe][MeB(C<sub>6</sub>F<sub>5</sub>)<sub>3</sub>]<sup>-</sup> (**21**). The attempts to synthesize similar kind of bowl structures with the triazine systems resulted in their bis substituted dinuclear dimethylaluminum complexes, [2,4-(Me<sub>3</sub>SiN)<sub>2</sub>-6-(R)-C<sub>3</sub>N<sub>3</sub>](AlMe<sub>2</sub>)<sub>2</sub> (R = Me (**22**), NHSiMe<sub>3</sub> (**23**), Ph (**24**)). We have also showed a facile synthesis of aluminum based cryptand, [2,6-(Me<sub>3</sub>SiN)<sub>2</sub>C<sub>5</sub>H<sub>3</sub>N]<sub>3</sub>Al<sub>2</sub> (**25**) by the reaction of bap with AlH<sub>3</sub>·NMe<sub>2</sub>Et.

## 4.4 Experimental Section

### 4.4.1 General procedure

All manipulations were performed under nitrogen/argon atmosphere using Schlenk line or glove box techniques. All the glassware were dried at 150 °C in an oven for at least 12 h and assembled hot and cooled *in vacuo* prior to use. Solvents were purified by MBRAUN solvent purification system MB SPS-800.

### 4.4.2 Starting materials

All chemicals were purchased from Sigma-Aldrich and used without further purification. Solution of Al<sub>2</sub>Me<sub>6</sub> (1 M in toluene) was used in all experiments and effective concentration with respect to the monomer AlMe<sub>3</sub> was 2 M. It is to be noted that the monomer AlMe<sub>3</sub> exists in vapor phase formed from its dimer Al<sub>2</sub>Me<sub>6</sub> (present in the condensed phase). The starting materials bis(trimethylsilyl)-N,N'-2,6-diaminopyridine (bap)<sup>[12]</sup> and bis(trimethylsilyl)-N,N'-

2,4-diamino-6-(R)-triazine (bat) systems (R = Me, NH(SiMe<sub>3</sub>), Ph)<sup>[13]</sup> were prepared by following the reported procedures.

#### 4.4.3 Physical measurements

The <sup>1</sup>H, <sup>13</sup>C, <sup>29</sup>Si, <sup>11</sup>B and <sup>19</sup>F NMR spectra were recorded with a Bruker 400 MHz spectrometer with TMS, BF<sub>3</sub>·OEt<sub>2</sub> and CFCl<sub>3</sub> respectively, as external references. Chemical shifts were reported in ppm. Downfield shifts relative to the reference were quoted positive while the upfield shifts were assigned negative values. High resolution mass spectra were recorded on a Waters SYNAPT G2-S instrument. IR spectra of the complexes were recorded in the range 4000–400 cm<sup>-1</sup> using a Perkin Elmer Lambda 35-spectrophotometer. The absorptions of the characteristic functional groups were only assigned and other absorptions (moderate to very strong) were only listed. Melting points were obtained in sealed capillaries on a Büchi B-540 melting point instrument.

All single crystal X-ray diffraction data were collected using a Rigaku XtaLAB mini diffractometer equipped with Mercury375M CCD detector. The data were collected with graphite monochromatic MoK $\alpha$  radiation ( $\lambda = 0.71073 \text{ \AA}$ ) at 100.0(2) K using scans. During the data collection, the detector distance was maintained at 50 mm (constant) and the detector was placed at  $2\theta = 29.85^\circ$  (fixed) for all the data sets. The data collection and data reduction were done using Crystal Clear suite.<sup>[14]</sup> The crystal structures were solved by using OLEX2<sup>[15]</sup> and the structure were refined using XL.<sup>[16]</sup> All non hydrogen atoms were refined anisotropically.

#### 4.4.4 Synthetic procedure

##### Synthesis of [2-(Me<sub>3</sub>SiN)-6-(Me<sub>3</sub>SiNH)C<sub>5</sub>H<sub>3</sub>N](AlMe<sub>2</sub>) (16):

AlMe<sub>3</sub> (12 mmol, 6.0 mL, 2.0 M in toluene) was added slowly to a stirred solution of bap (3.0 g, 11.8 mmol) in hexane (40 mL) at 0 °C. The reaction mixture was allowed to come to

room temperature and stirred for 6 h. All volatiles were removed under vacuum to give a sticky material, which was further crystallized from pentane at  $-30\text{ }^{\circ}\text{C}$ . Yield: 1.8 g (49.28 %). Mp:  $240\text{ }^{\circ}\text{C}$  (decomp.). IR (nujol)  $\nu$ : 3392 (N-H), 2955, 2922, 2853, 1596, 1457, 1392, 1298, 1249, 1196, 1049, 890, 840, 784, 694, 494,  $449\text{ cm}^{-1}$ .  $^1\text{H}$  NMR (400 MHz,  $\text{C}_6\text{D}_6$ ):  $\delta$  = 6.79 (t, 1H, Ar,  $^3J_{\text{H-H}} = 8.0\text{ Hz}$ ), 6.14 (d, 2H, Ar,  $^3J_{\text{H-H}} = 8\text{ Hz}$ ), 0.30 (s, 18H,  $\text{SiMe}_3$ ),  $-0.11$  (s, 3H,  $\text{AlMe}$ ),  $-0.97$  (s, 3H,  $\text{AlMe}$ ).  $^{13}\text{C}$  NMR (100 MHz,  $\text{C}_6\text{D}_6$ ):  $\delta$  = 165.1, 143.2, 111.9, 2.64 ( $\text{SiMe}_3$ ), 1.47 ( $\text{AlMe}$ ),  $-0.41$  ( $\text{AlMe}$ ).  $^{29}\text{Si}$  NMR (79.5 MHz,  $\text{C}_6\text{D}_6$ ):  $\delta$  = 8.58. HRMS ( $\text{AP}^+$ ):  $m/z$  calcd for  $\text{C}_{13}\text{H}_{29}\text{AlN}_3\text{Si}_2$ : (310.1715),  $[\text{M}+\text{H}]^+$ ; found: (310.1702).

#### **Synthesis of [2-( $\text{Me}_3\text{SiN}$ )-6-( $\text{Me}_3\text{SiNH}$ ) $\text{C}_5\text{H}_3\text{N}$ ] $_2\text{AlMe}$ (17):**

$\text{AlMe}_3$  (10.0 mmol, 5.0 mL, 2.0 M in toluene) was added slowly to a stirred solution of bap (5.0 g, 19.8 mmol) in hexane (60 mL) at  $0\text{ }^{\circ}\text{C}$ . The reaction mixture was allowed to come to room temperature and stirred for 24 h. All volatiles were removed under vacuum to give a sticky solid which was further crystallized with pentane at  $-30\text{ }^{\circ}\text{C}$ . Yield: 4.1 g (75.7 %). Mp:  $92\text{-}94\text{ }^{\circ}\text{C}$ . IR (nujol)  $\nu$ : 3393 (N-H), 2924, 2957, 1596, 1458, 1373, 1298, 1259, 1160, 1096, 1071, 1028, 840, 783, 719, 695, 620,  $492\text{ cm}^{-1}$ .  $^1\text{H}$  NMR (400 MHz,  $\text{CDCl}_3$ ):  $\delta$  = 7.21 (t, 2H, Ar,  $^3J_{\text{H-H}} = 8.0\text{ Hz}$ ), 5.87 (d, 2H, Ar,  $^3J_{\text{H-H}} = 8\text{ Hz}$ ), 5.66 (d, 2H, Ar,  $^3J_{\text{H-H}} = 8\text{ Hz}$ ), 3.89 (s, 2H, NH), 0.27 (s, 18H,  $\text{SiMe}_3$ ), 0.07 (s, 18H,  $\text{SiMe}_3$ )  $-0.72$  (s, 3H,  $\text{AlMe}_3$ ).  $^{13}\text{C}$  NMR (100 MHz,  $\text{CDCl}_3$ ):  $\delta$  = 165.45, 154.90, 141.70, 99.23, 95.35, 1.21 ( $\text{SiMe}_3$ ), 0.26 ( $\text{AlMe}_3$ ),  $-0.10$  ( $\text{SiMe}_3$ ).  $^{29}\text{Si}$  NMR (79.5 MHz,  $\text{CDCl}_3$ ):  $\delta$  = 4.70 ( $\text{SiMe}_3$ ),  $-1.45$  ( $\text{SiMe}_3$ ). HRMS ( $\text{AP}^+$ ):  $m/z$  calcd for  $\text{C}_{23}\text{H}_{50}\text{AlN}_6\text{Si}_4$ : (531.2520)  $[\text{M}-\text{Me}+\text{H}]^+$ ; obs: (531.2501).

#### **Synthesis of tetraazadialumino[3.3](2,6)pyridinophane, [2,6-( $\text{Me}_3\text{SiN}$ ) $_2\text{C}_5\text{H}_3\text{N}$ ] $_2\text{AlMe}$ (18):**

$\text{AlMe}_3$  (19.76 mmol, 9.9 mL, 2.0 M in toluene) was added slowly to a stirred solution of bis(trimethylsilyl)- $\text{N,N}'$ -2,6-diaminopyridine (5.0 g, 19.76 mmol) in toluene (80 mL) at  $0\text{ }^{\circ}\text{C}$ .

The reaction mixture was allowed to come to room temperature and stirred for 1 hour followed by 36 hours of reflux. All volatiles were removed under vacuum to give an oily material, which was crystallized with dry pentane (40 mL) at  $-30\text{ }^{\circ}\text{C}$ . Yield: 3.8 g (65.5 %). Mp: 268–272  $^{\circ}\text{C}$ . IR (nujol)  $\nu$ : 3084, 2956, 2928, 2857, 1593, 1547, 1454, 1394, 1351, 1256, 1192, 1159, 1064, 904, 844, 734, 687, 634, 531, 474  $\text{cm}^{-1}$ .  $^1\text{H}$  NMR (400 MHz,  $\text{CDCl}_3$ ):  $\delta$  = 7.16 (t, 2H, *p*-ArH, Ar,  $^3J_{\text{H-H}} = 8.0$  Hz), 5.79 (broad singlet, 4H, *m*-ArH, Ar), 0.13 (s, 36H,  $\text{SiMe}_3$ ),  $-0.49$  (s, 6H, AlMe) ppm.  $^{13}\text{C}$  NMR (100 MHz,  $\text{CDCl}_3$ ):  $\delta$  = 165.5, 154.9, 143.2, 109.5, 102.1, 2.3 ( $\text{SiMe}_3$ ), 0.5 ( $\text{SiMe}_3$ ),  $-10.5$  (AlMe) ppm.  $^{29}\text{Si}$  NMR (79.5 MHz,  $\text{CDCl}_3$ ):  $\delta$  = 3.76 ( $\text{SiMe}_3$ ),  $-2.38$  ( $\text{SiMe}_3$ ) ppm. HRMS ( $\text{AP}^+$ ):  $m/z$  calcd for  $\text{C}_{24}\text{H}_{49}\text{Al}_2\text{N}_6\text{Si}_4$ : (587.2726)  $[\text{M}+\text{H}]^+$ ; found: (587.2708).

**Synthesis of methoxy bridged dimer  $[\{2-(\text{Me}_3\text{SiN})-6-(\text{Me}_3\text{SiNH})\text{C}_5\text{H}_3\text{N}\}_2\text{Al}(\mu\text{-OMe})_2$  (19):**

A solution of **17** (1g, 1.83 mmol) in 40 mL hexane was stirred for 6 days under oxygen atmosphere. All volatiles were removed under vacuum and subsequently washed with cold pentane to afford compound **19** as white solid which was further crystallized from toluene at  $-20\text{ }^{\circ}\text{C}$ . Yield: 0.45 g (43.7 %). Mp: 268–272  $^{\circ}\text{C}$ . IR (nujol)  $\nu$ : 3390 (N-H), 2954, 2927, 2857, 1596, 1568, 1456, 1374, 1299, 1251, 1163, 1098 (O-Me), 1071, 839, 778, 747, 723, 689, 632, 594, 553, 468, 431  $\text{cm}^{-1}$ .  $^1\text{H}$  NMR (400 MHz,  $\text{CDCl}_3$ ):  $\delta$  = 7.09 (t, 4H, Ar,  $^3J_{\text{H-H}} = 8.0$  Hz), 5.77 (d, 4H, Ar,  $^3J_{\text{H-H}} = 8$  Hz), 5.43 (d, 4H, Ar,  $^3J_{\text{H-H}} = 8$  Hz), 4.07 (s, 4H, N-H), 3.55 (s, 12H, -OMe), 0.09 (s, 36H,  $\text{SiMe}_3$ ),  $-0.09$  (s, 36H,  $\text{SiMe}_3$ ).  $^{13}\text{C}$  NMR (100 MHz,  $\text{CDCl}_3$ ):  $\delta$  = 166.9, 156.2, 140.8, 98.9, 94.6, 51.3 (-OMe), 1.09 ( $\text{SiMe}_3$ ), 0.07 ( $\text{SiMe}_3$ ).  $^{29}\text{Si}$  NMR (79.5 MHz,  $\text{CDCl}_3$ ):  $\delta$  = 2.77 ( $\text{SiMe}_3$ ),  $-4.08$  ( $\text{SiMe}_3$ ). HRMS ( $\text{AP}^+$ ):  $m/z$  calcd for  $\text{C}_{46}\text{H}_{94}\text{Al}_2\text{N}_{12}\text{O}_2\text{Si}_8$ : (1125.5486)  $[\text{M}]^+$ ; found: (1125.5431).

**Synthesis of bowl shaped aluminum cage, [2,6-(Me<sub>3</sub>SiN)<sub>2</sub>C<sub>5</sub>H<sub>3</sub>N(AlMe<sub>2</sub>)<sub>2</sub>][AlMe] (20):**

AlMe<sub>3</sub> (6.0 mmol, 3.0 mL, 2.0 M in toluene) was added slowly to a stirred solution of bap (1.0 g, 3.9 mmol) in toluene (15 mL) at 0 °C. The reaction mixture was allowed to come to room temperature and stirred for 2 h. On evaporating all volatiles, a white solid was obtained which on crystallization with hexane at -30 °C afforded colorless crystals. Yield: 0.90 g (69.2 %). Mp: 161–164 °C. IR (nujol)  $\nu$ : 2956, 2921, 2857, 1600, 1547, 1458, 1390, 1337, 1256, 1192, 1170, 1085, 1050, 893, 847, 727, 691, 574, 489, 446 cm<sup>-1</sup>. <sup>1</sup>H NMR (400 MHz, CDCl<sub>3</sub>):  $\delta$  = 7.46 (t, 2H, Ar, <sup>3</sup>J<sub>H-H</sub> = 8.0 Hz), 6.35 (d, 4H, Ar, <sup>3</sup>J<sub>H-H</sub> = 8 Hz), 0.25 (s, 36H, SiMe<sub>3</sub>), -0.23 (s, 3H, AlMe), -0.55 (s, 6H, AlMe), -1.50 (s, 6H, AlMe). <sup>13</sup>C NMR (100 MHz, CDCl<sub>3</sub>):  $\delta$  = 164.86, 142.91, 111.54, 2.64 SiMe<sub>3</sub>, -0.06 (AlMe), -2.01 (AlMe), -8.23 (AlMe). <sup>29</sup>Si NMR (79.5 MHz, CDCl<sub>3</sub>):  $\delta$  = 8.88. HRMS (AP<sup>+</sup>): *m/z* calcd for C<sub>27</sub>H<sub>58</sub>Al<sub>3</sub>N<sub>6</sub>Si<sub>4</sub>: (659.3246) [M+H]<sup>+</sup>; obs: (659.3218).

**Synthesis of [2-(Me<sub>3</sub>SiN)<sub>2</sub>-6-(Me<sub>3</sub>SiN)<sub>2</sub>C<sub>5</sub>H<sub>3</sub>N]<sub>2</sub>(AlMe<sub>2</sub>)(AlMe)<sup>+</sup>[AlMe][MeB(C<sub>6</sub>F<sub>5</sub>)<sub>3</sub>]<sup>-</sup> (21):**

B(C<sub>6</sub>F<sub>5</sub>)<sub>3</sub> (0.4 mmol, 0.21 g) and [2,6-(Me<sub>3</sub>SiN)<sub>2</sub>C<sub>5</sub>H<sub>3</sub>N(AlMe<sub>2</sub>)<sub>2</sub>][AlMe] (20) (0.4 mmol, 0.26 g) were mixed in 5 mL of hexane and stirred for 1h. On evaporating all volatiles an oily product was obtained. Yield: 0.45 g (96.2 %). IR (nujol)  $\nu$  : 2955, 2924, 2855, 1604, 1549, 1460, 1378, 1264, 1172, 1089, 848, 800, 725 cm<sup>-1</sup>. <sup>1</sup>H NMR (400 MHz, CDCl<sub>3</sub>):  $\delta$  = 7.56 (t, 2H, Ar, <sup>3</sup>J<sub>H-H</sub> = 8.0 Hz), 6.53 (d, 2H, Ar, <sup>3</sup>J<sub>H-H</sub> = 8 Hz), 6.15 (d, 2H, Ar, <sup>3</sup>J<sub>H-H</sub> = 8 Hz), 0.52 (broad s, 3H, BMe), 0.41 (s, 18H, SiMe<sub>3</sub>), 0.31 (s, 18H, SiMe<sub>3</sub>), 0.15 (s, 3H, AlMe), -0.20 (s, 3H, AlMe), -0.25 (s, 3H, AlMe), -1.24 (s, 3H, <sup>+</sup>AlMe). <sup>13</sup>C NMR (100 MHz, CDCl<sub>3</sub>):  $\delta$  = 165.6, 155.3, 144.8, 112.3, 109.3, 1.66 (SiMe<sub>3</sub>), -5.17 (AlMe), -6.35 (AlMe), -6.86 (AlMe), -7.72 (AlMe). <sup>19</sup>F NMR (376 MHz, CDCl<sub>3</sub>):  $\delta$  = -132.6 (d, 6F, J<sub>F-F</sub> = 18.8 Hz, *o*-C<sub>6</sub>F<sub>5</sub>), -164.90 (t, 3F, J<sub>F-F</sub> = 18.8 Hz, *p*-C<sub>6</sub>F<sub>5</sub>), -167.31 (t, 6F, J<sub>F-F</sub> = 18.8 Hz, *m*-C<sub>6</sub>F<sub>5</sub>). <sup>11</sup>B NMR

(128 MHz, CDCl<sub>3</sub>):  $\delta = -14.92$ . <sup>29</sup>Si NMR (79.5 MHz, CDCl<sub>3</sub>):  $\delta = 20.23, 5.88$ . HRMS (AP<sup>+</sup>): *m/z* calcd for C<sub>26</sub>H<sub>54</sub>Al<sub>3</sub>N<sub>6</sub>Si<sub>4</sub>: (643.2933) [M-[MeB(C<sub>6</sub>F<sub>5</sub>)<sub>3</sub>]]<sup>+</sup>; found: (643.2921).

**Synthesis of [2,4-(Me<sub>3</sub>SiN)<sub>2</sub>-6-(Me)-C<sub>3</sub>N<sub>3</sub>](AlMe<sub>2</sub>)<sub>2</sub> (22):**

AlMe<sub>3</sub> (3.0 mmol, 1.5 mL, 2.0 M in toluene) was added slowly to a stirred solution of 6-methyl-bat (0.54 g, 2.0 mmol) in toluene (10 mL) at 0 °C. The reaction mixture was allowed to come to room temperature and stirred for 3 h. On evaporating all volatiles a white solid was obtained in good yield. Yield: 0.69 g (90.4 %). Mp: 161–164 °C. IR (nujol)  $\nu$  : 2956, 2921, 2855, 1603, 1494, 1459, 1378, 1355, 1251, 1193, 1150, 893, 876, 845, 756, 717, 690, 593, 427 cm<sup>-1</sup>. <sup>1</sup>H NMR (400 MHz, CDCl<sub>3</sub>):  $\delta = 2.07$  (s, 3H, Ar-Me), 0.22 (s, 18H, SiMe<sub>3</sub>), -0.69 (s, 12H, AlMe). <sup>13</sup>C NMR (100 MHz, CDCl<sub>3</sub>):  $\delta = 166.67, 165.73, 20.91$  (Ar-Me), -0.13 (SiMe<sub>3</sub>), -10.73 (AlMe). <sup>29</sup>Si NMR (79.5 MHz, CDCl<sub>3</sub>):  $\delta = 3.13$ . HRMS (AP<sup>+</sup>): *m/z* calcd for C<sub>14</sub>H<sub>34</sub>Al<sub>2</sub>N<sub>5</sub>Si<sub>2</sub>: (382.1984) [M]<sup>+</sup>; found: (382.1971).

**Synthesis of [2,4-(Me<sub>3</sub>SiN)<sub>2</sub>-6-(Me<sub>3</sub>SiNH)-C<sub>3</sub>N<sub>3</sub>](AlMe<sub>2</sub>)<sub>2</sub> (23):**

AlMe<sub>3</sub> (3.0 mmol, 1.5 mL, 2.0 M in toluene) was added slowly to a stirred solution of 6-Me<sub>3</sub>SiNH-triazine (0.68 g, 2.0 mmol) in toluene (10 mL) at 0 °C. The reaction mixture was allowed to come to room temperature and stirred for 3 h. On evaporating all volatiles, oily product was obtained which gave sticky compound after drying for a long period. Yield: 0.86 g (94.6 %). Mp: 185–190 °C. IR (nujol)  $\nu$ : 2956, 2926, 2856, 1590, 1551, 1466, 1389, 1155, 1097, 1024, 843, 804, 723, 689 cm<sup>-1</sup>. <sup>1</sup>H NMR (400 MHz, CDCl<sub>3</sub>):  $\delta = 0.34$  (s, 9H, SiMe<sub>3</sub>), 0.21 and 0.20 (s, 18H, SiMe<sub>3</sub>), -0.63 and -0.68 (s, 12H, AlMe). <sup>13</sup>C NMR (100 MHz, CDCl<sub>3</sub>):  $\delta = 168.0, 163.15, 161.79, 0.82$  (SiMe<sub>3</sub>), 0.38 (SiMe<sub>3</sub>), 0.11 (SiMe<sub>3</sub>), -9.01 (AlMe), -10.13 (AlMe). <sup>29</sup>Si NMR (79.5 MHz, CDCl<sub>3</sub>):  $\delta = 8.65, 1.32, 0.57$ . HRMS (AP<sup>+</sup>): *m/z* calcd for C<sub>16</sub>H<sub>39</sub>Al<sub>2</sub>N<sub>6</sub>Si<sub>3</sub>: (453.2175) [M]<sup>+</sup>; found: (453.2155).

**Synthesis of [2,4-(Me<sub>3</sub>SiN)<sub>2</sub>-6-(Ph)-C<sub>3</sub>N<sub>3</sub>](AlMe<sub>2</sub>)<sub>2</sub> (24):**

AlMe<sub>3</sub> (3.0 mmol, 1.5 mL, 2.0 M in toluene) was added slowly to a stirred solution of 6-phenyl-bat (0.66 g, 2.0 mmol) in toluene (10 mL) at 0 °C. The reaction mixture was allowed to come to room temperature and stirred for 3 h. On evaporating all volatiles a orange solid was obtained which on crystallization with pentane at -30 °C afforded colorless crystals. Yield: 0.83 g (93.5 %). Mp: 212–215 °C. IR (nujol)  $\nu$  : 2926, 2853, 1601, 1567, 1540, 1459, 1374, 1251, 1220, 1193, 1047, 1024, 954, 847, 781, 693, 592, 431 cm<sup>-1</sup>. <sup>1</sup>H NMR (400 MHz, CDCl<sub>3</sub>):  $\delta$  = 7.75, (d, 2H), 7.53 (m, 3H), 0.27 (s, 18H, SiMe<sub>3</sub>), -0.61 (s, 12H, AlMe). <sup>13</sup>C NMR (100 MHz, CDCl<sub>3</sub>):  $\delta$  = 166.99, 163.28, 133.62, 131.08, 129.66, 129.02, 128.14, 127.01, -0.07 SiMe<sub>3</sub>, -10.19 (AlMe). <sup>29</sup>Si NMR (79.5 MHz, CDCl<sub>3</sub>):  $\delta$  = 3.18. HRMS (AP<sup>+</sup>):  $m/z$  calcd for C<sub>19</sub>H<sub>36</sub>Al<sub>2</sub>N<sub>5</sub>Si<sub>2</sub>: (444.2140) [M]<sup>+</sup>; found: (444.2126).

**Synthesis of cryptand, [2,6-(Me<sub>3</sub>SiN)<sub>2</sub>C<sub>5</sub>H<sub>3</sub>N]<sub>3</sub>Al<sub>2</sub> (25):**

AlH<sub>3</sub>·NMe<sub>2</sub>Et (3.9 mmol, 8 mL, 0.5 M in toluene) was added slowly to a stirred solution of bap (1.0 g, 3.9 mmol) in toluene (40 mL) at 0 °C. The reaction mixture was allowed to come to room temperature and stirred for 12 h. All the volatiles were removed under vacuum to give a white solid, which was further crystallized from toluene at -20 °C. Yield: 0.59 g (56.2 %). Mp: 156-158 °C. IR (nujol)  $\nu$ : 2956, 2900, 1599, 1453, 1393, 1304, 1251, 1151, 1028, 842, 789, 718, 688, 622 cm<sup>-1</sup>. <sup>1</sup>H NMR (400 MHz, CDCl<sub>3</sub>):  $\delta$  = 7.20 (t, 3H, Ar, <sup>3</sup>J<sub>H-H</sub> = 8.0 Hz), 5.90 (d, 6H, Ar, <sup>3</sup>J<sub>H-H</sub> = 8 Hz), 0.11 (s, 54H, SiMe<sub>3</sub>). <sup>13</sup>C NMR (100 MHz, CDCl<sub>3</sub>):  $\delta$  = 163.7, 142.1, 102.2, 1.83 (SiMe<sub>3</sub>). <sup>29</sup>Si NMR (79.5 MHz, CDCl<sub>3</sub>):  $\delta$  = 0.02. HRMS (AP<sup>+</sup>):  $m/z$  calcd for C<sub>33</sub>H<sub>63</sub>Al<sub>2</sub>N<sub>9</sub>Si<sub>6</sub>: (807.3453) [M]<sup>+</sup>; found: (807.3423).

## 4.5 Crystallographic Data

**Table 4.1** Crystallographic data for compounds **16–18**.

Compound <sup>[a]</sup>	16	17	18-syn	18-anti
Chemical formula	C <sub>13</sub> H <sub>28</sub> AlN <sub>3</sub> Si <sub>2</sub>	C <sub>23</sub> H <sub>54</sub> AlN <sub>6</sub> Si <sub>4</sub>	C <sub>24</sub> H <sub>48</sub> Al <sub>2</sub> N <sub>6</sub> Si <sub>4</sub>	C <sub>24</sub> H <sub>48</sub> Al <sub>2</sub> N <sub>6</sub> Si <sub>4</sub>
Molar mass	309.54	590.09	587.00	587.00
Crystal system	monoclinic	monoclinic	monoclinic	monoclinic
Space group	<i>P2<sub>1</sub>/c</i>	<i>P2<sub>1</sub>/c</i>	<i>P2<sub>1</sub>/c</i>	<i>P2<sub>1</sub>/c</i>
<i>T</i> [K]	100(2)	100(2)	100(2)	100(2)
<i>a</i> [Å]	6.379(2)	12.1076(8)	17.2486(9)	11.6602(13)
<i>b</i> [Å]	13.613(3)	11.8845(8)	12.6136(7)	12.6412(10)
<i>c</i> [Å]	22.304(7)	24.8155(18)	16.1018(9)	12.9228(15)
$\alpha$ [°]	90	90	90	90
$\beta$ [°]	94.760(13)	94.202(4)	91.704(5)	116.275(14)
$\gamma$ [°]	90	90	90	90
<i>V</i> [Å <sup>3</sup> ]	1930.1(10)	3561.2(4)	3501.7(3)	1708.0(4)
<i>Z</i>	4	4	4	4
<i>D</i> (calcd.) [g·cm <sup>-3</sup> ]	1.065	1.101	1.113	1.141
$\mu$ (Mo- <i>K<math>\alpha</math></i> ) [mm <sup>-1</sup> ]	0.223	0.216	0.242	0.248
Reflections collected	10902	37445	48197	24025
Independent reflections	3410	8103	12480	6131
Data/restraints/parameters	3410/0/184	8103/0/356	12480/0/339	6131/0/170
<i>R</i> <sub>1</sub> , <i>wR</i> <sub>2</sub> [ <i>I</i> > 2 $\sigma$ ( <i>I</i> )] <sup>[a]</sup>	0.0651, 0.1657	0.0554, 0.1370	0.0715, 0.1627	0.0814/0.2115
<i>R</i> <sub>1</sub> , <i>wR</i> <sub>2</sub> (all data) <sup>[a]</sup>	0.0801, 0.1857	0.0687, 0.1491	0.1322, 0.1912	0.1129/0.2436
GOF	1.149	1.098	1.039	1.081

[a]  $RI = \Sigma||Fo|-|Fc||/\Sigma|Fo|$ ,  $wR_2 = [\Sigma w(|Fo|^2 - |Fc|^2)^2 / \Sigma w|Fo|^2]^1/2$

**Table 4.2** Crystallographic data for compounds **19**, **20**, **24** and **25**.

Compound <sup>[a]</sup>	19	20	24	25
Chemical formula	C <sub>23</sub> H <sub>47</sub> AlN <sub>6</sub> OSi <sub>4</sub>	C <sub>27</sub> H <sub>57</sub> Al <sub>3</sub> N <sub>6</sub> Si <sub>4</sub>	C <sub>19</sub> H <sub>35</sub> Al <sub>2</sub> N <sub>5</sub> Si <sub>2</sub>	C <sub>33</sub> H <sub>63</sub> Al <sub>2</sub> N <sub>9</sub> Si <sub>6</sub>
Molar mass	563.00	659.08	443.66	404.21
Crystal system	monoclinic	orthorhombic	triclinic	orthorhombic
Space group	<i>C</i> 2 <sub>1</sub> / <i>c</i>	<i>P</i> bcn	<i>P</i> $\bar{1}$	<i>C</i> 222 <sub>1</sub>
<i>T</i> [K]	100(3)	100(2)	100(2)	100(2)
<i>a</i> [Å]	22.068(9)	18.013(7)	6.4274(10)	17.001(3)
<i>b</i> [Å]	19.511(7)	14.239(6)	11.1271(18)	20.578(4)
<i>c</i> [Å]	15.850(6)	15.420(6)	18.495(3)	14.373(2)
$\alpha$ [°]	90	90	90.182(8)	90
$\beta$ [°]	110.104(14)	90	91.260(13)	90
$\gamma$ [°]	90	90	95.106(10)	90
<i>V</i> [Å <sup>3</sup> ]	6409(4)	3955(3)	1317.2(4)	5028.3(16)
<i>Z</i>	8	4	4	4
<i>D</i> (calcd.) [g·cm <sup>-3</sup> ]	1.167	1.107	1.119	1.068
$\mu$ (Mo- <i>K</i> $\alpha$ ) [mm <sup>-1</sup> ]	0.239	0.242	0.215	0.232
Reflections collected	12580	13462	13843	6914
Independent reflections	5488	4420	6007	5335
Data/restraints/parameters	5488/0/338	4420/0/191	6007/0/263	5335/0/236
<i>R</i> <sub>1</sub> , <i>wR</i> <sub>2</sub> [ <i>I</i> >2 $\sigma$ ( <i>I</i> )] <sup>[a]</sup>	0.0771, 0.2010	0.0722, 0.1886	0.0676, 0.1778	0.0710, 0.1327
<i>R</i> <sub>1</sub> , <i>wR</i> <sub>2</sub> (all data) <sup>[a]</sup>	0.1252, 0.2553	0.1098, 0.2223	0.0932, 0.2175	0.1139, 0.1630
GOF	1.009	1.069	1.222	0.988

[a]  $R_1 = \sum ||F_o| - |F_c|| / \sum |F_o|$ ,  $wR_2 = [\sum w(|F_o^2| - |F_c^2|)^2 / \sum w|F_o^2|]^2$

## 4.6 References

- [1] W. Zheng and H. W. Roesky, *J. Chem. Soc., Dalton Trans.* **2002**, 2787–2796.
- [2] M. L. Montero, A. Voigt, M. Teichert, I. Usón and H. W. Roesky, *Angew. Chem. Int. Ed. Engl.* **1995**, *34*, 2504–2506.
- [3] a) R. Duchateau, A. Meetsma and J. H. Teuben, *Chem. Commun.* **1996**, 223–224; b) A. L. Brazeau and S. T. Barry, *Chem. Mater.* **2008**, *20*, 7287–7291; c) N. E. Mansfield, M. P. Coles and P. B. Hitchcock, *Dalton Trans.* **2005**, 2833–2841; d) P. B. Hitchcock, M. F. Lappert and P. G. Merle, *Dalton Trans.* **2007**, 585–594; e) B. Clare, N. Sarker, R. Shoemaker and J. R. Hagadorn, *Inorg. Chem.* **2004**, *43*, 1159–1166; f) A. L. Brazeau, Z. Wang, C. N. Rowley and S. T. Barry, *Inorg. Chem.* **2006**, *45*, 2276–2281; g) J. A. R. Schmidt and J. Arnold, *Organometallics*, **2002**, *21*, 2306–2313; h) M. P. Coles and R. F. Jordan, *J. Am. Chem. Soc.* **1997**, *119*, 8125–8126; i) S. Dagorne, I. A. Guzei, M. P. Coles and R. F. Jordan, *J. Am. Chem. Soc.* **2000**, *122*, 274–289; j) R. T. Boere', M. L. Cole and P. C. Junk, *New J. Chem.* **2005**, *29*, 128–134; k) M. P. Coles, D. C. Swenson, and R. F. Jordan, *Organometallics* **1997**, *16*, 5183–5194; l) D. Abeysekera, K. N. Robertson, T. S. Cameron and J. A. C. Clyburne, *Organometallics* **2001**, *20*, 5532–5536; m) M. Bayram, D. Bläser, C. Wölper and S. Schulz, *Organometallics* **2014**, *33*, 2080–2087.
- [4] a) G. G. Skvortsov, G. K. Fukin, S. Y. Ketkov, A. V. Cherkasov, K. A. Lyssenko and A. A. Trifonov, *Eur. J. Inorg. Chem.* **2013**, 4173–4183; b) G. Glatz and R. Kempe, *Z. Kristallogr. NCS*, **2008**, *223*, 307–308; c) G. Glatz and R. Kempe, *Z. Kristallogr. NCS*, **2008**, *223*, 309–310; d) G. Glatz and R. Kempe, *Z. Kristallogr. NCS*, **2008**, *223*, 313–315; e) Y. L. Huang, D. Y. Lu, H. C. Yu, J. S. K. Yu, C.W. Hsu, T. S. Kuo, G. H. Lee, Y. Wang and Y. C. Tsai, *Angew. Chem. Int. Ed.* **2012**, *51*, 7781–7785; f) Y. T. Wey, F. S. Yang, H. C. Yu, T. S. Kuo and Y. C. Tsai, *Angew. Chem. Int. Ed.* **2017**, *56*,

- 15108–15112; g) V. Rad'kov, V. Dorcet, J. F. Carpentier, A. Trifonov and E. Kirillov, *Organometallics* **2013**, *32*, 1517–1527.
- [5] a) W. Uhl, M. Claesener, A. Hepp, B. Jasper, A. Vinogradov, L. van Wüllen and T. K.-J. Köster, *Dalton Trans.* **2009**, 10550–10562; b) W. Uhl, A. Hepp, M. Matar and A. Vinogradov, *Eur. J. Inorg. Chem.* **2007**, 4133–4137.
- [6] K. Maheswari and N. D. Reddy, *Organometallics* **2012**, *31*, 197–206.
- [7] Y. A. Wasslen, A. Kurek, P. A. Johnson, T. C. Pigeon, W. H. Monillas, G. P. A. Yap and S. T. Barry, *Dalton Trans.* **2010**, *39*, 9046–9054
- [8] S. L. Aeilts, M. P. Coles, D. C. Swenson and R. F. Jordan, *Organometallics*, **1998**, *17*, 3265–3270.
- [9] P. Shukla, J. C. Gordon, A. H. Cowley and J. N. Jones, *Inorg. Chim. Acta*, **2005**, *358*, 4407–4411.
- [10] H. M. T. Nguyen, Hsin-Yu Tang, W. F. Huang and M. C. Lin, *Computational and Theoretical Chem.* **2014**, *1035*, 39–43.
- [11] D. Zhang, *Eur. J. Inorg. Chem.* **2007**, 3077–3082.
- [12] L. Beer, J. F. Britten, J. L. Brusso, A. W. Cordes, R. C. Haddon, M. E. Itkis, D. S. MacGregor, R. T. Oakley, R. W. Reed, and C. M. Robertson *J. Am. Chem. Soc.* **2003**, *125*, 14394–14403.
- [13] B. Parker and D. Y. Son, *Inorg. Chem. Commun.* **2002**, *5*, 516–518.
- [14] CrystalClear 2.0; Rigaku Corporation: Tokyo, Japan, **2013**.
- [15] O. V. Dolomanov, L. J. Bourhis, R. J. Gildea, J. A. K. Howard and H. Puschmann, *J. Appl. Crystallogr.* **2009**, *42*, 339–341.
- [16] G. M. Sheldrick, *Acta Cryst. A*, **2015**, *71*, 3–8.



## List of Publications

1. [Deependra Bawari](#), Billa Prashanth, Satyam Ravi, K. R. Shamasundar, Sanjay Singh,\* and Dominic S. Wright, Two different pathways in the reduction of  $[(S=)PCl(\mu-NtBu)]_2$  with Na, *Chem. Eur. J.* **2016**, 22, 12027–12033 (**hot paper**). (Selected for the cover page and cover profile picture ([DOI: 10.1002/chem.201602882](https://doi.org/10.1002/chem.201602882)) of the journal).
2. [Deependra Bawari](#), Billa Prashanth, Kuldeep Jaiswal, Angshuman Roy Choudhury and Sanjay Singh,\* Product Isomer Distribution in the Sequential Functionalization of Cyclic-(P<sup>III</sup>)<sub>2</sub>N<sub>2</sub> Frameworks, *Eur. J. Inorg. Chem.* **2017**, 4123–4130.
3. [Deependra Bawari](#), Kuldeep Jaiswal, Billa Prashanth, Chandrakala Negi, Angshuman Roy Choudhury and Sanjay Singh,\* Group 13 element containing conformationally rigid “N-E-N” heteroatomic bridged [3.3](2,6)pyridinophanes (E = B, Al), *Chem. Commun.* **2018**, manuscript under revision.
4. [Deependra Bawari](#), Chandrakala Negi and Sanjay Singh\*, Assembly of molecular bowls and cryptands containing aluminium: The aesthetic use of pyridine and triazine modules and control of molecular topology. Manuscript under submission.
5. [Deependra Bawari](#), Chandrakala Negi, Vishal Kumar Porwal, and Sanjay Singh\*, First metal free dearomative hydroboration of triazine: A calix like trimer. Manuscript under preparation.
6. [Deependra Bawari](#), Bhupendra Goswami, Sabari V. R., Sandeep Kumar Thakur, R. V. Varun Tej, Angshuman Roy Choudhury and Sanjay Singh\* Neutral and cationic Cyclic (Alkyl)(Amino)carbene mercury [cAAC-Hg(II)] complexes: Scope of hydroamination of alkynes with organomercury compounds, *Dalton. Trans.* **2018**, [doi.org/10.1039/C7DT04589A](https://doi.org/10.1039/C7DT04589A).

7. Kuldeep Jaiswal, Billa Prashanth, [Deependra Bawari](#), and Sanjay Singh,\* Bis(phosphinimino)amide Supported Borondihydride and Heteroleptic Dihalo Compounds of Group 13, *Eur. J. Inorg. Chem.* **2015**, 2015, 2565–2573.
8. Piyush Mishra, Kanupriya Verma, [Deependra Bawari](#) and K. S. Viswanathan,\* Does Borazine-water Behave like Benzene–Water? A matrix Isolation Infrared and *ab initio* Study, *J. Chem. Phys.*, **2016**, 144, 234307–1–234307–9.
9. Billa Prashanth, [Deependra Bawari](#) and Sanjay Singh,\* Heteroleptic Iminophosphanamide In(III) Complexes: Source of Mild Lewis acid Indium Centers, *ChemistrySelect* **2017**, 2, 2039–2043.
10. Rishu, Billa Prashanth, [Deependra Bawari](#), Ushnish Mandal, Angshuman Roy Choudhury, Sanjay Singh\* and Aditya Verma, Hg(II) and Pd(II) complexes with a new selenoether bridged biscarbene ligand: Efficient mono- and bis-arylation of methyl acrylate with a pincer biscarbene Pd(II) precatalyst, *Dalton. Trans.* **2017**, 46, 6291–6302.